OPTIMIZATION OF
## AN ADVANCED HIGH SPEED HULL FORM

by
Henri W. Zajic

B.S. Marine Eng., United States Naval Academy, (1981)
MBA, Marymount University, (1989)

Submitted to the Department of
OCEAN ENGINEERING
in Partial Fulfillment of the Requirements for the Degrees of

NAVAL ENGINEER

and

MASTER OF SCIENCE IN NAVAL ARCHITECTURE
AND MARINE ENGINEERING

at the
MASSACHUSETTS INSTITUTE OF TECHNOLOGY
May 1995
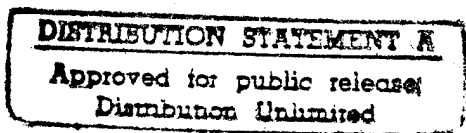
The author hereby grants to M.I.T. and to the U.S. Government permission to reproduce and to distribute
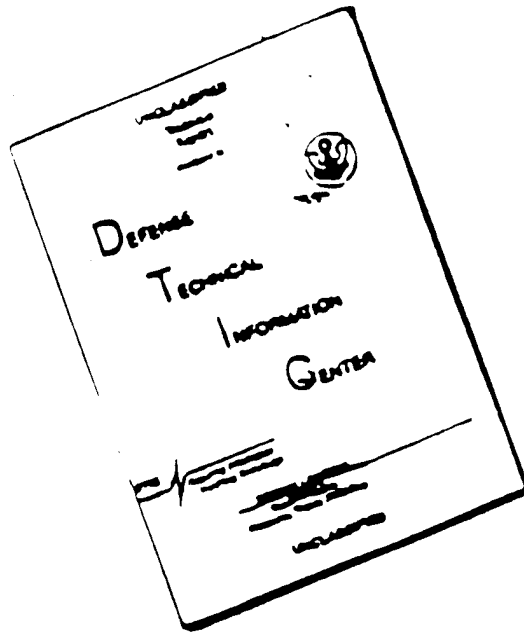copies of this thesis document in whole or in part.

Signature of author: _____
Department of Ocean Engineering, May 1995

Certified by: _____
Alan J. Brown
Professor of Naval Architecture and Marine Engineering
Thesis Supervisor

Accepted by: _____
A. Douglas Carmichael
Chairman, Department Committee on Graduate Students
Department of Ocean Engineering

1

DISCLAIMER NOTICE

THIS DOCUMENT IS BEST QUALITY AVAILABLE. THE COPY FURNISHED TO DTIC CONTAINED A SIGNIFICANT NUMBER OF PAGES WHICH DO NOT REPRODUCE LEGIBLY.

OPTIMIZATION OF
AN ADVANCED HIGH SPEED HULL FORM

by

Henri W. Zajic

Submitted to the Department of Ocean Engineering on 12 May 1995 in partial fulfillment of the requirements for the Degrees of Naval Engineer and Master of Science in Naval Architecture and Marine Engineering.

Abstract

It is the purpose of this research to examine the engineering process required to adequately predict the total resistance of unique hullforms. A comparison of the significant physical effects present in monohull and advanced hullforms testing is made. The historically accepted method of scaling using Froude's Hypothesis is studied and its underlying assumptions are considered in detail. An overall design philosophy is created for achieving resistance minimization through a range of operating speeds. This discussion is applied to a specific hullform called SLICE which is an adaptation of the Small Waterplane Area Twin Hull (SWATH) concept.

To further develop the body of available SLICE resistance data, three models were built and tested at the US Naval Academy's 380 feet towing tank in Annapolis Maryland. The results of these tests is reported on and a video demonstration of their performance is provided as part of this report.

Finally, a numerical method approach to the solution of Mitchell's integral is presented as a possible means of calculating SLICE wave making resistance. This is considered as an intermediate step tool in design optimization, useful after preliminary model tests are completed and before final designs are decided for powered model testing.

Thesis Supervisor: Dr. Alan J. Brown
Title: Professor of Naval Architecture and Marine Engineering

2

Acknowledgements

I would like to thank my advisor, Professor Alan Brown for his support, guidance and patience throughout the course of this work. I would also like to thank LCDR Jeff Reed for his intellectual support and willingness to talk through stumbling blocks to this project.

I would especially like to thank my parents Anna and Jerry Zajic for the love, patience, and sacrifice they gave over so many years to ensure that my foundation was a strong one. Without that, I would not have completed this work. I am only now beginning to understand the enormity of their contribution.

Sara, Katie and Greg are three great kids who have helped keep my MIT experience in perspective. Sara, thanks for singing "You are my sunshine..." whenever I was in a grumpy mood.

Although it is my name on the cover of this work, I received help from an enormous circle of people who contributed their expertise to my project. I feel I have developed a new family of friendships as a result:

Dr. Dave Moran and Dr. Paul Rispin of the Office of Naval Research. They allowed my initial access to the SLICE project and have supported my efforts throughout. Through their association, I received an extra year of education in program management and research development.

The LMSC team headed by Terry Schmidt as well as Steven Louie and Bill Clifford of Pacific Marine who provided me significant access to their development of SLICE.

Mr. Doug Jenkins of NSWC who educated me regarding model testing. Without his insight, my test program would not have been possible.

Dr. Michael Wilson and Mr C.C. Hsu of NWSC for their assistance in understand the mathematics behind their Wave Cancellation Multihull Ship concept. Dr. Takashi Maekawa of MIT for helping me with specific numerical methods problems.

Dr. Roger Compton, Mr. John Hill, Mr. Steve Enzinger and Mr. Don Bunker of the US Naval Academy Hydrodynamics Lab. They generously gave their facility, time and expertise to assist in executing my test plan.

Mr. Dave Barrett, who generously offered me a place to build models, access to equipment and building insight.

The team of dedicated model builders: Scott Miller, John Dannecker, Chris Warren, Chris Trost, Alex Deroches, Bob Meyer and Tim McCue who all contributed to inventing the model building process used and the actual construction.

To my fellow engineer and model builder, Jerry Zajic, who pushed the model building to completion. Without his drive, model three would never have been built. We don't always tackle a problem the same way but we make a great team.

3

I dedicate this project to my wife Melanie.

A chemical engineer in her own right. she chose to dedicate herself to our family. She has been my anchor during our lives together and especially here at MIT. She has been my cheerleader. study police. critic, friend. and strength throughout our MIT experience. She can keep three children quiet on a rainy Sunday afternoon while I study. Research work like mine is important only because wonderful people such as Melanie exist.

Table of Contents

Chapter 1   Introduction

The majority of the world's commerce is moved by monohull displacement ships. Ironically, in this age of supersonic air travel, guaranteed overnight mail delivery and fibre optic data transfer at the speed of light, modern displacement ships are capable of speeds no faster than those built fifty years ago. The apparent lack of progress in high speed ocean travel stems from the physical realities of the interaction between the displacement monohull form and the water in which it travels.

The total resistance curve for a ship is generally plotted as the Total Drag Coefficient, C_T versus Froude Number. $\mathscr{F}$. These are expressed as:

$$\mathscr{F} = V/\sqrt{(gL)} \tag{1-1}$$

$$R_T = (\frac{1}{2}\rho V^2 S)C_t \tag{1-2}$$

where L is some characteristic length, usually length of the waterline of the body, ρ is the density of the water, V is the ship's velocity and S is the Wetted Surface Area. Total resistance is generally recognized as the additive effects of friction. wave making and spray generation of both the main body and its appendages. The extent to which each of these components effects the total resistance is, however, the subject of ongoing debate even though it has been over one hundred years since Froude gave us this theory. For a monohull displacement ship, the wave making resistance portion of the total resistance curve has the characteristic shape shown in Figure (1-1). Since resistance is obtained by multiplying the coefficient shown in Figure (1-1) by V^2, the total resistance curve becomes nearly vertical and practically insurmountable by conventional hull forms at the speeds shown.
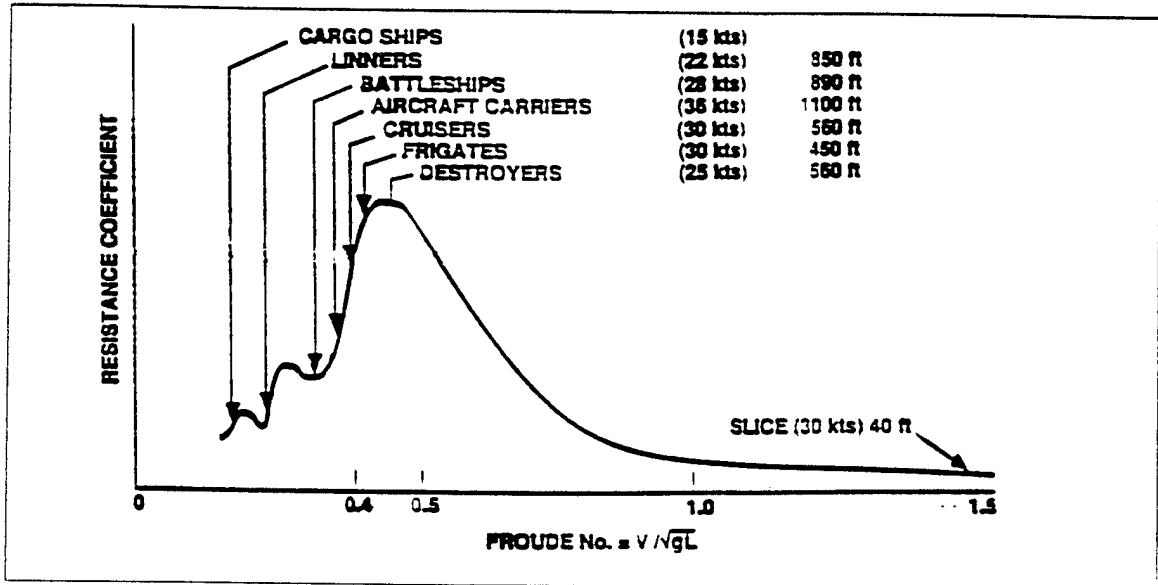
Figure 1-1: Characteristic Wave Making Resistance Curve
(from LMSC presentation)

For Naval Architects. the search is ongoing in advanced hull form design for a practical method to "get over the hump". Most advanced hull forms do not resemble the classic displacement monohull shape on which the vast majority of Naval Architecture experience is based. The purpose of this research is to examine the underlying assumptions regarding commonly accepted full scale resistance prediction methods in an effort to understand the important features of design optimization and draw some conclusions regarding resistance minimization methods . The Lockheed Missile and Space Company in conjunction with Pacific Marine (LMSC/PM) has proposed a hull form which is a modification of Small Waterplane Area Twin Hull (SWATH) concepts. Their proposal. called SLICE. will be presented to the United States Government as a 177 Lton vessel in an Advanced Technology Demonstration (ATD) in June 1996. A sketch of this hullform is shown in Figure 1-2. The SLICE vessel will be the subject hullform for the research conducted as part of this paper. SLICE is protected by Lockheed under patent law.
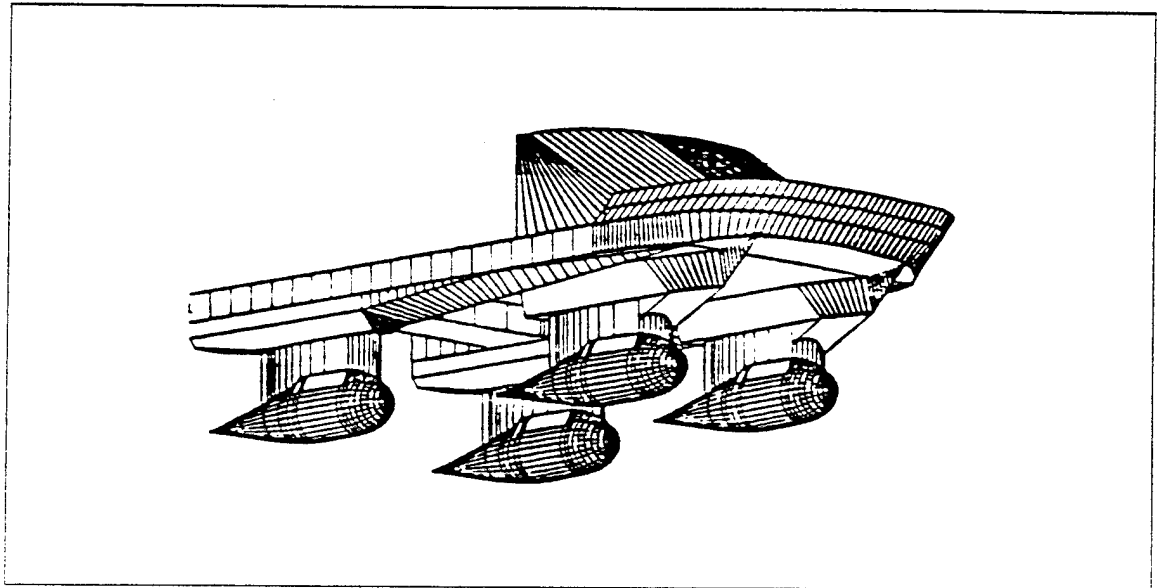
Figure 1-2: Artist's Concept of SLICE from an unpublished LMSC, Pacific Marine, ONR Article.

1.1 The SLICE Concept

High speed is not an inherent quality of SWATH ships. Although there may be some reduction of the wave making resistance due to smaller waterplane area, there is also an increase in the total wetted surface which increases frictional resistance. In SWATH ships, high speed is a design feature. When compared to an equivalent displacement monohull, SWATH design must be considered as a trade-off between a definite increase in frictional resistance and the potential for a decrease in wave making resistance. The design question becomes how to ensure that the decrease in wave making resistance is greater than the gain in frictional resistance.

LMSC's SLICE concept differs from traditional SWATH design in that the demi-hull is replaced by two shorter pods. Each pod is attached to the main box structure by a single strut. It is through this design feature that LMSC intends to minimize the impact of wave making resistance. By designing the vessel with an unusually short characteristic length, the hump of the wave making curve will in

theory be driven to a very low speed regime. Since resistance is a function of V^2, any left shift of the curve could have a substantial minimizing effect on the total resistance associated with the hump. It is further theorized that in the high speed regime, total resistance will be dominated by frictional effects and therefore design efforts focused on minimizing the wetted surface of the hullform will yield the best result. LMSC has chosen the length of the submerged pod as the characteristic length critical to design considerations. It should be emphasized that this hullform does not eliminate the hump effect characteristic of the wave making resistance curve. It does not specifically cause wave cancellation effects nor does it attempt to reduce viscous drag effects. Rather, the apparent thrust of the LMSC theory is to stagger the peak effects of wave and skin resistance, thereby reducing the overall resistance value at specific design speeds.

1.2 LMSC Model Test Synopsis

LMSC has conducted two different sets of model tests at the US Navy's Surface Warfare Center, Carderock Division, Bethesda, Maryland (NSWC). In the first series of tests, called the HM&E tests, several different configurations of struts, pods and foils were used to make a determination of the overall best configuration to use as the baseline for the production vessel. These tests were conducted in the Spring 1994.

The second set of tests, also conducted at NSWC, were used to obtain detailed resistance and control surface performance data for the baseline production vessel. These tests, conducted in August 1994 and continued in December 1994 were observed by several MIT students. The model that was tested was a 1/8th scale of the production vessel. It's construction was fiberglass bodies mounted to an aluminum box frame. For all the tests conducted, the model was fixed in pitch and heave and data was collected for forces and moments about the three principle axes. There were two major groupings of data collection runs performed. The first group was called the dynamic control tests and was primarily used to judge the required effectiveness of control surfaces to hold the ship at a constant draft with an even trim. Each run had a

slightly different model configuration with canards, stabilizers and rudders tested in different locations and with varying angles of attack. Each configuration was tested a single time unless there was some specific problem noted in the conduct of the test. The second major grouping of tests consisted of rather major modifications to the model configuration in an attempt to improve the design. Haunches on top of the struts were removed to allow for deeper strut length, wedges located at the top of the struts were added and removed to experiment with better surface piercing shapes, the overall draft of the model was adjusted to force a deeper submergence of the rather bluff pods and finally, a new model was tested in which the longitudinal position of the struts relative to the pods was altered to modify the flow over the pods.

Within these two major test categories, the test procedure remained consistent. The model remained fixed in pitch and heave for all tests. Two different speed regimes were tested. a lower speed run consisted of twelve speed increments ranging from 3.2- 8.8 feet per second (fps) corresponding to full scale speeds of 9-25 knots. A high speed run used seven increments from 5.7-12.4 fps which corresponds to full scale speeds of 10-35 knots. All speed increments were fit into a single pass along a tow tank length of approximately 1200 feet. All of the dynamic control tests were conducted only in the lower speed regime. the major model modification tests were conducted in both speed regimes.

1.3 Research Motivation

The US Navy has potential applications for relatively small (200-700 Lton) high endurance craft that embody the seakeeping attributes of SWATH. The Navy's interest in the SLICE program is demonstrated by the funding the Navy has committed to the ATD that LMSC will perform in June 1996. It was LMSC/PM's entrepreneurial spirit that initially brought the SLICE concept to the attention of the Navy but this same entrepreneurial spirit has the potential to limit the usefulness of the SLICE design as well. LMSC/PM's allocated timetable from concept development to final product delivery is just over two years, very short by Navy shipbuilding standards. As a result LMSC must focus on a relatively narrow set of engineering problems that

specifically address the needs of the 177 Lton ATD vessel. Broader based questions, such at an in-depth understanding of the effects of body interactions. how these interactions vary with modifications to the basic dimensions, the practicality of scaling the SLICE concept into a different size regime (1500 Lton, 5000 Lton, etc.) and a relative comparison of the merits of a SLICE ship as compared to a SWATH or Monohull design for a given mission are all facets of the development of this concept that are not specifically addressed by LMSC in the ATD.

This thesis will attempt to add to the developing body of SLICE knowledge by focusing on the resistance and powering aspects of the SLICE vessel in an academically rigorous manner. In so doing, three benefits will be realized:

1) Independent research into this hull form will give both the US Navy and LMSC a second hydrodynamic viewpoint of the 177 Lton vessel prior to the ATD.

2) Development of a sufficient body of data will aid optimization of the 177 Lton hull form.

3) A broader understanding of the hydrodynamic features of the hull form will facilitate deciding the merits of pursuing designs in other displacements more practical to the US Navy.

1.4 Approach

To achieve the objectives outlined above. there are several questions raised by the LMSC efforts that require answers. These questions and the method that will be pursued for answering them is outlined in this section.

THEORY

LMSC theorizes that the appropriate characteristic length for SLICE is the length of a single pod. In conventional designs. $\mathscr{F}$ is based on the length of the waterline (LWL). Representative characteristic lengths for SLICE would seem to be bounded on the low end by the length of a single strut and on the high end by the length between the leading edge of the forward strut to the trailing edge of the aft strut. LMSC's choice of an underwater body for the characteristic length is not an

obvious one. Understanding the appropriate characteristic length for the SLICE configuration is necessary to understand the magnitude of savings that can be expected over competing hull forms.

The interaction between bodies is the second area for further study. There are two specific situations that require detailed analysis. The first is the effect a strut and its attached pod have on one another, the second is the effect that a strut/pod combination have on any of the other three strut/pod combinations that form the underwater body. Understanding these effects is necessary for design optimization and also deciding the practical upper limit of displacement for a SLICE ship.

Finally, the LMSC proposed design places the forward struts inboard of the aft struts as illustrated in Figure 2. This arrangement may cause some significant outward lateral forces on the struts that must be considered in the structural design.

TESTING

There were several procedural questions raised by the model tests conducted by LMSC in August. Keeping the model fixed in pitch and heave was the most significant issue. Although it was intentionally done to facilitate the dynamic control analysis, it also left open significant questions regarding how the hull form behaves at different speeds. Considering the recognized sensitivity that SWATH type hulls have in tons per inch immersion (TPI) and the moment to trim one inch (MT1) this may be significant.

The short duration of each test run speed increment, the lack of repetition of tests, and the truncation of most data collection runs at the full scale equivalent of 25 knots for a ship required to achieve 30 knots raises questions regarding the thoroughness of the results. Although this is understandable considering the expense of model testing and the limited time available, more testing must be completed before the SLICE body of data can be utilized to make design decisions.

OPTIMIZING

There are several striking features incorporated in the LMSC design. The most

striking is the bluffness of the leading sections of the pods and struts, especially for a high speed craft. It would appear that minimizing the wetted surface to displacement ratio was LMSC's driving concern in hullform selection. Although this approach minimizes frictional resistance, it also introduces significant form drag. With a pod length to diameter ratio (L/D) of 4.2, SLICE cannot be thought of as a slender body. This introduces another concern in evaluating SLICE performance. The vast majority of traditional resistance analysis has slender body theory incorporated to some extent. Any evaluation process undertaken must be carefully scrutinized to ensure that the SLICE hullform does not violate this imbedded assumption. A design approach which more thoroughly addresses the entire speed spectrum is preferable even with a specific mission speed identified. All speeds from zero through the mission speed must be attainable so some design consideration must be given to the entire speed spectrum. With eight component bodies (4 struts and 4 pods), wave cancellation effects through body interaction should be a design focus.

RESEARCH METHOD

In an attempt to answer these questions the following work was accomplished:

1) A literature review that encompassed one hundred years of ship resistance research was performed. This was accomplished to ensure that the full body of assumptions made in this field of engineering is understood.

2) A study of model testing techniques was made to develop an appreciation for proper test methods.

3) Series 58 resistance data was studied for potential pod optimization.

4) A literature survey was conducted to ascertain the state of the science in spray drag predictions.

5) Three models were built and tested to expand the overall data bank.

6) A numerical calculation method for wave making resistance based on the solution to Mitchell's integral was attempted in an effort to expedite the hullform optimization process.

Chapter 2 Theory

The difficulty in predicting full scale resistance is in understanding the extent to which different physical phenomena contribute to total resistance. Although effects such as boundary layer development, wave making, spray generation and flow separation are known to be present as a body moves through the water, methods for quantitatively evaluating the contribution of each of these effects to total resistance and the extent to which these phenomenon may interact continues to be the subject of ongoing debate.

This chapter studies the two available approaches to resistance prediction, model testing and analysis. The objective is to identify those methods that will be best suited for SLICE resistance predictions. Since the vast majority of available resistance data was developed from displacement monohull analysis, care must be taken to ensure that underlying assumptions to these methods are not violated.

2.1 Model Testing

The classical approach to model testing is well documented. <u>Principles of Naval Architecture</u>[1] (PNA), and Rawson and Tupper[2] are probably the two most recognized authorities outlining this process. The textbook approach is definitively stated and easy to follow. Nonetheless, the SLICE experience has shown that specific model testing methodology and subsequent data reduction can be hotly contested. The difficulty lies in deciding if the model tested accurately replicates the physical phenomena that will be present in the full scale ship and what to do with the model scale data once it is obtained.

As background, the model testing/scaling process outlined by William Froude is presented. In this discussion the subscript m refers to the model and the subscript s

---

[1] Comstock, J.P., <u>Principles of Naval Architecture</u>, SNAME, New York, 1967, Chapter 7.

[2] Rawson,K.J. & Tupper,E.C. <u>Basic Ship Theory</u>, 3rd Edition, Vol 2, New York,1983.

refers to the full scale ship:

1) Build a model that is geometrically similar to the full scale ship. This is accomplished by choosing a scale factor to apply to all linear dimensions of the ship. The scale factor λ is then defined as:

$$\lambda = \frac{L_{ship}}{L_{model}} \qquad (2\text{-}1)$$

2) Test the model at equivalent speeds. Through dimensional analysis, it is easily shown that the full scale and model scale speeds are related through equation (1-1). Specifically:

$$V_{ship} = V_{model} \times \sqrt{\lambda} \qquad (2\text{-}2)$$

3) Convert the total model resistance measured R_{tm} to a coefficient of total resistance C_{tm} through relationship (1-2).

4) Calculate the coefficient of frictional resistance C_{fm}. The method for accomplishing this will be discussed shortly.

5) A quantity called the coefficient of residuary resistance C_{rm} is obtained by subtracting C_{fm} from C_{tm}. The reason C_{fm} is not subjected to the scaling law expressed in (2-2) will be discussed shortly.

6) The full scale coefficient of residuary resistance C_{rs} is then expressed at the same Froude Number as C_{rm}. Specifically,

$$C_{rs} = C_{rm} \qquad (2\text{-}3)$$

7) The full scale coefficient of frictional resistance C_{fs} is calculated in the

same manner as in step 4 and is added to C_{rs} to obtain the full scale coefficient of total resistance C_{ts}.

8) Full scale total resistance R_{ts} is then found using (1-2).

This process can be thought of as a system of one equation and one unknown. The unknown is C_{rs}; the equation is $C_{ts} = C_{rs} + C_{fs}$. This method of scaling data is useful only if the following conditions exist:

1) A geometrically similar model can be built and tested in compliance with the equalities set forth in (2-1) and (2-2).

2) The model is tested in a condition that can be considered equivalent to the normal operating condition of the full scale ship.

3) Frictional resistance can be reasonably calculated at both the model and full scale size.

4) All other physical phenomenon present must either obey equality (2-3) and therefore be lumped into the residuary component or be of such little concern that ignoring them is inconsequential to the final outcome.

If the last condition can not be satisfied for a particular phenomenon, then its effect must be calculated at both the model and full scale size and algebraically treated the same as the friction resistance component.

Froude's experiments were conducted on slender bodies, generally thought of as those with L/D > 10. Residuary resistance was defined as the combined effect of wave making resistance and eddy resistance. At low speeds, eddies appear to be a by product of the boundary layer and therefore part of frictional resistance. Experimentally, Froude demonstrated that eddy resistance did not change proportionally with skin friction as parallel midbody was added to a given hull form. He concluded that eddy resistance was actually related to the form of the hull. Since wave making and eddy resistance are both related to form and are pressure related phenomenon, they historically have remained combined as the residuary resistance

component[3]. For slender bodies the only significant physical phenomena are friction, waves and eddy formation. The process outlined above was developed with slender bodies and only these three phenomena in mind.

2.2 Frictional Resistance

The problem of calculating the frictional resistance of a ship was first studied by considering flat plates. The essential issue focuses on the development of the boundary layer along the length of the plate and its transition from a laminar to a turbulent regime. Frictional resistance is usually expressed as a coefficient of friction in the form of (1-2) and is generally plotted as a function of the Reynolds Number, $\Re$:

$$\Re = \frac{V*L}{v} \qquad (2-4)$$

where L is some characteristic length, usually length of the waterline of the body, υ is the kinematic viscosity of the water and V is the ship's velocity. The development of a laminar flow equation was the work of Blasius (1904), while the turbulent solution was formulated independently by Prandtl and von Karman in the 1920's. In the range of Reynolds Number between 5×10^5 and 9×10^6, neither the turbulent nor the laminar expression yields accurate results. This region of uncertainty is known as the transition region. Experimentally it has been shown that the transition from laminar to turbulent flow occurs gradually across the length of a plate as its speed increases. This gives physical meaning to the rather large band of uncertainty between fully laminar and fully turbulent flow. The curves of laminar, transition and turbulent plate flow are shown in Figure (2-1).

Model testing through the 1940's attempted to draw parallels between monohull

---

[3] Gilmer,T.C and Johnson.B. Introduction to Naval Architecture. Naval Institute Press, Annapolis, 1982, p.217.

18

forms and the known flat plate solution. The most accepted flat plate solution to frictional resistance adapted to ship form use is the Schoenherr Formula. This flat plate formulation is frequently seen in the literature labeled as the ATTC Line. In an attempt to account for the effect of hull form on boundary layer formation the International Towing Tank Conference (ITTC) adopted an *interim* solution that was derived from a correlation of previously obtained model tests.
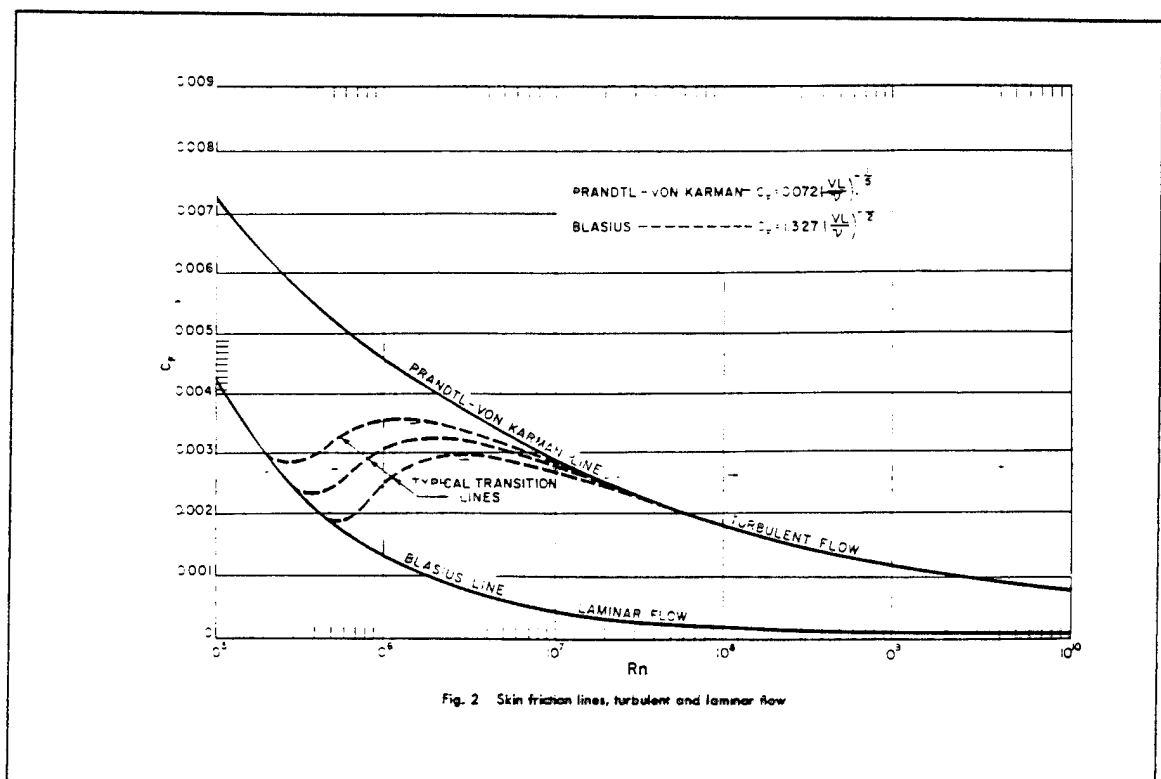

Fig. 2 Skin friction lines, turbulent and laminar flow

Figure 2-1: Laminar and Turbulent Flow Skin Friction Lines[4]

---

[4] Principles of Naval Architecture. op.cit., p295.

This formulation, known as the ITTC 1957 line is given as:

$$C_f = \frac{0.075}{(\log_{10} \Re - 2)^2}$$
(2-5)

It should be stressed that this line was developed from a correlation of model data, it does not physically represent the behavior of a flat plate and it was not obtained by extrapolating flat plate data to ship like forms. Forty years later, the ITTC has not replaced this interim solution with a better alternative.

At the same time that the ITTC 1957 formulation was published, Hughes proposed a method for calculating flat plate frictional resistance given by:

$$C_f = \frac{0.066}{(\log_{10} \Re - 2.03)^2}$$
(2-6)

To the basic Hughes line, a form factor is then added. The purpose of this form factor is to help account for the differences in the laminar to turbulent transition seen by a flat plate and a fuller body. The attractiveness of Hugh's method is that it attempts to keep friction and eddy resistance linked. Physical observation of a body moving through the water would seem to make this reasonable. The method proposed by Hughes has not received the same acceptance within the Naval Architecture community as the ITTC 1957 line. The earliest criticism was the low value that equation (2-6) yields when compared to flat plate testing. Additionally, the use of a form factor is also questionable as outlined by Oosterveld[5], quoted below:

" It has now become clear that in many cases the wave
pattern resistance is less than the residuary resistance estimated

---

[5] Oosterveld. M.W.C. ed., "Report of the Resistance Committee", 15th International Towing Tank Conference, The Hague, 1978, p.21.

by assuming a form factor independent of Froude number and Reynolds number. This will certainly be the case whenever bow wave breaking occurs. One possible reason for this is that the viscous resistance may vary significantly with Froude number (which effects the flow at the edge of the boundary layer) as well as with Reynolds number, so that it is not well predicted on a constant form factor basis. However it is conceivable that this variation arises at least in part from an interaction of the boundary layer and wake with the wave system, so that energy losses which originate with wave making, and are primarily Froude number dependent, may manifest themselves as an apparent increase in the viscous wake losses."

The frictional lines discussed in this section are shown in Figure (2-2).
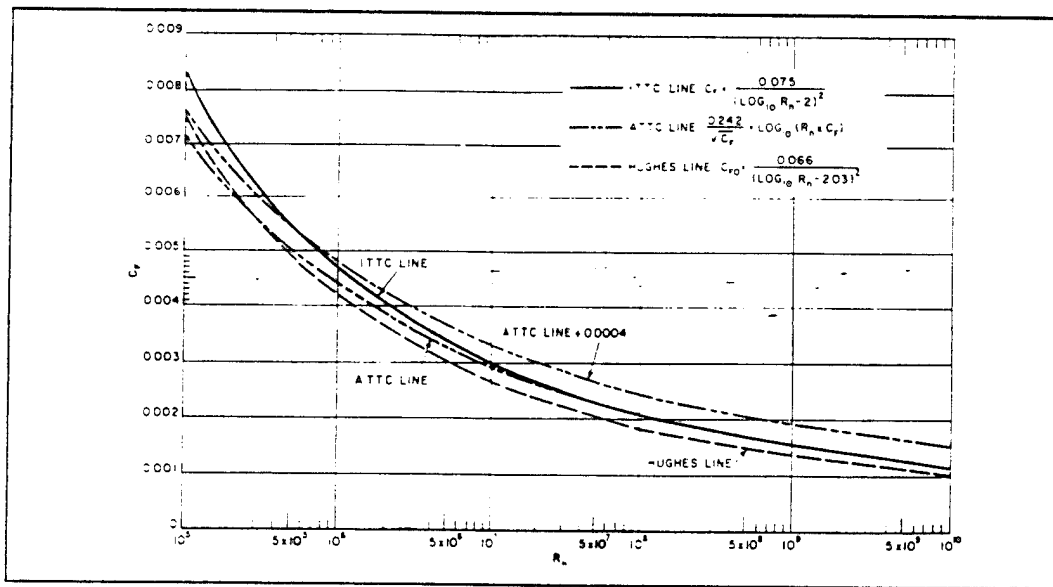
Figure 2-2: Standard Skin Friction Lines[6]

This discussion of frictional resistance has bearing on the SLICE project in two

[6] Principles of Naval Architecture, op.cit., p. 298.

respects. First there is the issue of turbulent flow. The general practice in model testing is to artificially stimulate turbulence. This is done so that the model and the full scale ship operate in the same regime. Without turbulence tripping, most models would operate at least partially in the transition regime shown in Figure (2-1), making data interpretation difficult since C_f is highly variable in this regime. Hughes[7] describes standard methods of stimulation (usually pins, wires or sand strips), methods of accounting for the resistance caused by these devices and the uncertainty involved in insuring that turbulence is actually achieved. The values of $\Re$ at which the SLICE models and full scale ship operate are shown in Table (2-1). A comparison of these values to Figure (2-1) would appear to demand that some form of turbulence tripping be used in testing.

	Full Scale	1/8th Scale	1/16th Scale
Low End Reynolds Number	2.0×10^7 (Turbulent in Fig 2-1)	2.5×10^6 (Transition in Fig 2-1)	1.2×10^6 (Transition in Fig 2-1)
High End Reynolds Number	2.1×10^8 (Turbulent in Fig 2-1)	3.0×10^7 (Turbulent in Fig 2-1)	1.3×10^7 (Transition in Fig 2-1)

Table 2-1: Operating Reynolds Numbers for SLICE based on Strut and Pod Length

Figure (2-1) however shows the laminar to turbulent transition for a *flat plate*. SLICE, with a nearly hemispherical nose shape and an overall L/D ≈ 4.5 cannot be likened to a flat plate. The laminar to turbulent transition for a sphere is known to occur in the

---

[7] Hughes,G. and Allan,J., "Turbulence Stimulation on Ship Models, SNAME Transactions, 1951, p281-314.

region $\Re = 4.5 \times 10^4 - 5 \times 10^5$ or two orders of magnitude lower than that of a flat plate. The actual transition for SLICE probably lies somewhere between these two extreme boundaries. When viewed in this light, turbulence stimulation is probably not worth the uncertainty involved in mathematically removing the resistance effects of the trip device. For the purposes of testing in this project, at the model scale, turbulent flow will be assumed even though turbulence stimulation is not provided.

The second issue is to decide the most appropriate method to compute the frictional component of SLICE resistance. The ATTC line should be excluded since it is derived strictly from flat plate results. The Hughes line with form factor corrections may initially appear attractive since it incorporates calculated adjustments for form. The fullness of the SLICE body and the definite appearance of a breaking bow wave may cause the inaccurate accounting discussed by Oosterveld. The ITTC 1957 line is the best choice. It is based on actual ship and model results. Even though there may be uncertainty in describing the details of laminar to turbulent transition, and the impact the fullness of a ship shape has on that transition, the ITTC 1957 line must be thought of as correctly including the phenomenon since it is based solely on test results. This is a fallout of the model to ship correlation method used to derive the line. It is the only line discussed that was developed in this fashion. Further work in this project will utilize the ITTC 1957 line as the basis for calculating frictional resistance.

2.3 Wave Making Resistance

Wave making resistance has two parts. In an obvious way it accounts for the energy expended creating the visible wave system seen as a body moves through the water. It also accounts for the energy expended overcoming drag due to the pressure distribution created by unseparated inviscid flow around a body. The literature is vague on the second part of this definition of wave making resistance. The pressure distribution around the body is directly related to the form of the body but this effect is not the commonly termed "form drag". "Form drag" is a Reynolds scaled viscous effect that is best thought of as the correlation between flat plate frictional resistance

prediction and actual ship friction results. The form part of wave making resistance should not be confused with eddy resistance either which accounts for the effects of separated flow. Since both parts of the definition of wave making resistance are pressure effects, this phenomenon will follow Froude scaling.

One of the reasons that model testing is performed is because the ability to calculate wave making resistance remains an elusive goal. This section reviews the classical work that has been accomplished in this area. The objective is to gain some insights into the physical phenomenon and how it applies to the SLICE hullform. The foundation for a mathematical approach to wave resistance was set in place at nearly the same time that Froude was developing his model testing methods. J.H. Mitchell gave an analytic solution for wave resistance of the form[8]:

$$R_w = \frac{4\rho g^2}{\pi V^2} \int \sec^3\theta \left| \int\int \sigma \exp\{(\frac{g}{V^2})\sec^2\theta(y-ix\cos\theta)\}dxdy \right|^2 d\theta \qquad (2\text{-}7)$$

Where ρ is the density of water, V is velocity and σ is the potential function that represents the body of interest. The combined complexity of writing σ to comply with the necessary boundary conditions at the free surface as well as with the relatively complex form of a monohull and the difficulty in actually solving this integral without the advantage of numerical computing techniques, were serious setbacks to the popularity of this approach. The most significant pursuit of Mitchell's work was undertaken by T. Havelock and W.C. Wigley. Wigley was the first to successfully decompose the waves generated by a hullform into components and thus gain an understanding of how they are formed. This was first achieved with what is now called the Wigley hull, a wedge followed by parallel midbody followed by an identical wedge pointed opposite to the bow. Eventually Wigley refined the hull to a smooth

---

[8] Newman, J.N., Marine Hydrodynamics, The MIT Press, Cambridge,1989. p.282.

form. He discovered that there are actually four waves produced by this shape. The first is produced by the leading edge of the hull, the next two are produced by the two shoulders formed by the intersection of the fore and aft wedge with the parallel midbody and the final one is produced by the trailing edge of the aft wedge. This decomposition held true for hullforms with continuous lines as well. Figure (2-3) is reproduced from Wigley's writings[9] which graphically demonstrates this additive effect.

This discussion is useful to the SLICE program because it gives insights to an approach at hullform optimization. Since the amplitude of the wave system generated is related to the form of the body, maintaining lines that are reasonably fine should help to minimize the hump of the wave making curve. As a approximation without actual calculations, the shape of the struts and pods of the SLICE form will be adjusted in an effort to find a reasonable compromise between frictional and wave making resistance. This is different from the LMSC approach which appears to have concentrated on the operating range of $\mathscr{F} > 0.9$ with effort focused on minimizing frictional resistance.

The SLICE hullform can be decomposed into eight different bodies, four struts and four pods. Each of these component bodies has a form that is reasonably similar to the hullforms tested by Wigley. If each of these bodies can be thought of as producing four waves that combine into a single wave system for the body, then an approach to optimizing wave making resistance can be created by adjusting body spacing once form issues are decided. A three tier system of looking at this problem is proposed:

1) First consider the interaction between a strut and its attached pod. This step can be thought of as creating an oversized bulbous bow for the strut.

2) Next consider the effect of longitudinally aligned strut pod combinations. This will probably have a diminished effectiveness compared to step 1

---

[9] Wigley,W.C.S., "A Comparison of Experiment and Calculated Wave-Profiles and Wave-Resistances for a form having Parabolic Waterlines", Proceedings of the Royal Society, Series A, London, 1934. pp 144-159.

Fig. 2.—Model 1254. Comparison of calculated and observed wave-profiles.

A. Broken line is observed wave-profile at 10·78 feet per second $(c/\sqrt{gl} = 0·694)$. (No experimental values of wave-height are available aft of the point marked B for this speed.)
C. Full line is calculated wave-profile at 10·78 feet per second $(c/\sqrt{gl} = 0·694)$.
D. Broken line is observed wave-profile at 10·50 feet per second $(c/\sqrt{gl} = 0·675)$.
E. Full line is calculated wave-profile at 10·50 feet per second $(c/\sqrt{gl} = 0·675)$.
F. Broken line is observed wave-profile at 9·20 feet per second $(c/\sqrt{gl} = 0·592)$.
G. Full line is calculated wave-profile at 9·20 feet per second $(c/\sqrt{gl} = 0·592)$.
H. Broken line is observed wave-profile at 7·95 feet per second $(c/\sqrt{gl} = 0·512)$.
I. Full line is calculated wave-profile at 7·95 feet per second $(c/\sqrt{gl} = 0·512)$.
J. Broken line is observed wave-profile at 6·74 feet per second $(c/\sqrt{gl} = 0·433)$.
K. Full line is calculated wave-profile at 6·74 feet per second $(c/\sqrt{gl} = 0·433)$.
L. Broken line is observed wave-profile at 5·45 feet per second $(c/\sqrt{gl} = 0·351)$.
M. Full line is calculated wave-profile at 5·45 feet per second $(c/\sqrt{gl} = 0·351)$.
N. Broken line is observed wave-profile at 4·22 feet per second $(c/\sqrt{gl} = 0·272)$.
O. Full line is calculated wave-profile at 4·22 feet per second $(c/\sqrt{gl} = 0·272)$.

Figure 2-3: Calculated Wave Profile Analysis

since the amplitude of the forward system will not equal that of the aft system once they interact.

3) Finally consider the interactions of the transversely and diagonally aligned strut pod combinations. Since these are not in the principle direction of motion, it is expected that the effectiveness of these interactions will again be diminished from the previous step.

2.4 Eddy Resistance

As previously noted, the literature is noticeably vague in defining both form and eddy resistance. They are frequently used together but are not used interchangeably. Articles written about resistance prediction usually account for eddy resistance as an input to residuary resistance. The research for this thesis uncovered no direct usage of form resistance in prediction schemes. As discussed in Chapter 2-2, this thesis considers form drag to be the increase in frictional resistance felt by a ship shape compared to an equivalent flat plate. The ITTC 1957 line directly accounts for form drag since it is based on experimental data from monohull forms. Other schemes such as the ATTC line and Hughes Line require some form compensation for accurate use since they are based on flat plate resistance.

Eddy resistance on the other hand has physical origins. In this thesis it is taken to mean the result of separation effects from discontinuities in the hull form. These can result from actual breaks in the ships lines such as the intersection of the strut and pod at both the leading and trailing edge, intersection of appendages and the main body, or radii of curvature which are too hard for the flow to follow. As discussed in chapter 2-1, eddy resistance is a pressure effect and therefore should be scaled as part of the residuary resistance component.

Following the classic approach, the minor swirling seen along the sides of a ship are associated with viscous effects of well behaved flow and are accounted for in the frictional component[10]. Significant swirling that can be associated with flow

---

[10] Principles of Naval Architecture, op.cit. p.312.

27

separation, such as that seen at the transom, describes the type of effect accounted for by eddy resistance. There is some obvious room for interpretation of cause and effects in these definitions of form and eddy drag. This highlights the importance of observing physical behavior through model testing.

2.5 Spray Resistance

The formation of spray and the impact it has on total drag has historically been assumed insignificant to monohull testing. Simple observation of full and model scale monohulls operating at speed validates this assumption. Although spray is generated, the region of generation is highly localized and the quantity of spray generated is usually small. With the increased interest in advanced hullforms such as hydrofoils and planing craft, neglecting spray was recognized as a poor assumption but the body of available knowledge regarding the mechanism of spray generation and the appropriate method of scaling spray results is relatively small.

When spray becomes a major concern, the one equation, one unknown analogy used in section 2-1 becomes one equation and two unknowns. The typical solution to this problem has been to test at very high speeds ($\mathscr{F} > 3.0$) to eliminate wave making. This allows spray drag to be analyzed separately but is only a partial answer. A gap exists at the lower, more practical values of $\mathscr{F}$. In 1971, Chapman[11] conducted a significant test program on strut forms with parabolic leading and trailing edges. He concluded the following:

1. Spray drag is partially dependent on both strut form and thickness. Blunt leading edges produce more spray.

2. The spray mass flow rate of spray depends on the thickness to chord ratio (t/c) and on $\mathscr{F}$. Blunt bodies send the spray up at higher angles causing greater wetting.

3. Skin friction due to wetting is the primary source of spray drag.

---

[11] Chapman. R.B. , Spray Drag of Surface Piercing Struts, Naval Undersea Research and Development Center Report AD 730710, 1971.

4. The momentum in the spray sheet is sufficient to create a large pressure drag on any object it strikes.

Chapman's work was expanded by Zhu Bing-quan in 1986[12]. A total of twelve struts were tested, all with parabolic trailing and leading edges. The objective was to correlate strut performance to the parameters c (chord length), t (maximum thickness) and x (longitudinal position of the maximum thickness). The relationship derived is:

$$R_s = \rho V^2 x^2 C_s \qquad (2\text{-}8)$$

and C_s is given as:

$$C_s = 0.068\frac{x}{t} - 0.555(\frac{x}{t})^2 + 0.696(\frac{x}{t})^3 + 0.083(\frac{x}{t})^2 \mathscr{F} \qquad (2\text{-}9)$$

The research also showed that the spray drag was minimized when $t\,x = 0.313$.

This has applications to the SLICE analysis. The strut form selected by LMSC is contrary to that recommended by the published literature for minimizing spray drag. The apparent design goal of minimizing frictional resistance fails to consider spray effects. In deciding the extent to which the spray effects will scale from model size to full scale, the dependence of (2-9) on $\mathscr{F}$ implies that spray drag will follow Froude scaling. The conclusion reached by Chapman and Zhu Bing-quan that the initiation of spray is highly form dependent also supports this assertion.

The following is recommended when dealing with spray effects. Choose strut shapes that are known to minimize spray generation. Unless there is a significant structural or interior arrangements reason to do otherwise, struts should have parabolic leading and trailing edges and $t\,x$ should be reasonably close to 0.313. For the ATD,

---

[12] Zhu Bing-quan, Ge Wei-zhen. "Experimental Study on Spray Performance of Surface Piercing Struts, Journal of Hydrodynamics, ser 2 no 4, 1990, pp 91-98.

this will help minimize spray effects and allow the research efforts to focus on the area of principle interest, the wave making resistance. Any spray that is observed in testing should be treated as part of the residuary resistance. If the tentative conclusion that spray follows Froude scaling is wrong, then this process will over predict the total resistance. Considering the uniqueness of the SLICE hullform, a conservative error of this nature is well justified for the first full scale ship. Design work in this project will follow these conclusions.

2.6 Appendage Resistance

The effect of appendages on total drag has historically been assumed small in monohull testing. This assumption is based on the fact that the overall size of the appendages is usually one or two orders of magnitude less than the main hull. For comparative testing of hulls, it is reasonable to ignore the appendages. For obtaining exact resistance predictions, appendages are usually included in the final testing and stripping tests have been devised to help account for their effects. In stripping tests, the model is towed first with all the appendages on. In subsequent tests, the appendages are removed one at a time. In this manner the impact of each appendage can be assessed. This approach assumes that the interaction effects of the appendages with each other and with the main hull are negligible.

For SLICE, appendages occupy a larger percentage of total volume compared to monohulls. The flow around SLICE is more complex and therefore interactions may be more pronounced. A full stripping test is warranted in the case of SLICE. Since this project is focused a comparison of alternate hull forms, appendages will be excluded, leaving the stripping test to future work.

2.7 The SLICE Data Scaling Method

Based on the above discussion, the traditional method of data scaling outlined in section 2-1 is recommended for the SLICE project and will be used in this research. Calculating the frictional resistance using the ITTC 1957 line will yield a moderately conservative answer. Although the ITTC 1957 line was derived from monohull tests, it

is the only method that naturally accounts for the Froude Number dependence of boundary layer development. All other phenomena (wave making, eddy formation and spray development) will be treated as part of residuary resistance and scaled accordingly.

It is important to recognize is that this technique of data scaling is considered reliable due to the enormous volume of model testing that has been performed on numerous series of monohull models. The validation of this process for SLICE will only come when the full scale ship is built and tested. This is the real value of the ATD. Building and properly testing the full scale ship will significantly contribute to the Naval Architecture community's understanding of the robustness of current testing and scaling techniques.

2.8 A Numerical Approach

Model testing is a time consuming, detail intensive process that requires significant capital expenditure. For a new hull form, some degree of model testing is mandatory in the early stages of design so observations of physical behavior can be made. This is critical to validating assumptions, but from a cost savings perspective, the ability to numerically model the ship's behavior is attractive. Small changes to the hull can be made and tested without the expense of building a new model. If the numerical model can be kept mathematically simple, comparative results can be obtained quickly and cheaply. There must be a degree of confidence however that the computer model fully represents actual resistance.

The physical phenomena of interest are friction, wave, spray and eddy resistance. Friction and spray resistance can be calculated using (2-5), (2-8) and (2-9). If there is no significant separation or vortex phenomena, it is reasonable to neglect eddy resistance (only observation can answer this) and a prediction for full scale resistance can be obtained if a method of solving (2-7) can be found. This is significant to the SLICE discussion since it may provide a simple and fundamental tool for predicting and minimizing the wave making hump magnitude.

A solution to Mitchell's integral was outlined by Lunde[13] in 1951. The process was further applied to a ship called the Wave Cancellation Multi-hull Ship Concept by Wilson and Hsu[14]. They express the total wave making resistance as the summation of body and interaction terms as shown:

$$R_{w_{i,j}} = 16\pi\rho\kappa^2 \int_0^{\frac{\pi}{2}} (\sum_1^N\sum_1^N P_i P_j + \sum_1^N\sum_1^N Q_i Q_j)\sec^3\theta d\theta \qquad (2\text{-}10)$$

where N represents the number of bodies the overall hull can be divided into and:

$$P = \int_0^T\int_0^L \sigma(x,z)\cos[\kappa(x\cos\theta + y\sin\theta)\sec^2\theta]e^{\kappa z\sec^2\theta}dxdz \qquad (2\text{-}10a)$$

$$Q = \int_0^T\int_0^L \sigma(x,z)\sin[\kappa(x\cos\theta + y\sin\theta)\sec^2\theta]e^{\kappa z\sec^2\theta}dxdz \qquad (2\text{-}10b)$$

$$\sigma = -\frac{V}{2\pi}\frac{\delta}{\delta x}(f(x,z)) \qquad (2\text{-}10c)$$

[13] Lunde, J.K., "On the Linearized Theory of Wave Resistance for Displacement Ships in Steady and Accelerated Motion", SNAME Transactions, Vol 59, 1951, pp. 25-76.

[14] Wilson, M.B., and Hsu, C.C., "Wave Cancellation Multihull Ship Concept", Presented at the Intersociety High Performance Marine Vehicle Conference, Arlington, Va., 24-27 June 1992.

$$\kappa = \frac{g}{V^2} \qquad\qquad (2\text{-}10d)$$

In these expressions, the like product terms are the body terms and the cross product terms are the interaction terms.

The underlying assumptions to Lunde's approach are :

1. The fluid is incompressible, irrotational and inviscid.

2. The wave height is small compared to wave length.

3. The ship motion can be reasonably represented by a fine distribution of sources and sinks along the centerline of the body.

Prior observation of SLICE models in the towing tank indicates that conditions 2 and 3 may not be satisfied ideally. Each of these phenomenon must be watched closely in subsequent tests and considered in the interpretation of results. Havelock[15] demonstrated good correlation using this technique with hull forms having L/B as small as 10.6. Data presented by Newman[16] indicates that there is better correlation between model test data and thin ship theory at higher values of $\mathscr{F}$. SLICE is a full form with L/D = 4.5-5.0 but operates at $\mathscr{F}$ = 0.9-1.2. Although SLICE is not an exact fit for thin ship theory, the approach may be reasonable.

---

[15] Havelock, T.H., "Wave Resistance Theory and its Application to Ship Problems", SNAME Transactions, 1951, pp. 13-24.

[16] Newman, J.N. , op.cit., p282.

Chapter 3 Model Testing

As part of this research, three models were designed, built and tested. Appendix A provides detailed lessons learned from this testing experience which may be useful to other students attempting to undertake similar model testing projects.

3.1 Model Test Objectives

There were three objectives underlying the model testing phase of this project:

1. Expand the quantity of available model scale resistance data for the baseline SLICE configuration.

2. Visually observe model performance in sufficient detail to understand the physical behavior of this hullform. As discussed in chapter 2, this is important for justifying the scaling technique selected.

3. Test operationally equivalent hullforms to help assess baseline SLICE advantages and disadvantages.

The models were tested at the United States Naval Academy's 380' tow tank facility during the week of 6-10 March 1995.

3.2 Model Descriptions

The three models tested as part of this research were designed to meet the same operational constraints. This was done to ensure that comparisons made at the end of the testing could be made on the basis of similar ships. All models when scaled to full scale have a displacement of 177 Lton, a pod diameter of 7-8 feet and a strut beam of 3.25 feet. These dimensions are the working dimensions of the ATD vessel, driven by requirements other than hydrodynamic performance. The pod diameter is controlled by engine size requirements and the strut beam is controlled by access trunks into the pods. With these requirements imposed on all three models, they are considered equivalent hulls.

The three models tested were designated M-1, M-2 and M-3. Detailed tables

of hull offsets and design calculations for each model are contained in Appendices B, C and D respectively. Individual descriptions of each model follow.

MODEL M-1 BASELINE:

This model utilizes LMSC's offsets as tested in December 1994 with the exception that the fillets at the strut/pod interface and the haunch structures are excluded. The fillets were excluded to help simplify model building. This modification is not considered detrimental to the testing outcome. The combination of the pod, strut and fillet in the LMSC model creates a effective L/D of 3.9, the omission of the fillets increases this ratio to a more favorable 4.2. This modification should result in slightly lower resistance values. The bow wedges installed in the December LMSC model are replicated in this model. The purpose of this model is twofold. First, it provides a means of correlating the data obtained in these tests with the data obtained by LMSC in December 1994. This is considered important since the tests were conducted in two different facilities, under different conditions with different scale models. The ability to correlate data between Model M-1 and the LMSC model will be valuable in demonstrating repeatability of results. The second use of Model M-1 is to expand the available range of data for the baseline SLICE. Model tests were conducted at model equivalent speeds through 40 knots to ensure that the entire operating range was properly represented by data.

Table 3-1 provides the principle dimensions of Model M-1. Profile and top view sketches of the forward and aft strut/pod combinations are in Figure 3-1. In this drawing the alignment of the struts with the corresponding pods is correctly represented. The spacing between the forward and aft combination is not preserved however in the interest of fitting the drawing onto one page. This model was constructed with 29 lbf of reserve buoyancy. The struts are manufactured from balsa wood with a fiberglass shell, the pods are molded fiberglass.

35

Scale Factor	17.26:1
Displacement	75 Lbf
Beam	36.15 inches
Draft	8.34 inches
Pod Diameter	5.5625 inches
Fwd Pod Length	22.9 inches
Aft Pod Length	25 inches
Fwd Pod Separation (CL to CL)	23.4 inches
Aft Pod Separation (CL to CL)	30.25 inches
Strut Length	16.68 inches
Strut Max Beam	2.26 inches

**Table 3-1: Model M-1 Baseline
Principle Dimensions**
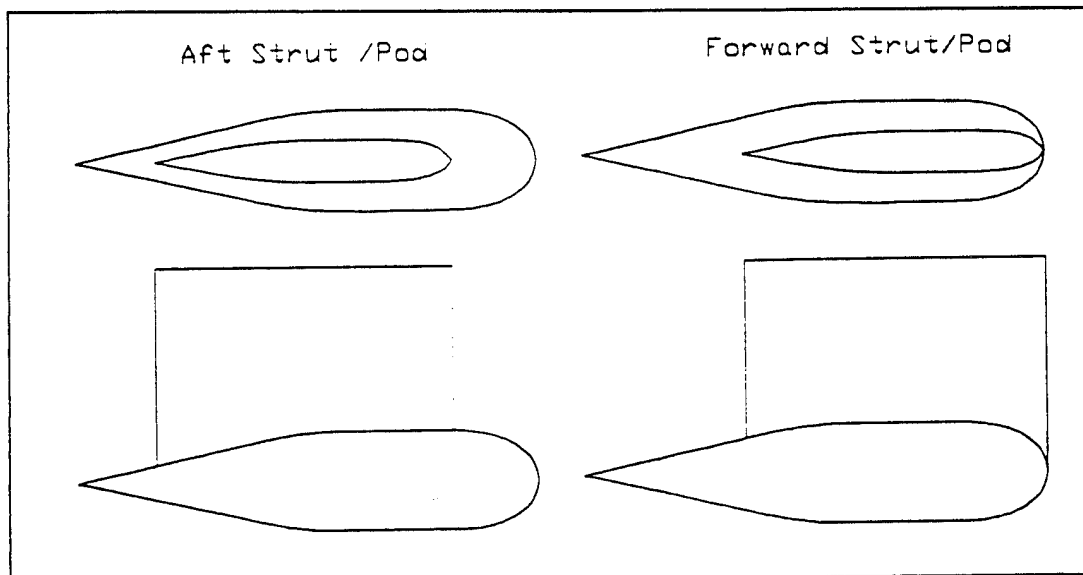
Figure 3-1: Model M-1 Forward and Aft Strut/Pod
(Note: In this drawing the fwd-aft pod spacing is not preserved)

MODEL M-2 RATIONAL DESIGN:

The purpose of this model is to explore the effects on total resistance of using finer offsets for the struts and pods . To avoid changing too many variables in a single test, this model maintains all the gross parameters of the Model M-1 Baseline (ie: Strut/Pod alignment, fore/aft spacing and centerline to centerline spacing). The expectation for this design is that by comparing this model's results with that of M-1, some conclusions can be drawn about the relative magnitude of both friction and wave making resistance through the range of speeds tested. The anticipated result from this model is that the amplitude of the wave making hump will be diminished.

The offsets for the pods are adapted from Series 58 data[17]. This series was selected since it represents a concerted effort to optimize submarine hull forms. The model selected from the series was Model 4155. This model was selected based on its length to diameter (L/D) ratio of 5 which is similar but finer than the baseline SLICE L/D of 4.2. It should be noted that within the Series 58 results, Model 4155 falls outside the range of optimum L D which was found to be between 6 and 8. Model 4155 was selected despite this drawback in order to satisfy the operational requirement of creating a full scale 177 Lton vessel with pod diameters of 7-8 feet. These criteria could not be satisfied with a series 58 hull with a L/D of 6-8.

A trait of the Series 58 hullforms is that they have no parallel midbody. Although hydrodynamically this is superior, it would significantly complicate the building of the full scale ship. The Model M-2 therefore incorporates a modification to Model 4155 by replacing some of the midships shape with parallel midbody.

The strut offsets utilize a symmetric parabolic leading and trailing edge. The general parameters of this strut are outlined in Chapter 2-5 but are also constrained by the design requirement that the full scale maximum beam must be at least 3.25 feet. The calculations used to develop the strut and pod offsets and a table of the actual

---

[17] Gertler, M. "Resistance Experiments on a Systematic Series of Streamlined Bodies of Revolution for Application to the Design of High Speed Submarines", David Taylor Model Basin Report C-297. unclassified and approved for public release 18 Dec 1972, April 1950.

offsets used are contained in Appendix C.

Model M-2 represents a partial optimization. The offsets for the struts and pods are based on research conducted in optimizing these types of shapes. The optimized values are then adjusted to conform to design requirements. Model M-2 make no attempt to optimize the placement of the strut pod combinations relative to one another. Table 3-2 provides the principle dimensions of Model M-2. Profile and top view sketches of a the forward and aft strut/pod combinations are at Figure 3-2. This model was constructed with 30 lbf of reserve buoyancy. The struts are manufactured from balsa wood with a fiberglass shell, the pods are molded fiberglass.

MODEL M-3 OPTIMIZED HIGH SPEED SWATH:

The purpose of this model is to compare SLICE performance to a more conventional SWATH. The offsets used for the high speed SWATH were reported by McGregor[18]. The demihull diameter was forced to meet the 7-8 foot full scale requirement, the strut maximum beam was forced to meet the 3.25 foot full scale requirement and the overall displacement was forced to meet the 177 Lton full scale requirement established earlier. In order to meet these requirements, the demihull L/D was established at 12.86. This corresponds to a full scale demihull length of 90 feet, about 15 feet shorter than the Length Overall (LOA) of the proposed ATD SLICE. The consequence of this is that although Model M-3 is hydrodynamically equivalent to Model M-1, depending on the extent to which the box structure is cantilevered forward and aft of the struts, the SWATH will end up with as much as 600 square feet less arrangable deck space. This is an 11% decrease from the SLICE ATD vessel.

A tandem strut arrangement was selected in order to minimize the displacement occupied by the struts. This was necessary in order to maximize the demihull displacement and maintain a reasonable demihull length. As with model M-2, the

---

[18] McGregor, R.C. and Chun, H.H., "On the Potential of SWATH Ships for Very High Speed Operation", Fast 91, pp. 491-506.

strut offsets are based on the guidance provided in Chapter 2-5. In his SWATH design, McGregor provided guidance for the optimum placement of the struts in relation to the pods. This placement was utilized in Model M-3. The calculations used to develop the strut and pod offsets and a table of offsets are contained in Appendix D. Table 3-3 provides the principle dimensions of Model M-3. A profile and top view sketch of a the demihull is at Figure 3-3. The struts of this model are manufactured from balsa wood with a fiberglass shell, the demihulls are hollowed PVC rod, shaped to the proper offsets. There is 10 lbf of reserve buoyancy.

The reason the three models were not all built to the same scale factor stems from the actual building process. There is a slight variation in the full scale diameter of the three underwater hull diameters. In full scale, M-1 is 8 feet, M-2 is 7.74 feet and M-3 is 7 feet. PVC pipe was used to mold parallel midbody sections. This material is relatively inexpensive and comes in a standard pipe outer diameter dimension of 5.5625 inches. This dimension became the driver for determining the model scale factor. Since the three models have different full scale diameters, the scale factors vary accordingly.

Scale Factor	16.68:1
Displacement	83.3 lbf
Beam	37.41 inches
Draft	8.63 inches
Pod Diameter	5.5625 inches
Fwd Pod Length	27.8 inches
Aft Pod Length	27.8 inches
Fwd Pod Separation (CL to CL)	24.17 inches
Aft Pod Separation (CL to CL)	36.26 inches
Strut Length	17.25 inches
Strut Max Beam	2.34 inches

**Table 3-2: Model M-2 Modified Baseline
Principle Dimensions**
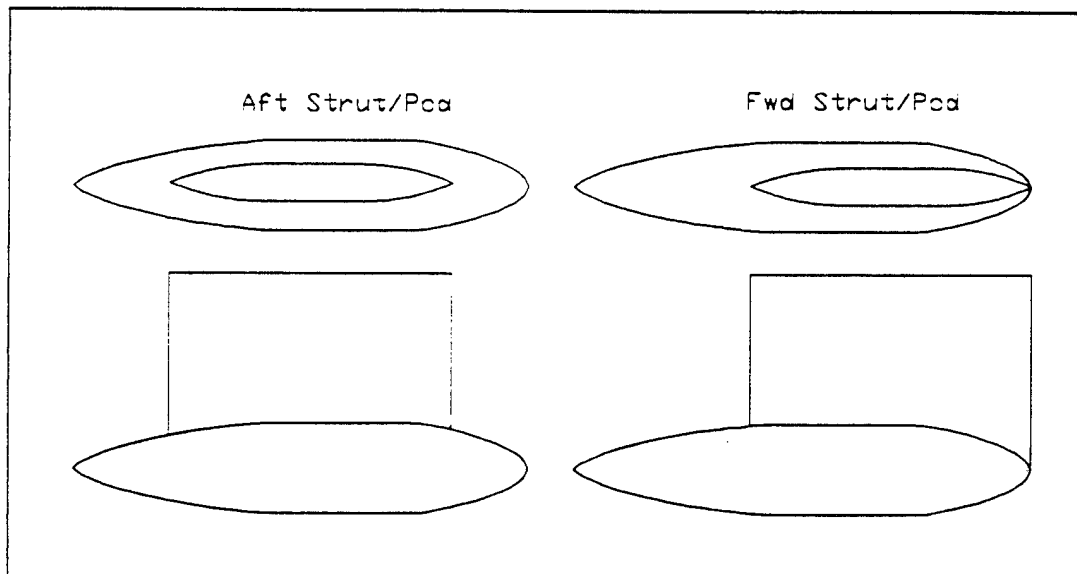
Figure 3-2: Model M-2 Forward and Aft Strut/Pod
(Note: In this drawing the fwd-aft pod spacing is not preserved)

40

Scale Factor	15.10:1
Displacement	115.1 lbf
Beam	39.93 inches
Draft	11.13 inches
Demihull Diameter	5.5625 inches
Demihull Length	71.5 inches
Strut Length	19.10 inches
Strut Max Beam	2.58 inches

Table 3-3: Model M-3 McGregor's High Speed SWATH Principle Dimensions
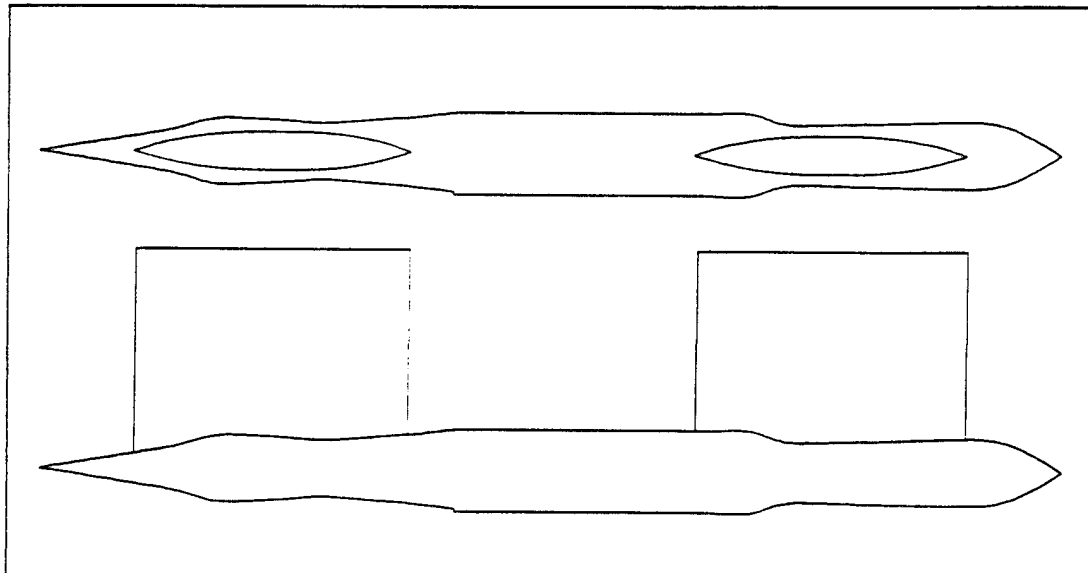
Figure 3-3: Model M-3 Demihull and Strut

3.3 Test Description

A copy of the test plan developed for the Naval Academy Tow Tank tests is included as Appendix E. This enclosure explains the planned tests in detail.

Two basic tests were planned for the models. The first measures resistance and lift with the models fixed in pitch and heave. This test replicates the test configuration used by LMSC thereby allowing for correlation with the LMSC data. Data collection runs consisted of the model held at its design draft with no trim. At the slow end of the speed spectrum, one speed change was allowed during data collection. At higher speeds only one speed was used per test run. Data was collected at full scale equivalent speeds from 3-40 knots with the following model configurations:

1) Model M-1 Baseline in the LMSC configuration.
2) Model M-1 Baseline with the forward and aft struts in line.
3) Model M-1 Baseline in the LMSC configuration at varying drafts.
4) Model M-2 Modified Baseline in the LMSC configuration.
5) Model M-3 McGregor's SWATH.

The second test, quasi free in heave, was not conducted. The intent of this test was to replicate the effects of control surfaces through a counterweight system with the hope that information could be gained regarding the necessary sensitivity of the control system. Conceptually, the counterweight would provide the same lift as the control surfaces without added model building complexity. The model would then be free to respond to small perturbations and its stability qualitatively assessed. This test was considered a second priority to the project and time in the test facility ran out before it could be accomplished. It is considered a worthwhile area of further study.

The test plan indicates that a fourth model, the Midfoil, was tested. This model was built and tested at the request of ONR but is not considered part of this research. It is not reported in this thesis.

3.4 Physical Observations

The importance of observing the behavior of the models can not be overstated. A videotape of the model tests is included as part of this thesis. Shown in the tape is a port beam perspective, both above and underwater as well as a stern view of all the models tested. The video is organized by speed increment, showing each model first at the peak of the wave making hump (10 and 12 knot full scale equivalent) then in the post hump valley (16 knot full scale equivalent) and finally at three high speed increments (25, 30 and 35 knot full scale equivalents). The following qualitative observations are made regarding the performance of the models.

PROPELLER SUBMERGENCE

The ATD vessel will have propellers mounted on the aft end of the forward pods. After the August LMSC model tests, there was significant concern that the wave system created in the hump was large enough to expose the propeller. This evaluation was made by observing the wake from above the free surface but was difficult to assess properly due to spray and distortion. With M-1, the underwater camera used in this project reveals that there is better submergence at the propeller than apparent when viewed from above.

HUMP SPEED PERFORMANCE

It was expected that M-2 with its finer lines would exhibit less wave making than the very bluff M-1 in the hump speed range. In fact, the surprising result was that the wakes produced were nearly identical. The wake of M-3 at the same speed was much smaller than either M-1 or M-2. The implications of this observation are unclear without examining actual data. The similarity between the M-1 and M-2 wakes would suggest that the form of the bodies, both strut and pod, is not a controlling factor in hump speed resistance. The vast difference between M-1/M-2 and M-3 suggests that the underwater body plays a role in wave cancellation.

The correct conclusion may simply be that this is a demonstration of the flow differences of bluff bodies (M-1 L/D = 4.2, M-2 L/D = 5.0) and more slender bodies

(M-3 L/D = 12.9) or there may be some more complicated mechanism of wave cancellation that needs to be explored.

HIGH SPEED PERFORMANCE

In the full scale range of 25-40 knots, there is a significant difference in the performance of M-1 and M-2. At these speeds, M-1 creates a very large vortex at the aft intersection of the strut and the pod. Above the surface, this is manifest as a rooster tail. As the speed increases, the inception point of this vortex travels further aft along the pod tail and at the full scale equivalent of 40 knots almost reaches the end of the pod. This effect is absent in M-2 and M-3.

This effect does not appear to be caused by the relatively small scale of the models. Reviewing footage of the LMSC tests, the same phenomenon is apparent. It is more pronounced in the August tests than the December tests, but it is difficult to tell if that can be attributed to the design changes LMSC made. There is not enough quality video footage of the December tests to draw this conclusion. It is possible that the August and December tests did not allow a full steady state condition to be established. In both the August and December tests, speed increments were maintained on average for 10 seconds measured from the start of a speed change to the start of the subsequent speed change. As observed in the March tests, this amount of time is barely adequate to establish steady state conditions. When accelerated from rest, the March data shows that forces did not stabilize until 8-10 seconds after the steady state speed was achieved. The LMSC testing may have stabilized sooner since the acceleration was only between speed increments and not from rest. Nonetheless, the data collection period was extremely short. The inception speed of the rooster tail appears to be comparable in both the LMSC tests and this project's tests. This indicates that the effect follows Froude scaling.

After the August LMSC tests, much attention was focused on scaling spray effects. This was in response to the extreme wake created at high speed. LMSC's position was that spray effects could be ignored in full scale predictions and designed out using spray rails. The underwater observation of M-1 demonstrates that much of

what was called spray in August was actually produced by an entirely different mechanism. The vortex that creates the rooster tail is a separation effect created as the flow unsuccessfully attempts to conform to the hullform. When M-1, M-2 and M-3 are compared at the same speed, it becomes obvious that only a very little of the splashing seen above the surface in M-1 can be attributed to spray generated by the struts. The majority of the splashing effect is more accurately accounted for as a by-product of eddy resistance.

WAKE CHARACTERISTICS

The wake produced by the SLICE hullform is compact and has a greater amplitude than that of the SWATH. The SWATH produces a relatively flat but significantly longer wake. From an energy in the water standpoint, comparison becomes difficult since the entire volume of the wake must be considered.

3.5 Test Data

Raw data collected during the testing is presented in Appendix F. Test 1 results (fixed in pitch and heave measurements of drag and lift) are presented graphically in. Drag (positive x) is taken to be opposite the direction of forward motion. Sinkage (positive z) is down from the free surface. Several speed settings were repeated during the testing. Repeated speeds are recorded in these figures and are designated Dual Point (DP). No direct comparison of performance using Figures (3-4) - (3-6)should be done since each model is built to a slightly different scale factor .

Figures (3-7) and (3-8) present model scale data at the same scale factor. This required scaling M-2 and M-3 data to the M-1 scale. Data scaling was accomplished using the process outlined in Chapter 2-7. Scaling between models was accomplished using the composite scale factors shown:

$$\lambda_2 = \frac{\lambda_{model2}}{\lambda_{model1}} = \frac{16.68}{17.26} = 0.966 \qquad (3-1)$$

$$\lambda_3 = \frac{\lambda_{model3}}{\lambda_{model1}} = \frac{15.10}{17.26} = 0.875 \qquad (3-2)$$

The calculations used in this process are in Appendix G.

Figure (3-9) shows the data collected for Model M-1 tested in both the Baseline configuration and an in-line configuration of the forward and aft strut/pod groups. The results of testing Model M-1 at varying depths was inconclusive. Insufficient data was collected to develop a trend.
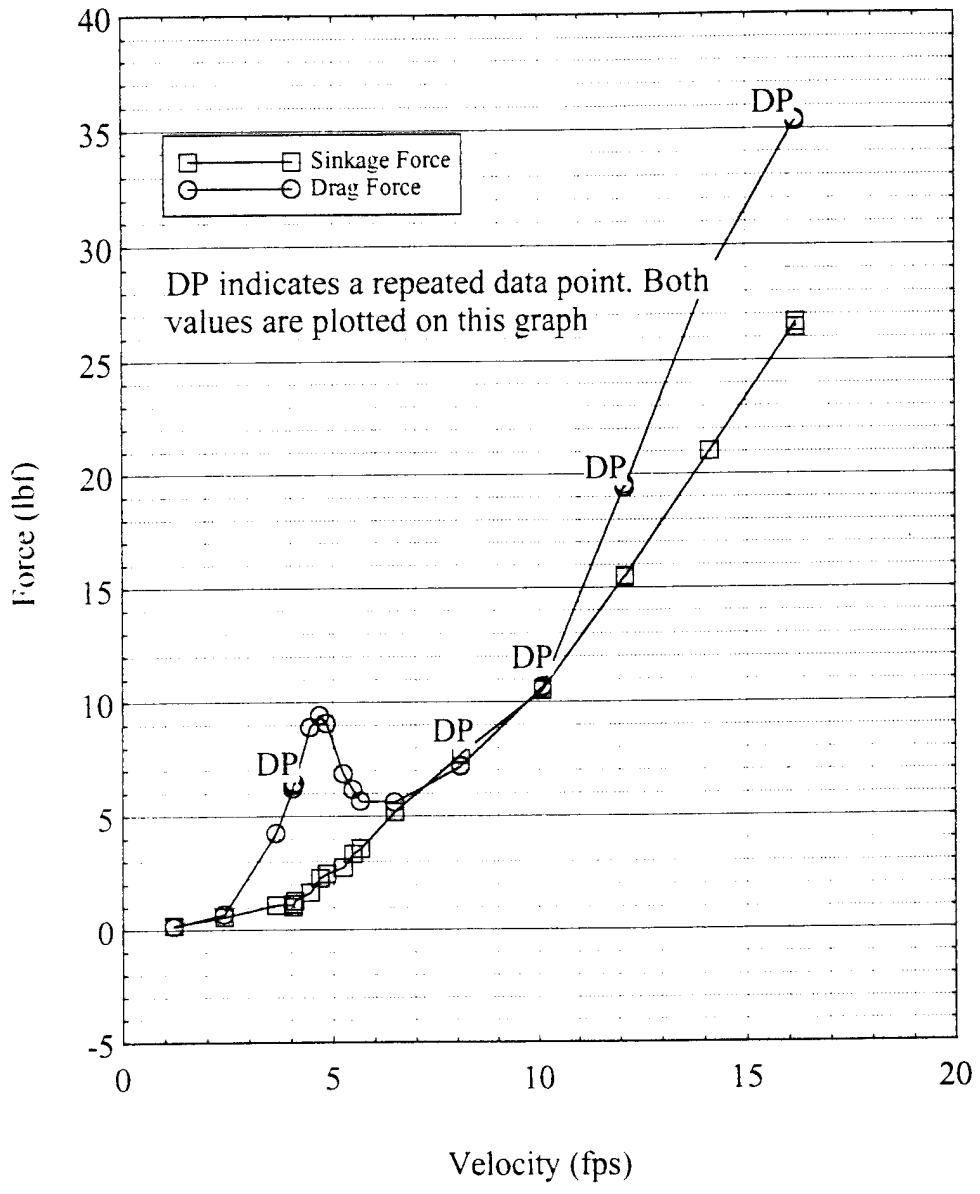
Figure 3-4: Model M-1 Fixed in Pitch and Heave
Unscaled Data
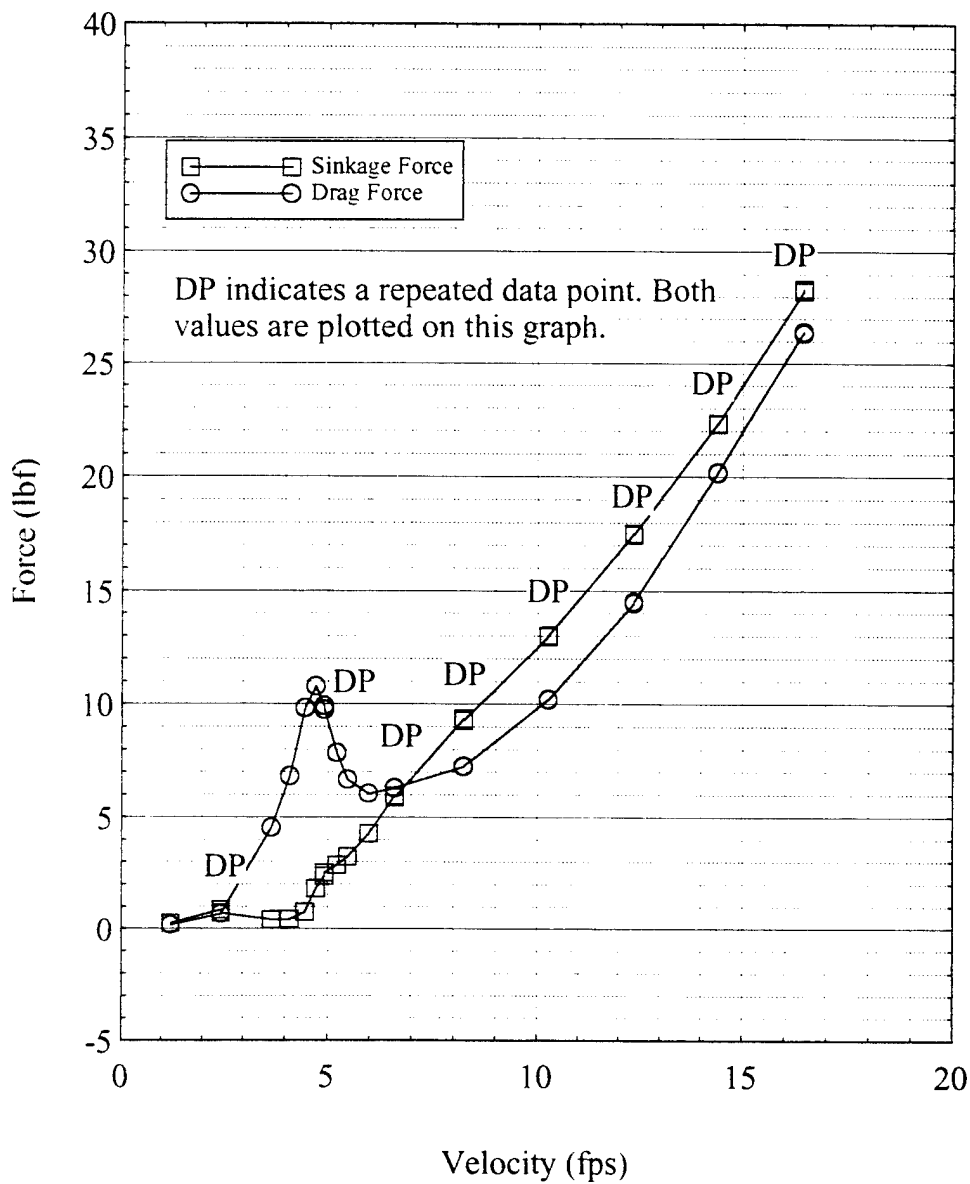
**Figure 3-5: Model M-2 Fixed in Pitch and Heave
Unscaled Data**
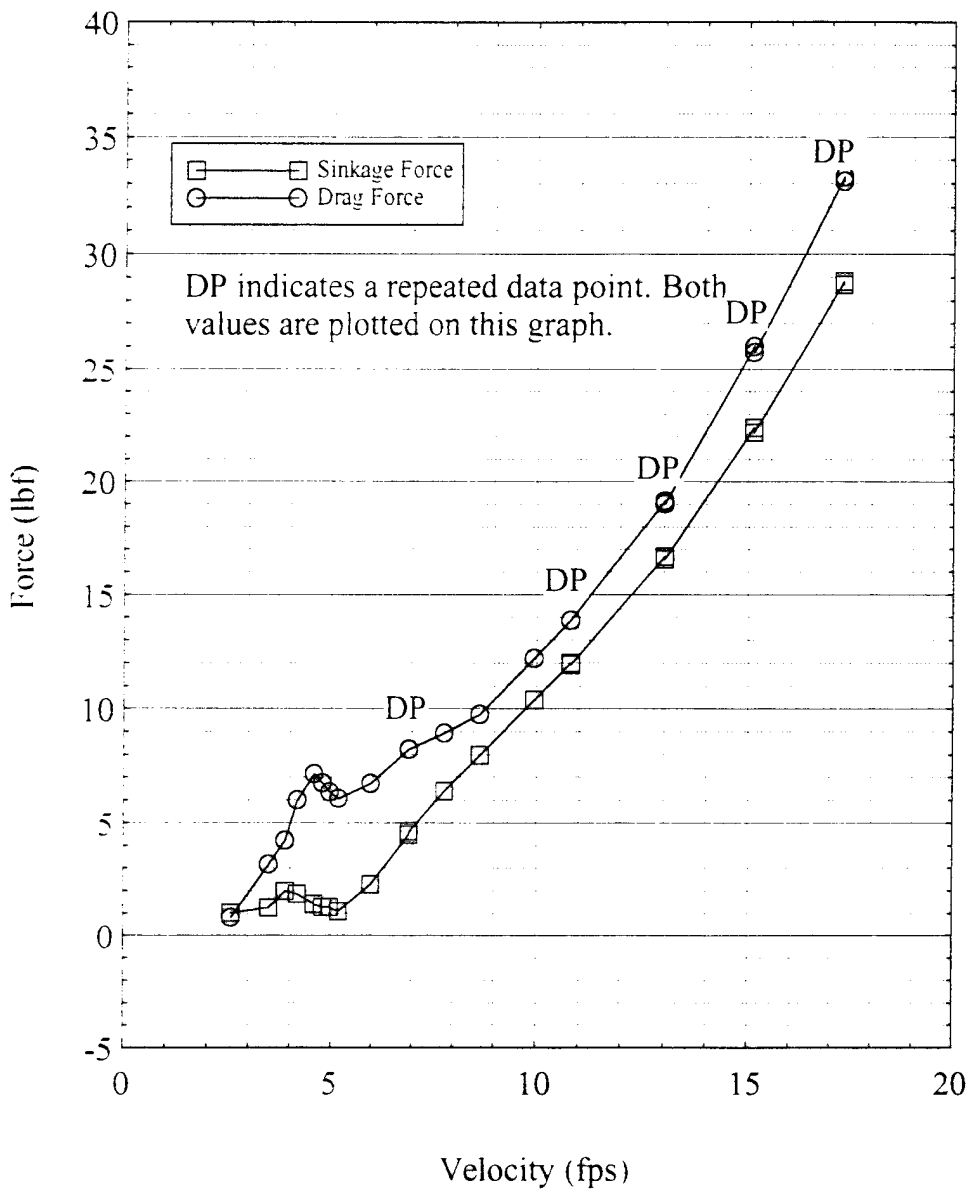
**Figure 3-6: Model M-3 Fixed in Pitch and Heave
Unscaled Data**

data at 17.26:1 scale
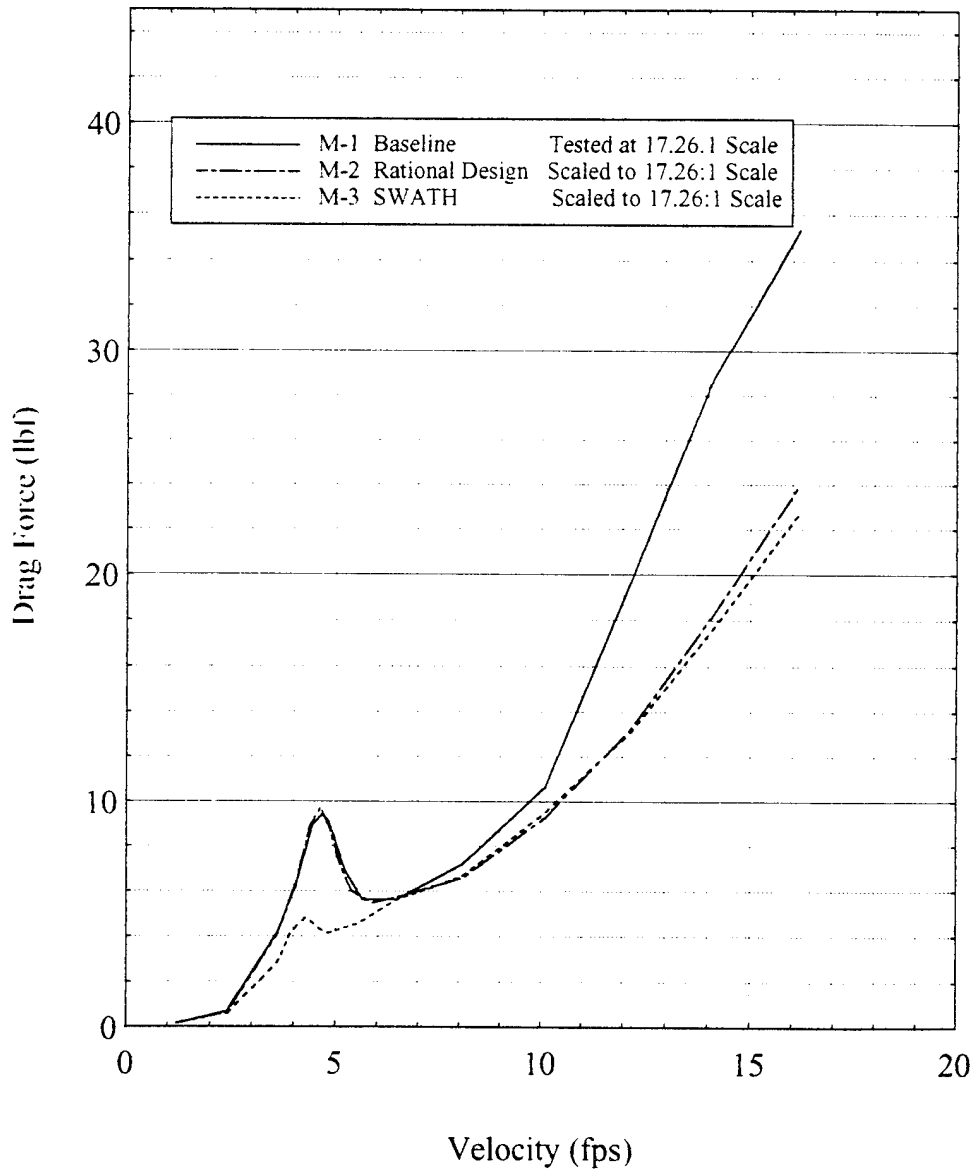
Figure 3-7: Models M-1/M-2 and M-3 Fixed in Pitch and Heave Data Presented in 17.26:1 Scale

data at 17.26:1 scale
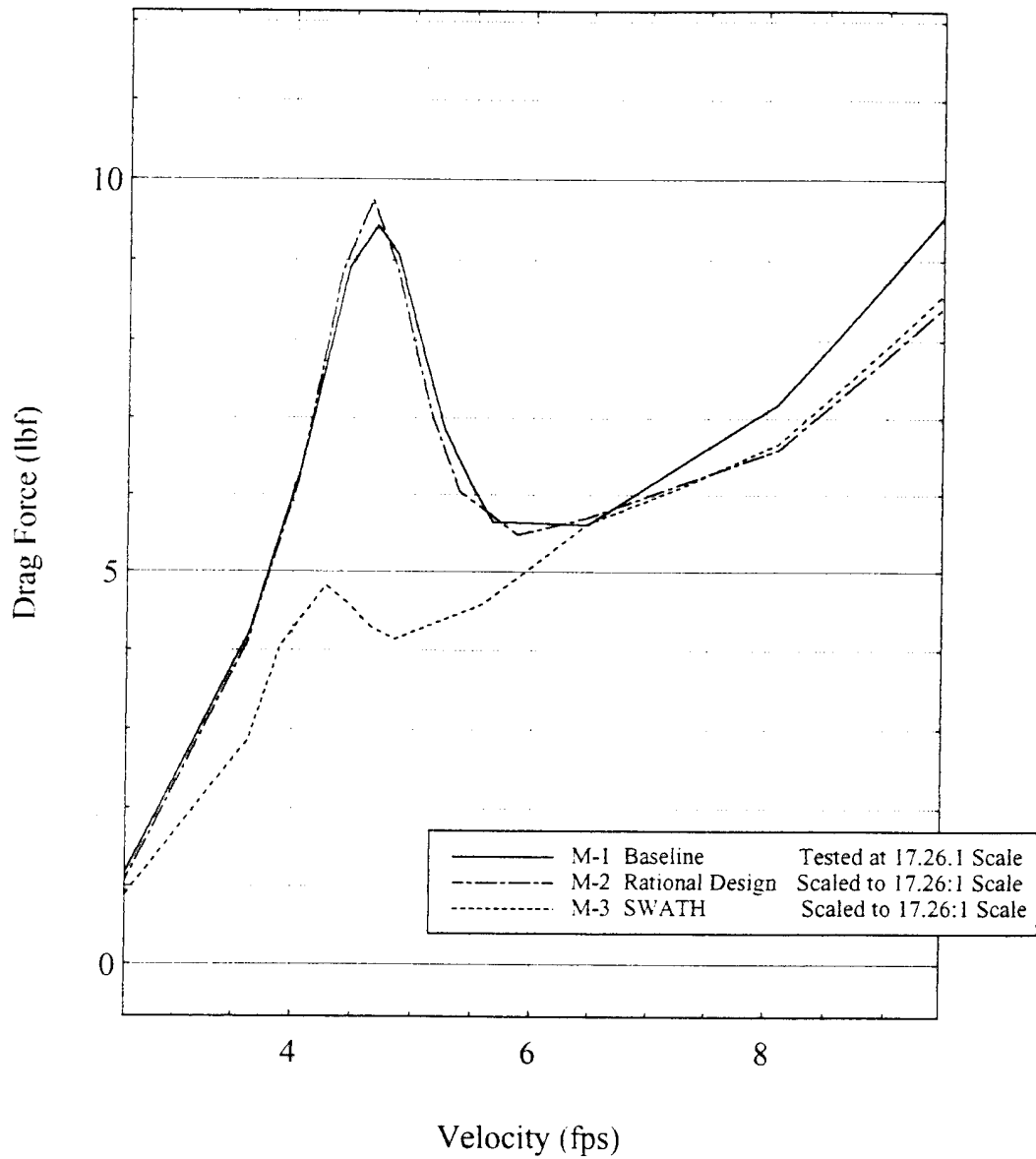
Figure 3-8: Models M-1/M-2 and M-3 Fixed in Pitch and Heave
Data Presented in 17.26:1 Scale
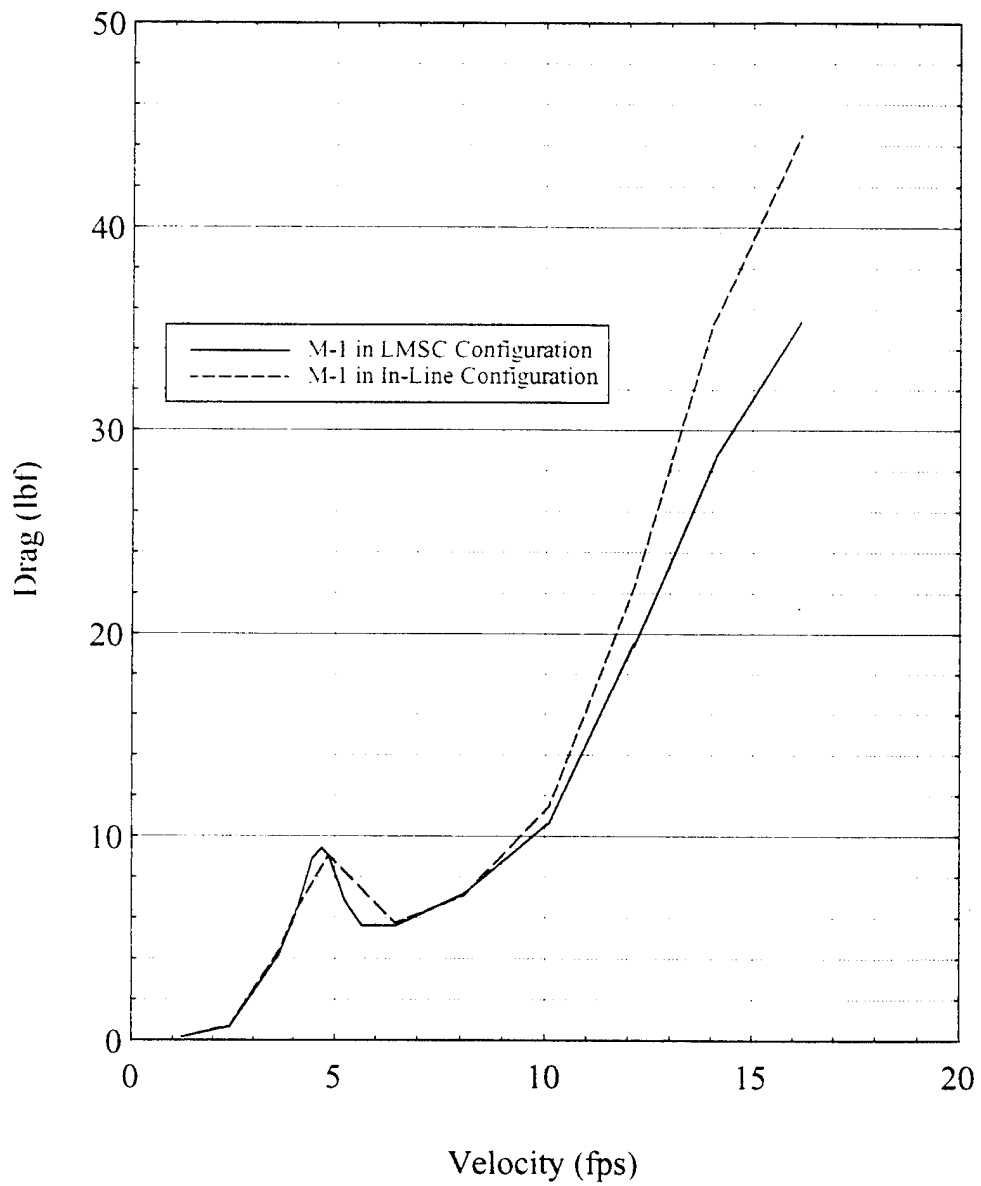
**Figure 3-9: Models M-1 Fixed in Pitch and Heave
Tested in the Baseline and In-Line Configurations
Data Presented in 17.26:1 Scale**

Several comments can be made about this data.

REPEATABILITY OF RESULTS

A large number of data points were repeated through the course of the testing. Without exception, the difference in recorded data is statistically insignificant. Most repeated data was recorded in successive runs down the tank. A notable exception to this are runs 70 and 71 in Appendix F. In this case, testing of Model M-1 was completed, Model M-2 and Model M-3 were tested, then Model M-1 was remounted and realigned on the carriage and five data points collected. There was excellent correlation between these points and data collected two days earlier.

HUMP SPEED MODEL PERFORMANCE

The resistance values for M-1 and M-2 through the hump, Figure 3-7, support the observation made earlier that the wakes are very similar. The similarity in resistance values was an unanticipated result. M-2 represents the extent to which L/D can be extended and still retain the features of SLICE. Since this variation was insufficient to impact the amplitude of the hump, the only other alternative for diminishing the hump magnitude is altering the relative position of struts and pods.

The fact that the hump for M-1, M-2 and M-3 all occur at essentially the same speed indicates that the Strut Length is the appropriate length to characterize SLICE. This conclusion is reached by considering M-3 in contrast to M-1 and M-2. The hump is expected to occur at $\mathscr{F}= 0.45$. For the demihull of M-3 this corresponds to V= 6.25 fps. for the struts it corresponds to V= 3.2 fps. The hump actually occurs at V=4.5,

demonstrating dominance by the struts. The pods of M-1 and M-2 are less than half the length of M-3's demihulls and yet the hump for all three is at the same speed. The struts for all three models were essentially the same length. The underwater bodies may be contributing to wave making through cancellation effects but the position of the hump is driven by the surface piercing bodies.

HIGH SPEED MODEL PERFORMANCE

In the range 6.5-10 fps (full scale equivalent: 16-25 knots), M-1 total resistance is up to 20% greater than that of M-2 even though M-1 has less wetted surface and therefore less frictional resistance than M-2. This is the first indication that model form must be traded off with friction to optimize post hump resistance.

For speeds greater than 10 fps, the rapid increase in M-1 resistance can be directly correlated with the appearance of the trailing edge vortex noted in the physical observations.

M-1/ LMSC COMPARISON

One test objective for M-1 was to compare M-1 results with the December LMSC model. Figure 3-10 presents the M-1 data as collected as well as a sample of LMSC data from both August and December scaled to 17.26:1. Model M-2 results are also presented scaled accordingly. The August LMSC curve represents LMSC data runs 106-121, The December LMSC curve represents LMSC data runs 86-97. These models were tested with appendages and haunch structures in place.

M-1 correlation with the December tests is good below 8.25 fps (full scale: 20 knots), becomes marginal from 8.25-10 fps (full scale:20-25 knots), and does not exist above this value. M-1 correlation is more satisfactory with the August test results. The lack of high speed correlation requires comment.

Of concern is the vortex created at 10 fps (full scale: 25 knots). The phenomenon is documented as existing in the August and December tests as well as the tests conducted on M-1. The question is deciding if the lack of correlation indicates that effect does not scale, or if there is some other mechanism that is causing the difference. The possibility that the LMSC data may have been obtained before steady state was achieved has already been discussed. Although this is a fault of the LMSC test program, it is difficult to attribute the entire difference in test results on this shortcoming alone.
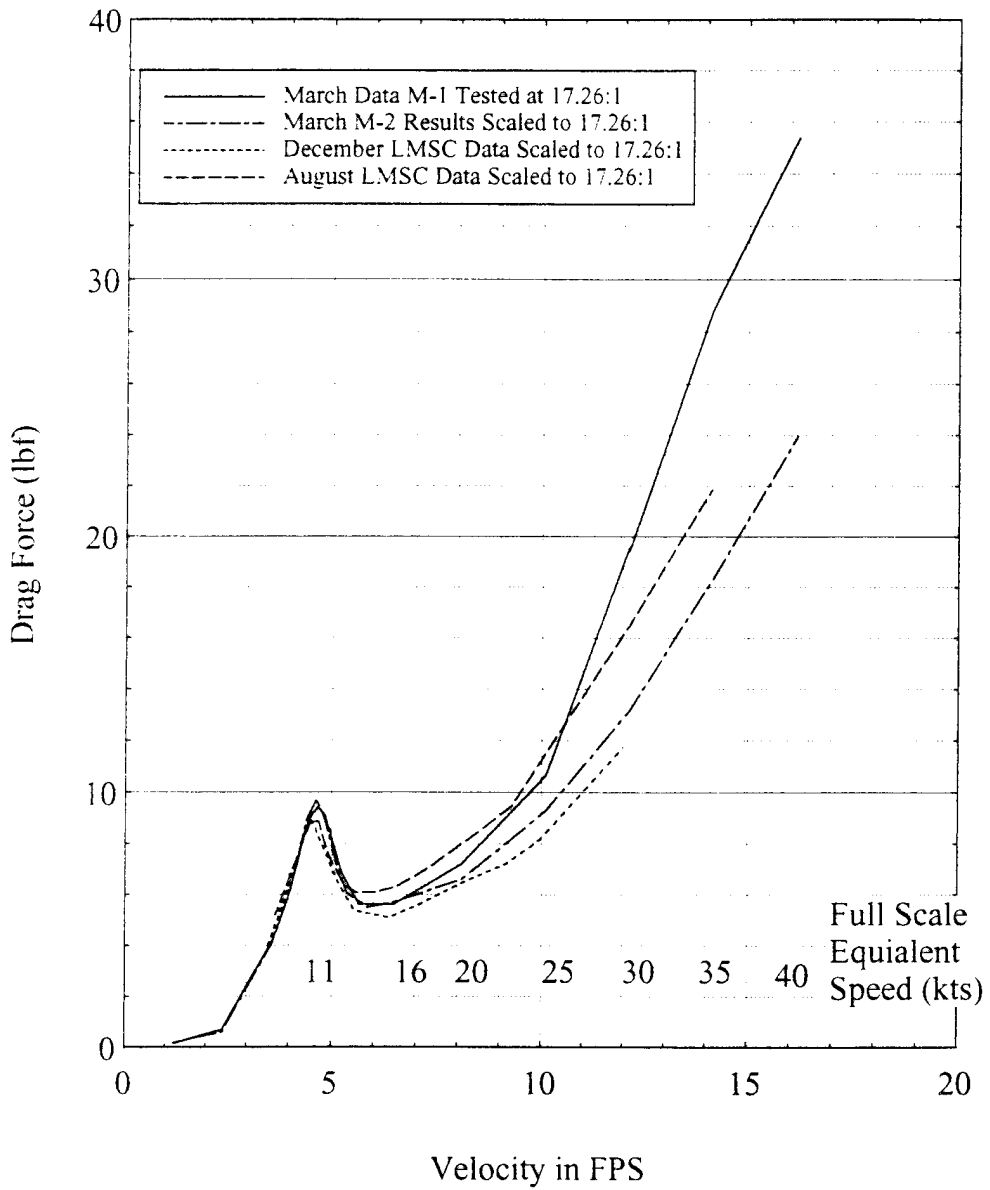
Figure 3-10: Models M-1 Performance Compared With LMSC Results Data Presented in 17.26:1 Scale

In the tests of M-1, there is direct impingement of the rooster tail on the model frame. During the testing, this was considered acceptable for two reasons: 1) Impingement also occurred in the LMSC model tests and will occur in the full scale ship depending on the construction of the box structure. 2) During the testing, the impingement was considered a minor effect since the profile of the frame structure was small (60 in^2 total). Reviewing video footage of these tests, the direction of rooster tail flow was perpendicular to the frame, thereby maximizing the force of impingement. In the LMSC tests impingement was not as direct. Appendix H provides a calculation that demonstrates that impingement could account for up to 11 pounds of the measured force at 15 fps.

There are enough differences in test configurations to preclude a definitive explanation for the lack of correlation. The rooster tail impingement may contribute to the lack of correlation. The conclusion drawn at this point is that the trailing vortex is real and will scale but may not directly contribute to overall resistance to the extent indicated by the Model M-1 results in Figure (3-7). Failure to achieve steady state in the LMSC test may also be a significant factor in this difference. Re-testing M-1 with the frame isolated will help eliminate this ambiguity but ultimately full scale test results are required.

3.6 Full Scale Predictions and Discussion

With the understanding that the M-1 results may over predict full scale resistance, figures (3-11) and (3-12) present full scale data for all three models. Figure (3-13) provides power requirements based on these values. Data scaling was accomplished using the process outlined in Chapter 2-7. The calculations used in this process are at Appendix G. Based on figure (3-11), the high speed SWATH offers the best resistance performance through the entire speed range.

Figures (3-14)- (3-19) present M-1, M-2 and M-3 data in model and full scale, decomposed into the frictional, residuary and correlation factor components. In the post hump region of the resistance curve, residuary (ie wave making) resistance accounts for at least 60% of the total resistance value. This further supports the

concept that the hull form must be designed as a compromise between frictional and wave making resistance, not a single component optimization.

Full scale data
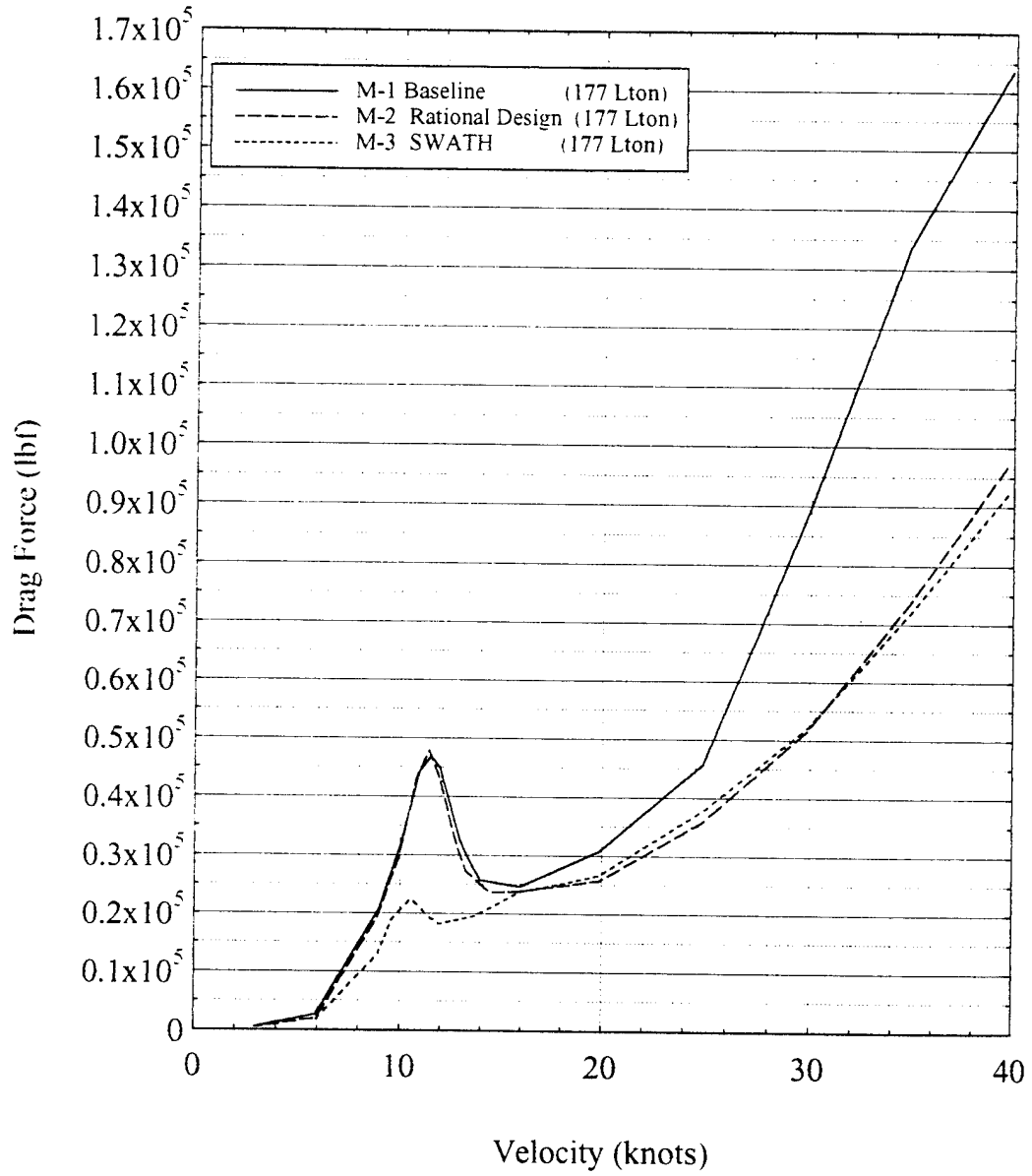
**Figure 3-11: Models M-1/M-2 and M-3 Fixed in Pitch and Heave
Full Scale Resistance Data**

58
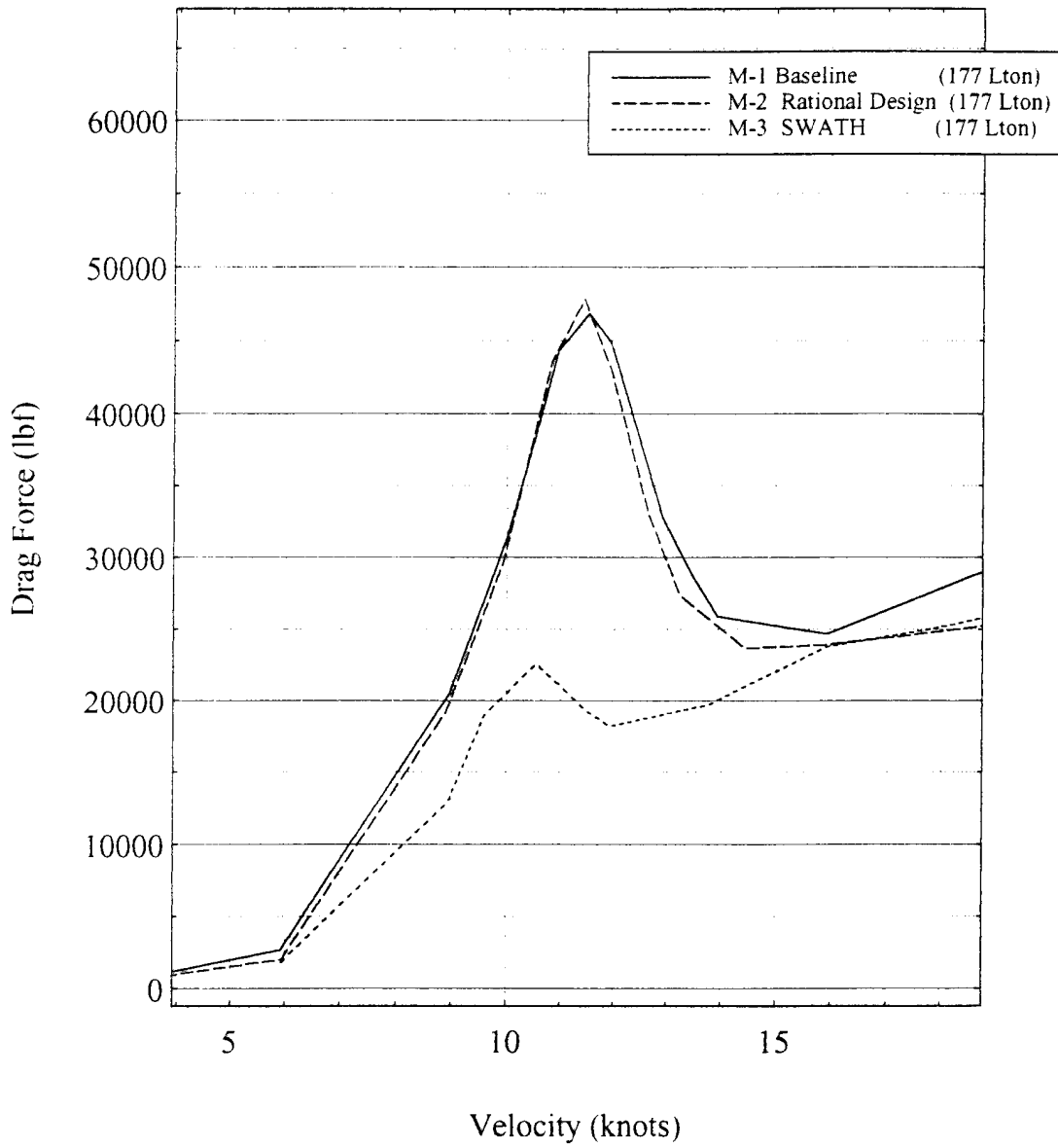
Full scale data

Figure 3-12: Models M-1/M-2 and M-3 Fixed in Pitch and Heave Full Scale Resistance Data
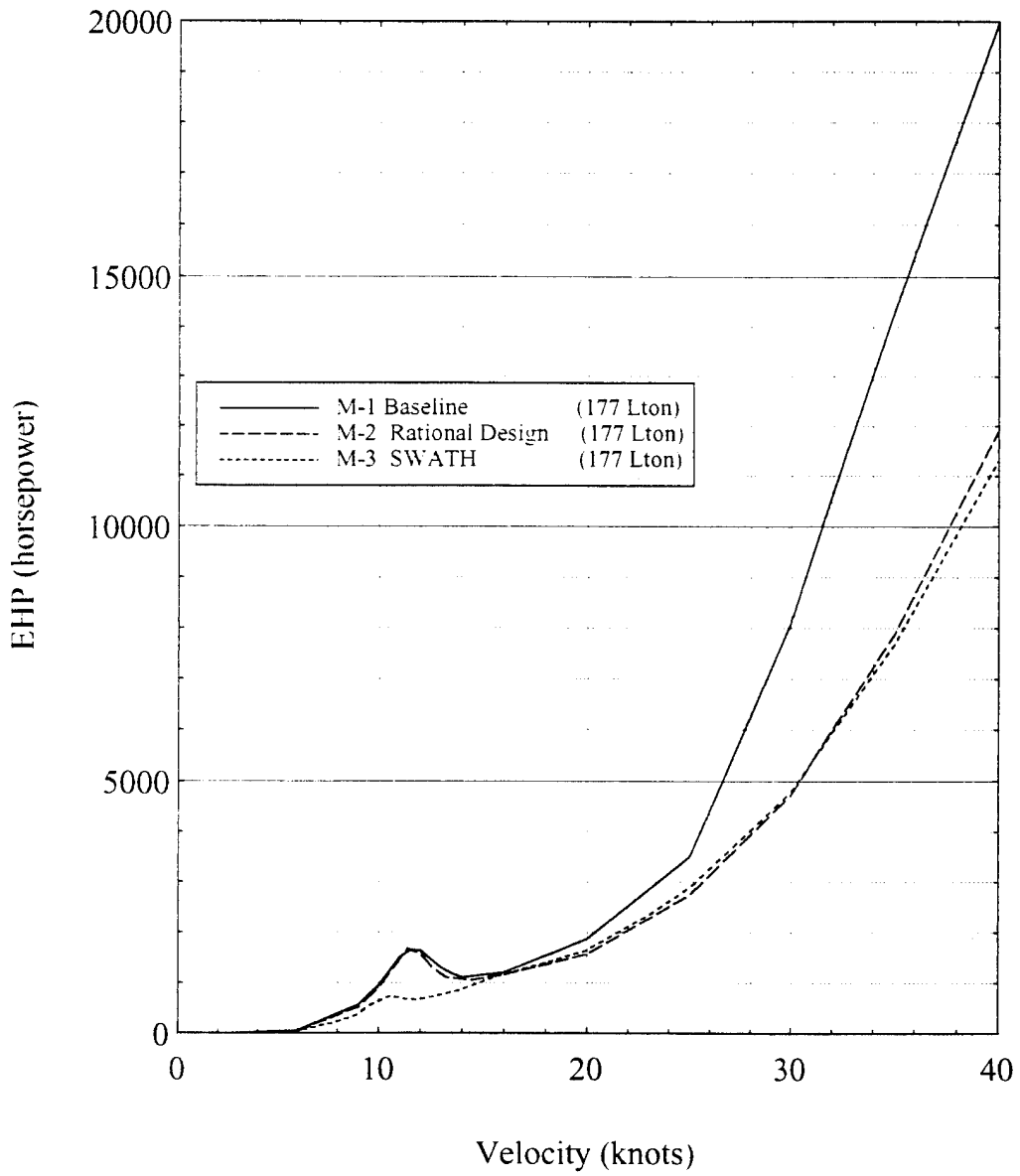
Figure 3-13: Models M-1/M-2 and M-3 Fixed in Pitch and Heave Powering Data
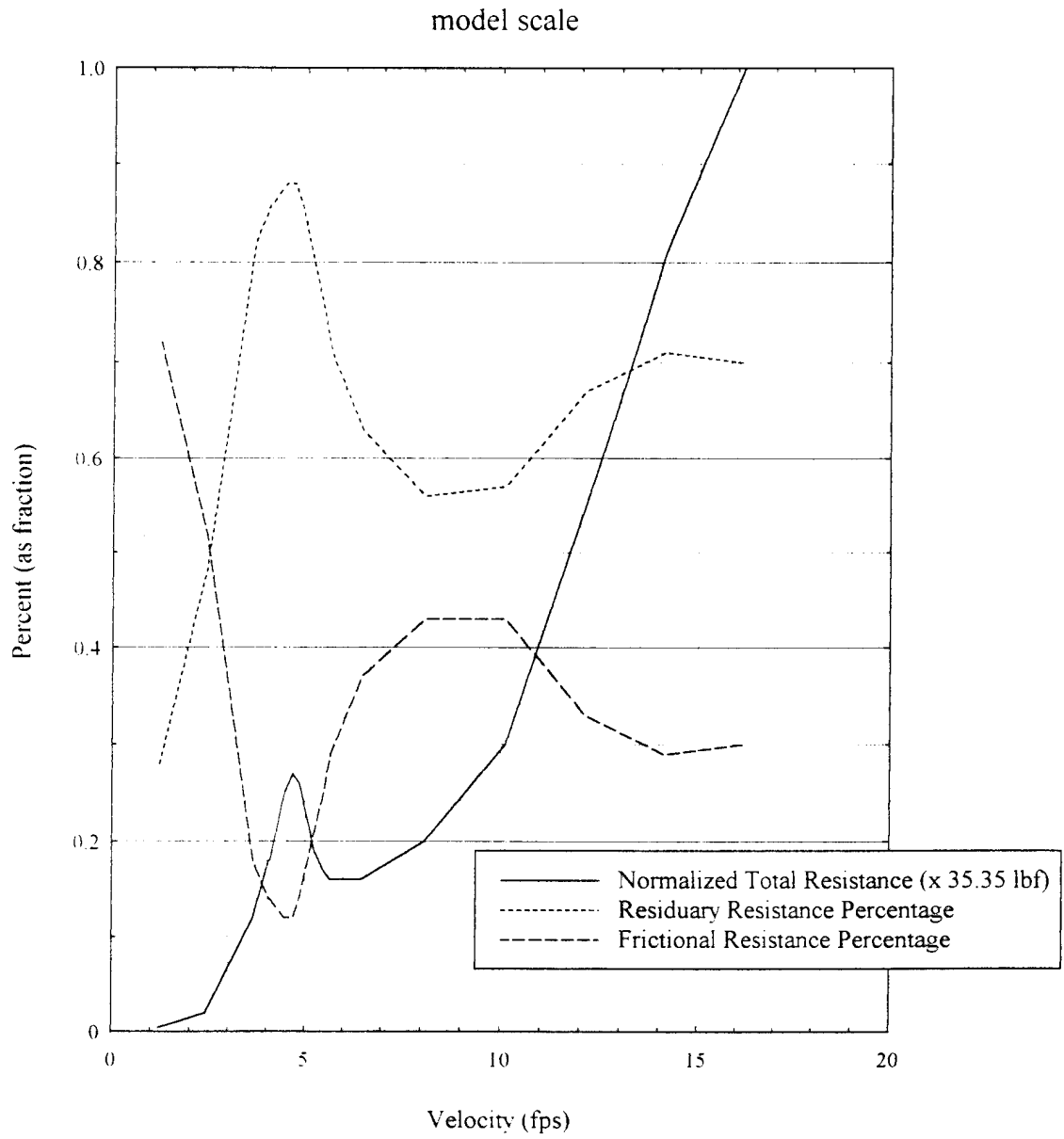
model scale

Figure 3-14: Model M-1 Resistance Components as a Percent of Total Resistance
Derived from Unscaled Test Data
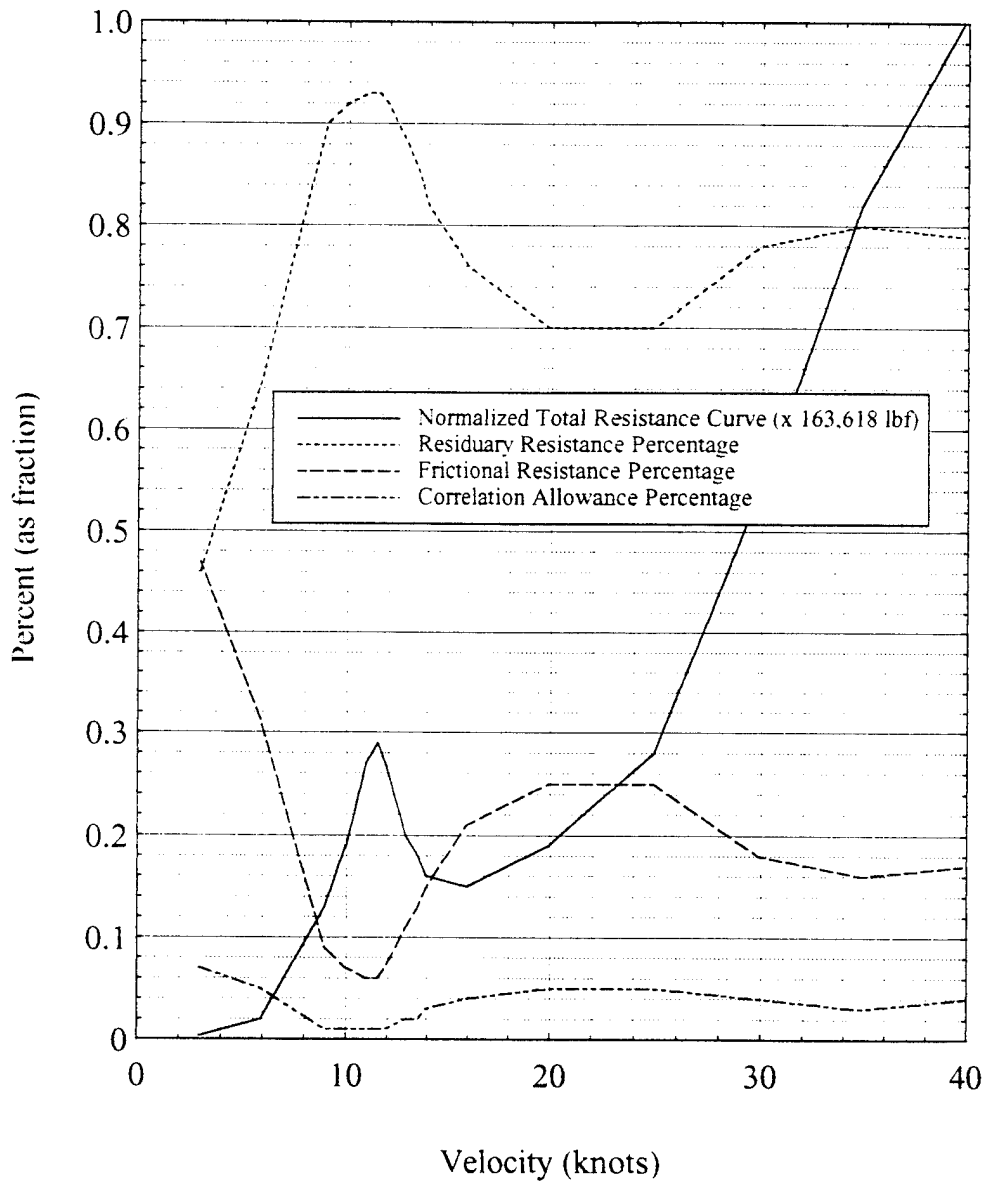
Full scale

Figure 3-15: Model M-1 Resistance Components as a Percent of Total Resistance Based on Full Scale Results

62
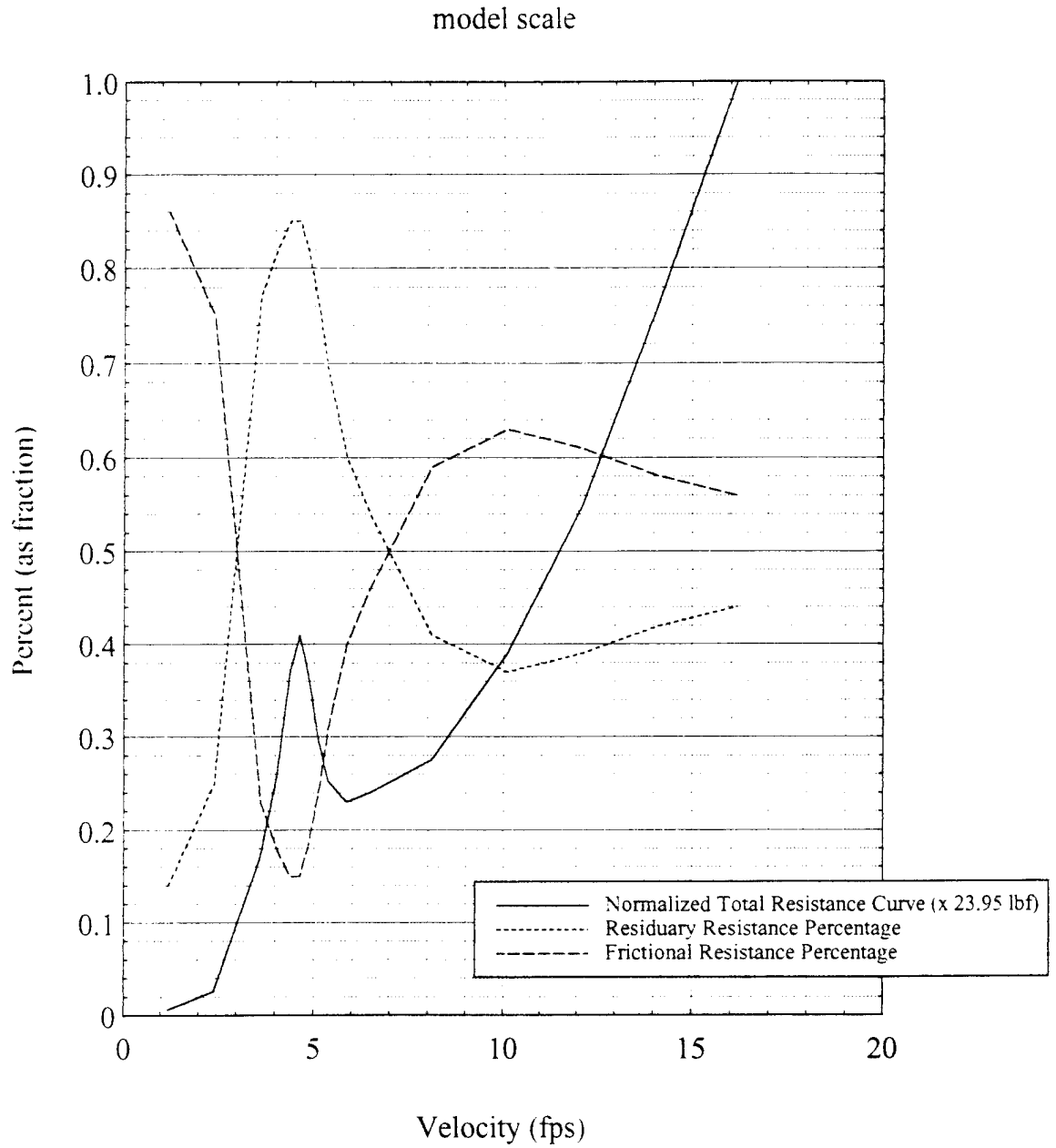
model scale

Figure 3-16: Model M-2 Resistance Components as a Percent of Total Resistance
Derived from Unscaled Test Data
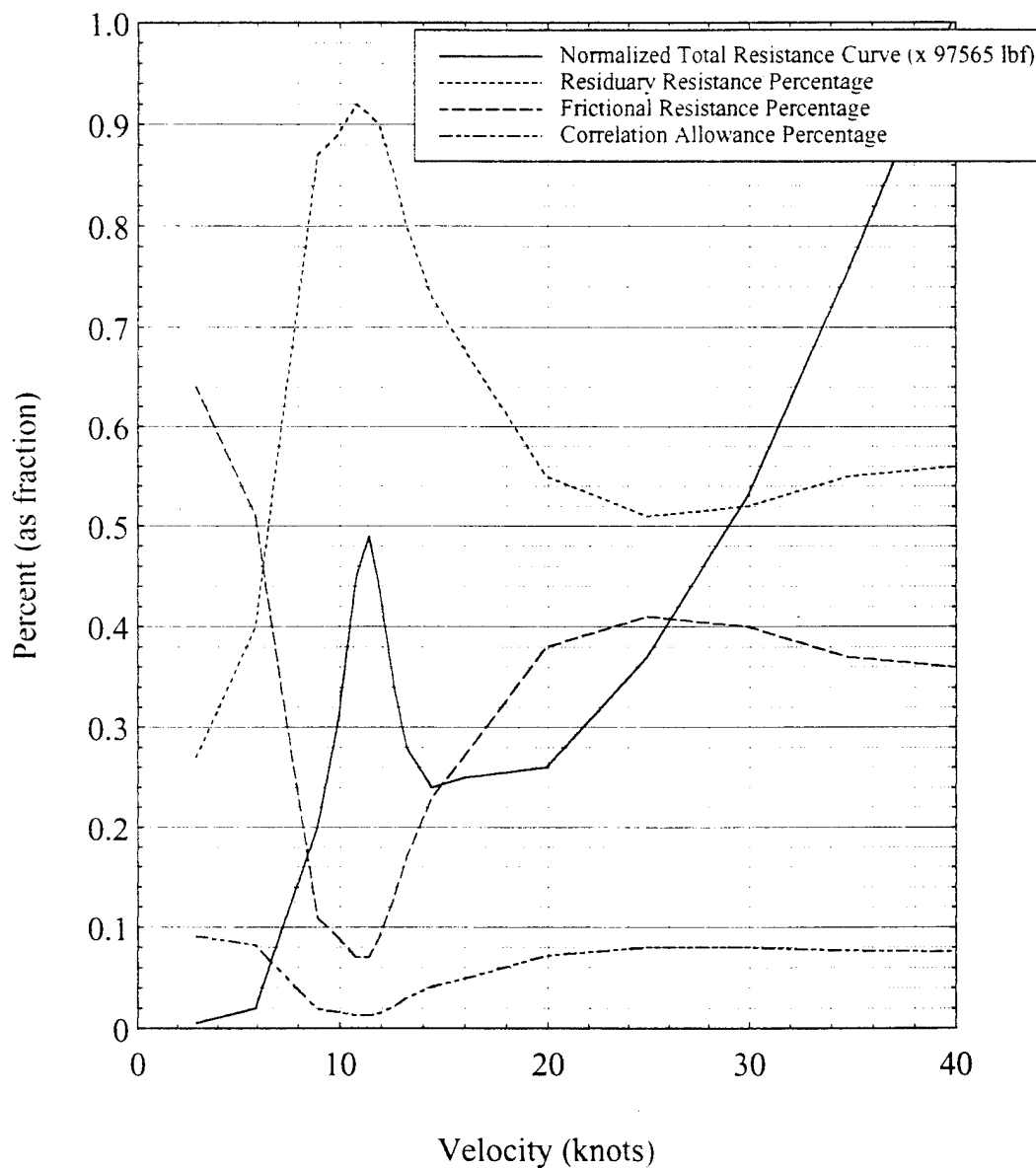
full scale

Figure 3-17: Model M-2 Resistance Components as a Percent of Total Resistance Based on Full Scale Results
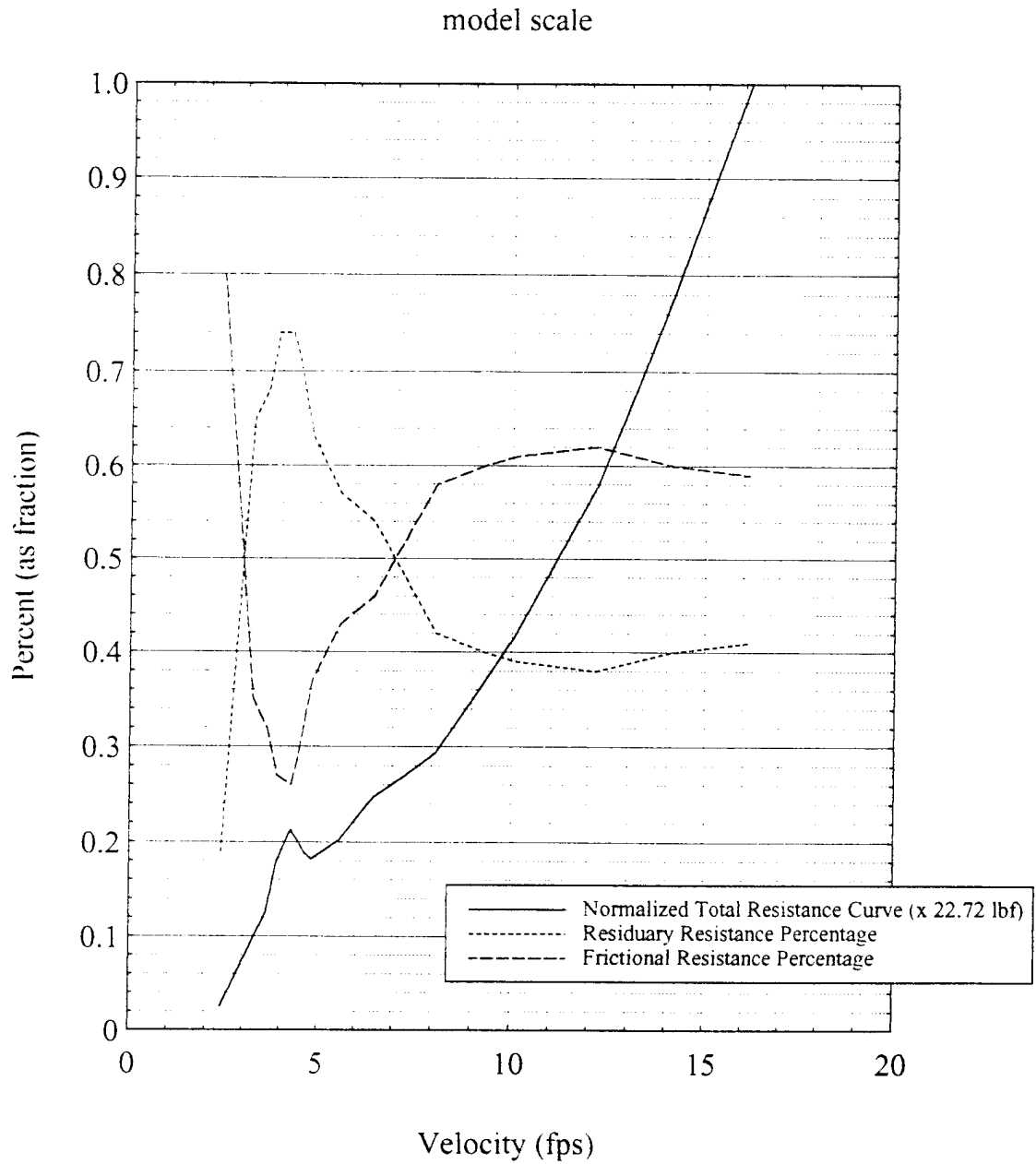
model scale

Figure 3-18: Model M-3 Resistance Components as a Percent of Total Resistance Derived from Unscaled Test Data
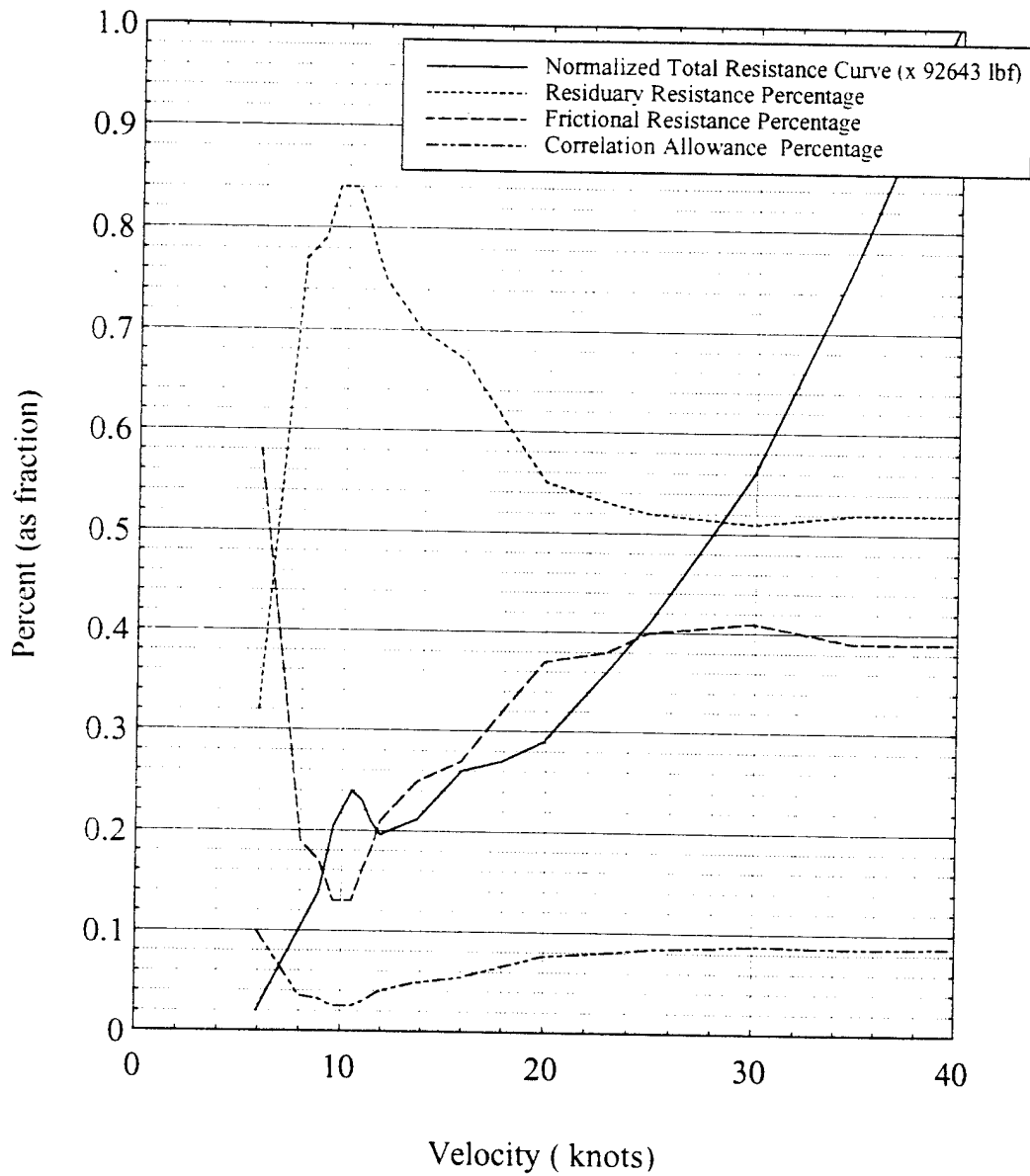
Figure 3-19: Model M-3 Resistance Components as a Percent of Total Resistance Based on Full Scale Results

Chapter 4 Numerical Solution

4.1 Objective of a Numerical Approach

The ability to predict a ship's resistance using numerical methods has many advantages. If an appropriate method can be found, the expense and time of model testing may be reduced. Current state of the science is approaching realistic treatment of the free surface (ie: non linearized theory) but these methods are still too expensive to use as an iterative design tool. Simpler less expensive methods may not be accurate enough to exactly predict resistance but can be extremely useful for comparative analysis of small changes to the same hullform. These methods require tow tank model testing as verification to ensure that all physical phenomena are properly represented.

This thesis attempts to validate the SLICE applicability of a numerical method solution of Mitchell's integral as an approximation for wave resistance. As cited in Chapter 2, the approach first outlined by Lunde, was used by Wilson in the Wave Cancellation Multihull Ship concept. It is not expected that this thin ship approximation will provide exact resistance values. The goal of this chapter is to develop an understanding of the body interactions in the SLICE hullform to assist resistance optimization through body placement. Of specific interest is reducing the magnitude of the wave making hump. The thin ship approach is useful since it allows wave making resistance to be segregated into all component body and interaction terms. This is important while studying the effect of small geometry changes on total resistance.

Model M-2 is selected as the subject for this study. Physical observation during the model tests demonstrate that this model has a reasonable chance of satisfying thin ship flow requirements.

4.2 Solution Technique

Restated from Chapter 2.8, the equation to be solved is:

$$R_{w_{ij}} = 16\pi\rho\kappa^2 \int_0^{\frac{\pi}{2}} (\sum_1^N\sum_1^N P_i P_j + \sum_1^N\sum_1^N Q_i Q_j)\sec^3\theta \, d\theta \tag{4-1}$$

where:

$$P = \int_0^T\int_0^L \sigma(x,z)\cos[\kappa(x\cos\theta + y\sin\theta)\sec^2\theta]e^{\kappa z\sec^2\theta}dxdz \tag{4-1a}$$

$$Q = \int_0^T\int_0^L \sigma(x,z)\sin[\kappa(x\cos\theta + y\sin\theta)\sec^2\theta]e^{\kappa z\sec^2\theta}dxdz \tag{4-1b}$$

$$\sigma = -\frac{V}{2\pi}\frac{\delta}{\delta x}(f(x,z)) \tag{4-1c}$$

$$\kappa = \frac{g}{V^2} \tag{4-1d}$$

The coordinate system that will be used has its origin in the undisturbed free surface with +X in the direction of ship motion, +Z vertically up from the free surface and +Y in accordance with the right hand rule.

DEVELOPMENT OF THE BODY AND POTENTIAL FUNCTIONS

The first requirement is to write a function that describes the strut and pod forms. This function is written with the bodies at the global origin. Later, these bodies will be translated to their actual relative positions through the X, Y and Z terms in

68

Equation (4-1a) and (4-1b).

For M-2, the strut form was developed using an identical parabolic nose and tail shape with parallel midbody in between. The equations used to describe the strut shapes are:

$$NoseOffsets = \frac{B}{2} * [1 - (\frac{L_n - x}{L_n})^{n_{strut}}]$$

(4-2)

$$MidbodyOffsets = \frac{B}{2}$$

(4-3)

$$TailOffsets = \frac{B}{2} * [1 - (\frac{x - L_n - L_{pmb}}{L_t})^{n_{strut}}]$$

(4-4)

where for this specific strut,

B (the maximum beam) = 0.195 ft
L_n (nose length) = L_t (tail length) = 0.51 ft
L_{pmb} (parallel midbody length) = 0.42 ft
n_{strut} = 2.25

To reduce the complexity of the strut body potential function as applied in (4-1a) and (4-1b), the offsets calculated by (4-2), (4-3) and (4-4) were curve fit to a single high order polynomial given by:

$$Strut = 0.4893 * x^6 + 2.1126 * x^5 + 3.1328 * x^4 + 1.7248 * x^3 - 0.0786 * x^2 - 0.3890 * x + 0.0008$$

(4-5)

The source distribution representing the strut is written as:

$$\sigma_{strut} = -\frac{V}{2\pi} * (2.936 * x^5 + 10.563 * x^4 + 12.531 * x^3 + 5.174 * x^2 - 0.1572 * x - 0.389)$$

The pod shapes are created in a similar fashion. Now however, the nose is represented by an ellipse and the tail by a parabola. The pod offsets are given by the following:

$$PodNose = \frac{D}{2} * [1 - (\frac{L_n - x}{L_n})^{n_{nose}}]^{\frac{1}{n_{nose}}} \tag{4-7}$$

$$PodMidbody = \frac{D}{2} \tag{4-8}$$

$$PodTail = \frac{D}{2} * [1 - (\frac{x - L_n - L_{pmb}}{L_t})^{n_{tail}}] \tag{4-9}$$

where for this specific pod,

> D (the maximum diameter) = 0.4635 ft
> L_n (nose length) = 0.67 ft
> L_t (tail length) = 1.1 ft
> L_{pmb} (parallel midbody length) = 0.60 ft
> n_{nose} = 2.00
> n_{tail} = 2.40

Again a single high order polynomial was generated to represent the pod and is given by:

$$Pod = -0.04 * x^7 - 0.32 * x^6 - 1.16 * x^5 - 2.37 * x^4 - 2.96 * x^3 - 2.27 * x^2 - 0.99 * x + 0.038$$

The source distribution representing the pod is written as:

$$\sigma_{pod} = -\frac{V}{2\pi} * (-0.253 * x^6 - 1.93 * x^5 - 5.82 * x^4 - 9.49 * x^3 - 8.88 * x^2 - 4.54 * x - 0.99$$

The pods are treated as a line source in (4-1a) and (4-1b) by fixing the z term in the exponential as a constant equal to the strut depth plus the maximum radius of the pod. This follows the example provided by Chapman[19] for dealing with submerged bodies of revolution.

PAIRING OF TERMS

Struts and pods are numbered in the traditional naval manner. The scheme is presented in Figure (4-1). There are a total of 36 possible combinations of the eight bodies that form the SLICE hull. Eight combinations are "like" or body terms and 28 combinations are different or "cross product" terms. These terms are presented below grouped by relative position in the hull. The numbers indicate which bodies are interacting in the term calculated:

1) Body Terms:

1-1, 2-2, 3-3, 4-4, 5-5, 6-6, 7-7, 8-8

2) Same Corner Cross Terms:

[19] Chapman, R.B., Hydrodynamic Drag of Semisubmerged Ships, American Society of Mechanical Engineers, paper number 72-Wa, 1972, pp 879-884.

1-5, 2-6, 3-7, 4-8

3) Longitudinal Cross Terms:

1-3, 1-7, 5-3, 5-7, 2-4, 2-8, 6-4, 6-8

4) Diagonal Cross Terms:

1-4, 1-8, 5-4, 5-8, 2-3, 2-7, 6-3, 6-7

5) Transverse Cross Terms:

1-2, 1-6, 5-2, 5-6, 3-4, 3-8, 7-4, 7-8

This physical grouping is retained through the calculations to simplify comparisons.
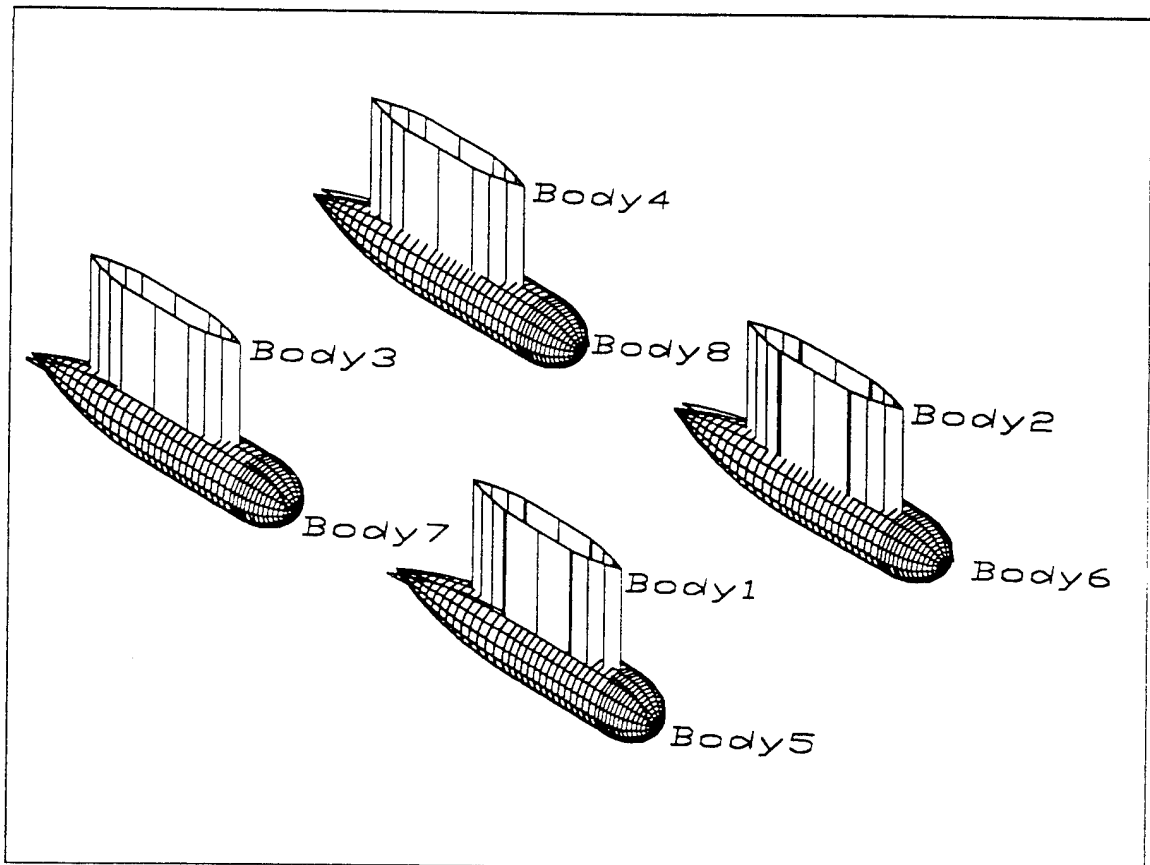
Figure 4-1: SLICE Body Numbering Scheme

CODING

MATLAB was used for the required computations. This choice was made to utilize the installed graphics capabilities of the program. Plotting results as computations were made was useful both in validating geometry assumptions and debugging. A logic flow chart of the overall computation scheme is at Appendix I. The routines used are also presented in this appendix. The pod and strut geometries were developed in the files PODGEO.m and STRUTGEO.m, The main wave making resistance routine is contained in the file Q.m. The solution to equations (4-1), (4-1a) and (4-1b) are solved in called subroutines for each of the thirty six paired terms in files named for the bodies that are paired. Samples of a strut body, pod body and strut/pod cross term are contained in the files ONEONE.m, SIXSIX.m and ONESIX.m. All other body and cross product subroutines are patterned after these files. This apparently cumbersome organization had one significant advantage. Once the files were written and assembles, bodies could be toggled on and off in the computation simply by adding a "%" at the head of the appropriate subroutine call line. This allows the overall SLICE geometry to be reduced into smaller pieces rather easily and helped demonstrate the complex interactions that occur in the full multibodied hull.

4.3 Results

Only partial results were obtained for the numerical solution during the allocated period of study for this thesis. Complete validation of results was not obtained and the results contained in this section require further analysis before design decisions can be made. Sufficient progress was made to draw some preliminary conclusions. Model M-2 was computed in the speed range of 3-9 fps (full scale 11-22 knots) using the values shown in Table (4-1). The results presented in Figure (4-2) and Table (4-2) are based on using fifty subdivisions in the x integration, 12 divisions in the z integration and 10 divisions in the θ integration. Testing was conducted varying the number of divisions and this was found to be a minimum acceptable limit with the integrity of the result maintained.

Strut Length	1.44 ft
Strut Beam (max)	0.195 ft
Strut Height	0.36 ft
Fwd Strut Set Back (x axis reference)	0.0 ft
Fwd Strut Offset (y axis reference)	± 0.979 ft
Aft Strut Set Back (x axis reference)	-3.48 ft
Aft Strut Offset (y axis reference)	± 1.396 ft
Strut Submergence (z axis reference)	-0.18 ft
Pod Length	2.321 ft
Pod Diameter (max)	0.4635 ft
Fwd Pod Setback (x axis reference)	0.0 ft
Fwd Pod Offset (y axis reference)	± 0.979 ft
Aft Pod Set Back (x axis reference)	-3.16 ft
Aft Pod Offset (y axis reference)	± 1.396 ft
Pod Submergence (z axis reference)	-0.59 ft

Table 4-1: M-2 Gross Parameters Used For Calculation

Figure 4-2 presents only the wavemaking portion of resistance as predicted by the numerical scheme. The negative overall result is attributed to the overall sign convention that is used in the calculation which has x positive in the direction of motion. An unresolved problem with this conclusion is that the body terms (1-1 through 8-8) should have been negative on their own. This however was not the case.

With negative Rw Values the curve is
flipped and this is the peak of the wave
making hump.
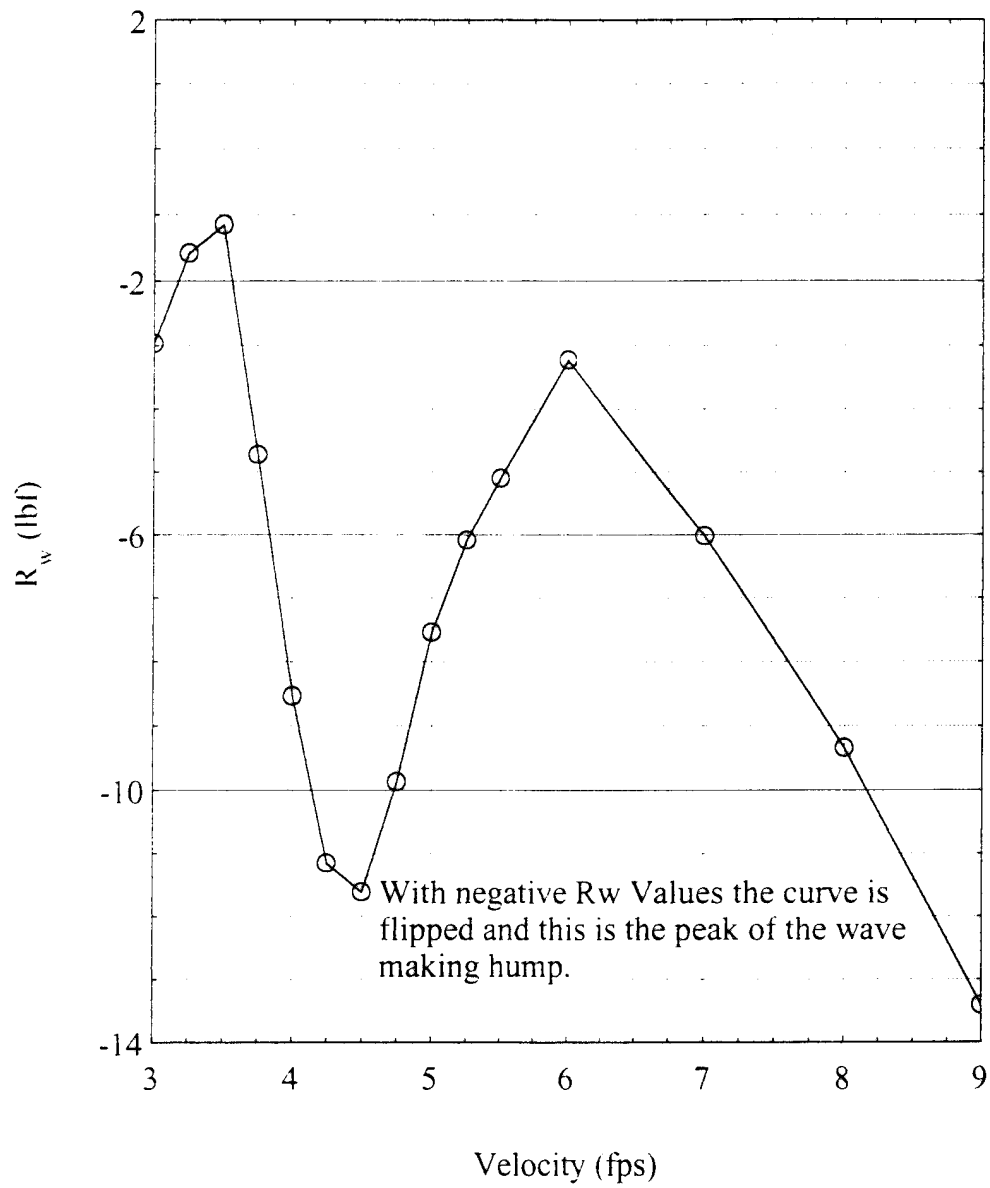
Figure 4-2: Wave Making Resistance of SLICE calculated from Thin Ship Theory

Speed (fps)	1-1 (lbf)	2-2 (lbf)	3-3 (lbf)	4-4 (lbf)	5-5 (lbf)	6-6 (lbf)	7-7 (lbf)	8-8 (lbf)
3	0.39E-3	0.39E-3	0.39E-3	0.39E-3	0.0004	0.0004	0.0004	0.0004
4	0.56E-3	0.56E-3	0.56E-3	0.56E-3	0.0020	0.0020	0.0020	0.0020
5	0.62E-3	0.62E-3	0.62E-3	0.62E-3	0.0038	0.0038	0.0038	0.0038
6	0.65E-3	0.65E-3	0.65E-3	0.65E-3	0.0052	0.0052	0.0052	0.0052
7	0.65E-3	0.65E-3	0.65E-3	0.65E-3	0.0061	0.0061	0.0061	0.0061
8	0.64E-3	0.64E-3	0.64E-3	0.64E-3	0.0067	0.0067	0.0067	0.0067
9	0.63E-3	0.63E-3	0.63E-3	0.63E-3	0.0070	0.0070	0.0070	0.0070

Table 4-2a: Wave Making Resistance Component Terms
BODY TERMS

Speed (fps)	1-5 (lbf)	2-6 (lbf)	3-7 (lbf)	4-8 (lbf)
3	-0.556	-0.556	-0.181	-0.181
4	-1.413	-1.413	-1.037	-1.037
5	-2.043	-2.043	-1.773	-1.773
6	-2.406	-2.406	-2.220	-2.220
7	-2.598	-2.598	-2.466	-2.466
8	-2.700	-2.700	-2.601	-2.601
9	-2.751	-2.751	-2.675	-2.675

Table 4-2b: Wave Making Resistance Component Terms
SAME CORNER CROSS TERMS

Speed (fps)	1-3 (lbf)	1-7 (lbf)	5-3 (lbf)	5-7 (lbf)	2-4 (lbf)	2-8 (lbf)	6-4 (lbf)	6-8 (lbf)
3	0.276	-0.249	-0.245	0.001	0.421	-0.241	-0.436	0.0
4	0.11	-0.547	-0.103	0.002	0.141	-1.054	-0.488	0.004
5	0.356	-0.135	-0.528	0.0	0.350	0.383	-0.371	-0.003
6	-0.264	1.128	0.922	-0.007	-0.422	2.035	1.709	-0.010
7	-0.412	1.325	1.248	-0.008	-0.882	1.879	2.059	-0.008
8	-0.388	1.142	1.264	-0.006	-0.903	1.106	1.527	-0.004
9	-0.103	0.682	0.811	-0.004	-0.626	0.302	0.799	0.0

Table 4-2c: Wave Making Resistance Component Terms
LONGITUDINAL CROSS TERMS

Speed (fps)	1-4 (lbf)	1-8 (lbf)	5-4 (lbf)	5-8 (lbf)	2-3 (lbf)	2-7 (lbf)	6-3 (lbf)	6-7 (lbf)
3	0.04E-3	0.119	-0.018	0.0	0.02E-3	-0.043	-0.018	0.0
4	0.33E-3	-0.250	-0.574	0.001	-.11E-3	-0.045	-0.57	0.001
5	-.58E-3	0.986	1.090	-0.005	-.09E-3	-0.016	1.089	0.001
6	-.29E-3	0.401	0.815	-0.003	-.30E-3	0.870	0.815	-0.004
7	0.08E-3	-0.447	-0.241	0.002	-.09E-3	0.540	-0.242	-0.004
8	0.75E-3	-1.308	-1.240	0.006	-.31E-3	0.986	-1.240	-0.005
9	0.58E-3	-1.711	-1.580	0.009	0.01E-3	0.072	-1.380	-0.002

Table 4-2d: Wave Making Resistance Component Terms
DIAGONAL CROSS TERMS

Speed (fps)	1-2 (lbf)	1-6 (lbf)	5-2 (lbf)	5-6 (lbf)	3-4 (lbf)	3-8 (lbf)	7-4 (lbf)	7-8 (lbf)
3	0.0	-0.079	-0.079	0.0	0.0	0.06	-0.115	0.0
4	-.03E-3	-0.213	-0.213	0.001	0.24E-3	0.112	-0.403	0.001
5	0.25E-3	-0.492	-0.492	0.003	-.23E-3	0.131	-0.383	0.001
6	0.13E-3	-0.484	-0.484	0.003	0.28E-3	-0.406	-0.489	0.003
7	0.52E-3	-0.840	-0.840	0.005	0.20E-3	-0.048	-0.541	0.003
8	-.25E-3	-0.404	-0.404	0.005	0.34E-3	-0.491	-0.944	0.004
9	0.07E-3	-0.472	-0.472	0.005	0.16E-3	-0.612	-0.417	0.004

Table 4-2e: Wave Making Resistance Component Terms
TRANSVERSE CROSS TERMS

Understanding that the code used is only partially validated, the following observations are made:

STRUTS

The contribution made by the struts is small. This is true both of the body terms and the cross terms between any two struts. This is reasonable for the strut geometry used. There is symmetry about midships, the nose and tail sections are slender and the overall L/D is 7.4. To verify that the low values obtained were not a code problem, an alternate geometry was selected that did not possess midships symmetry but retained the same L/D. A significant increase in resistance values was noted. These results follow the conclusions drawn by Chapman and Zhu Bing-quan on strut optimization cited in Chapter 2.5.

CROSS TERMS

As anticipated, the Same Corner Cross terms have the largest impact on wave

making resistance. This is followed in importance by the Longitudinal Cross Terms. The Diagonal and Transverse Cross Terms had more significant impact than was anticipated. Although smaller than the other terms, it would not be correct to eliminate the Transverse terms from optimizing iterations. Also clear from a review of Table (4-2) is the complexity of the body interactions. At a given speed, the transverse term for a specific body may have an additive effect while the longitudinal term for that same body has a subtracting term etc. Additionally, due to the lack of fore aft symmetry in the baseline SLICE layout, similar body groupings do not behave the same at a given speed. Note the difference between 3-8 and 7-4 in the Transverse Terms Table as an example of this. This decomposition of SLICE wavemaking resistance demonstrates that optimization work must be conducted with the entire hullform present. Attempting to sub-optimize a component body (such as a single strut pod combination) without observing the impact on the entire hullform may lead to erroneous conclusions.

Chapter 5 Conclusions

5.1 Restatement of Thesis Objectives

This thesis attempted to add to the developing body of SLICE knowledge by focusing on the resistance and powering aspects of the SLICE vessel in an academically rigorous manner. Three specific objectives were identified:

1) Independent research into the SLICE hullform to give both the US Navy and LMSC a second hydrodynamic viewpoint of the 177 Lton vessel prior to the ATD.

2) Development of a larger body of data to aid in optimizing the 177 Lton hull form.

3) A broader understanding of the hydrodynamic features of the hull to facilitate deciding the merits of pursuing designs in other displacements more practical to the US Navy.

In order to meet these objectives, several questions required answers:

1) LMSC theorizes that the appropriate characteristic length for SLICE is the length of a single pod. Is this valid?

2) The specific interaction between bodies has not been defined by LMSC. What is the relative importance of form; strut/pod alignment; and the effects that a strut/pod combination have on any of the other three strut/pod combinations that form the underwater body? Understanding these effects is necessary for design optimization.

3) The LMSC proposed design places the forward struts inboard of the aft struts. Is the outward lateral force (y axis lift) created by an effective angle of attack on the aft struts significant enough to create structural concerns?

4) The LMSC model tests were all conducted with models fixed in pitch and heave. Is this an accurate enough representation of reality to make predictions?

5) The LMSC tests maintained speed increments for an extremely short

duration (usually less than 10 seconds) and frequently truncated test runs at a model scale equivalent of 25 knots full scale. Was this sufficient to characterize a ship with an intended speed of 30+ knots?

6) Is the apparent focus on skin friction reduction, as reflected in the body forms selected, reasonable?

7) Does SLICE offer the stated hydrodynamic advantage over a SWATH ship.

5.2 Conclusions

CHARACTERISTIC LENGTH

The appropriate characteristic length for SLICE is the strut length, not the pod length. This is illustrated in the resistance curves for M-1,M-2 and M-3. These models had significantly different underwater bodies but very similar strut lengths. On a resistance vs speed plot, the position of the wave making hump for all three hullforms is nearly identical. In order to align these with $\mathcal{F}$= 4.5, strut length must be chosen as the characteristic length used in the definition $\mathcal{F}$.

THE IMPORTANCE OF BODY FORM AND BODY INTERACTION

Model M-2 was developed with the expectation that finer lines would help improve the hump speed performance of the baseline SLICE hullform. The offsets selected for the pods increased the constructive L/D of the pods from 4.1 in the baseline to 5.0 in M-2. This was the maximum improvement that could be made to L/D and still maintain the gross characteristics of the Baseline SLICE. This change in L/D was not sufficient to impact the hump speed performance. If the SLICE hullform is maintained, improvements in hump speed resistance must come from body interaction. Underwater photography showed that propeller submergence is better through the hump speed than previously thought.

The finer lines of M-2 did make a significant improvement in the resistance measured in the high speed range. Underwater photography revealed that the bluff lines of M-1 causes the shedding of a significant vortex at the trailing edge of the

81

struts starting at model scale equivalents of 25 knots. These vortices were incorrectly interpreted as spray phenomenon in previous testing. In the full scale ATD ship, the flow modification caused by the propellers may cause these vortices to be ingested into the propellers with a significant loss of thrust.

MODEL TEST CONDITIONS

Attempting to test the SLICE hullform in a condition other than fixed in pitch and heave introduces a significant level of complexity to the model design. The added complexity does not necessarily make the results more useful. The difficulty lies in developing a system that connects the model to the tow carriage through the line of force. With four underwater bodies all towed from a central point, this is extremely complex to manufacture. Any connection point somewhere other than in the line of force is easier to manufacture but creates variable applied moment. This effect cannot simply be subtracted out since it is impossible to separate it from the effects of real hydrodynamic forces. The remaining option then is to lock the model in pitch and heave. For the purposes of conducting comparative testing, this simplification is justified and was a reasonable simplification made by LMSC.

The tests conducted as part of this thesis showed that there was a significant transient time associated with acceleration from rest. In the higher speed ranges, forces required 4-6 seconds to achieve steady state after the steady state speed was achieved. The LMSC tests incorporated more speeds in a single run with fewer accelerations from rest. LMSC allowed for significantly less data collection time at each speed increment (less than 10 seconds compared with greater than 20 seconds). This may not have been sufficient time to achieve steady state and may contribute to the differences in LMSC's test results and those conducted as part of this thesis.

The numerical analysis conducted in Chapter 4 highlighted the extreme complexity of the flow around SLICE. Relationships presumed negligible such as the transverse and diagonal body interactions were shown to contribute noticibly to the overall resistance value. This has an implication in the LMSC test results. When the August control surface tests were conducted, only one side of the model (starboard)

was adjusted for various angles of attack. Based on the results of the wave making decomposition however, drawing conclusions about whole body behavior based on partial body measurements may lead to incorrect results.

HULLFORM OPTIMIZATION

The data decomposition presented at the end of Chapter 3 demonstrates that it is incorrect to optimize the hull for high speed operation by focusing on frictional resistance. Powering through the wave making hump does not imply that wave making resistance becomes negligible. It is true that the coefficient of wave making resistance C_w becomes a small number but resistance continues to increase as velocity squared. The design perspective should be that Froude scalable effects will account for at least half the total resistance and the hull should be optimized accordingly.

SLICE APPLICABILITY TO THE US NAVY

Figure (5-1), obtained from a set of presentation graphics used by Dr. R. Compton at the U.S. Naval Academy, depicts a predecessor to SLICE. The literature survey conducted as part of this thesis did not uncover any design work accomplished on this hull.

The comparison of either M-1 or M-2 with M-3 indicate that if there is an advantage to the SLICE hullform over conventional SWATH hullforms, it must be found somewhere other than in powering performance. M-3 demonstrates that it is possible to create a SWATH to the design constraints of SLICE and still meet or exceeded SLICE resistance performance through the entire speed range.

SLICE offers a possible advantage in the ratio of Deck Area to Displacement. The development of M-3 showed that the 177 Lton SWATH could have up to 600 ft^2 less deck area than the equivalent SLICE. The extent to which the crossbox is cantilevered fore and aft of the struts becomes the controlling factor. For low density payloads, such as ferry traffic, this is significant. For higher density payloads typical of military craft, the advantage is diminished.

April 8, 1930.   W. R. BLAIR   1,753,399

OCEAN-GOING WATER CRAFT

Filed June 29, 1929
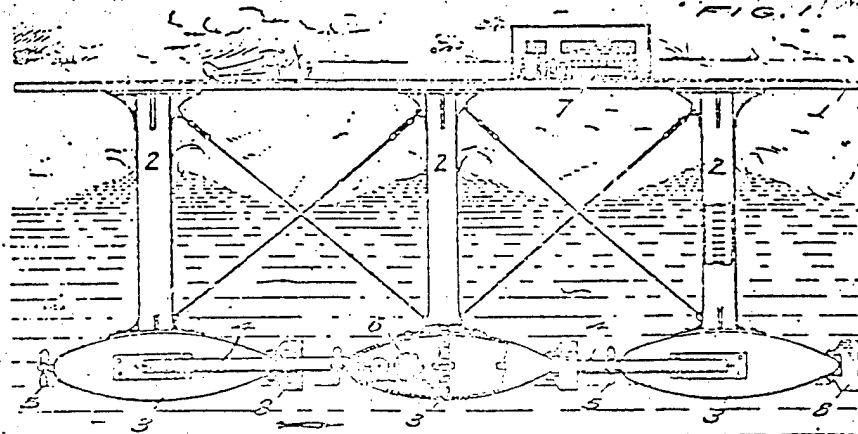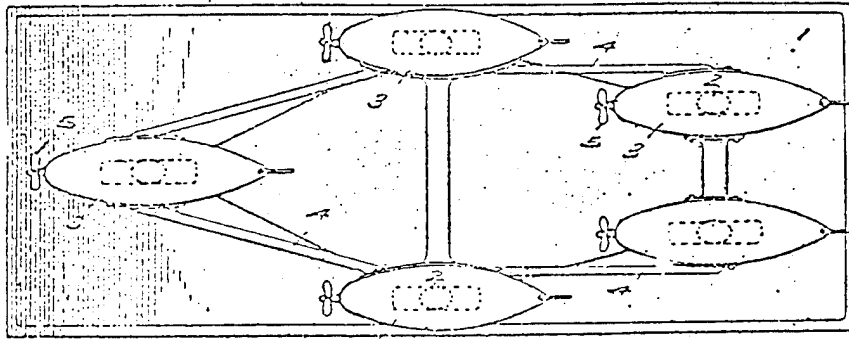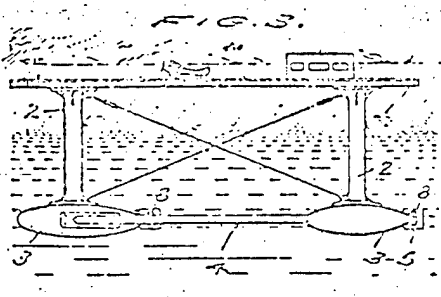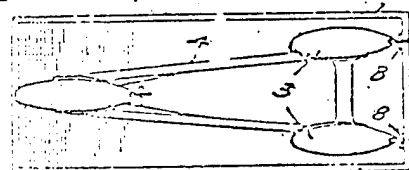
Figure 5-1: A SLICE Predecessor

The following recommendations are made for future study of SLICE technology:

1) The question of lateral lift on the aft struts created by the flow direction remains unanswered. This question should be addressed before the ATD vessel is placed in service to ensure a structural issue, either from an integrity or fatigue standpoint, is not overlooked.

2) This thesis presented a reasoned approach to scaling model data to full scale. The ATD will be the validating test of assumptions and decisions made in presenting the case for using traditional methods of data scaling. If conducted properly, the ATD will be invaluable in demonstrating the robustness of Froude hypothesis. During the ATD, significant effort should be invested in photographically documenting flow behavior both above and below the surface. Without this observation of physical phenomena, specific conclusions about scaling issues will not be possible.

3) The numerical approach used in this thesis requires further development before tuning of the SLICE hullform can be fully demonstrated. Thin ship theory appears to be reasonable for comparative analysis purposes and this approach should be further developed. After further validation, SLICE component positioning can be optimized and then a model of the final outcome should be built and tested in a similar scale to M-2 so that results can be compared. This could be the subject of a reasonable follow on thesis.

4) The SLICE ATD has the potential to answer many questions that have been raised regarding the classical naval architecture approach to resistance predictions. With careful planning, the ATD will be much more than a demonstration of a single ship's performance. It has the potential to contribute to the Naval Architecture community's understanding of the robustness of current testing and scaling techniques.

Appendix A

Model Testing Lessons Learned

The Science and Art of Model Testing

The purpose of this appendix is to outline the thought process that was used in designing the experiments and the models that were used in this thesis. The tone of this section will be conversational and it represents a compilation of lessons learned as the research for this paper progressed. It is hoped that this appendix may be of use to other students who may choose to undertake a similar type of research effort.

When the work for this paper began, it was decided that in support of a Naval Construction program, there would be a wealth of experience to be gained from designing and building a ship (albeit a small one) that actually had to work. With this decided, I embarked on a challenging, frustrating, rewarding, extremely time consuming, detail intensive process.

The title to this appendix is not meant to be trite. There are clearly scientific/engineering principles that may not be violated if reasonable test results are expected. Geometric similitude must be maintained, tolerances must be decided on, load and material strength estimates must be reasonably predicted, scaling must be calculated properly and data reduction must be interpreted accurately. Beyond this however, I discovered an entire world of additional issues regarding the planning of the experiment, actual construction of the models and successful time and resource management during the critical and always too short time allocated in the test facility. You cannot gain an appreciation for this facet of experimentation by taking a course or reading a book.

RECOMMENDATION #1: Prior to doing anything on your own experiment, observe similar projects for several days. In the case of this research, I had the opportunity to observe the SLICE testing conducted at NSWC in August and December. For eight days that I was able to watch other people devise solutions and cope with frustrations without impacting my own work. Many ideas for my own project were born during these eight days and most importantly, I met the experts in the field of model testing. Later, these associations were invaluable to me.

If this period of observation does not scare you away from proceeding with your own experiment, the next question you must honestly answer is: How handy are you and what resources do you have at your disposal? When I began building the models, I considered myself reasonably proficient with tools but I had never undertaken a project of this magnitude before.

RECOMMENDATION #2: As a means of determining your handiness, I suggest you consider the type tolerances you will have to build to if the model is to be considered a reasonable geosim. For argument, lets say that in full scale, the greatest building error that will be tolerated is 6 inches (pretty big error!). If the scale that you are building to is 16:1, inaccuracies in your model of greater than 3/8 inch exceed the building tolerance and you have introduced a level of uncertainty as to the actual geometric similarity of your model to the real ship. If your personality is such that you fail to recognize the difference between 3/8 and 1/2 inch when measuring things, then model building may not be the thing for you. Scaling errors to full scale to determine reasonableness was a process that slowly evolved during my own project

At this stage, some decisions need to be made regarding the specific test objectives. To a large measure, this will determine the complexity of the model to be built. The speeds to be modeled must be matched with tow tank capabilities. For this project, full scale speeds of 40 knots were desired. Based on the maximum carriage speed at the MIT tow tank, this would have required building the models in a 100:1 scale, a size so small that no useful data would be collected. The alternatives were to either slow the maximum speed or find another facility. The United States Naval Academy was literally the closest facility with the necessary capability. In addition to these concerns, there were also the questions regarding what the model should be capable of doing. Early on in the project it was decided that the models would have no control surfaces. This removed a significant level of complexity from the model design. It was also decided that the models should be capable of being modified for self propulsion at some point in the future. Additionally, since the general test scheme called for a test free in heave, the models had to be built with sufficient reserve buoyancy to support themselves, the mounting frame, the towing carriage heave post and force blocks and an estimated reserve for propulsion equipment. This simple

exercise placed many constraints on the model:

1) The models would have to be particularly rugged to enhance the chance of survival during the 400+ mile trip to the test facility in the back of a van. I eliminated the conventional foam construction in deference to this requirement.

2) By understanding what the models had to do, I could make a weight budget to build to. It turned out that the heave post and force block weighed 25 pounds collectively. Properly scaled, I could estimate the displacement of the models (between 75, 83 and 115 lbf for models M-1, M-2 and M-3 respectively). I then budgeted 10% for reserve buoyancy and allocated 15 lbf for frame weight. The remainder could be used in materials to actually build the models. This weight budget further drove the building plan. The material selected had to be strong, extremely light and simple enough for an amateur to work with.

RECOMMENDATION #3: Design your models only for the capability you plan to test. Build only what you need. Clearly establish exactly what the models will be used for before planning their construction. Eliminate multiple functions where possible since multiple functions will most likely increase the model's level of complexity. In the case of this project, significant effort was expended to meet an established weight budget. The weight budget was based on the assumption that the model would be tested in a free to heave condition but this test was never performed. For the fixed in heave tests, the models would have been acceptable even if they were negatively buoyant.

At this stage there is almost enough preliminary groundwork set to begin building. With any luck you will be able to enlist the help of others in the actual building process. The models built for this project represent the collective work of 9 individuals with a total of roughly 700 manhours invested between December and March. Admittedly a portion of this time was expended inefficiently, devising solutions to emergent problems, obtaining supplies etc. but these are the facts of model building and this sort of time expenditure should be planned for.

RECOMMENDATION #4 If you are not literate in a CAD system, develop that proficiency well in advance of the model building. As early as possible, make full

scale working drawings. This is critical if other people are helping you. It is the only way to know that you helpers understand what to build. If the drawings are done soon enough in advance, they may help point out errors in the design. I did not develop a good set of working drawings early enough in the process and it hindered progress on several occasions. Once the drawing process was brought under control, I found it handy to cut up the rather disposable drawings for templates.

Originally PVC was the material of choice for the model construction. It is easy to shape and bond and is a relatively inexpensive alternative. Additionally, water absorption is not a concern. There are two drawbacks though. PVC is relatively dense. At 81 lb/in^3, it can be made to float if rather thin walled sections are used. This is useful for long stretches of parallel midbody but becomes a significant drawback for the shaped pieces which must be turned on a lathe. Hollowing these sections out to an appropriate wall thickness was not practical. Additionally, the time to turn a single nose cone (inside and outside) was fund to be about 10 hours after considerable practice. A total of 16 nose and tail cones were required for two models. 160 hours was considered excessive to finish this single piece of the project. The second drawback of PVC is also one of its advantages. PVC is relatively easy to cut because it is soft. Although there was little danger of it deforming in a gross sense, it is very easy to gouge and scratch. Once damaged in this fashion, it is difficult to repair because although it is easy to sand and it bonds well to itself with the proper adhesive, other bonding and filling agents do not adhere well. In short the probability of achieving a satisfactory repair once damaged is small. In light of the trip the models would take to the test facility and the potential for damage during this trip, this was considered a major drawback.

RECOMMENDATION #5 Treat your model building project like an actual shipbuilding project in the preliminary phase. Account for weight and buoyancy to the greatest accuracy possible. I developed a weight budget for Structure (the frame), Propulsion (the tow pad), the Payload (the heave post), a building margin of 10% and a design reserve buoyancy of 10% (allocated because there is some intention to eventually convert my models to self propulsion so there may be some growth). By calculating the displacement, I then knew how much each component could weigh and I did weigh them frequently through the building process. As work

proceeded, building margin was allowed to be utilized at a rate commensurate with the stage of building. I incorporated this method early enough in the project to abandon PVC as a building material before too much work was done, but not soon enough to avoid buying a quantity of material that was not useful.

RECOMMENDATION #6 Make frequent tests of methods you think you will use, well in advance of when you need them in the building project. If you plan to use a particular machine, check it out to ensure all the pieces are there and it functions properly. If you plan to use a particular adhesive to bond two different materials, try it out early on with two scrap pieces, even if the adhesive claims to be formulated to do the job. I had significant difficulty with this on several occasions. Testing gave me the time to either call the manufacturer for assistance or to find a different product. The two times I did not perform tests on intended procedures resulted in near disaster. The one time I did not perform a bonding test was with PVC and PVC cement, items I had worked with in the past and was assured by the PVC supplier would work. For a reason I never determined, the cement did not bond. This occurred late on a Saturday immediately proceeding the Sunday I was to depart for Annapolis. The search for a new bonding agent was frustrating since it was not supposed to happen, difficult because of the hour, and nearly cost me a significant piece of the test program (the high speed SWATH model did not require significant reserve buoyancy and so was built from PVC to utilize the material purchased.). I intended to paint the models bright yellow with marine paint. Yellow is the color of choice for model testing because it enhances contrast and is useful for photography. The marine paint was difficult to apply, did not cover well and was slow to dry. This provided for extreme frustration at the already frantic end of the building phase. In the end analysis, any spray enamel with a 10-15 minute dry time would have performed equally well in the tow tank tests, and I would have known that if I tested the paint systems in February rather than waiting until the end of the project.

For the SLICE hullforms, molded fiberglass was found to be the best construction method. With other materials such as shaped foam, PVC rod turned on a lathe or stacked wood, construction is a 100% hands on process. Only one piece can be manufactured at a time. Each SLICE model has the following components: 4 struts, 4 nose cones, 4 tail cones and 4 parallel midbody sections. There were two SLICE models, therefore requiring the manufacture of 32 components. Hand crafting each component would not only have been prohibitively time consuming but also would have introduced slight variations between components that should have been identical (the four nose cones for example). Molded fiberglass construction offered the following advantages:

91

1. A mold insures that the four components have the same shape.

2. Once the molds are made, component fabrication time is primarily epoxy curing time. This frees up time for the builder to do something else.

3. By laying in the fiberglass cloth in the correct fashion, excellent strength is obtained for very little weight.

4. Using the proper additives in the epoxy provides an outside surface that requires no finish work once the piece is removed from the mold.

The West Epoxy System was the material of choice for this project. It is relatively expensive but is readily available at Marine Supply stores, very easy to use, and is associated with an excellent consumer product hotline that is responsive and helpful. Most of the products referred to in the building process are West System names. The West system can be used with either a fast setting hardener or a regular hardener. The fast hardener cuts the working time and also the curing time of the mixture in half. Additives which are called for in some of the steps also reduce working time. Times cited below are based on using the fast hardener. The West System sells a set of proportioning pumps which helps to ensure that the correct mix of resin and hardener is achieved. The pumps are a worthwhile investment.

Note: The epoxy will not adhere well to plastic so working on a plastic drop cloth will help cleanup. Mixing the epoxy in plastic pails can be reused. Just let the epoxy harden and the tap the pail.

The following outlines the steps used constructing the pods:

1. A CAD drawing was made of the pod. Five or six tangent lines were drawn along the curvature. Angles with the vertical and insets from the leading edge were calculated. This is shown in figure A-1.

2. A male plug was cut out of PVC rod on a lathe. This was done by marking the insets, and then cutting at the appropriate angle from the inset mark to the leading edge. The transitions between angles was fared with a file and the entire plug polished

with consecutive applications of 200, 320 and 400 grit wet sandpaper followed by an abrasive cleanser and finally brass polish. All these steps were performed on the lathe to ensure roundness.

3. A female mold was then made from the male plug. This was done with the West System. First the Plug is coated with a layer of wax. This is necessary to ensure the epoxy does not adhere to the plug. The first epoxy coat consists of the appropriate mix resin and hardener with sufficient microfibers added to give the mixture the consistency of paste. Since the additives decrease the working time, I suggest you pump the resin into the mixing pail, add the additive and mix it thoroughly and then as a last step, add the correct amount of hardener. This method will save a few minutes of working life. This mixture is painted onto the plug and serves as very smooth gel-coat layer. Brushes can be conserved by washing them with acetone after use but I recommend always doing this first layer with a new brush. This application is allowed to begin to harden but not cure (approx 2-3 hours). Even with steep angles, this mixture should be thick enough so there is very little running of the coat while it sets. A second layer is added which is also a paste like consistency. This time, the additive is a 50%-50% mix of microfibers and colloidal silica, which will be less smooth but has greater strength. This also is set aside to begin to harden but not cure (2-3 hours). Finally, the real strength layer is added. For the molds. this consisted of squares of fiber matting soaked in mixed epoxy (no additives in the mixture this time). The matting has a random fiber lay and tends to be fairly (0.125" thick). Do not let the matting get too wet or else it will tend to slide when placed on the plug. The most effective way to do this step is with your hands. Latex gloves are an absolute requirement. This step is just like working with paper mache. When the matting has begun to harden (2-3 hours) a layer of 12 ounce woven fiberglass cloth is added as a final step. Pre-cutting the cloth into smaller patches will help since your gloved hands will be covered in epoxy. Since there are no additives in the epoxy in the last two steps, use the epoxy sparingly, just enough to barely wet the cloth. Allow the entire mold to cure for the appropriate time (8 hours with fast hardener). The mold may have to be beaten pretty hard to pull it free. In the case of my shapes, I found that

removing the plug actually drew a significant vacuum because of the closeness of the fit. The mold is strong enough to be beaten pretty hard with a rubber mallet. A small hole drilled into the mold and later patched may also help.

4. Manufacturing pieces is now essentially a repeat of step 3 with a few exceptions. I chose to leave out the fiberglass matting in the final pieces. There was sufficient strength with the two initial coats and the 12 ounce cloth and I wanted to reduce weight.   *Take Note*: The epoxy cures using an exothermic process. In the steps used up till now, this was insignificant. Since the female mold is a cup, as you manufacture the component pieces, any excess resin will pool in the bottom of the mold. On two occasions I cracked my molds because of the heat released by the excess pool. I recommend that you set the mold into a pot of cold water at least during the final step (glass cloth and epoxy). This seems to be adequate to control the temperature.   *Take Note:* You need to provide a method of pulling the piece out of the mold. I did this by setting two 12" pieces of nylon string into the wet epoxy of the final coat and covering the end with a square of fiberglass cloth. This gave a secure method of pulling the piece out.

5. After the components are pulled from the mold, they should be washed with acetone to remove any residual wax. If this is not done later epoxying during assembly may not bond well.

6. When all the components are manufactured, they can easily be assembled by epoxying them together. I cut rings out of balsa wood that were fitted into the joints to increase the gluing surface. The timing of this assembly is dependent on how the struts get attached. For the SLICE models, the struts are bolted to the pods. In order to facilitate this, the tails were joined to the parallel midbody sections. The struts were then attached to the sub assembly and finally the nose cones sealed the assembly.

The following process was used to build the struts.

1. A full scale CAD drawing of the strut cross section was made. This was cut out and glued to a piece of thin plywood. The cross section shape was cut out of the

wood so that a "slip over template was created.

2. Blocks of balsa wood were cut to rough dimensions of the strut and glued together to create the correct strut length.

3. Once dry, the balsa wood was sanded to shape so that the template made a loose fit over the balsa wood.

4. The balsa wood was sealed using a coating of epoxy painted onto it. This was left to cure.

5. The strut was sanded to remove large defects. (The balsa wood will cause a fair amount of bubbling in the epoxy). It is then covered in 12 ounce fiberglass cloth.
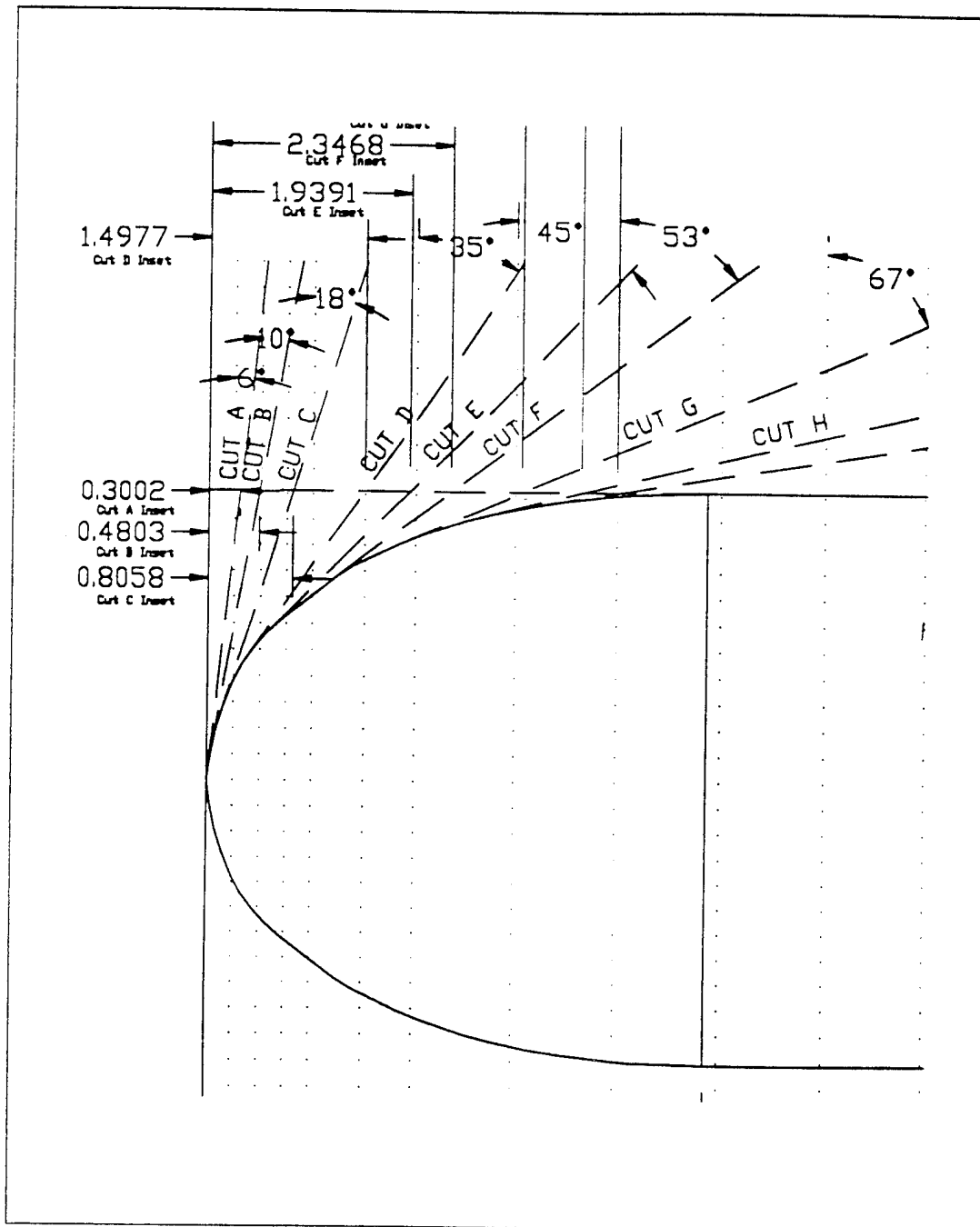
Figure A-1: Example of Nose Cone Template

Appendix B

Model M-1 Baseline

Table of Offsets

and

Design Worksheet

Model M-1 Table of Offsets

Foward Pod in Inches   Aft Pod in Inches   Struts in Inches

$X_{fp}(x_{fp})$	$Y_{fp}(y_{fp})$	$X_{ap}(x_{ap})$	$Y_{ap}(y_{ap})$	$X_s(x_s)$	$Y_s(y_s)$
0	0	0	0	0	0
0.695	1.534	0.695	1.534	0.695	0.658
1.391	2.05	1.391	2.05	1.391	0.91
2.086	2.364	2.086	2.364	2.086	1.037
2.781	2.568	2.781	2.568	2.781	1.1
3.477	2.692	3.477	2.692	3.456	1.13
4.172	2.762	4.172	2.762	9.06	1.13
4.867	2.781	4.867	2.781	9.734	1.105
11.82	2.781	11.125	2.781	10.43	1.048
13.211	2.663	12.516	2.663	11.125	0.978
14.602	2.441	13.906	2.441	11.82	0.892
15.992	2.155	15.297	2.155	12.516	0.788
17.383	1.849	16.687	1.849	13.211	0.672
18.773	1.541	18.078	1.541	13.906	0.542
20.164	1.233	19.469	1.233	14.602	0.406
21.555	0.925	20.859	0.925	15.297	0.271
22.945	0.617	22.25	0.617	15.992	0.136
24.336	0.308	23.641	0.308	16.687	0
25.727	0	25.031	0		

98

These are the full scale SLICE offsets taken from the December 1994 LMSC variant used to generate Model M-1 offsets.

Pod X Coord (ft)	Pod Y Coord (ft)	Strut X Coord (ft)	Strut Y Coord (ft)
0	0	0	0
1	2.21	1	0.95
2	2.95	2	1.31
3	3.40	3	1.49
4	3.69	4	1.58
5	3.87	4.97	1.625
6	3.97	13.03	1.625
7	4.00	14	1.59
16	4.00	15	1.51
18	3.81	16	1.41
20	3.51	17	1.28
22	3.10	18	1.13
24	2.66	19	0.97
26	2.22	20	0.78
28	1.77	21	0.58
30	1.33	22	0.39
32	0.89	23	0.20
34	0.44	24	0
36	0		

Model M-1 Baseline LMSC SLICE

This is based on the drawings provided by LMSC for the December baseline ship.

1a. Units Defined

$$ft \equiv 1L \qquad lb \equiv 1M \qquad sec \equiv 1T \qquad \text{Base Units}$$

$$nm = 6076 \cdot ft \qquad \text{Nautical Mile}$$

$$kt = 1 \cdot \frac{nm}{hr} \qquad \text{Knot}$$

$$lton = 2240 \cdot lb \qquad \text{Long Ton}$$

1b. Foward Pod Offsets in Full Scale

$$i = 0 .. 18$$

$$x_{fp_i} = READ(m1pfx) \qquad y_{fp_i} = READ(m1pfy)$$

Aft Pod Offsets in Full Scale

$$x_{ap_i} = READ(m1pax) \qquad y_{ap_i} = READ(m1pay)$$

Strut Offsets in Full Scale

$$j = 0 .. 17$$

$$x_{s_j} = READ(m1sx) \qquad y_{s_j} = READ(m1sy)$$

Model Scale Factor

$$\lambda = \frac{8 \cdot ft}{5.5625 \cdot in} \qquad \lambda = 17.258$$

Model Offsets

$$X_{fp}(x_{fp}) = x_{fp_i} \cdot \lambda^{-1} \cdot 12 \qquad Y_{fp}(y_{fp}) = y_{fp_i} \cdot \lambda^{-1} \cdot 12 \qquad \text{Foward Pod}$$

$$X_{ap}(x_{ap}) = x_{ap_i} \cdot \lambda^{-1} \cdot 12 \qquad Y_{ap}(y_{ap}) = y_{ap_i} \cdot \lambda^{-1} \cdot 12 \qquad \text{Aft Pod}$$

$$X_{s}(x_{s}) = x_{s_j} \cdot \lambda^{-1} \cdot 12 \qquad Y_{s}(y_{s}) = y_{s_j} \cdot \lambda^{-1} \cdot 12 \qquad \text{Struts}$$

1c. Model Scale Weight Balance

Fixed Variables

$\lambda := 17.258$

$\rho_{sw} = 1.9912 \cdot lb \cdot \dfrac{sec^2}{ft^4}$ Density of Salt Water at 56° F. An assumed average operating temperature.

$\nu_{sw} = 1.3343 \cdot 10^{-5} \cdot \dfrac{ft^2}{sec}$ Kinematic Viscosity of Salt Water at 56° F.

$\rho_{fw} = 1.9367 \cdot lb \cdot \dfrac{sec^2}{ft^4}$ Density of Fresh Water at 68° F. An assumed average tow tank temperature. Use this if prediction is for a model test.

$\nu_{fw} = 1.0804 \cdot 10^{-5} \cdot \dfrac{ft^2}{sec}$ Kinematic Viscosity of Fresh Water at 68° F.

$g = 32.174 \cdot ft \cdot sec^{-2}$ Acceleration due to gravity

$\ast\ast\ast$ $V = 0 \cdot kt, 1 \cdot kt .. 35 \cdot kt$ Modify this to reflect the velocity range of interest.

Indicator Settings

Water

$SW = 0$ "1" indicates the ship is operating in Salt Water
"0" indicates the ship is operating in Fresh Water

$\rho = if(SW = 1, \rho_{sw}, \rho_{fw})$

$\nu = if(SW = 1, \nu_{sw}, \nu_{fw})$

Hull Displacement Definition

$\ldots$ $\Delta_d = \dfrac{170 \cdot \text{lton}}{\lambda^3}$ This defines the the requireded $(_d)$ displacement of the vessel

note: 170 lton is used here since that is the displacement of the "filletless" hull.

$V_d = \Delta_d \cdot \dfrac{1}{\rho \cdot g}$ $V_d = 1 \cdot \text{ft}^3$ The requireded $(_d)$ displaced volume

Bouyant Force

$$F_b = V_d \cdot \rho \cdot g \qquad\qquad F_b = 74.084 \cdot \text{lb}$$

Weight Account

FRAME

$$W_f = 18 \cdot \text{lb}$$

Force Block + Heave Post

$$W_{bl} = 25 \cdot \text{lb}$$

Other Model Supplies

$$W_{oth} = 2 \cdot \text{lb}$$

Desired Reserve Bouyancy

$$F_{brd} = 0.06 \cdot F_b$$

$$F_{brd} = 4.445 \cdot \text{lb}$$

Allowed Weight of a single strut pod

$$W_{sp} = \dfrac{F_b - W_f - W_{bl} - W_{oth} - F_{brd}}{4} \qquad\qquad W_{sp} = 6.16 \cdot \text{lb}$$

103

Appendix C

Model M-2 Modified Baseline

Table of Offsets

and

Design Worksheet

Model M-2 Table of Offsets

Pods (both fwd and aft have the same offsets)   Struts
in inches   in inches

$xm(x)_i$ in^{-1}	$ym(y)_i$ in^{-1}	$xm(x)_j$ in^{-1}	$ym(y)_j$ in^{-1}	$xscale(x1)_i$ in^{-1}	$\dfrac{yscale(x1)_i}{ft}$
0	0	14.463	2.716	0	0
0.556	0.8	15.019	2.694	0.72	0.287
1.112	1.145	15.575	2.669	1.44	0.529
1.669	1.411	16.131	2.642	2.16	0.729
2.225	1.632	16.687	2.61	2.87	0.889
2.781	1.82	17.244	2.575	3.59	1.009
3.337	1.983	17.8	2.535	4.31	1.093
3.894	2.124	18.356	2.491	5.03	1.144
4.45	2.246	18.912	2.441	5.75	1.166
5.006	2.351	19.469	2.385	6.47	1.168
5.562	2.441	20.025	2.322	7.19	1.168
6.119	2.518	20.581	2.251	7.91	1.168
6.675	2.582	21.137	2.172	8.62	1.168
7.231	2.635	21.694	2.083	9.34	1.168
7.788	2.678	22.25	1.984	10.06	1.168
8.344	2.713	22.806	1.873	10.78	1.168
8.9	2.74	23.362	1.75	11.5	1.166
9.456	2.758	23.919	1.614	12.22	1.144
10.012	2.771	24.475	1.463	12.94	1.093
10.569	2.779	25.031	1.296	13.65	1.009
11.125	2.781	25.588	1.113	14.37	0.889
11.681	2.78	26.144	0.909	15.09	0.729
12.238	2.773	26.7	0.684	15.81	0.529
12.794	2.763	27.256	0.429	16.53	0.287
13.35	2.75	27.812	0	17.25	0
13.906	2.735				

Model M-2 The Better Slice

This variant uses the same gross dimmensions as the baseline SLICE but varies the body shapes to follow more traditional forms. The struts use parabolic leading and trailing edges and the pods are based on series 58 shapes.

1a. Units Defined

$ft \equiv 1L$ $lb \equiv 1M$ $sec \equiv 1T$ Base Units

$nm := 6076 \cdot ft$ Nautical Mile

$kt := 1 \cdot \dfrac{nm}{hr}$ Knot

$lton = 2240 \cdot lb$ Long Ton

1b. Fixed Variables

$\rho_{sw} = 1.9912 \cdot lb \cdot \dfrac{sec^2}{ft^4}$ Density of Salt Water at 56° F. An assumed average operating temperature.

$\nu_{sw} = 1.3343 \cdot 10^{-5} \cdot \dfrac{ft^2}{sec}$ Kinematic Viscosity of Salt Water at 56° F.

$\rho_{fw} = 1.9367 \cdot lb \cdot \dfrac{sec^2}{ft^4}$ Density of Fresh Water at 68° F. An assumed average tow tank temperature. Use this if prediction is for a model test.

$\nu_{fw} = 1.0804 \cdot 10^{-5} \cdot \dfrac{ft^2}{sec}$ Kinematic Viscosity of Fresh Water at 68° F.

$g = 32.174 \cdot ft \cdot sec^{-2}$ Acceleration due to gravity

*** $V := 0 \cdot kt, 1 \cdot kt .. 35 \cdot kt$ Modify this to reflect the velocity range of interest.

1c. Indicator Settings

Water

$$$ $SW := 1$ "1" indicates the ship is operating in Salt Water
                        "0" indicates the ship is operating in Fresh Water

$$\rho := if\left(SW=1, \rho_{sw}, \rho_{fw}\right)$$

$$v := if\left(SW=1, v_{sw}, v_{fw}\right)$$

Body Segmentation

$$$ $seg := 1 \cdot ft$

2a. Hull Component and Required Displacement Definition

••• $\Delta_d = 177 \cdot lton$ This defines the the requireded ($_d$) displacement of the vessel

$$V_d := \Delta_d \cdot \frac{1}{\rho \cdot g}$$ $V_d = 6189 \cdot ft^3$ The requireded ($_d$) displaced volume

Strut Height

$H := 6 \cdot ft$ Ammount of Strut in the Water *Defined per the Baseline*

Strut Beam

••• $D_1 = 3.25 \cdot ft$ Maximum Strut Beam Required *Defind per the Baseline*
                             Considered a required parameter.

Overall Strut Length

••• $L_1 = 24 \cdot ft$ Overall Strut Length

Length to Beam Ratio

$$LD1 := \frac{L_1}{D_1}$$ $LD1 = 7.385$ Length to Maximum Diameter Ratio

Length Breakdown

*** $L_{pmb1} = 7 \cdot ft$ Length of Parallel Midbody

*** $L_{n1} = 0.5 \cdot (L_1 - L_{pmb1})$ $L_{n1} = 8.5 \cdot ft$ Strut Nose Length *(2.4 x D is optimum)*

     $L_{t1} = L_1 - L_{pmb1} - L_{n1}$ $L_{t1} = 8.5 \cdot ft$ Strut Tail Length *(3.6 x D is optimum)*

Nose and Tail Shape Exponent

*** $n_{n1} \equiv 2.25$ *** $n_{t1} \equiv 2.25$

Calculation of Nose and Midbody Shape

$$x1 := 0 \cdot ft, \cdot seg.. \cdot (L_{n1} + L_{pmb1})$$

defines the x values of the subdivisions

$$yn1(x1) := \frac{D_1}{2} \cdot \left[1 - \left(\frac{L_{n1} - |x1|}{L_{n1}} \right)^{n_{n1}} \right]$$

defines the y values of the nose based on a parabola

$$ypmb1(x1) := \frac{D_1}{2}$$

defines the y values of the midsection

$$A1(x1) := if(|x1| \leq L_{n1}, yn1(x1), ypmb1(x1))$$

Calculation of Tail Shape

$$x1 := 0 \cdot ft, \cdot seg.. \cdot (L_{n1} + L_{pmb1} + L_{t1})$$

defines the x values of the subdivisions

$$yt1(x1) := \frac{D_1}{2} \cdot \left[1 - \left[\frac{|x1| - (L_{n1} + L_{pmb1})}{L_{t1}} \right]^{n_{t1}} \right]$$

defines the y values based on a parabola

$$body1(x1) := if(|x1| \leq L_{n1} + L_{pmb1}, A1(x1), yt1(x1))$$

Function that defines the body geometry

Strut Section

— Body 1
— Body 1
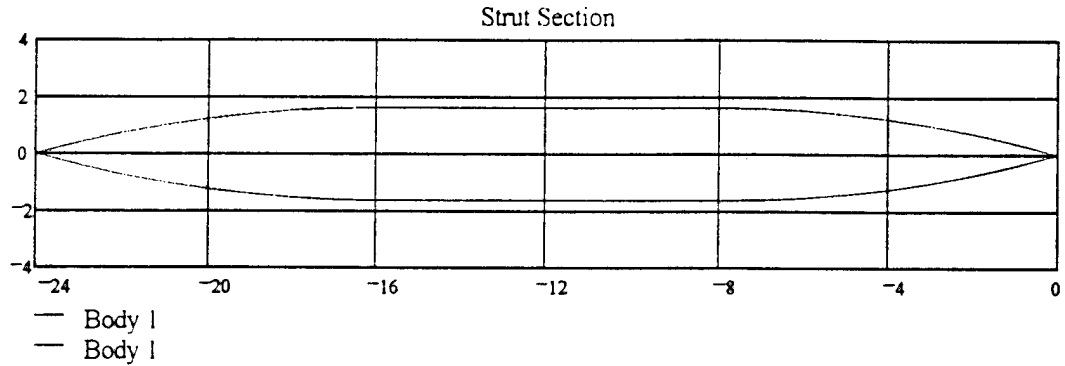
Wetted Surface and Volume Calculation

Perimeter

Nose

$$N_p = 0.5 \cdot \sqrt{D_1{}^2 + 16 \cdot L_{nl}{}^2} + \frac{D_1{}^2}{8 \cdot L_{nl}} \cdot \ln\left(\frac{4 \cdot L_{nl} - \sqrt{D_1{}^2 - 16 \cdot L_{nl}{}^2}}{D_1}\right)$$

$$N_p = 17.55 \cdot ft$$

Tail

$$T_p = 0.5 \cdot \sqrt{D_1{}^2 + 16 \cdot L_{tl}{}^2} + \frac{D_1{}^2}{8 \cdot L_{tl}} \cdot \ln\left(\frac{4 \cdot L_{tl} + \sqrt{D_1{}^2 + 16 \cdot L_{tl}{}^2}}{D_1}\right)$$

$$T_p = 17.55 \cdot ft$$

Midsection

$$S_p = 2 \cdot L_{pmbl}$$

$$S_p = 14 \cdot ft$$

Total Perimeter

$$P = N_p + S_p + T_p$$

$$P = 49.1 \cdot ft$$

Wetted Surface of the Strut

$$WS_s = P \cdot H \qquad WS_s = 294.602 \cdot ft^2 \qquad \text{for one strut}$$

Areas

nose area

$$N_a = \frac{2}{3} \cdot L_{nl} \cdot D_l \qquad N_a = 18.417 \cdot ft^2$$

tail area

$$T_a = \frac{2}{3} \cdot L_{tl} \cdot D_l \qquad T_a = 18.417 \cdot ft^2$$

mid section area

$$S_a = D_l \cdot L_{pmbl} \qquad S_a = 22.75 \cdot ft^2$$

Total Area

$$Area = N_a + S_a + T_a \qquad Area = 59.583 \cdot ft^2$$

Volume per Strut

$$vol = Area \cdot H \qquad vol = 357.5 \cdot ft^3$$

Total Strut Volume

$$VOL = 4 \cdot vol \qquad VOL = 1430 \cdot ft^3$$

Pod Volume Required

$$V_{pods} = V_d - VOL \qquad V_{pods} = 4759 \cdot ft^3 \qquad \text{for four pods}$$

$$V_{pod} = \frac{V_{pods}}{4} \qquad V_{pod} = 1190 \cdot ft^3 \qquad \text{per pod}$$

Pod Definition based on the Model 4155 of Series 58

$$\lambda_1 = 4.3 \qquad$$ the scale factor used to get from the data on page 49 of series 58 (Lpod= 9 ft) to the size needed per baseline Lpod= 38.7 ft) is 4.3

$$L_p = 9 \cdot ft \cdot \lambda_1 \qquad D_p = 1.8 \cdot ft \cdot \lambda_1 \qquad D_p = 7.74 \cdot ft$$

$$i = 0, 1 .. 53$$

$$x_i = READ(betx) \qquad y_i = READ(bety) \qquad \text{non dimmensional}$$

$$xfs(x) = x \cdot L_p \qquad yfs(y) = y \cdot D_p \qquad \text{full scale dimmensions}$$

$$WS_{58} = 39.75 \cdot ft^2$$

$$WS_{fs} = WS_{58} \cdot \lambda_1^{2} \qquad WS_{fs} = 734.977 \cdot ft^2 \qquad \text{for one pod}$$

$$Vol_{58} = 14.89 \cdot ft^3 \qquad \text{As printed in the Series 58 data}$$

$$Vol_{fs} = Vol_{58} \cdot \lambda_1^{3} \qquad Vol_{fs} = 1183.859 \cdot ft^3$$

$$VOLUME = 4 \cdot Vol_{fs} - 4 \cdot vol$$

$$VOLUME = 6165.437 \cdot ft^3 \qquad V_d = 6188.727 \cdot ft^3 \qquad \textbf{Compares calculated volume}$$
$$\textbf{to needed volume.}$$

$$\Delta = VOLUME \cdot \rho \cdot g \qquad \Delta = 176.334 \cdot lton$$

Now Scale to Model Size

$$\lambda_2 = \frac{5.5625 \cdot in}{D_p} \qquad \lambda_2 = 0.06 \qquad \frac{1}{\lambda_2} = 16.698$$

$$i = 0,1..25 \qquad j = 26,27..50$$

$$xm(x) = xfs(x) \cdot \lambda_2 \qquad ym(y) = yfs(y) \cdot \lambda_2$$

Better Slice Strut Offsets $\qquad \lambda_2 = 0.06$

$$xscale(x1) = \frac{x1 \cdot 12 \cdot \lambda_2}{ft} \qquad\qquad yscale(x1) = body1(x1) \cdot 12 \cdot \lambda_2$$

Weight / Volume Balance

Density of PVC

$$D_r = 6.1875 \cdot in \qquad L_r = 7.9375 \cdot in$$

diameter and length of rod weighed

$$V_r = \pi \cdot \left(\frac{D_r}{2}\right)^2 \cdot L_r \qquad V_r = 0.138 \cdot ft^3$$

volume of 1 foot of rod

$$\rho_{pvc} = \frac{11.7 \cdot lb}{V_r} \qquad \rho_{pvc} = 84.708 \cdot lb \cdot ft^{-3}$$

density of the PVC

$$\rho_{fw} = 62.311 \cdot lb \cdot ft^{-3}$$

density of FW at 68°F.

Displaced Volume

$$V_{model} = VOLUME \cdot \lambda_2^3$$

$$V_{model} = 1.324 \cdot ft^3$$

Bouyant Force

$$F_b = V_{model} \cdot \rho_{fw} \qquad F_b = 82.523 \cdot lb$$

Weight Account

FRAME

$$W_f = 15 \cdot lb$$

Force Block + Heave Post

$$W_{bl} = 25 \cdot lb$$

Parallel Midbody X 4 pods

$$L_{pmb} = 6.7 \cdot in$$

$$V_{pvcpmb} = \left[\pi \cdot \left(\frac{5.5625}{2} \cdot in \right)^2 - \pi \cdot \left(\frac{5.5625 - 0.5}{2} \cdot in \right)^2 \right] \cdot L_{pmb} \cdot 4$$

$$V_{pvcpmb} = 0.065 \cdot ft^3$$

$$W_{pmb} = V_{pvcpmb} \cdot \rho_{pvc} \qquad\qquad W_{pmb} = 5.482 \cdot lb$$

Pod Nose and Tail x 4 pods

$$V_{podnt} = V_{pods} \cdot 2 - 4 \cdot L_{pmb} \cdot \pi \cdot \left(\frac{5.5625}{2} \cdot in \right)^2 \qquad \text{volume of the nose and tail}$$

$$V_{podnt} = 0.645 \cdot ft^3$$

$$V_{nbore1} = \pi \cdot (2.25 \cdot in)^2 \cdot 1.25 \cdot in \cdot 2 \qquad V_{nbore1} = 39.761 \cdot in^3$$

$$V_{nbore2} = \pi \cdot (2.0 \cdot in)^2 \cdot 1 \cdot in \cdot 2 \qquad V_{nbore2} = 25.133 \cdot in^3$$

$$V_{nbore3} = \pi \cdot (1.5 \cdot in)^2 \cdot 2 \cdot in \cdot 2 \qquad V_{nbore3} = 28.274 \cdot in^3$$

$$V_{nbore4} = \pi \cdot (1.25 \cdot in)^2 \cdot 1.0 \cdot in \cdot 2 \qquad V_{nbore4} = 9.817 \cdot in^3$$

$$V_{nbore5} = \pi \cdot (0.75 \cdot in)^2 \cdot 1.0 \cdot in \cdot 2 \qquad V_{nbore5} = 3.534 \cdot in^3$$

$$V_{tbore1} = \pi \cdot (2.25 \cdot in)^2 \cdot 2 \cdot in \cdot 2 \qquad V_{tbore1} = 63.617 \cdot in^3$$

$$V_{tbore2} = \pi \cdot (2.0 \cdot in)^2 \cdot 3 \cdot in \cdot 2 \qquad V_{tbore2} = 75.398 \cdot in^3$$

$$V_{tbore3} = \pi \cdot (1.5 \cdot in)^2 \cdot 2 \cdot in \cdot 2 \qquad V_{tbore3} = 28.274 \cdot in^3$$

$$V_{tbore4} = \pi \cdot (1.0 \cdot in)^2 \cdot 2 \cdot in \cdot 2 \qquad V_{tbore4} = 12.566 \cdot in^3$$

$$V_{tbore5} = \pi \cdot (0.5 \cdot in)^2 \cdot 1 \cdot in \cdot 2 \qquad V_{tbore5} = 1.571 \cdot in^3$$

113

$$V_{bore} \quad V_{nbore1} - V_{nbore2} - V_{nbore3} + V_{nbore4} - V_{nbore5} + V_{tbore1} \cdots$$
$$+ V_{tbore2} - V_{tbore3} - V_{tbore4} + V_{tbore5}$$

$$V_{bore} = 287.947 \cdot in^3$$

$$V_{pvcpod} = V_{podnt} - V_{bore}$$

$$V_{pvcpod} = 0.479 \cdot ft^3$$

$$W_{podnt} = V_{pvcpod} \cdot \rho_{pvc} \qquad W_{podnt} = 40.547 \cdot lb$$

4 Struts

$$V_s = Area + \lambda_2^2 \cdot 6 \cdot in \qquad V_s = 0.427 \cdot ft^3$$

$$V_{sbore} = 4 \cdot (10 \cdot in \cdot 1.8 \cdot in \cdot 6 \cdot in) \qquad V_{sbore} = 0.25 \cdot ft^3$$

$$V_{sbore2} = 4 \cdot (2.75 \cdot in \cdot 0.7 \cdot in \cdot 6 \cdot in) \cdot 2 \qquad V_{sbore2} = 0.053 \cdot ft^3$$

$$V_{pvcstr} = V_s - V_{sbore} - V_{sbore2} \qquad V_{pvcstr} = 0.124 \cdot ft^3$$

$$W_{struts} = V_{pvcstr} \cdot \rho_{pvc}$$

$$W_{struts} = 10.499 \cdot lb$$

Other Model Supplies

$$W_{oth} = 5 \cdot lb$$

Checking for a Balance

$F_{brd} = 10 \cdot lb$ Desired Reserve Bouyancy

$$W_{model} = W_f + W_{bl} + W_{pmb} - W_{podnt} - W_{struts} - W_{oth}$$

$W_{model} = 101.527 \cdot lb$ Actual Model Weight

$F_{bra} = F_b - W_{model}$ Actual Reserve Bouyancy (Should = R_{bd})

$F_{bra} = -19.005 \cdot lb$

$F_{bra} \quad F_{brd} = -29.005 \cdot lb$ Must be 0 or greater.

Areas to Help the Balance

reserve = areas with excess weight included that can be trimmed down by the indicated ammount

$$r_f = 2 \cdot lb \quad \text{frame} \qquad r_{bl} = 0 \cdot lb \quad \text{force block} \qquad r_{oth} = 1 \cdot lb \quad \text{other model items}$$

$$\text{reserve} = r_f + r_{bl} + r_{oth}$$

$$\text{fixed} = W_f + W_{bl} + W_{oth} - \text{reserve} \qquad \text{Weights that are unchangable}$$

excess = reserve bouyancy that is desired but not needed

$$\text{excess} = 0 \cdot lb$$

$$F_{br} = F_{brd} - \text{excess}$$

Calculate the upper limits for strut/nose and tail cone weights

$$W_{modelmax} = F_b - F_{br}$$

$$W_{spa} = \frac{W_{modelmax} - \text{fixed}}{4} \qquad \text{The Max Allowed weight for a single strut/pod combination}$$

$$W_{spa} = 7.631 \cdot lb$$

$$\frac{W_{struts}}{4} - \frac{W_{podnt}}{4} - \frac{W_{pmb}}{4} = 14.132 \cdot lb \qquad \text{Calculated Weight of a single strut/pod combination}$$

Summation of Allowed Weights

$$W_f - r_f = 13 \cdot lb \qquad \text{Frame Weight}$$

$$W_{bl} - r_{bl} = 25 \cdot lb \qquad \text{Force Block and Heave Post}$$

$$W_{oth} - r_{oth} = 4 \cdot lb \qquad \text{Miscalleanous Weight Allowed}$$

$$W_{spa} = 7.631 \cdot lb \qquad \text{The Max Allowed weight for a single strut/pod combination}$$

115

Model Dimmensions

$$\lambda_m = \frac{1}{16.68}$$

$$Lstrut_m = L_l \cdot \lambda_m \qquad\qquad Lstrut_m = 1.439 \cdot ft$$

$$WSstrut_m = WS_s \cdot \lambda_m^2 \qquad\qquad WSstrut_m = 1.059 \cdot ft^2$$

$$Lpod_m = L_p \cdot \lambda_m \qquad\qquad Lpod_m = 2.32 \cdot ft$$

$$WSpod_m = WS_{fs} \cdot \lambda_m^2 \qquad\qquad WSpod_m = 2.642 \cdot ft^2$$

Appendix D

Model M-3 Optimized SWATH
Table of Offsets
and
Design Worksheet

Model M-3 Table of Offsets

Demihull Offsets
in inches

Strut Offsets
in inches

$xh12 \cdot ft^{-1} \cdot 12$ $OFF(xh12) \cdot ft^{-1} \cdot 12$

$x1 \cdot ft^{-1} \cdot 12$ $body1(x1) \cdot ft^{-1} \cdot 12$

$xh12 \cdot ft^{-1} \cdot 12$	$OFF(xh12) \cdot ft^{-1} \cdot 12$		$x1 \cdot ft^{-1} \cdot 12$	$body1(x1) \cdot ft^{-1} \cdot 12$
0	0		0	0
0.794	0.667		0.794	0.26
1.589	1.212		1.589	0.488
2.383	1.641		2.383	0.685
3.178	1.959		3.178	0.852
3.972	2.173		3.972	0.99
4.766	2.294		4.766	1.099
5.561	2.335		5.561	1.182
6.355	2.303		6.355	1.24
7.15	2.285		7.15	1.275
7.944	2.268		7.944	1.29
8.738	2.25		8.738	1.291
9.533	2.232		9.533	1.291
10.327	2.214		10.327	1.291
11.122	2.196		11.122	1.29
11.916	2.178		11.916	1.275
12.71	2.16		12.71	1.24
13.505	2.142		13.505	1.182
14.299	2.124		14.299	1.099
15.094	2.107		15.094	0.99
15.888	2.089		15.888	0.852
16.682	2.071		16.682	0.685
17.477	2.053		17.477	0.488
18.271	2.035		18.271	0.26
19.066	2.017		19.066	$-1.147 \cdot 10^{-15}$
19.86	2.313			
20.654	2.48			
21.449	2.647			
22.243	2.814			
23.038	2.78			
23.832	2.78			
24.626	2.78			
25.421	2.78			
26.215	2.78			
27.01	2.78			
27.804	2.78			
28.598	2.78			
29.393	2.78			

Model M-3 The High Speed Swath

This variant uses the same gross dimmensions as the baseline SLICE but uses a shape characteristic of a high speed swath. Tandem strut design was selected to minimize strut displacement.

1a. Units Defined

$ft \equiv 1 L$ $lb \equiv 1 M$ $sec \equiv 1 T$ Base Units

$nm = 6076 \cdot ft$ Nautical Mile

$kt = 1 \dfrac{nm}{hr}$ Knot

$lton = 2240 \cdot lb$ Long Ton

1b. Fixed Variables

$\lambda = 0.0662$

$\rho_{sw} = 1.9912 \cdot lb \cdot \dfrac{sec^2}{ft^4}$ Density of Salt Water at 56° F. An assumed average operating temperature.

$\nu_{sw} = 1.3343 \cdot 10^{-5} \cdot \dfrac{ft^2}{sec}$ Kinematic Viscosity of Salt Water at 56° F.

$\rho_{fw} = 1.9367 \cdot lb \cdot \dfrac{sec^2}{ft^4}$ Density of Fresh Water at 68° F. An assumed average tow tank temperature. Use this if prediction is for a model test.

$\nu_{fw} = 1.0804 \cdot 10^{-5} \cdot \dfrac{ft^2}{sec}$ Kinematic Viscosity of Fresh Water at 68° F.

$g = 32.174 \cdot ft \cdot sec^{-2}$ Acceleration due to gravity

*** $V = 0 \cdot kt, 1 \cdot kt .. 35 \cdot kt$ Modify this to reflect the velocity range of interest.

1c. Indicator Settings

Water

$$SW = 0$$

"1" indicates the ship is operating in Salt Water
"0" indicates the ship is operating in Fresh Water

$$\rho = if(SW=1, \rho_{sw}, \rho_{fw})$$

$$\nu = if(SW=1, \nu_{sw}, \nu_{fw})$$

Body Segmentation

$$seg = 1 \cdot ft \cdot \lambda$$

2a. Hull Component and Required Displacement Definition

*** $\Delta_d = 177 \cdot lton \cdot \lambda^3$ This defines the the requireded ($_d$) displacement of the vessel

$$V_d = \Delta_d \cdot \frac{1}{\rho \cdot g} \qquad V_d = 2 \cdot ft^3 \qquad \text{The requireded ($_d$) displaced volume}$$

2a.i. Strut Creation

Strut Height

$H = 8 \cdot ft \cdot \lambda$ Desired to allow demi hull submergence of at least one diameter.

$H = 6.355 \cdot in$

Strut Beam

*** $B_1 = 3.25 \cdot ft \cdot \lambda$ Maximum Strut Beam Required *Defind per the Baseline Considered a required parameter.*

$B_1 = 2.582 \cdot in$

Overall Strut Length

••• $L_1 = 24 \cdot ft \cdot \lambda$ Overall Strut Length

$L_1 = 19.066 \cdot in$

Length to Beam Ratio

$$LB1 = \frac{L_1}{B_1} \qquad LB1 = 7.385 \quad \text{Length to Maximum Beam Ratio}$$

120

Length Breakdown

$$\text{***} \quad L_{pmbl} = 3 \cdot ft \cdot \lambda \qquad \text{Length of Parallel Midbody}$$

$$\text{***} \quad L_{nl} = 0.5 \cdot L_l - L_{pmbl} \qquad L_{nl} = 0.695 \cdot ft \; \text{Strut Nose Length} \; \textit{(2.4 x D is optimum)}$$

$$L_{tl} = L_l - L_{pmbl} - L_{nl} \qquad L_{tl} = 0.695 \cdot ft \; \text{Strut Tail Length} \; \textit{(3.6 x D is optimum)}$$

Strut Nose and Tail Shape Exponent

$$\text{***} \quad n_{ns} \equiv 2.25 \qquad\qquad \text{***} \quad n_{ts} \equiv 2.25$$

Calculation of Nose and Midbody Shape

$$xl = 0 \cdot ft, seg.. \; L_{nl} - L_{pmbl} \qquad \text{defines the x values of the subdivisions}$$

$$ynl(xl) = \frac{B_l}{2} \left[1 - \left(\frac{L_{nl} - xl}{L_{nl}} \right)^{n_{ns}} \right] \qquad \text{defines the y values of the nose based on a parabola}$$

$$ypmbl(xl) = \frac{B_l}{2} \qquad\qquad\qquad \text{defines the y values of the midsection}$$

$$Al(xl) = if\left(xl \leq L_{nl}, ynl(xl), ypmbl(xl) \right)$$

Calculation of Tail Shape

$$xl = 0 \cdot ft, seg.. \; L_{nl} - L_{pmbl} - L_{tl} \qquad \text{defines the x values of the subdivisions}$$

$$ytl(xl) = \frac{B_l}{2} \left[1 - \left(\frac{xl - L_{nl} - L_{pmbl}}{L_{tl}} \right)^{n_{ts}} \right] \qquad \text{defines the y values based on a parabola}$$

$$bodyl(xl) = if\left(xl \leq L_{nl} - L_{pmbl}, Al(xl), ytl(xl) \right) \qquad \text{Function that defines the body geometry}$$

Strut Section

2.a.ii. Wetted Surface and Volume Calculation For the Struts

Perimeter

Nose

$$N_p = 0.5 \cdot \overline{B_1^2 - 16 \cdot L_{nl}^2} - \frac{B_1^2}{8 \cdot L_{nl}} \cdot \ln\left(\frac{4 \cdot L_{nl} - \overline{B_1^2 - 16 \cdot L_{nl}^2}}{B_1}\right)$$

$$N_p = 1.421 \cdot ft$$

Tail

$$T_p = 0.5 \cdot \overline{B_1^2 - 16 \cdot L_{tl}^2} - \frac{B_1^2}{8 \cdot L_{tl}} \cdot \ln\left(\frac{4 \cdot L_{tl} - \overline{B_1^2 - 16 \cdot L_{tl}^2}}{B_1}\right)$$

$$T_p = 1.421 \cdot ft$$

Midsection

$$S_p = 2 \cdot L_{pmbl}$$

$$S_p = 0.397 \cdot ft$$

Total Perimeter

$$P = N_p - S_p + T_p$$

$$P = 3.24 \cdot ft$$

Wetted Surface of the Strut

$$WS_s = P \cdot H \qquad WS_s = 1.716 \cdot ft^2 \qquad \text{for one strut}$$

Areas

nose area

$$N_a = \frac{2}{3} \cdot L_{nl} \cdot B_l \qquad N_a = 0.1 \cdot ft^2$$

tail area

$$T_a = \frac{2}{3} \cdot L_{tl} \cdot B_l \qquad T_a = 0.1 \cdot ft^2$$

mid section area

$$S_a = B_l \cdot L_{pmbl} \qquad S_a = 0.043 \cdot ft^2$$

Total Area

$$Area = N_a + S_a + T_a \qquad Area = 0.242 \cdot ft^2$$

Volume per Strut

$$vol = Area \cdot H \qquad vol = 0.128 \cdot ft^3$$

Total Strut Volume

$$VOL_s = 4 \cdot vol \qquad VOL_s = 0.513 \cdot ft^3$$

2.a.iii Demi-Hull Creation

Demi Hull Volume Required

$$V_{dh} = V_d - VOL_s \qquad V_{dh} = 1 \cdot ft^3 \qquad \text{for two hulls}$$

$$\frac{V_{dh}}{2} = 0.7 \cdot ft^3 \qquad \text{per demihull}$$

Demi Hull Shape

$$D_h = 7 \cdot ft \cdot \lambda$$ Max diameter of the Hull $D_h = 5.561 \cdot in$

$D_{h1} = 0.84 \cdot D_h$	$D_{h1} = 4.671 \cdot in$	Section #1-2 interface
$D_{h2} = .73 \cdot D_h$	$D_{h2} = 4.059 \cdot in$	Section #2-3 interface
$D_{h3} = D_h$	$D_{h3} = 5.561 \cdot in$	Section #3-4 interface
$D_{h4} = D_h$	$D_{h4} = 5.561 \cdot in$	Section #4-5 interface
$D_{h5} = .73 \cdot D_h$	$D_{h5} = 4.059 \cdot in$	Section #5-6 interface
$D_{h6} = .84 \cdot D_h$	$D_{h6} = 4.671 \cdot in$	Section #6-7 interface

$$L_h = 90 \cdot ft \cdot \lambda$$ Overall Length of the hull. $L_h = 5.958 \cdot ft$

$L_{h1} = 0.08 \cdot L_h$	$L_{h1} = 5.72 \cdot in$	Section #1
$L_{h2} = .19 \cdot L_h$	$L_{h2} = 13.584 \cdot in$	Section #2
$L_{h3} = 0.05 \cdot L_h$	$L_{h3} = 3.575 \cdot in$	Section #3
$L_{h4} = 0.25 \cdot L_h$	$L_{h4} = 17.874 \cdot in$	Section #4
$L_{h5} = 0.15 \cdot L_h$	$L_{h5} = 10.724 \cdot in$	Section #5
$L_{h6} = 0.09 \cdot L_h$	$L_{h6} = 6.435 \cdot in$	Section #6
$L_{h7} = 0.19 \cdot L_h$	$L_{h7} = 13.584 \cdot in$	Section #7

$$L2D = \frac{L_h}{D_h} \qquad L2D = 12.857$$

Segment 1 & 2

Calculation of Nose Cone Shape

$$n_{n1} = 2.25$$ Nose cone shape exponent

$$xh12 = 0 \cdot ft, \cdot seg.. \cdot (L_{h1} + L_{h2})$$ defines the x values of
the subdivisions

the subdivisions

$$yh1(xh12) = \frac{D_{h1}}{2}\left[1 - \left(\frac{L_{h1} - xh12}{L_{h1}}\right)^{n\,n1}\right]$$

defines the y values of the nose based on an ellipse

$$yh2(xh12) = \frac{D_{h1}}{2} - \frac{D_{h2} - D_{h1}}{2\,L_{h2}}\left[\left(xh12 - L_{h1} - seg\right)\right]$$

defines the y values of section 2

$$A1(xh12) = if\left(|xh12| < L_{h1}, yh1(xh12), yh2(xh12)\right)$$

offsets for the first two body segments.

Adding in Segment 3

$$xh12 = 0\,ft, -seg.. \; L_{h1} - L_{h2} - L_{h3}/$$

defines the x values of the subdivisions

$$yh3(xh12) = \frac{D_{h2}}{2} - \frac{D_{h3} - D_{h2}}{2\,L_{h3}}\left(xh12 - L_{h1} - L_{h2} - seg\right)$$

defines the y values of section 3

$$B1(xh12) = if\left(xh12 < L_{h1} - L_{h2}, A1(xh12), yh3(xh12)\right)$$

offsets for the first three body segments.

Adding in Segment 4

$$xh12 = 0\,ft, -seg.. \; L_{h1} - L_{h2} - L_{h3} - L_{h4}/$$

defines the x values of the subdivisions

$$yh4(xh12) = \frac{D_{h3}}{2}$$

defines the y values of section 4

$$C1(xh12) = if\left(xh12 < L_{h1} - L_{h2} - L_{h3}, B1(xh12), yh4(xh12)\right)$$

offsets for the first three body segments.

Adding in Segment 5

$$xh12 = 0\,ft, -seg.. \; L_{h1} - L_{h2} - L_{h3} - L_{h4} - L_{h5}$$

defines the x values of the subdivisions

$$yh5(xh12) = \frac{D_{h4}}{2} - \frac{D_{h5} - D_{h4}}{2\,L_{h5}}\left(xh12 + L_{h1} - L_{h2} - L_{h3} + L_{h4} - seg\right)$$

defines the y values of section 5

$$D1(xh12) = \text{if}\left(xh12 < L_{h1} + L_{h2} + L_{h3} + L_{h4}, C1(xh12), yh5(xh12)\right)$$

offsets for the first three body segments.

Adding in Segment 6

$$xh12 = 0 \cdot ft, \cdot seg.. \cdot L_{h1} + L_{h2} + L_{h3} + L_{h4} + L_{h5} + L_{h6}/ \qquad \text{defines the x values of the subdivisions}$$

$$yh6(xh12) = \frac{D_{h5}}{2} - \frac{D_{h6} - D_{h5}}{2 \cdot L_{h6}} \cdot \left[xh12 + L_{h1} + L_{h2} + L_{h3} + L_{h4} + L_{h5}/ - seg \right]$$

defines the y values of section 6

$$E1(xh12) = \text{if}\left(xh12 < L_{h1} + L_{h2} + L_{h3} + L_{h4} + L_{h5}, D1(xh12), yh6(xh12) \right)$$

offsets for the first three body segments.

Adding in Segment 7

$$xh12 = 0 \cdot ft, \cdot seg.. \cdot L_{h1} + L_{h2} + L_{h3} + L_{h4} + L_{h5} + L_{h6} + L_{h7}/ \qquad \text{defines the x values of the subdivisions}$$

$$yh7(xh12) = \frac{D_{h6}}{2} - \frac{-D_{h6}}{2 \cdot L_{h7}} \cdot \left[xh12 + L_{h1} + L_{h2} + L_{h3} + L_{h4} + L_{h5} + L_{h6} - seg \right]$$

defines the y values of section 7

$$OFF(xh12) = \text{if}\left(xh12 < L_{h1} + L_{h2} + L_{h3} + L_{h4} + L_{h5} + L_{h6}, E1(xh12), yh7(xh12) \right)$$

offsets for the first three body segments.

126
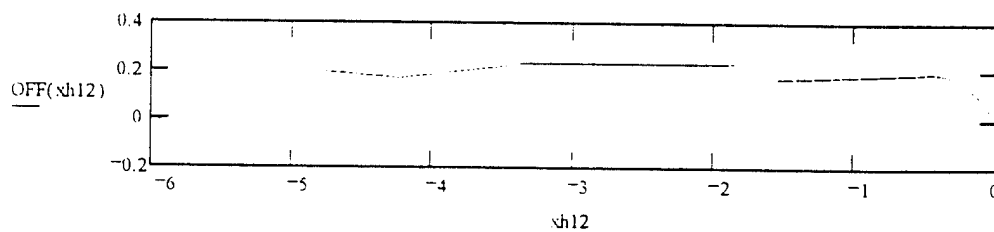
Wetted Surface of TWO demihulls

$$WS_h = 2 \cdot \int_{-0\cdot ft}^{\cdot L_h} 2\cdot\pi\cdot OFF(xh12)\,dxh12 \qquad WS_h = 13.2\cdot ft^2$$

Volume of TWO demihulls

$$VOL_h = 2 \cdot \int_{-0\cdot ft}^{\cdot L_h} \pi\cdot OFF(xh12)^2\,dxh12 \qquad VOL_h = 1.3\cdot ft^3$$

Volume Balance

Available

$$VOL_{avail} = VOL_h - VOL_s$$

$$VOL_{avail} = 1.8\cdot ft^3$$

$$\Delta_{avail} = VOL_{avail}\cdot\rho\cdot g$$

$$\Delta_{avail} = 112.5\cdot lb$$

Required

$$V_d = 1.8\cdot ft^3$$

Excess Volume

$$VOL_{avail} - V_d = 0\cdot ft^3 \qquad \text{(negative implies insufficient volume)}$$

Deck Area Lost compared to SLICE

$C = 3\cdot ft$ This is the combined ammount the bow/stern are cantelivered over the ends of the hulls.

$$\left(105\cdot ft - \frac{L_h}{2} - C\right)\cdot 55\cdot ft = 660\cdot ft^2 \qquad \text{(negative implies a gain in deck area)}$$

127

Model Building Balance

Bouyant Force

$$F_b = \Delta_{avail} \qquad\qquad F_b = 112.496 \cdot lb$$

Weight Account

FRAME

$$W_f = 18 \cdot lb$$

Force Block + Heave Post

$$W_{bl} = 25 \cdot lb$$

Other Model Supplies

$$W_{oth} = 2 \cdot lb$$

Desired Reserve Bouyancy

$$F_{brd} = 0.05 \cdot F_b$$

$$F_{brd} = 5.625 \cdot lb$$

Allowed Weight of a demihull + 2 Strut combo

$$W_{sp} = \frac{F_b - W_f - W_{bl} - W_{oth} - F_{brd}}{2}$$

$$W_{sp} = 30.936 \cdot lb$$

Appendix E

Project Test Plan

and

Test Journal

SLICE Project Test Plan for the Week of 6-10 March 1995

Anticipated Number of Models to Test: 4

Desired Data to Obtain: Resistance (x) for all 4 models, Dynamic Sinkage (z) for 2 models.

Model Descriptions: Model M-1 is the LMSC baseline design.
Model M-2 anticipates improvements to the LMSC baseline by improving the shape of the bodies but retaining the gross geometry of the baseline ship.
Model M-3 is an optimized SWATH based on the results presented by McGregor
Model M-4 is the Mid Foil Concept.

Desired Testing Schedule:

6 March 95	Set-Up M-1; M-1 Test 1	20runs
7 March 95	M-1 Test 2; Set-Up M-2; M-2 Test 1	30 runs
8 March 95	M-2 Test 1(finish) ; Set-Up M-3; M-3 Test 1	30runs
9 March 95	M-3 Test 1 (finish); M-3 Test 2	30 runs
10 March 95	Set-Up M-4; M-4 Test 1	20 runs

Test Description:

Test 1: Resistance Locked in Heave and Pitch.

Objective: To measure forces in the X and Z directions over the operating range of speeds.

Discussion: Previous testing has indicated that a significant Z force is generated and that the magnitude of the force is geometry dependent. This method of testing replicates the LMSC methodology and therefore allows for a basis of model comparison with LMSC results. The LMSC justification for this methodology is that control surfaces will be employed to fix the operational draft.

Description: With the model rigidly fixed to the carriage, the following sequence of speeds will be used to collect data for both X and Z forces : Model Scale Equivalent (MSE) of 3,6,9,12,16,20,25,30,35,40 kts for basic data. Each speed will accomplished with one run. Then MSE of 20,25,30,35,40 kts to demonstrate repeatability. If time in the day permits then additional runs will be made at MSE of 10,11,13,14 and 22 kts to fill in hump data and the high speed knuckle. This represents a total of 20 runs for the test completion.

Test 2: Free to Heave.

Objective: To quantify the difference in resistance results for a model rigidly fixed and one that is allowed to oscillate about a desired waterline.

Discussion: Although control surfaces may hold the ship to a fixed depth in a gross sense of the word, it is unlikely that the system's sensitivity will exactly replicate a rigid mounting. This test will use a counterbalance to replicate the control surface but allow the model to oscillate about this point.

Description: This test will use the Z force results from Test 1 to determine the counterbalance weight required. The model will be attached to the carriage free to heave but locked in all other respects. The necessary counterbalance weight be added and the model towed at the given speed. *(Note, due to the small TPI associated with SWATH vessels, a method for adding the weight as the carriage comes to speed may be necessary. This is a Discussion Point for the 3 Feb meeting.)* The test rig will require a positive stop in the negative z direction with a method of determining that the stop has been reached. This stop must be set to no more than 3 inches above the design waterline of the model.

The following sequence of speeds will be used to collect data for X force only with note being taken of the counterbalance weight added. Model Scale Equivalent (MSE) of 9,12,16,20,25,30,35,40 kts for basic data. Each speed will accomplished with one run. Then MSE of 20,25,30,35,40 kts to demonstrate repeatability. If time in the day permits then additional runs will be made at MSE of 3, 6,10,11,13,14 and 22 kts to fill in hump data and the high speed knuckle. This represents a total of 20 runs for the test completion.

3/6/95

0800 ARRIVED USNA

0830 VAN UNLOADED, checked over models, all
      Travelled undamaged.

0911 Discussed Model Construction techniques
      w/ Don Bunker. Construction Technique
      appears reasonable in all 4 models.

1100 Marked waterlines on Baseline Model.
      To Level out, following shims are
      Required:

          Pod #1 FWD   0.224"   4
          Pod #1 AFT   0.174"   3
          Pod #2 FWD   0.039"   3
          Pod #2 AFT   0"   0
          Pod #3 FWD   0.014"   0
          Pod #3 AFT   0.254"   4
          Pod #4 FWD   0.19"   3
          Pod #4 AFT   0.21"   3   0.218" actual
                                        ↑

      Decided to add shim in whole # increments of
      washers of 0.06" Thickness. Max
      error this should induce is 0.03" or
      an angle of attack of 0.17° ⟷
      This is a building error of 0.5"

1230 Wedges installed in M-1

1400 FRAME ASSEMBLED AND FULLY ALIGNED.

1430 INSTALLING MATLAB 5.0 — writing Data Reduction

132

3/6/99

ORGANIZED

1445 Called Cambridge to check in.

1515 Working on Shimming/Aligning Model.

Required Separation (TRANSVERSE) between Pods
Set as:

        FWD (23") Measured Lead EDGE   23 1/16"

                  Measured Trail EDGE   23 1/16"

      AFT (32.5") Measured Lead EDGE   32 3/16"

                  TRAIL EDGE   32 1/4"

Also measured Top to Bottom of Trail Edge of
Struts to check for Toe in:
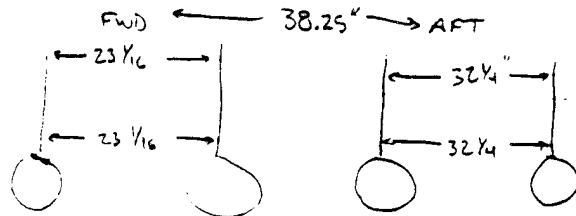
1551 Model in water to be connected to Carriage.

1610 M-2 is attached to the carriage for final in heave test.

1630 Sanding Gloss off #1(M-2) — Don Banka did same for M-1 earlier today. Note: Gloss finish tends to overly optimistic results. Should use a matte finish!

133

3/6/95

1745   Made DWL markings on one pod of M-2

3/7/95

0735   Don/STEVE SETTING UP INSTRUMENTATION, I AM
        FINISHING MARKINGS ON M-2. ⟷ NOTE: MARKINGS
        IN ALL models are done a 1-inch spacing.

0835   CALCULATED SHIM REQUIREMENTS FOR M-2

              Pod # 1   FWD
                        AFT
              Pod # 2   FWD
                        AFT
              Pod # 3   FWD
                        AFT
              Pod # 4   FWD
                        AFT

0927   Model M-2 drafts are finished/ shim reqs' calculated
        Finishing Instrumentation /photo set up.

        Collecting data about 1300. Mapping out the Baseline
        ship before we move. ___ at high speed on 2
        pump is significant. Not so on low speed ___

1315   Completed data collection for the Base- Requirements

134

____ of M-1 T20T _____

Now we are modifying the model to add
a spray rail on 3rd fwd edge of the aft
pod.

HUM
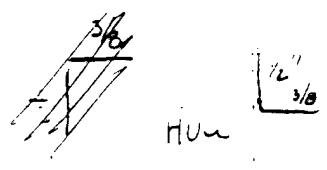
Total length = 15"   pit 6"/9"

→ The spray rail test was done at 30, 35, 40 ±5
set there as no conclusive measurable result.
Enjoyment in the prime appe to se
more from the rooster tail of the ag trailing
edge of the fwd strut/pod rather than
sni. from the sides of the struts — spray
rails won't help this

TP View   Small
                           amount
                           spray.

         small
         amount of
         spray

                  Serious Spray.

1515- Setting up M-2 for Test 1 -

FWD ← -1" → AFT
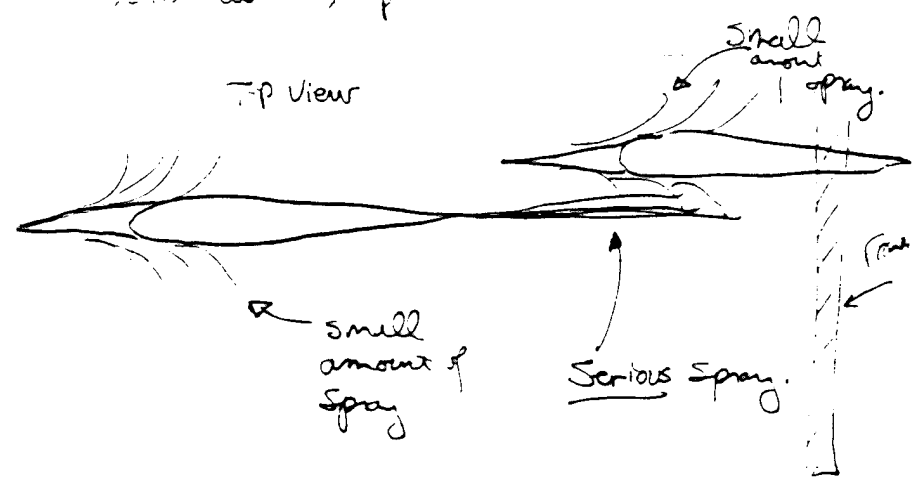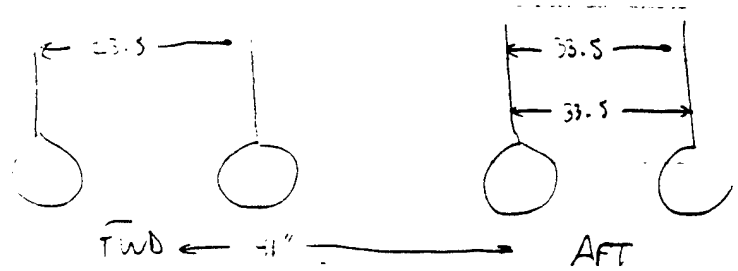
FWD	L.E. measured	23.5
	T.E. Measured	23 7/8
AFT	L.E. Measured	33.5
	T.E. MEASURED	33.5

1550 Began testing M-2 For Test 1

1620 STOPPED TESTING FOR THE DAY

2200 Reducing Data —
        Synopsis of Data collected for M-2 Test 1

          # of INDIVIDUAL DATA POINTS : 21
          # of REPEATED VALUES   5
        TOTAL # of POINTS TO define Curve 16

FULL SCALE SPEEDS DATA COLLECTED AT (in knots)

3, 6, 9, 10(x4), 11, 12, 13, 13.5, 14, 15, 16,
20(x4), 25(x4), 30(x4), 35, 40(x4)

The 13.5 knot data point was an incidental
carriage set-up point, not intentionally
sought after.

Test 1 analyzed for spray rails.
\# of individual data points: 3
\# of repeats   0
Total points to define curve 3

Overall, the usefulness of the spray rails
was not apparent. The effect in the 3 runs
was sporadic and the principle spray
rail data appears to be the
effects seen in the Boston Tail (see
the ...)

2230   I have been getting unthread files
       prepared to compare M-1, M-2, M-3
       on an equal footing (i.e same scale factor).

       with the initial spar points n, M-2
       data close fits into a large full scale
       0-12 kts) but data is incomplete

①

3/7/95

2245   GAVE M-3 final Paint Coat.

3/8/95

0745   Marked W/L's on one side of M-3

0900   Water temp = 59.2°F

____   Finished Data runs for M-2 Test 1 ____
        ____ for ____

____   ____ Drawings ____ for M-3 Dennhell ?

1400   Began Swapping M-2 & M-3. Have been Stalling for
        Dave's arrival. Can't wait longer.

1425   Steve Gore/Dave Rossi Show up. Rispa = little later,
        Moran after that. This ties in my afternoon. Don't Gore
        yet M-3 rigged. ℄ spacing is set at ~7¾" 17⅞".

1600   Start getting some data for M-3.

3-9-95.

0900   Resumed Testing M-3

0946   Distance from Tail of M-3 to beginning
        of aft platform = 3ft. ← Important to judge

138

3/9/95

0946 (gnd) water Temp = 59.2°F

1307 Setting M-1 back up for further testing.
              Gross Settings.

         FWD ⟵——— 38¼ ———⟶ AFT

       ⟵— 23" —⟶   ⟵— 32¼ —⟶
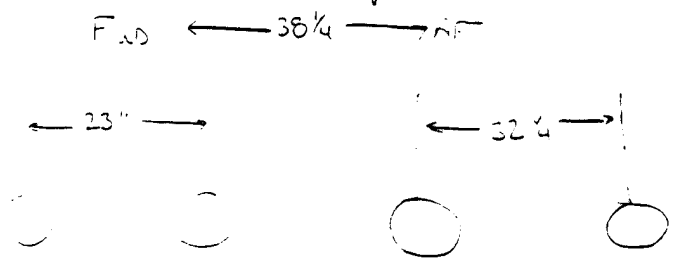
              Final Settings

         F D   L.E.   23⅛"
                T.E.   23¼"
         AFT   L.E.   32"
                T.E.   31½"

1342   M- to be tested to get a few more points
       in the rump.

1346- M-1 Test 2 — This will try to get a
       missing point in the rump map. Second is the
       single point out a few will be trying
       to try to determine any of model
       alignment since model was taken down

3/9/95

1505 – Finished 3 speed test of Z place.
Done at 4?? & 3 fps
Sinking model & below DWL at 1/8"
increments to see if Z would even go to
Zero, or cross zero.

It did cross zero at 4?? & ? fps, not
for 3 fps.

Did again at 7 fps. got zero crossing a
1.25" below dwl.

1507   Reconfiguring M— for Incline Test.

1600   Completed Incline Test. Chatted w/ Steve Louie
        & Art Anderson Engs.

3/10/95

0745   Began making mockup on M-4. Do not
        have a DWL to marked Inches above baseline.

AFT measurements   FWD

T-O View

140

3/10/?5

FWD TO AFT SETUP

1430   First ... test ... data
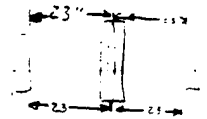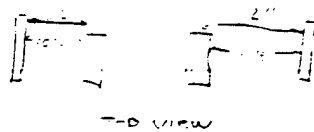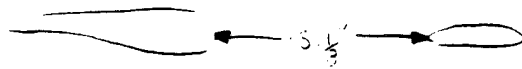
1455   Next test ... constant acceleration at $2.7 f/s^2$
        from ... to ... fps.

447   Conducting constant acc acc test.

540   Conducting spray test = 30 ± 10

Appendix F

Model Test Results

Raw Data

Index of Test Runs Conducted 6-10 March 1995

Run #	Model/Test	Full Scale Equivalent V (Kts)	Test Velocity (FPS)	Drag (Lbf)	Lift (Lbf)
1	M-1 in Baseline Config.	10	4.08	6.46	1.27
2	M-1 in Baseline Config.	3	1.21	0.151	0.191
	M-1 in Baseline Config.	6	2.41	0.689	0.562
	M-1 in Baseline Config.	9	3.64	4.24	1.09
3	M-1 in Baseline Config.	12	4.85	9.08	2.42
	M-1 in Baseline Config.	13.5	5.47	6.16	3.33
6	M-1 in Baseline Config.	16	6.47	5.61	5.18
7	M-1 in Baseline Config.	20	8.08	7.19	7.73
R7	M-1 in Baseline Config.	20	8.08	7.17	7.7
8	M-1 in Baseline Config.	25	10.11	10.66	10.53
9	M-1 in Baseline Config.	30	12.13	19.54	15.52
R9	M-1 in Baseline Config.	30	12.13	19.39	15.46
10	M-1 in Baseline Config.	35	14.14	28.82	21.02
11	M-1 in Baseline Config.	40	16.18	35.32	26.42
12	M-1 in Baseline Config.	10	4.05	6.21	1.02
	M-1 in Baseline Config.	11	4.45	8.91	1.64
14	M-1 in Baseline Config.	13	5.25	6.86	2.74
	M-1 in Baseline Config.	14	5.66	5.65	3.57
16	M-1 in Baseline Config.	15	6.02	5.48	4.25
17	M-1 in Baseline Config.	40	16.18	35.38	26.65
18	M-1 with Spray Rail Aft	30	12.13	19.45	15.48
19	M-1 with Spray Rail Aft	35	14.14	27.95	20.61
20	M-1 with Spray Rail Aft	40	16.18	36.87	26.87
24	M-2 in Baseline Config.	10	4.11	6.83	0.443
25	M-2 in Baseline Config.	3	1.22	0.172	0.247
	M-2 in Baseline Config.	6	2.46	0.667	0.845
27	M-2 in Baseline Config.	9	3.68	4.52	0.416
	M-2 in Baseline Config.	12	4.93	9.92	2.37
28	M-2 in Baseline Config.	6	2.46	0.679	0.724
29	M-2 in Baseline Config.	12	4.93	9.76	2.51
30	M-2 in Baseline Config.	16	6.58	6.28	5.95
31	M-2 in Baseline Config.	16	6.58	6.3	5.89
32	M-2 in Baseline Config.	20	8.23	7.25	9.35
R32	M-2 in Baseline Config.	20	8.23	7.26	9.29
34	M-2 in Baseline Config.	25	10.28	10.23	12.97
R34	M-2 in Baseline Config.	25	10.28	10.19	13.03
36	M-2 in Baseline Config.	30	12.35	14.54	17.52
R36	M-2 in Baseline Config.	30	12.35	14.53	17.48
38	M-2 in Baseline Config.	35	14.4	20.17	22.33
R38	M-2 in Baseline Config.	35	14.4	20.19	22.3
40	M-2 in Baseline Config.	40	16.45	26.42	28.25
R40	M-2 in Baseline Config.	40	16.45	26.36	28.35
42	M-2 in Baseline Config.	11	4.47	9.81	0.77
43	M-2 in Baseline Config.	11.5	4.72	10.78	1.82
44	M-2 in Baseline Config.	13.5	5.47	6.68	3.25
45	M-2 in Baseline Config.	12.5	5.22	7.85	2.86
46	M-2 in Baseline Config.	14.5	5.97	6.05	4.27

48	M-3	6	2.58	0.801	1.01
	M-3	9	3.88	4.22	1.98
49	M-3	12	5.18	6.08	1.08
53	M-3	16	6.91	8.24	4.48
55	M-3	16	6.92	8.22	4.63
56	M-3	18	7.78	8.93	6.4
57	M-3	20	8.65	9.74	7.9
58	M-3 Towed Backwards	7.5	3.48	3.17	1.26
59	M-3	25	10.81	13.87	12
R59	M-3	25	10.81	13.86	11.92
61	M-3	30	13	19.13	16.68
R61	M-3	30	13	19.03	16.56
63	M-3	35	15.13	26	22.39
R63	M-3	35	15.13	25.75	22.19
66	M-3	40	17.29	33.27	28.84
R66	M-3	40	17.29	33.1	28.7
68	M-3	11.5	4.97	6.35	1.27
69	M-3	14	5.97	6.74	2.27
70	M-1 in Baseline Config.	10.25	4.17	6.01	1.87
	M-1 in Baseline Config.	11.25	4.58	7.14	1.42
	M-1 in Baseline Config.	12	4.78	6.75	1.27
71	M-1 in Baseline Config.	10	4.05	6.37	1.13
	M-1 in Baseline Config.	11.5	4.68	9.43	2.29
72	M-1 T+0.5"	11.5	4.71	9.59	-1.13
	M-1 T+1.0"	11.5	4.71		
74	M-1 T+0.25"	11.5	4.67	9.42	0.89
R74	M-1 T+0.375"	11.5	4.7	9.45	0.4
76	M-1 Towed Backwards	20	8.07	-9.91	10.22
77	M-1 Draft Adjustment	15	5.97	See Plots	See Plots
	M-1 Draft Adjustment	15	5.97	See Plots	See Plots
78	M-1 Draft Adjustment	15	5.97	See Plots	See Plots
	M-1 Draft Adjustment	15	5.97	See Plots	See Plots
	M-1 Draft Adjustment	15	5.97	See Plots	See Plots
79	M-1 Draft Adjustment	17.5	6.97	See Plots	See Plots
80	M-1 Draft Adjustment	17.5	6.97	See Plots	See Plots
81	M-1 Draft Adjustment	17.5	6.97	See Plots	See Plots
82	M-1 In Line Config		4.05	6.32	1.27
	M-1 In Line Config		4.85	9.07	2.67
83	M-1 In Line Config		1.21	0.158	0.175
	M-1 In Line Config		2.41	0.693	0.6
84	M-1 In Line Config		3.64	4.41	1
	M-1 In Line Config		6.47	5.74	5.36
85	M-1 In Line Config		8.08	7.1	7.54
86	M-1 In Line Config		10.11	11.48	10.26
87	M-1 In Line Config		12.13	22.29	14.22
88	M-1 In Line Config		14.01	35.17	19.67
89	M-1 In Line Config		16.19	44.51	26.45

144

TEST: Model M-1 Test 1 RUN NO:001
05/30/95 01:44:43

LIFT00.001(LB)-ALL T229/S0
DRAG00.001(LB)-ALL T229/S0
VELO00.001(FPS)-ALL T229/S0

TIME(SEC)
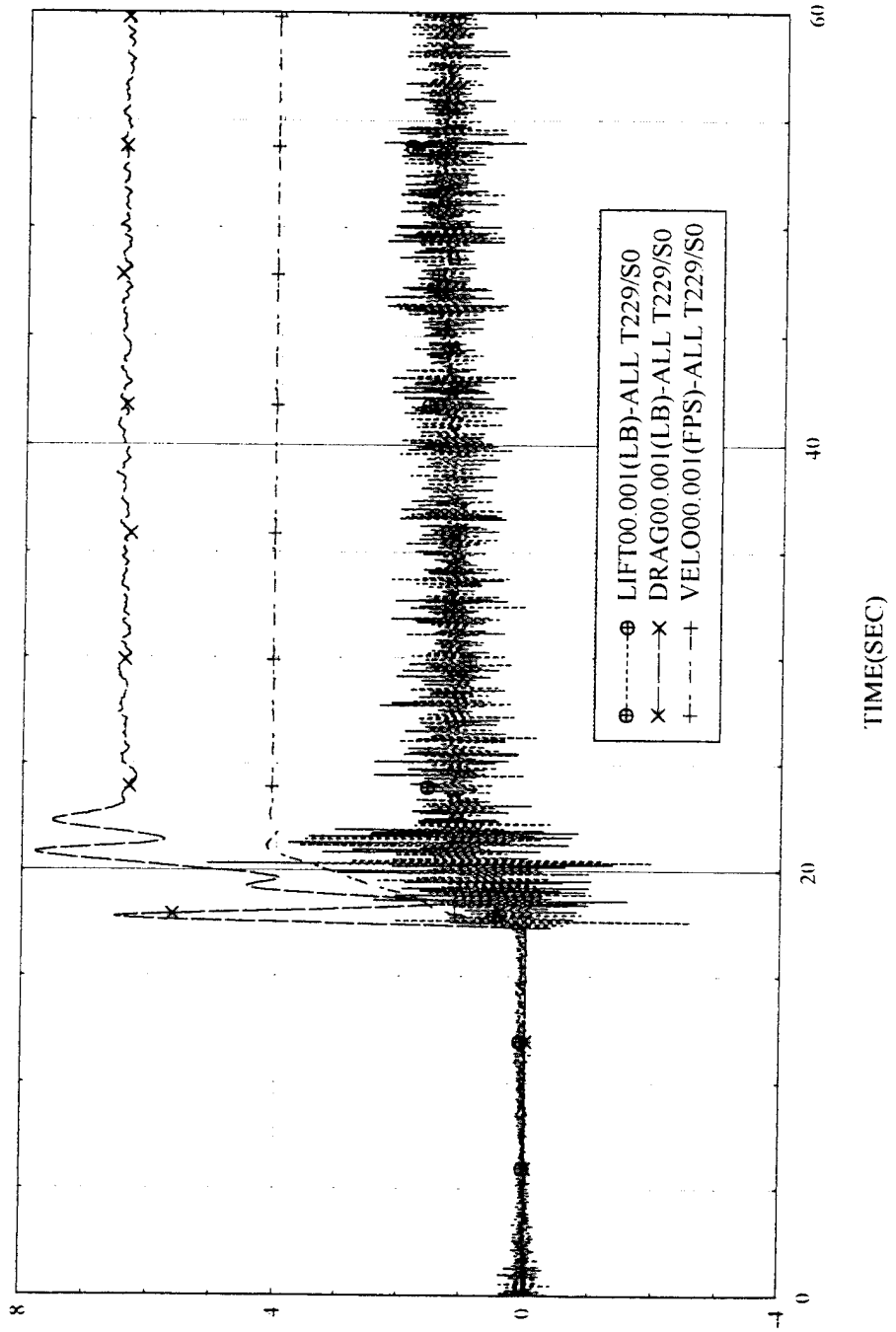
TEST:Model M-1 Test 1 RUN NO:002
05/30/95 01:48:09

TIME(SEC)

TEST:Model M-1 Test 1 RUN NO:003

TIME(SEC)

Legend:
- ⊕ ┈┈ LIFT00.003(LB)-ALL T229/S0
- ✕ ─── DRAG00.003(LB)-ALL T229/S0
- + ─·─ VELO00.003(FPS)-ALL T229/S0

147

TEST:Model M-1 RUN NO.006

LIFT00.006(LB)-ALL T229/S0
DRAG00.006(LB)-ALL T229/S0
VELO00.006(FPS)-ALL T229/S0

TIME(SEC)
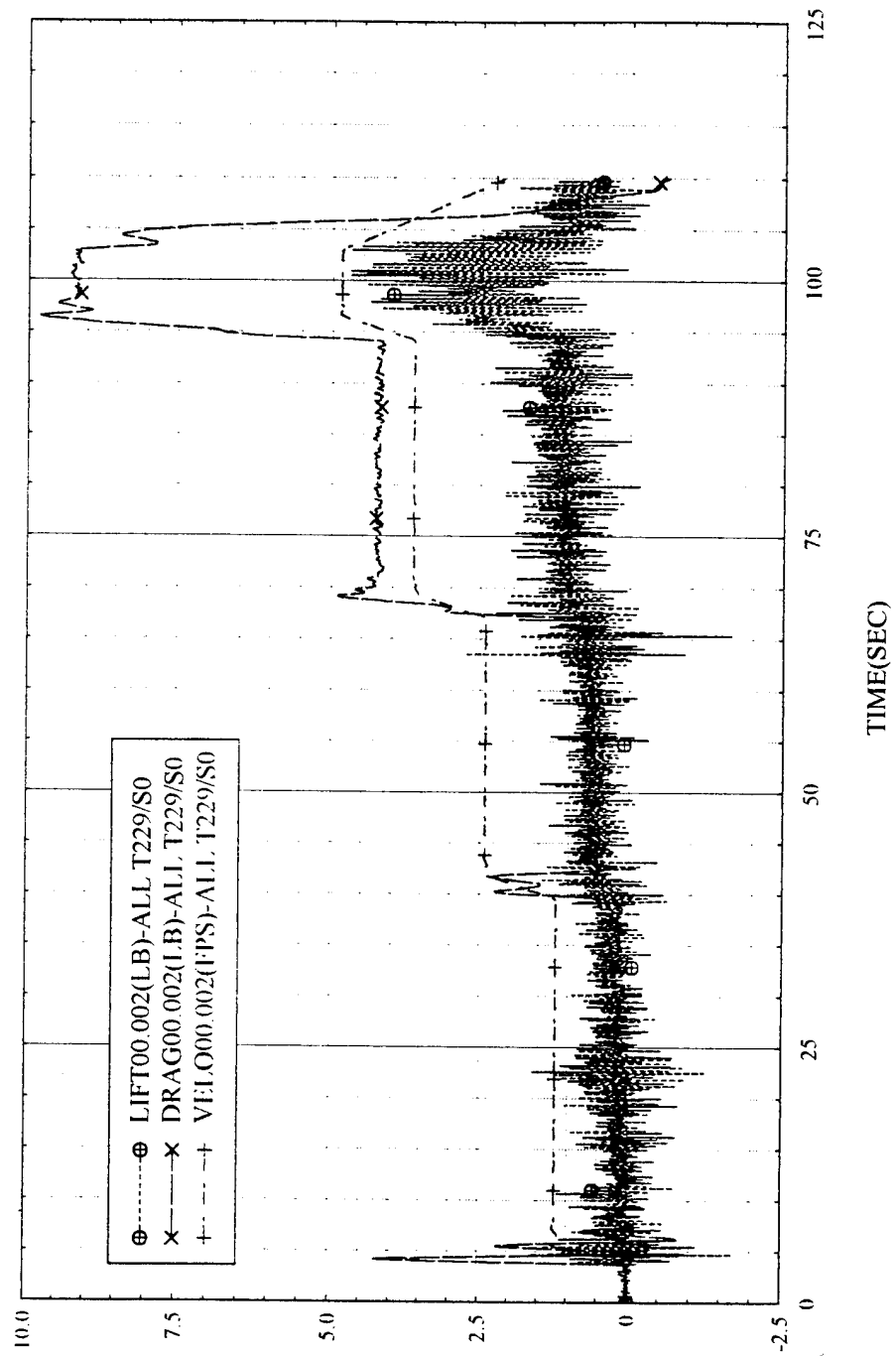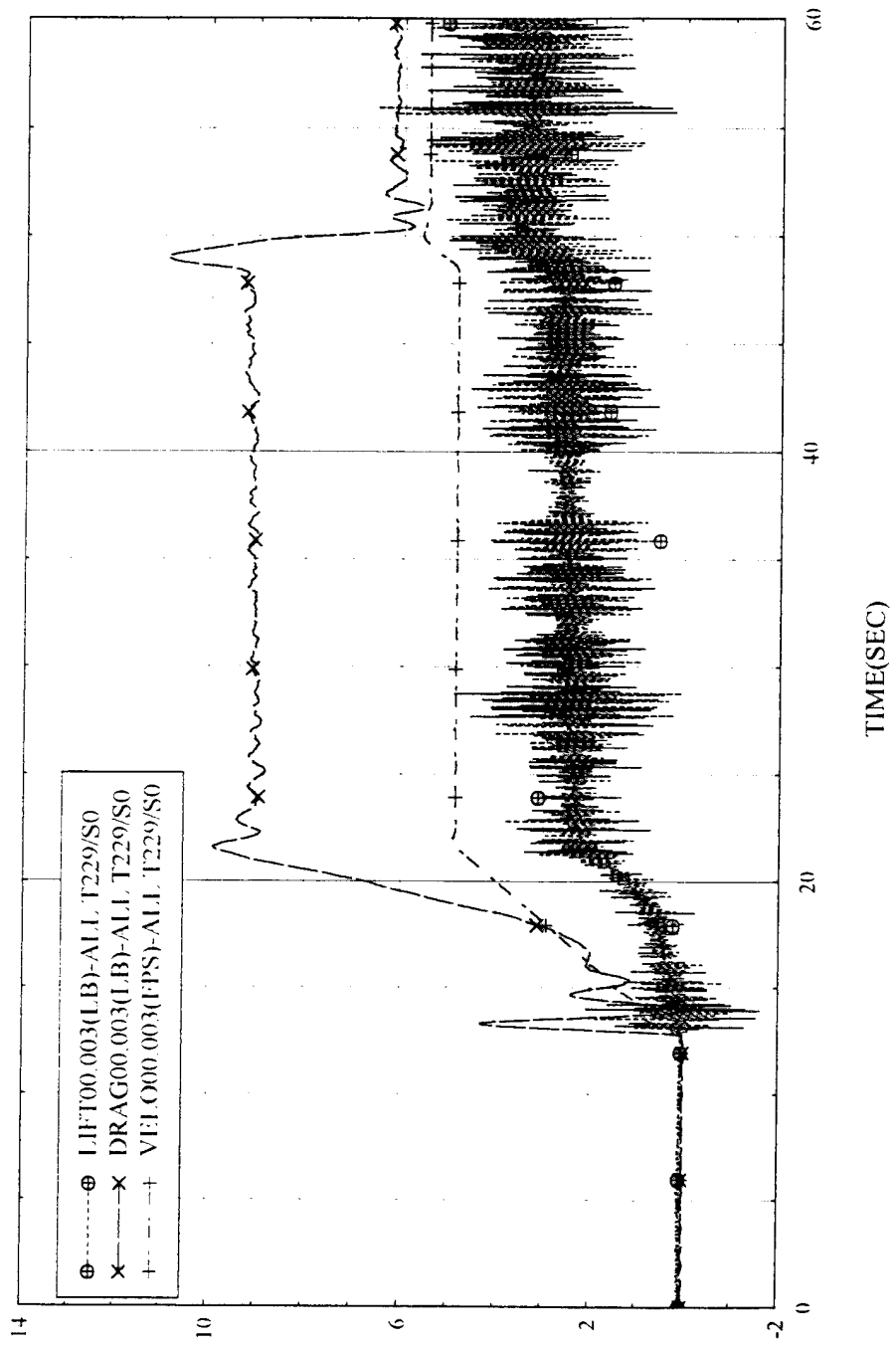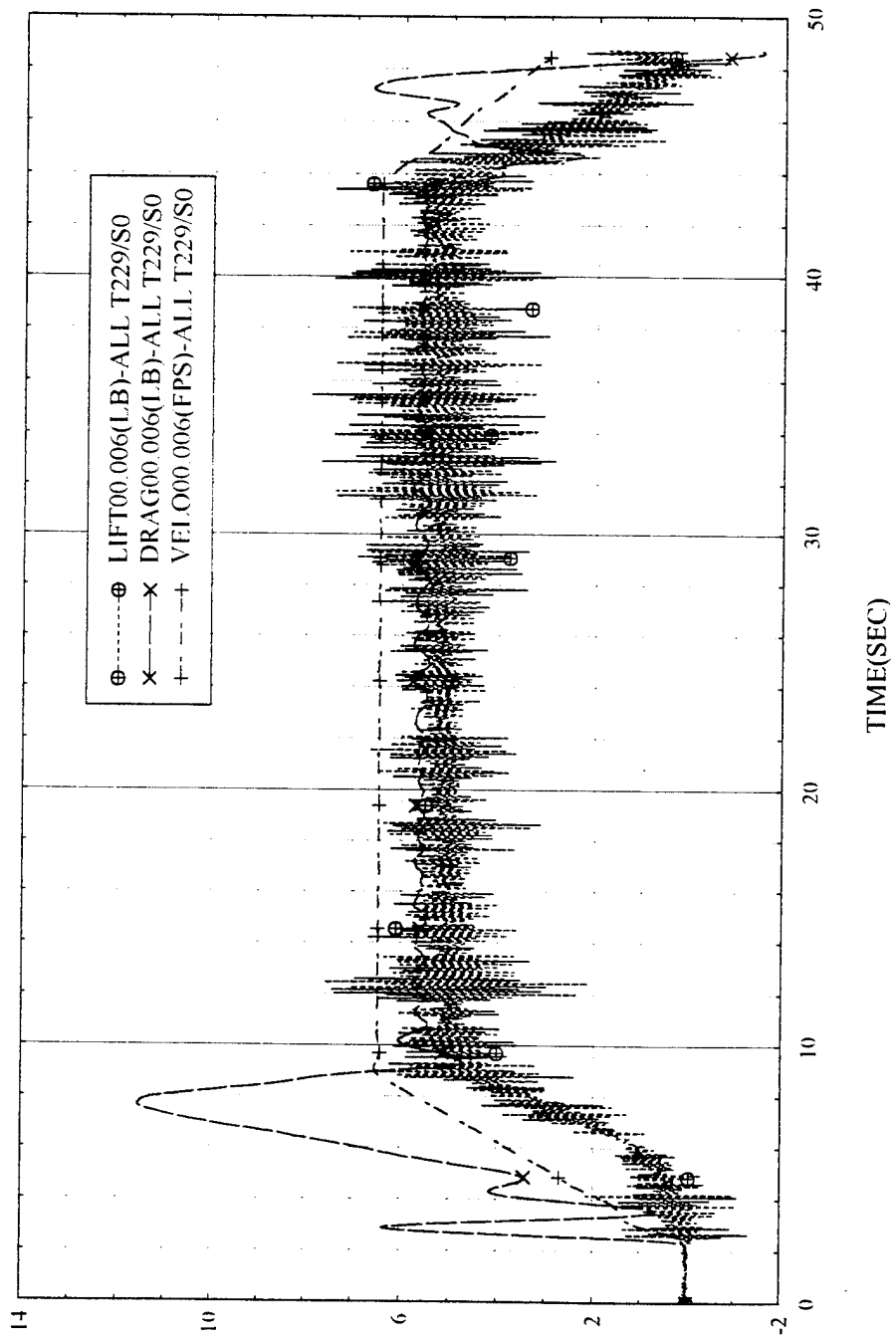
TEST:Model M-1 Test 1 RUN NO. 007
05/30/95 01:59:58
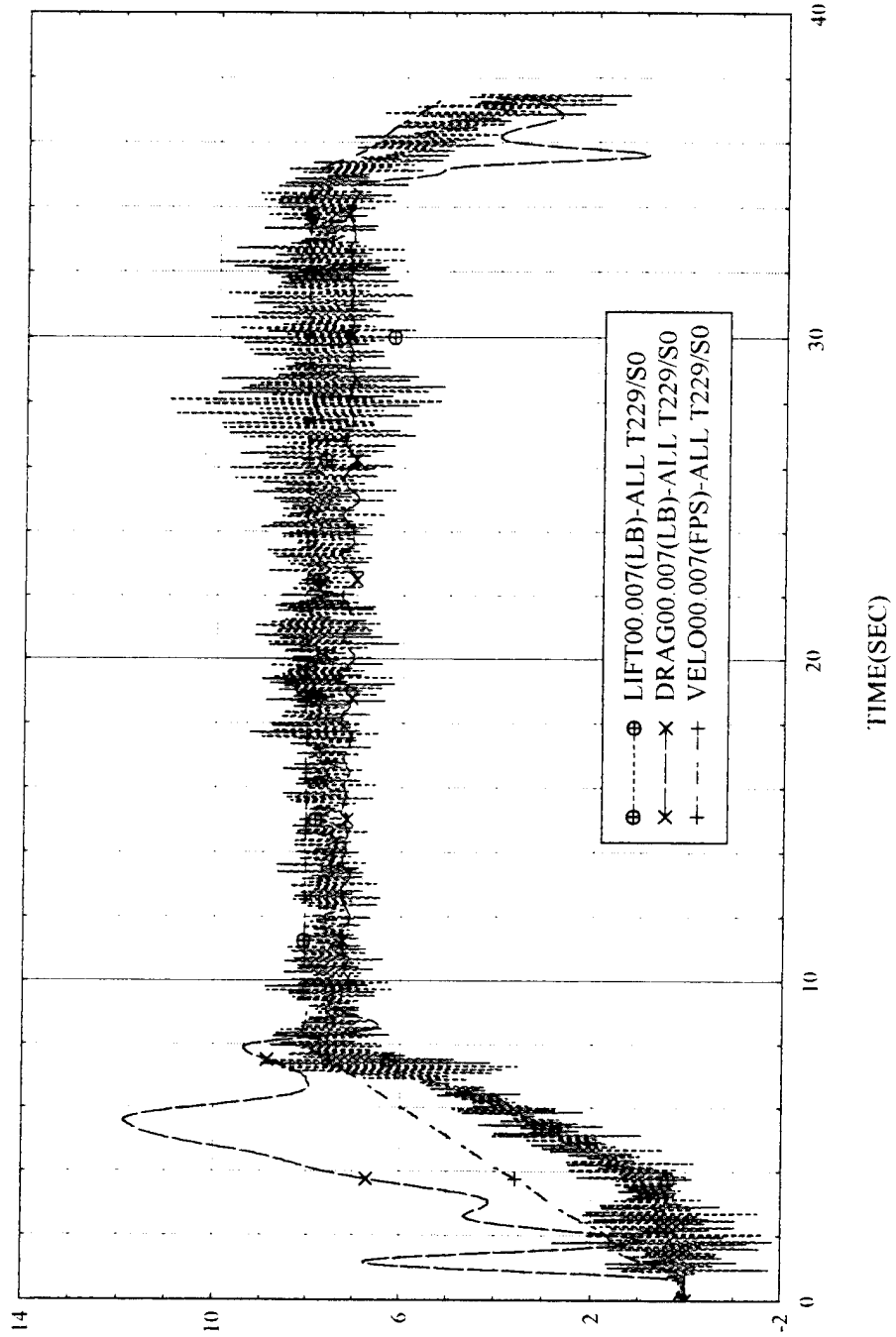
TEST:Model M-1 Test 1 RUN NO:008
05/30/95 02:03:35

⊕	LIFT00.008(LB)-ALL T229/S0
×	DRAG00.008(LB)-ALL T229/S0
+	VELO00.008(FPS)-ALL T229/S0

TIME(SEC)
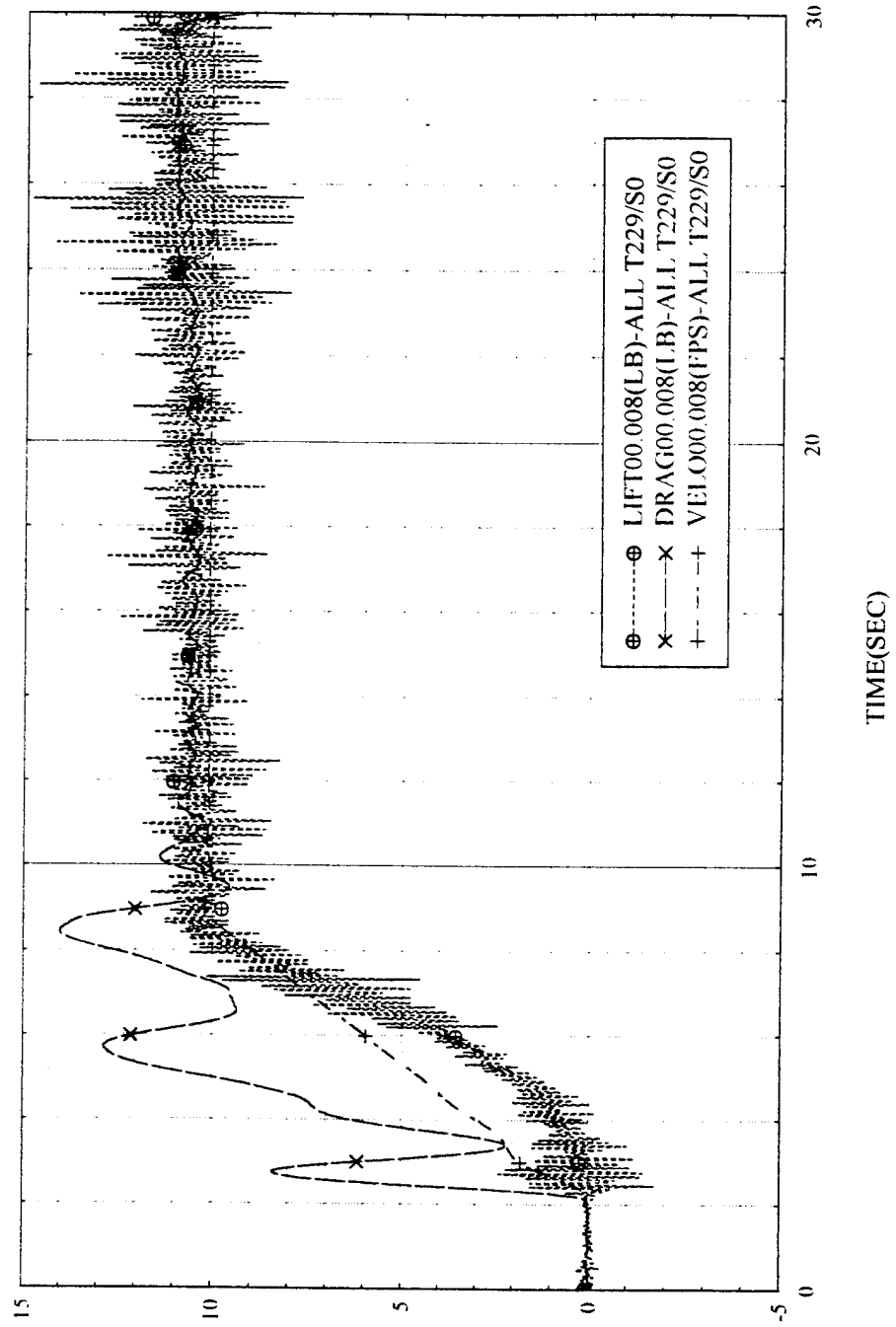
TEST:Model M-1 Test 1 RUN NO:009
05/30/95 02:06:40

LIFT00.009(LB)-ALL T229/S0
DRAG00.009(LB)-ALL T229/S0
VEL000.009(FPS)-ALL T229/S0

TIME(SEC)
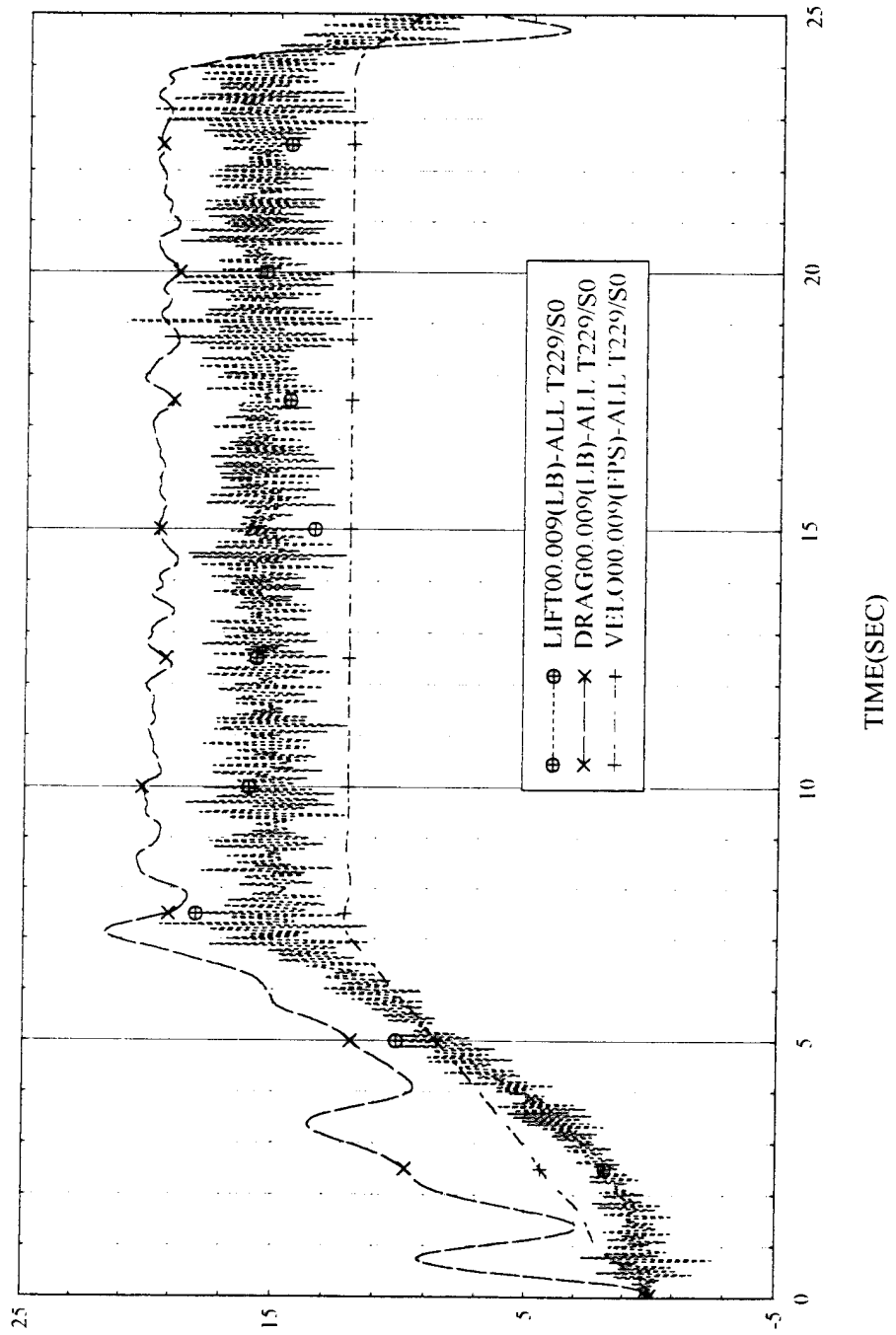
TEST:Model M-1 Test 1 RUN NO:R09
05/30/95 02:10:44

TIME(SEC)

LIFT00.R09(LB)-ALL T229/S0
DRAG00.R09(LB)-ALL T229/S0
VELO00.R09(FPS)-ALL T229/S0

152
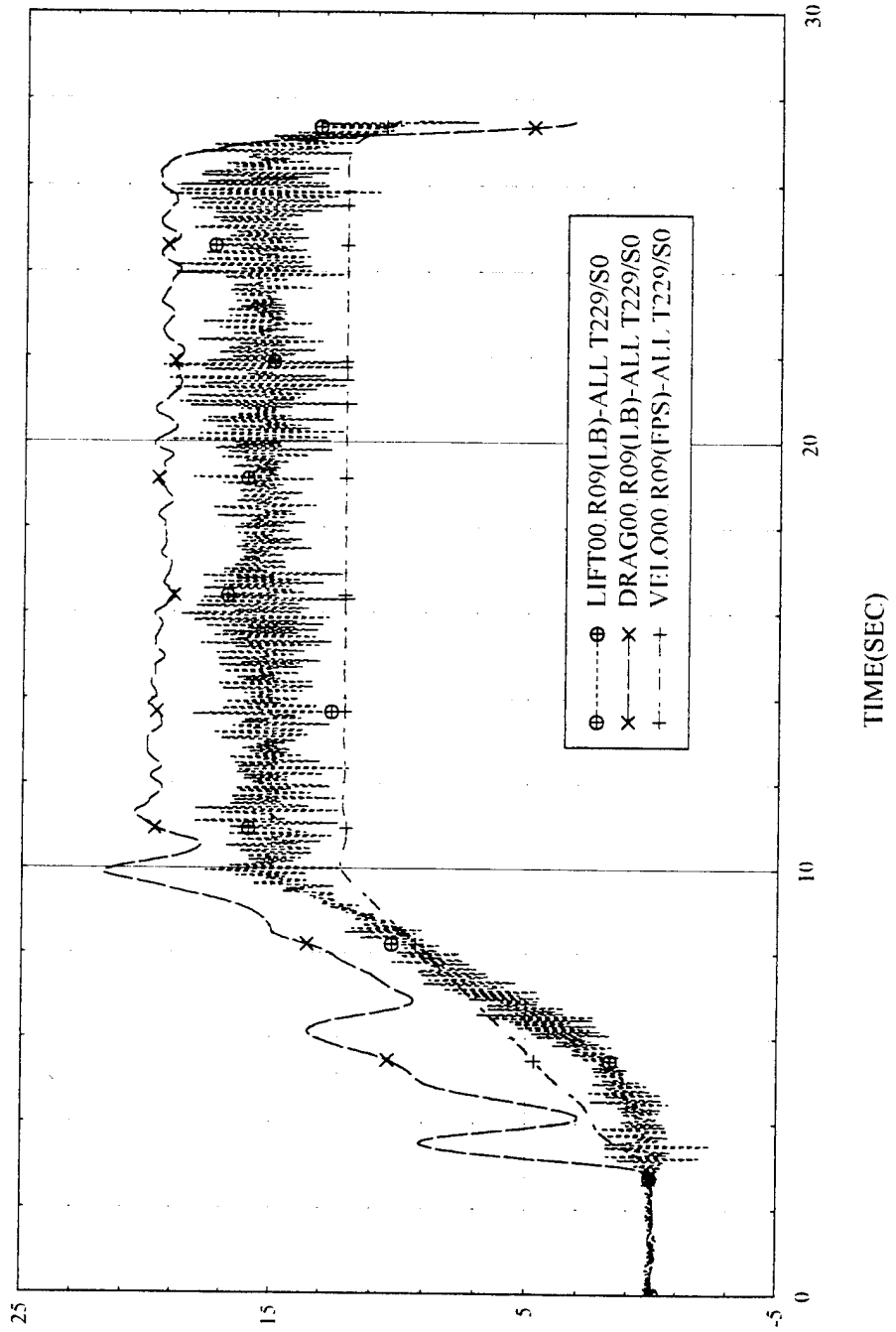
TEST:Model M-1 Test 1 RUN NO:011
05/30/95 02:17:02

TIME(SEC)

⊕ LIFT00.011(LB)-ALL T229/S0
✕ DRAG00.011(LB)-ALL T229/S0
+ VELO00.011(FPS)-ALL T229/S0

153
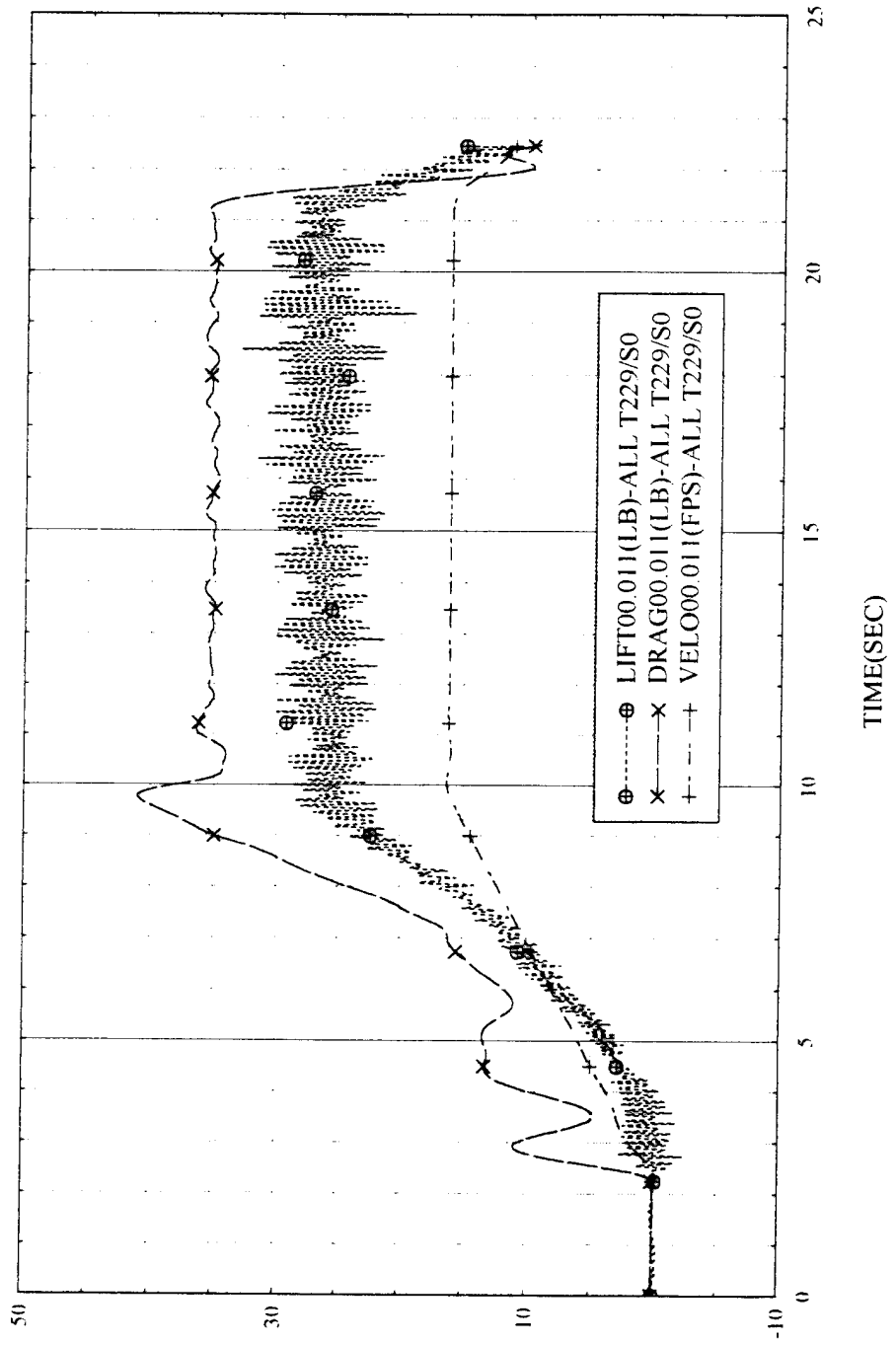
TEST:Model M-1 Test I RUN NO:012
05/30/95 02:20:27

LIFT00.012(LB)-ALL T229/S0
DRAG00.012(LB)-ALL T229/S0
VELO00.012(FPS)-ALL T229/S0

TIME(SEC)

154

TEST:Model M-1 Test 1 RUN NO.014
05/30/95 02:24:06

LIFT00.014(LB)-ALL T229/S0
DRAG00.014(LB)-ALL T229/S0
VELO00.014(FPS)-ALL T229/S0

TIME(SEC)
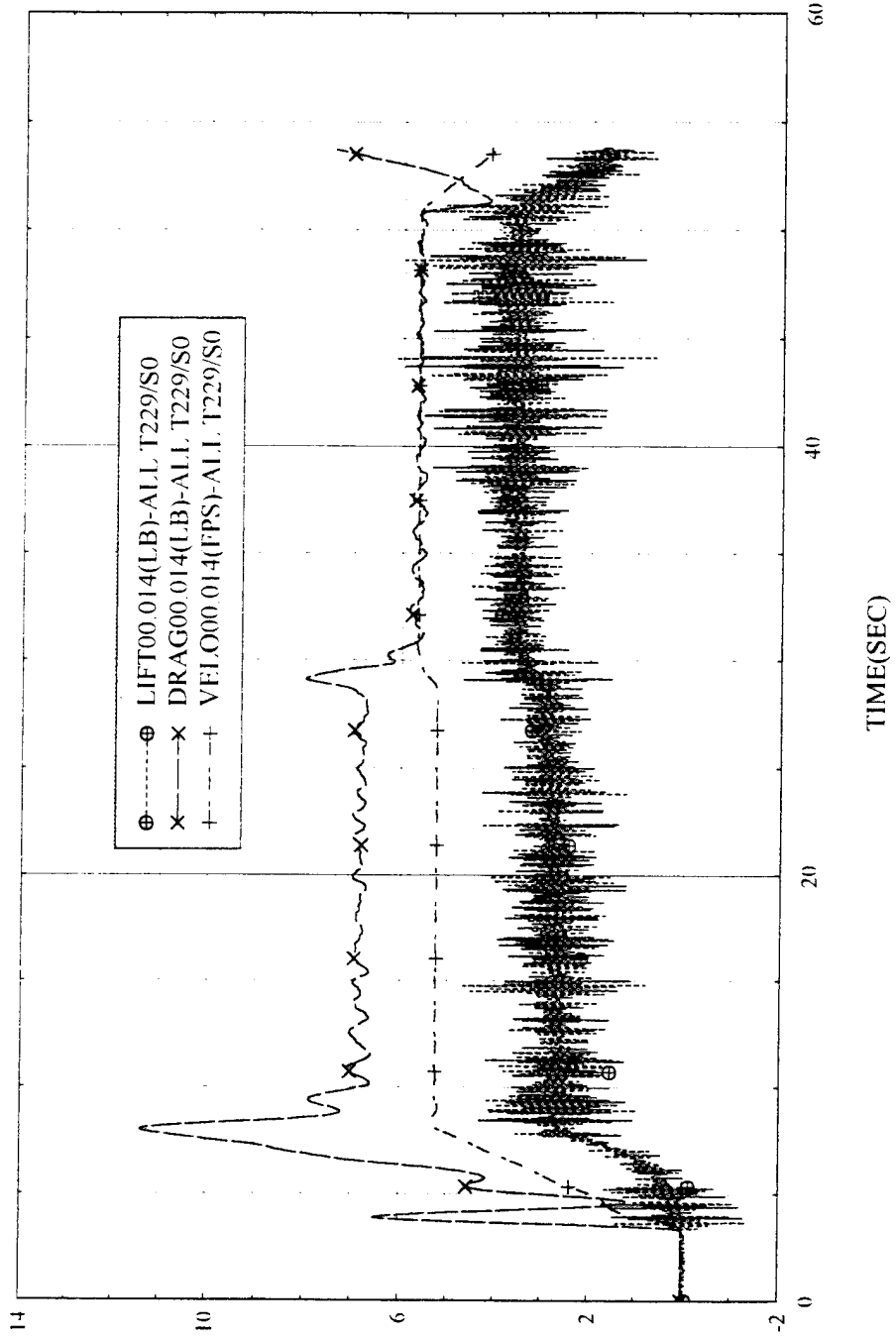
TEST:Model M-1 Test 1 RUN NO:016
05/30/95 02:28:26

TIME(SEC)

LIFT00.016(LB)-ALL T229/S0
DRAG00.016(LB)-ALL T229/S0
VELO00.016(FPS)-ALL T229/S0
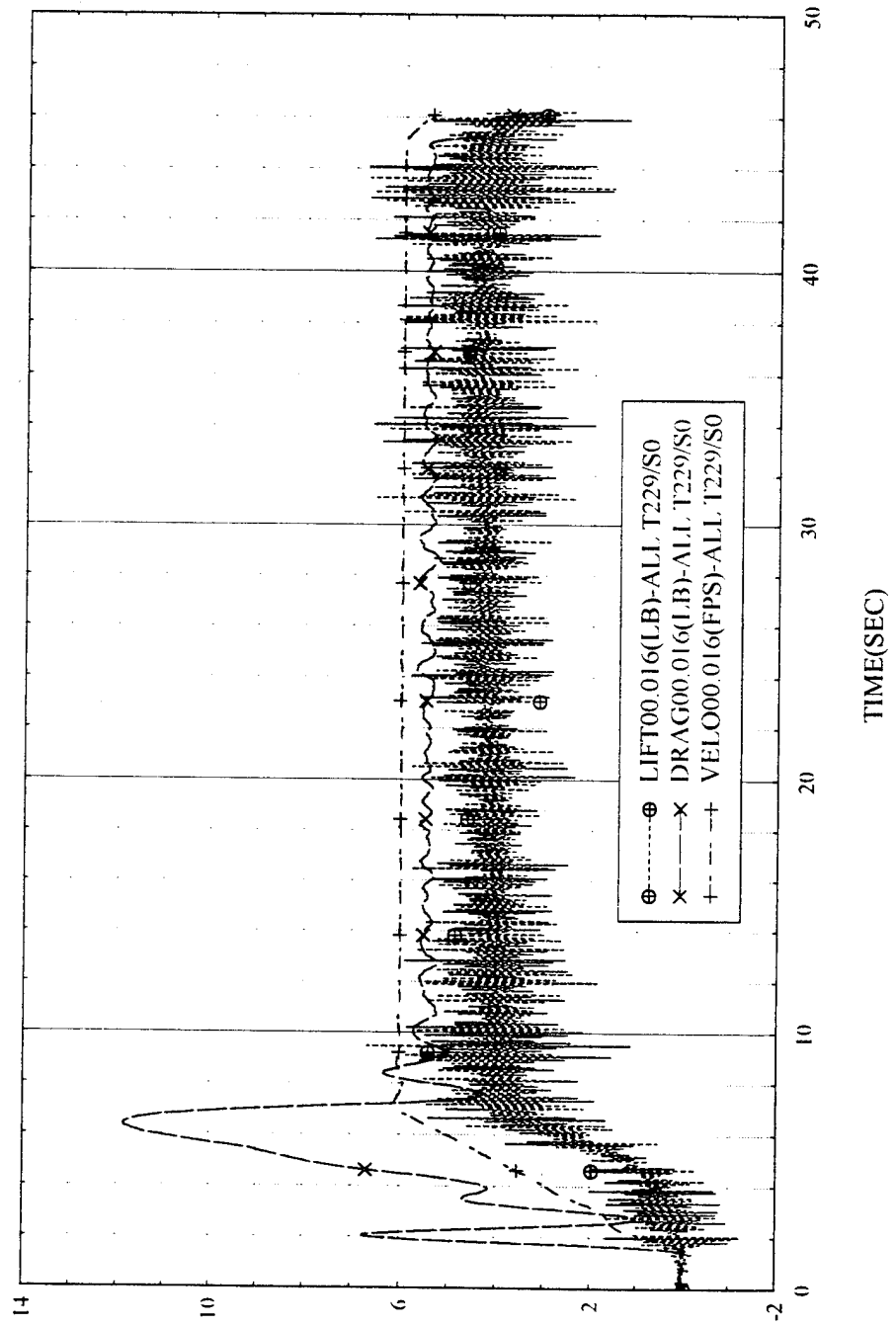
TEST:Model M-I Test I RUN NO:017
05/30/95 02:33:17
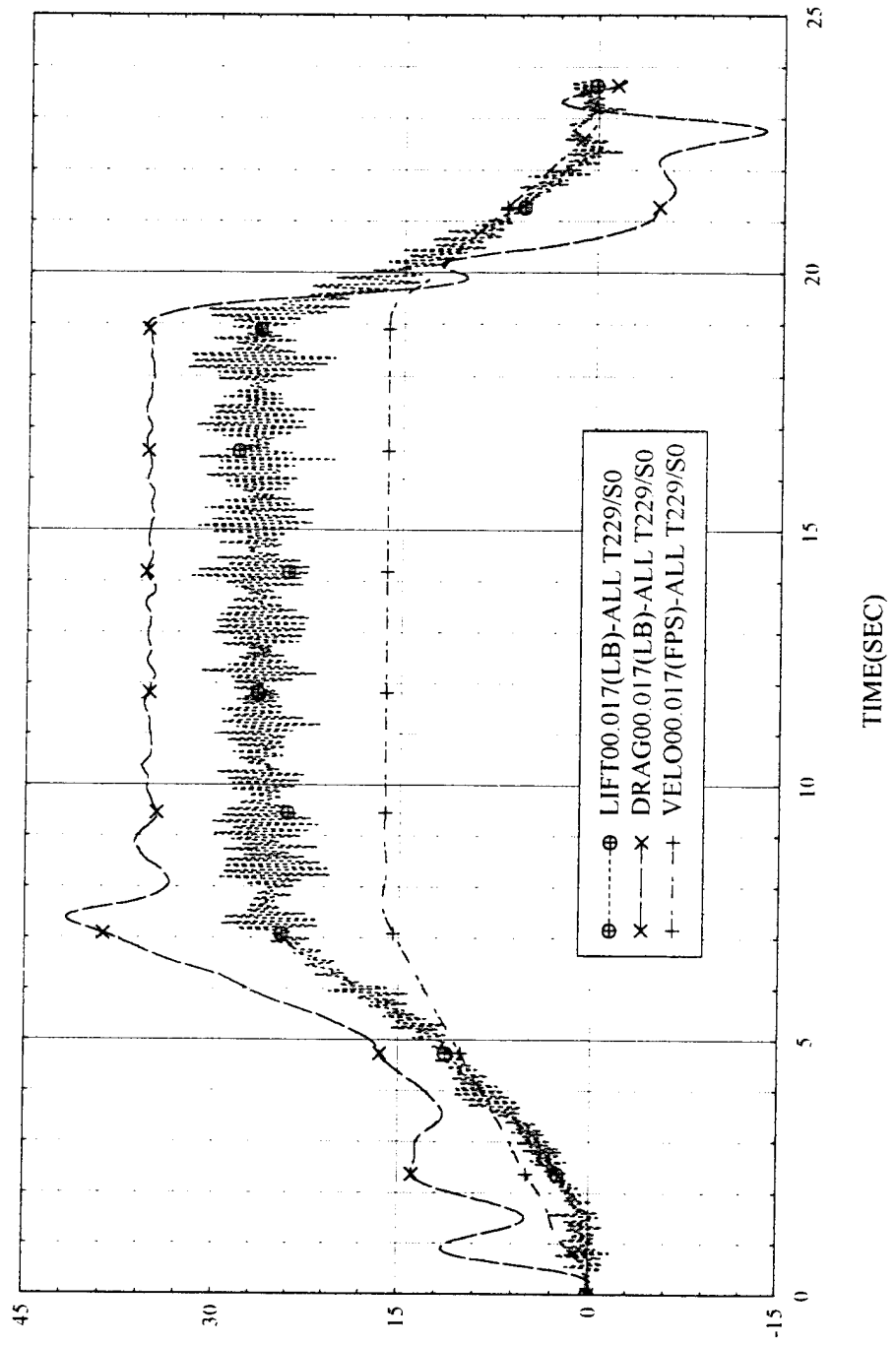
TEST:Model M-1 Test 1 with Spray Rail RUN NO.018
05/30/95 02:36:11

	LIFT00.018(LB)-ALL T229/S0
⊕	
×	DRAG00.018(LB)-ALL T229/S0
+	VELO00.018(FPS)-ALL T229/S0

TIME(SEC)
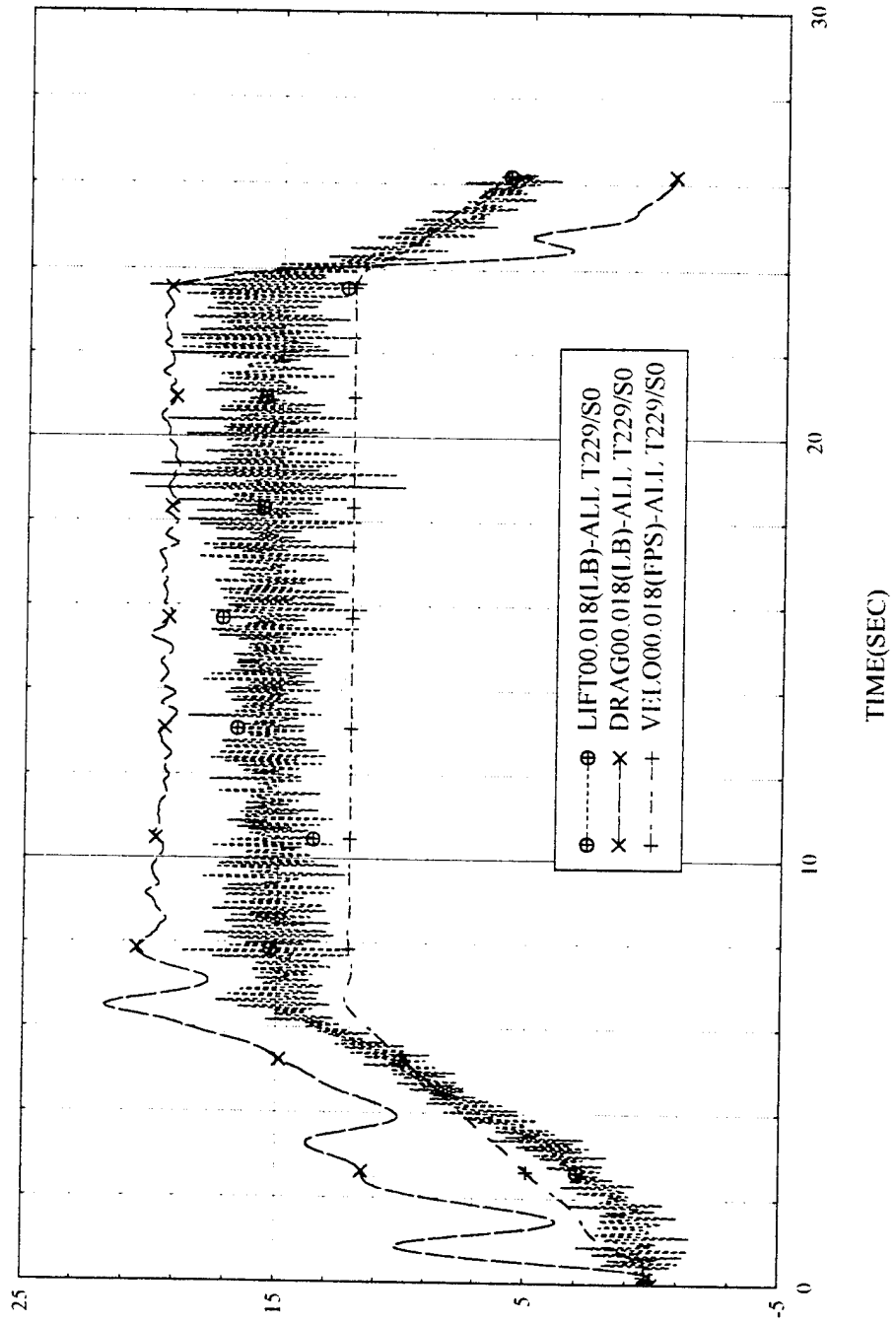
TEST:Model M-1 Test 1 with Spray Rail RUN NO:019
05/30/95 02:40:01

TIME(SEC)

Legend:
⊕ LIFT00.019(LB)-ALL T229/S0
✕ DRAG00.019(LB)-ALL T229/S0
+ VELO00.019(FPS)-ALL T229/S0
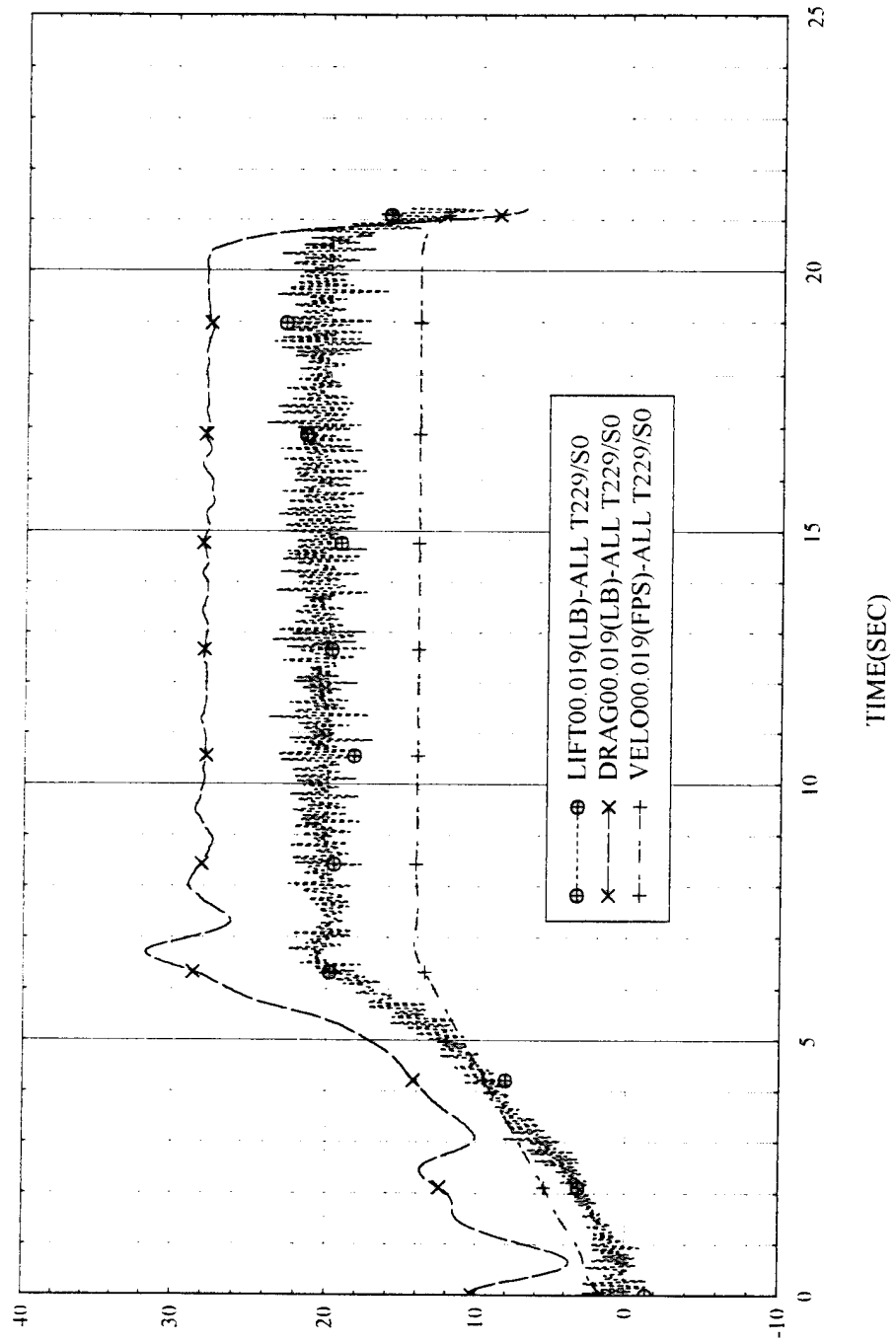
TEST:Model M-1 Test 1 with Spray Rail RUN NO:020
05/30/95 02:42:55

TIME(SEC)

LIFT00.020(LB)-ALL T229/S0
DRAG00.020(LB)-ALL T229/S0
VELO00.020(FPS)-ALL T229/S0
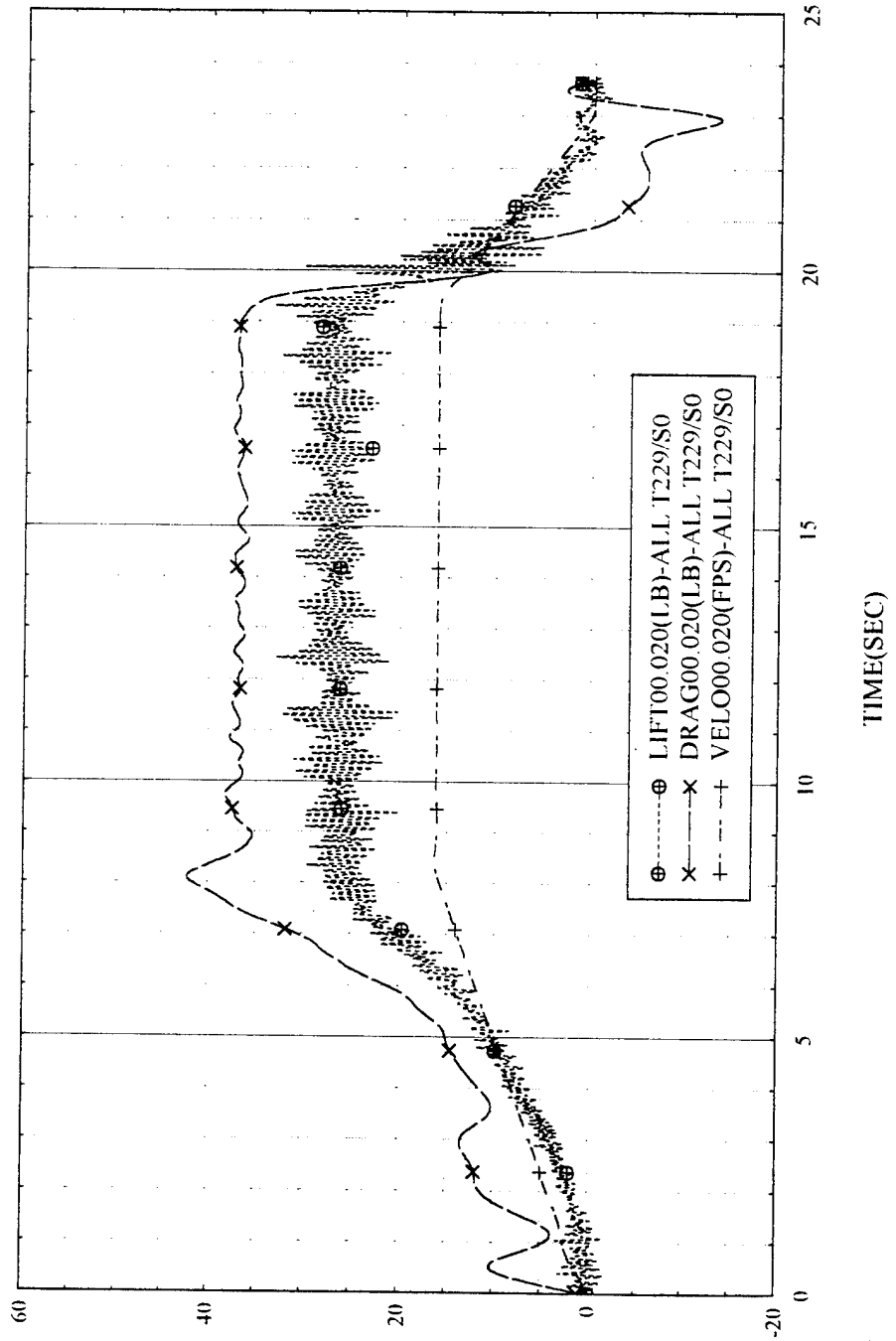
TEST:Model M-2 Test 1 RUN NO.025
05/30/95 02:48:08

LIFT00.025(LB)-ALL T229/S0
DRAG00.025(LB)-ALL T229/S0
VELO00.025(FPS)-ALL T229/S0

TIME(SEC)
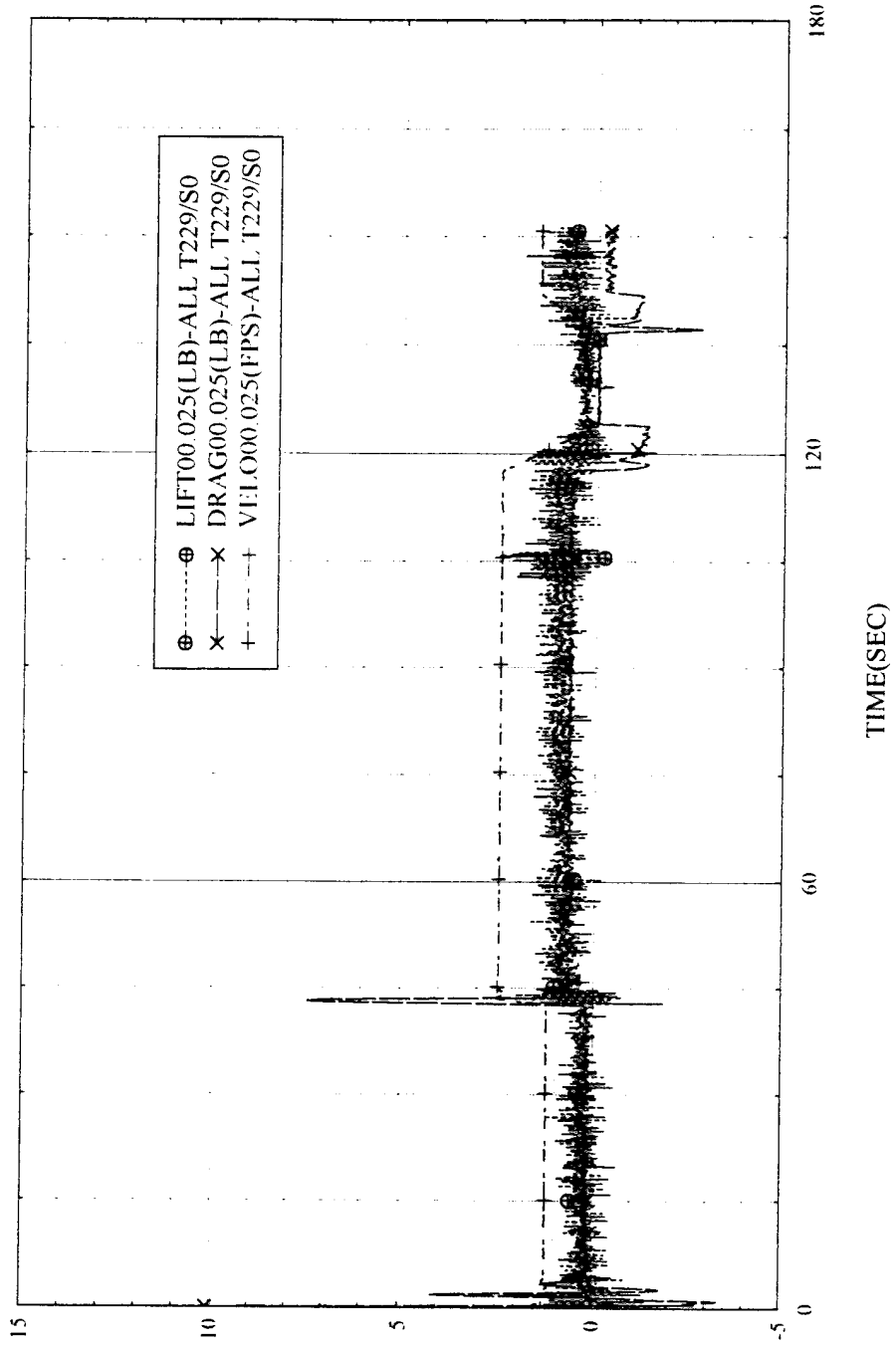
TEST:Model M-2 Test 1 RUN NO:027
05/30/95 02:51:38

LIFT00.027(LB)-ALL T229/S0
DRAG00.027(LB)-ALL T229/S0
VELO00.027(FPS)-ALL T229/S0

TIME(SEC)
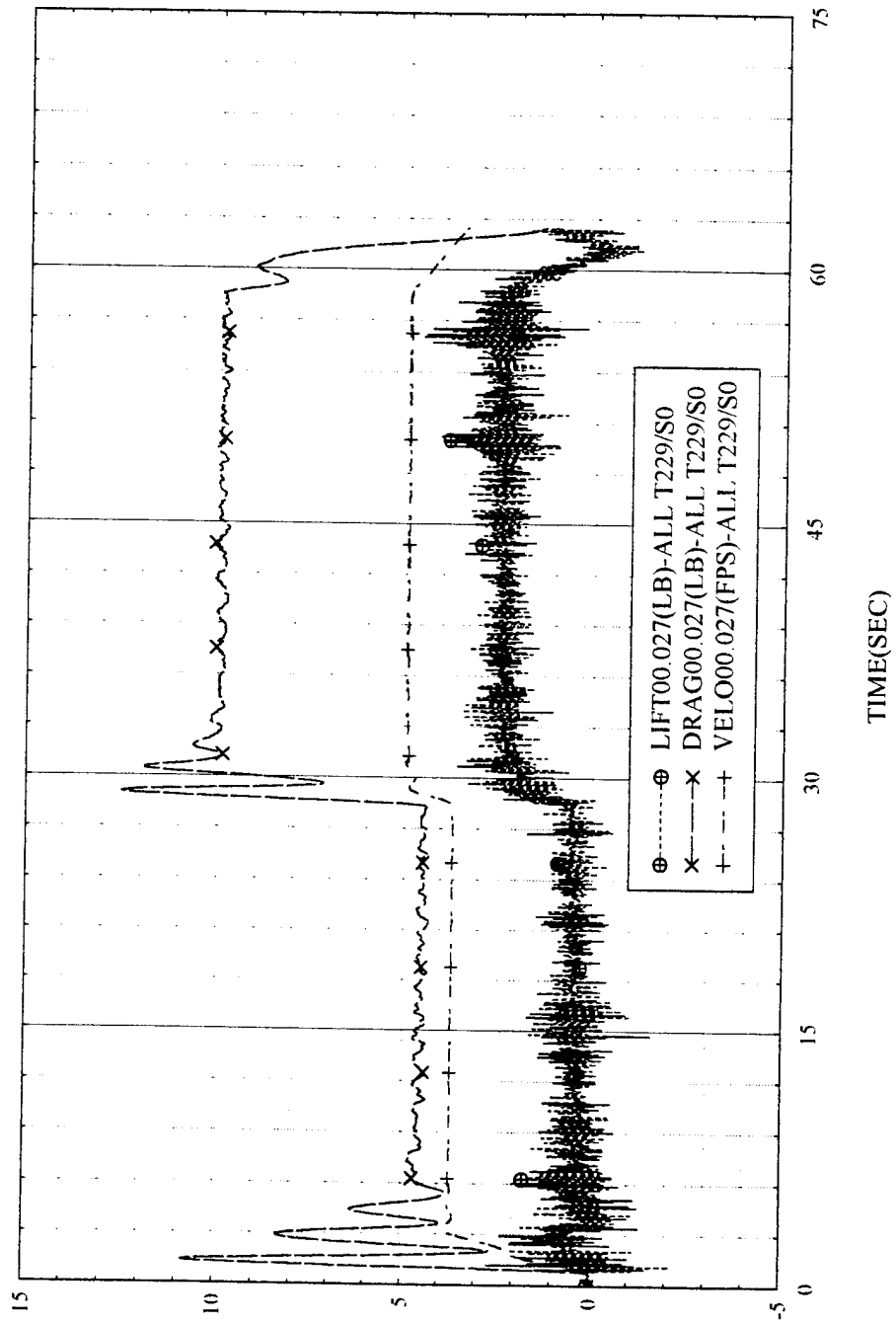
TEST:Model M-2 Test 1 RUN NO:028
05/30/95 02:55:44

Legend:
⊕ LIFT00.028(LB)-ALL T229/S0
✕ DRAG00.028(LB)-ALL T229/S0
+ VELO00.028(FPS)-ALL T229/S0

TIME(SEC)
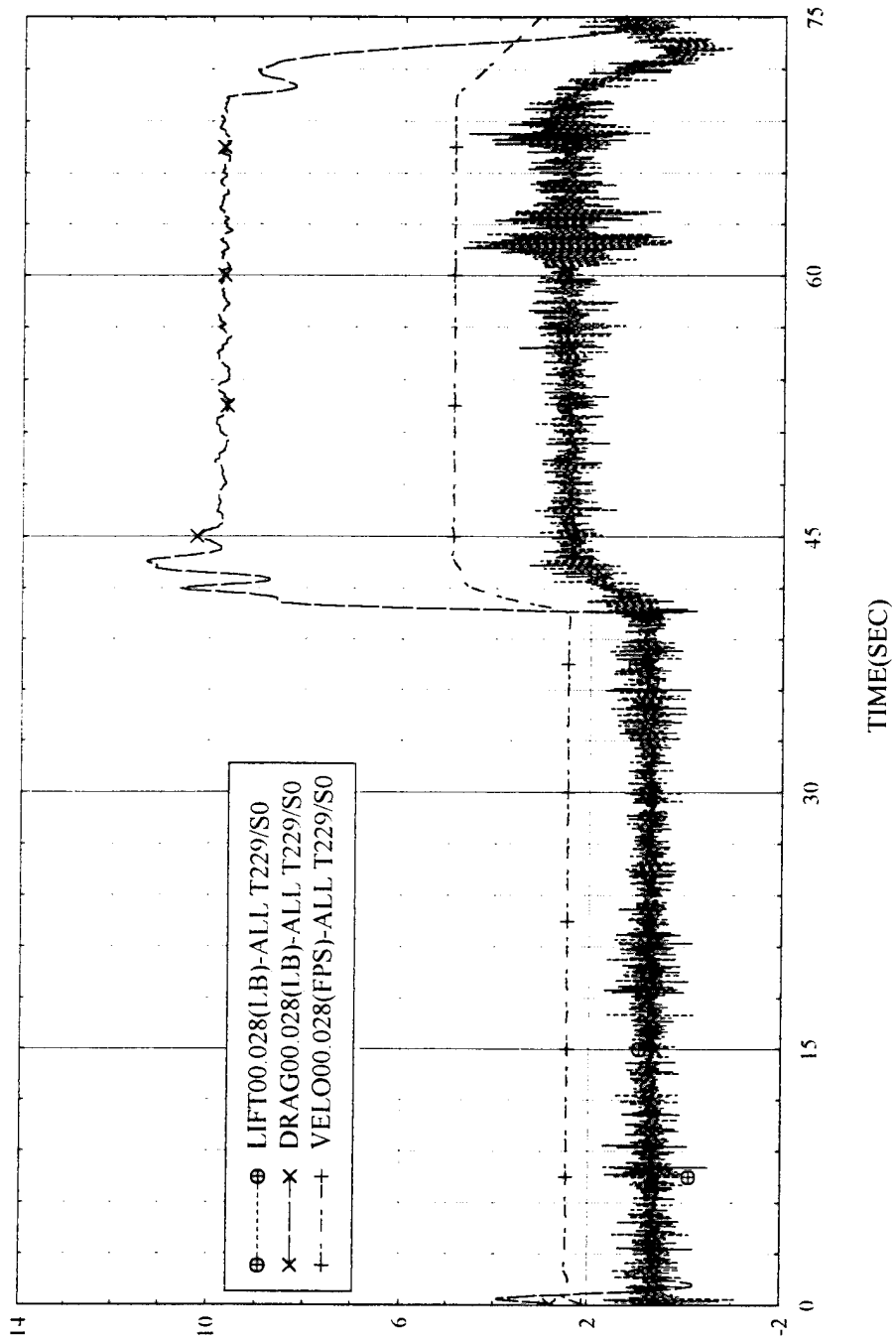
TEST:Model M-2 Test 1 RUN NO.030
05/30/95 03:27:50

LIFT00.030(LB)-ALL T229/S0
DRAG00.030(LB)-ALL T229/S0
VELO00.030(FPS)-ALL T229/S0

TIME(SEC)
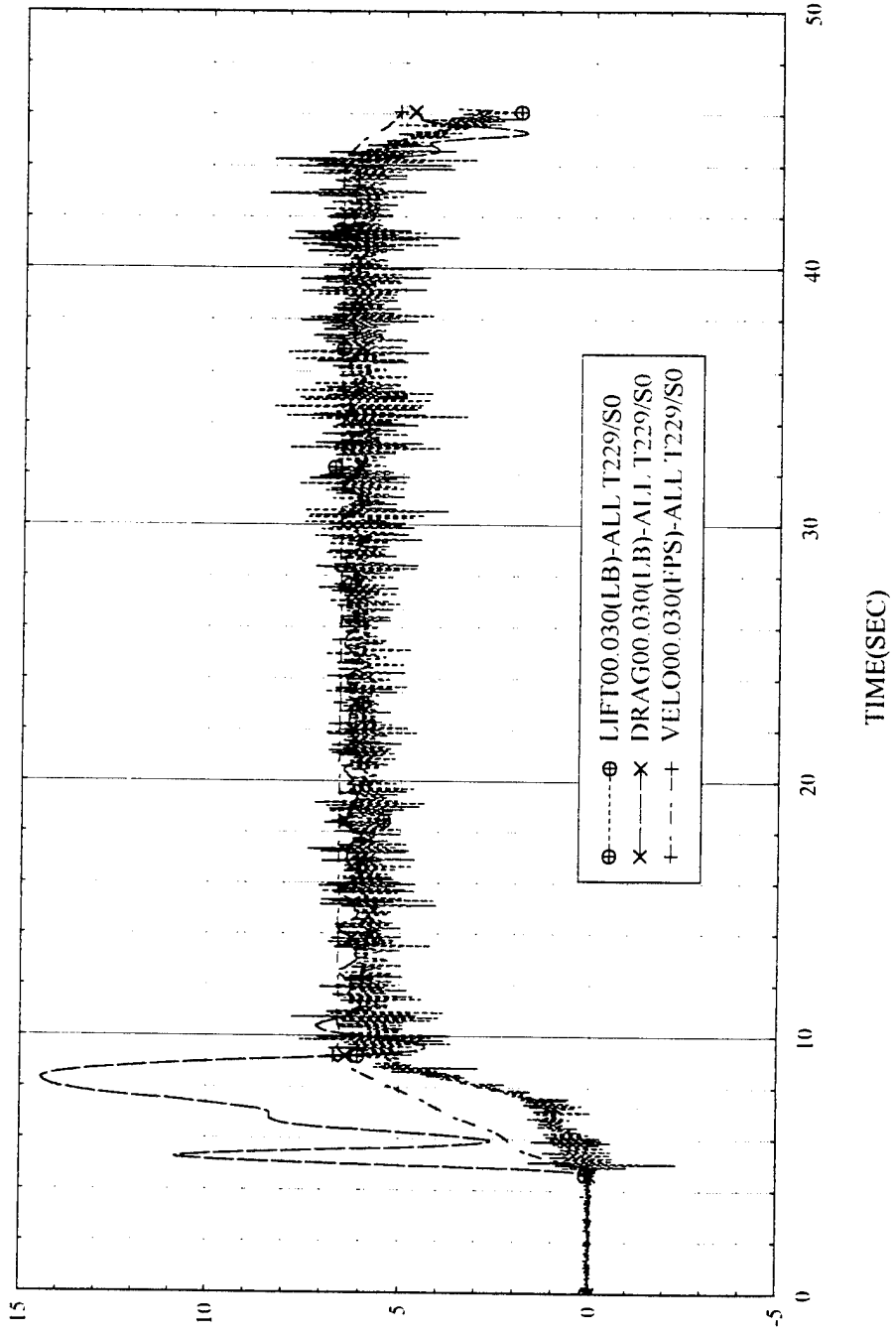
TEST:Model M-2 Test 1 RUN NO:031
05/30/95 03:31:35

LIFT00.031(LB)-ALL T229/S0
DRAG00.031(LB)-ALL T229/S0
VELO00.031(FPS)-ALL T229/S0

TIME(SEC)

TEST:Model M-2 Test 1 RUN NO:032
05/30/95 03:34:52

TEST:Model M-2 Test 1 RUN NO:R32
05/30/95 13:38:43

LIFT00.R32(LB)-ALL T229/S0
DRAG00.R32(LB)-ALL T229/S0
VELO00.R32(FPS)-ALL T229/S0

TIME(SEC)
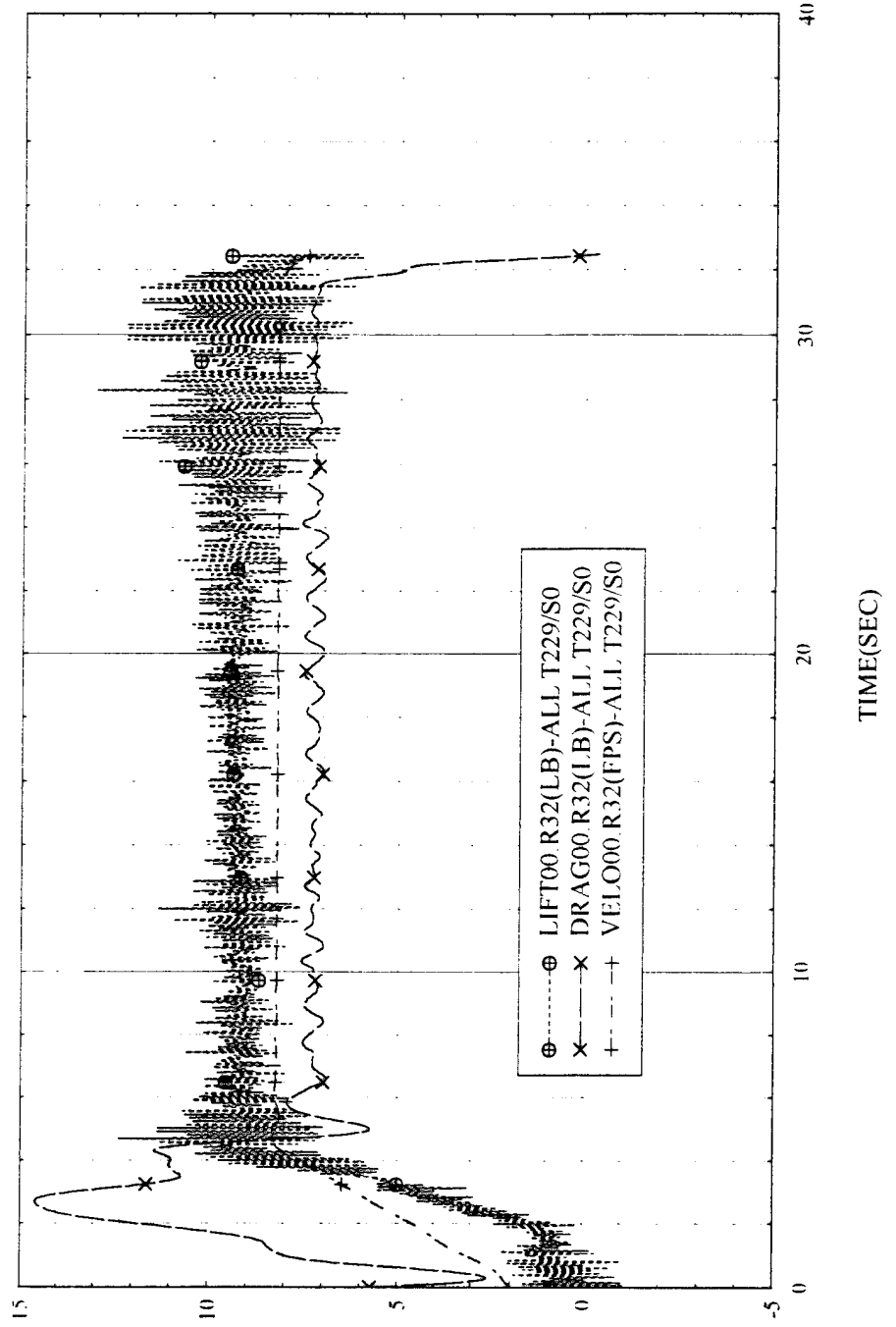
TEST:Model M-2 Test 1 RUN NO.034
05/30/95 13:41:51

TIME(SEC)

LIFT00.034(LB)-ALL T229/S0
DRAG00.034(LB)-ALL T229/S0
VELO00.034(FPS)-ALL T229/S0
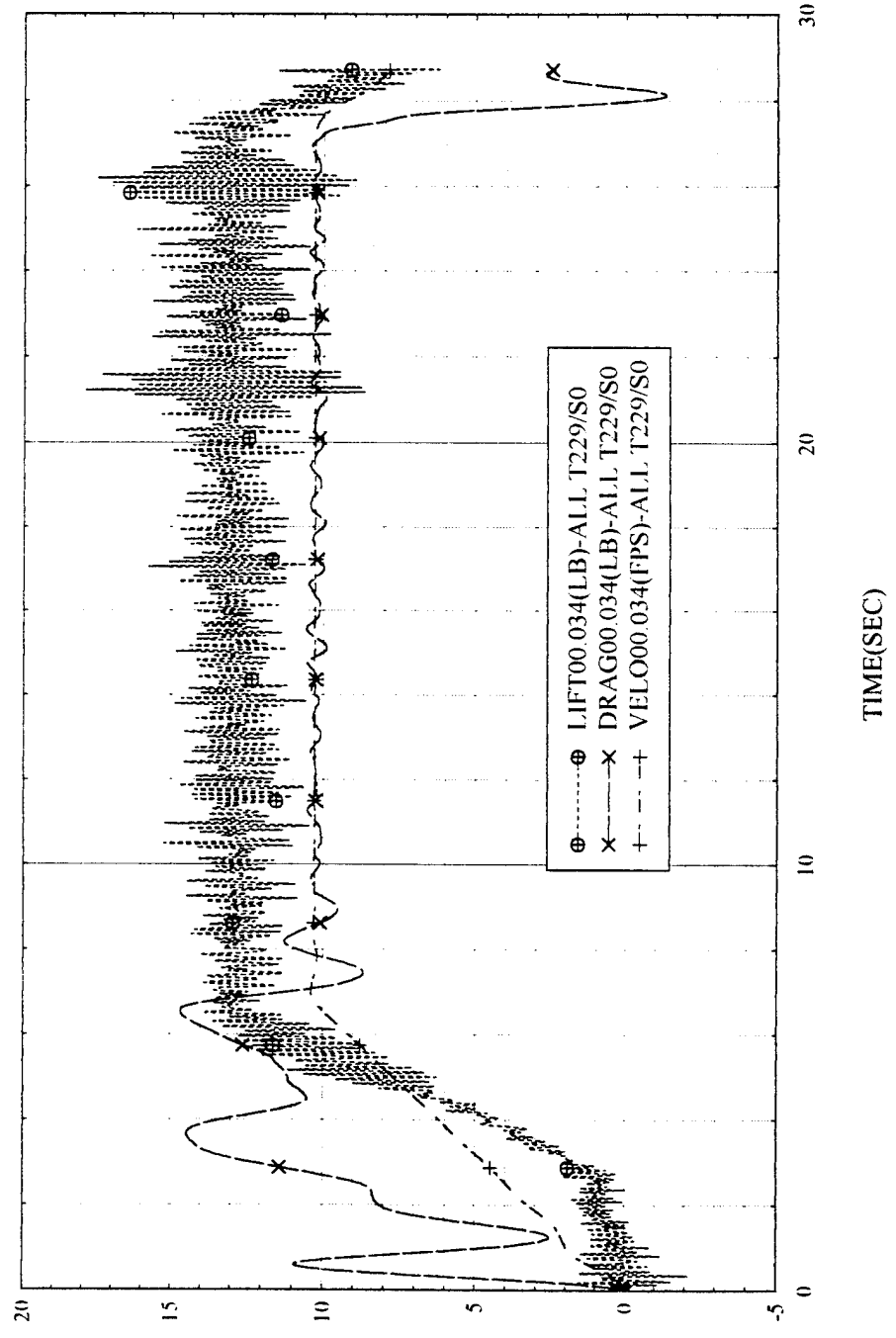
TEST: Model M-2 Test 1 RUN NO:R34
05/30/95 13:43:50

LIFT00.R34(LB)-ALL T229/S0
DRAG00.R34(LB)-ALL T229/S0
VELO00.R34(FPS)-ALL T229/S0

TIME(SEC)
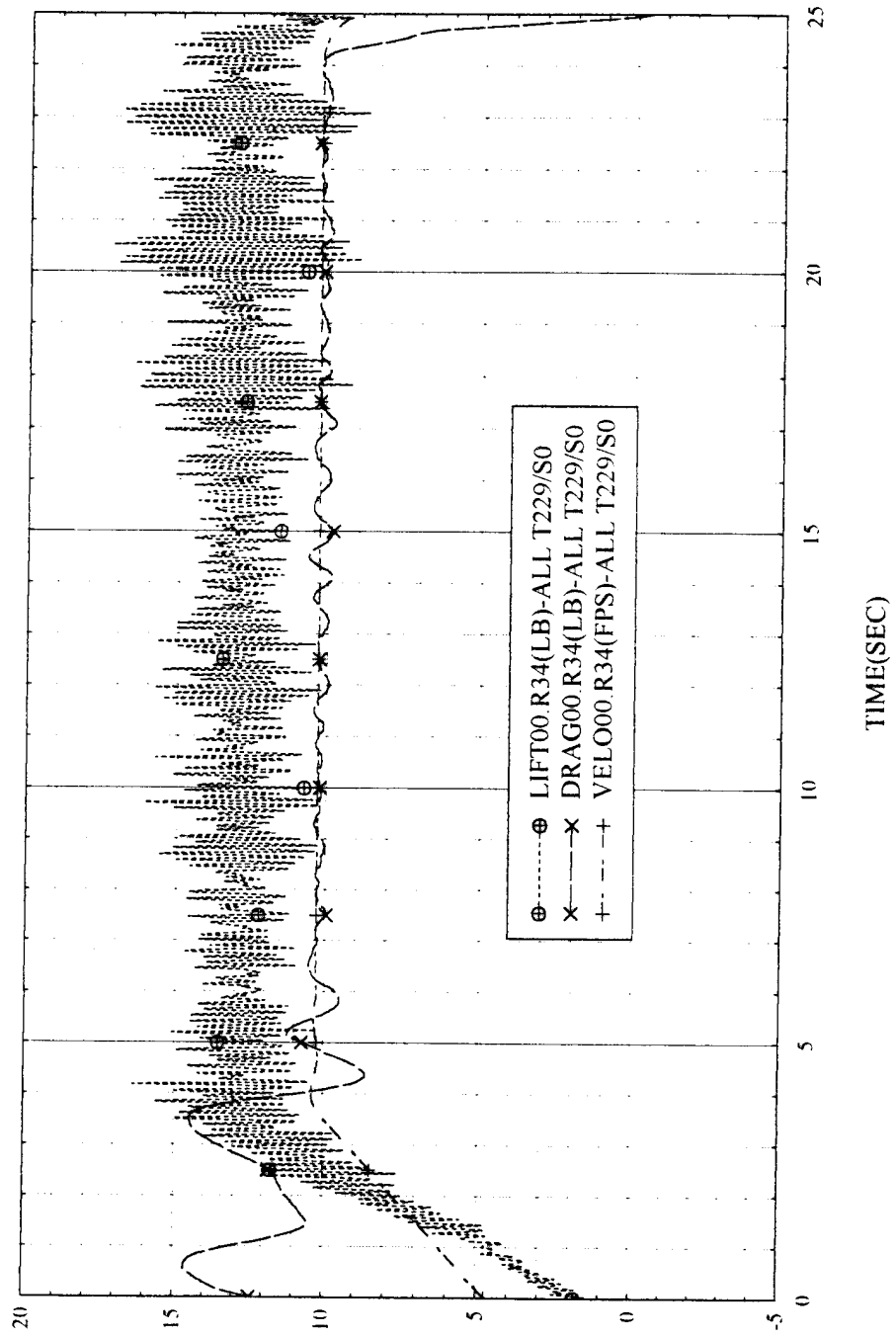
TEST:Model M-2 Test 1 RUN NO:036
05/30/95 13:45:37

TIME(SEC)

LIFT00.036(LB)-ALL T229/S0
DRAG00.036(LB)-ALL T229/S0
VELO00.036(FPS)-ALL T229/S0

TEST:Model M-2 TestI RUN NO:R36
05/30/95 13:47:25

LIFT00.R36(LB)-ALL T229/S0
DRAG00.R36(LB)-ALL T229/S0
VELO00.R36(FPS)-ALL T229/S0

TIME(SEC)
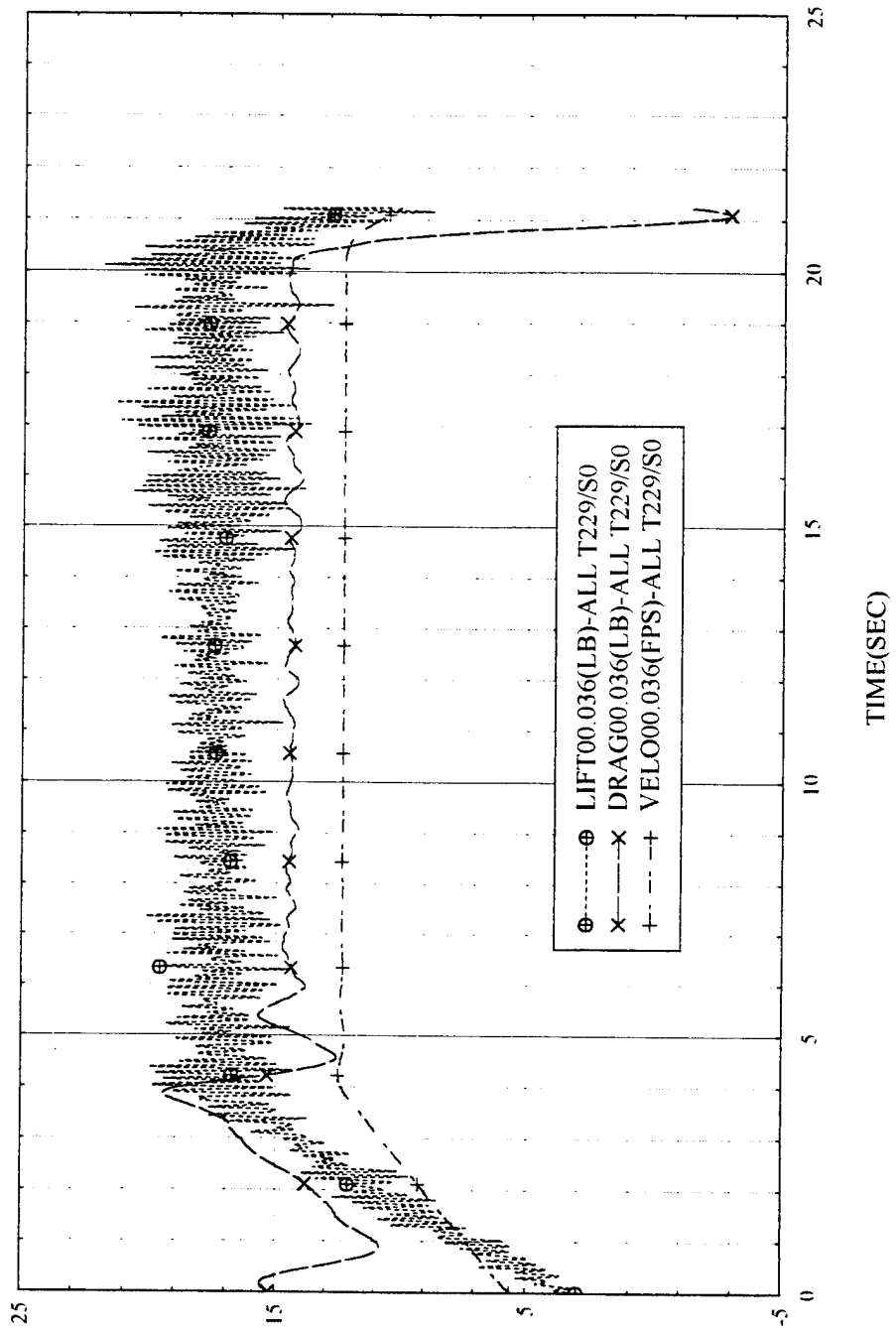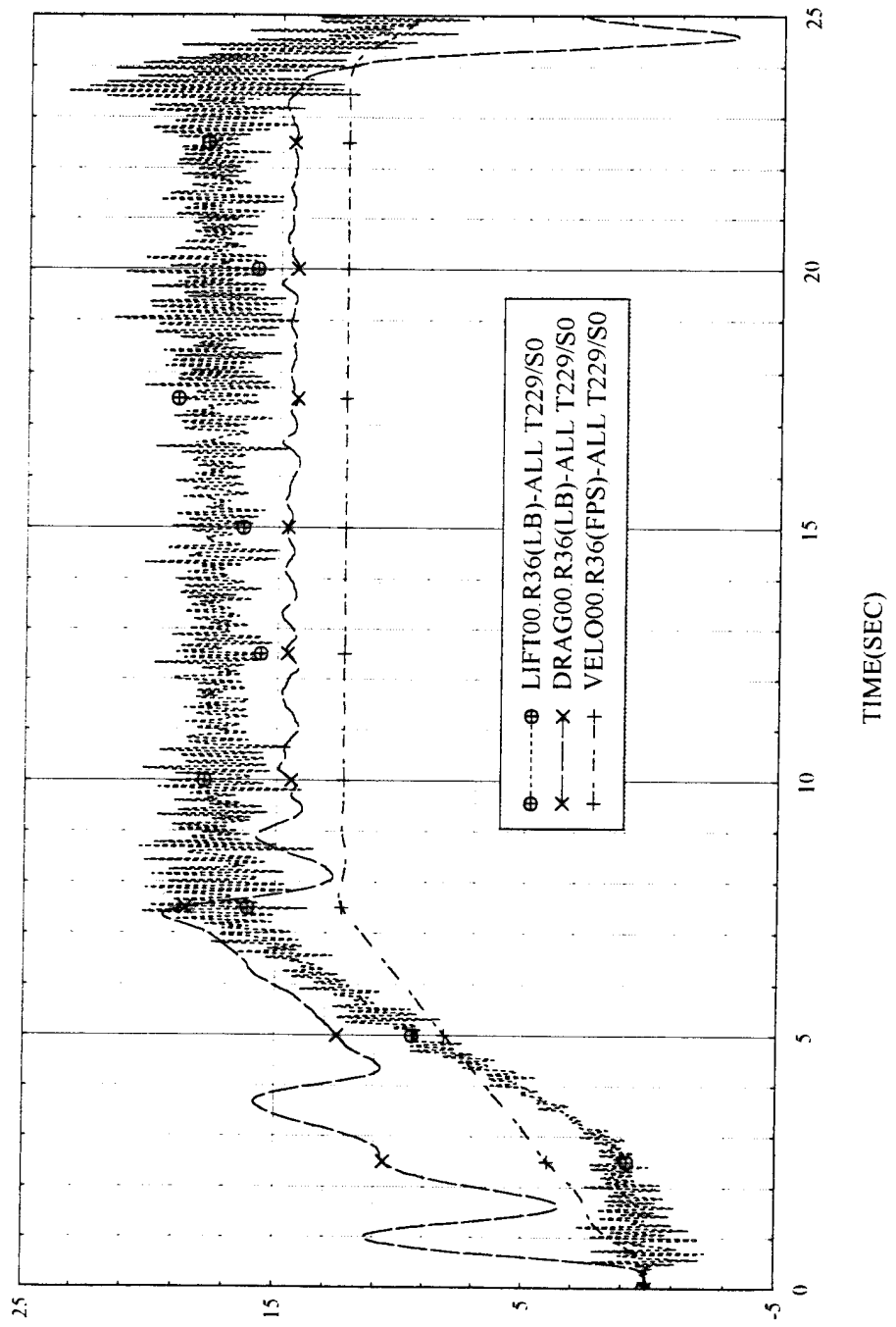
TEST:Model M-2 Test 1 RUN NO:038
05/30/95 13:49:19

LIFT00.038(LB)-ALL T229/S0
DRAG00.038(LB)-ALL T229/S0
VELO00.038(FPS)-ALL T229/S0

TIME(SEC)
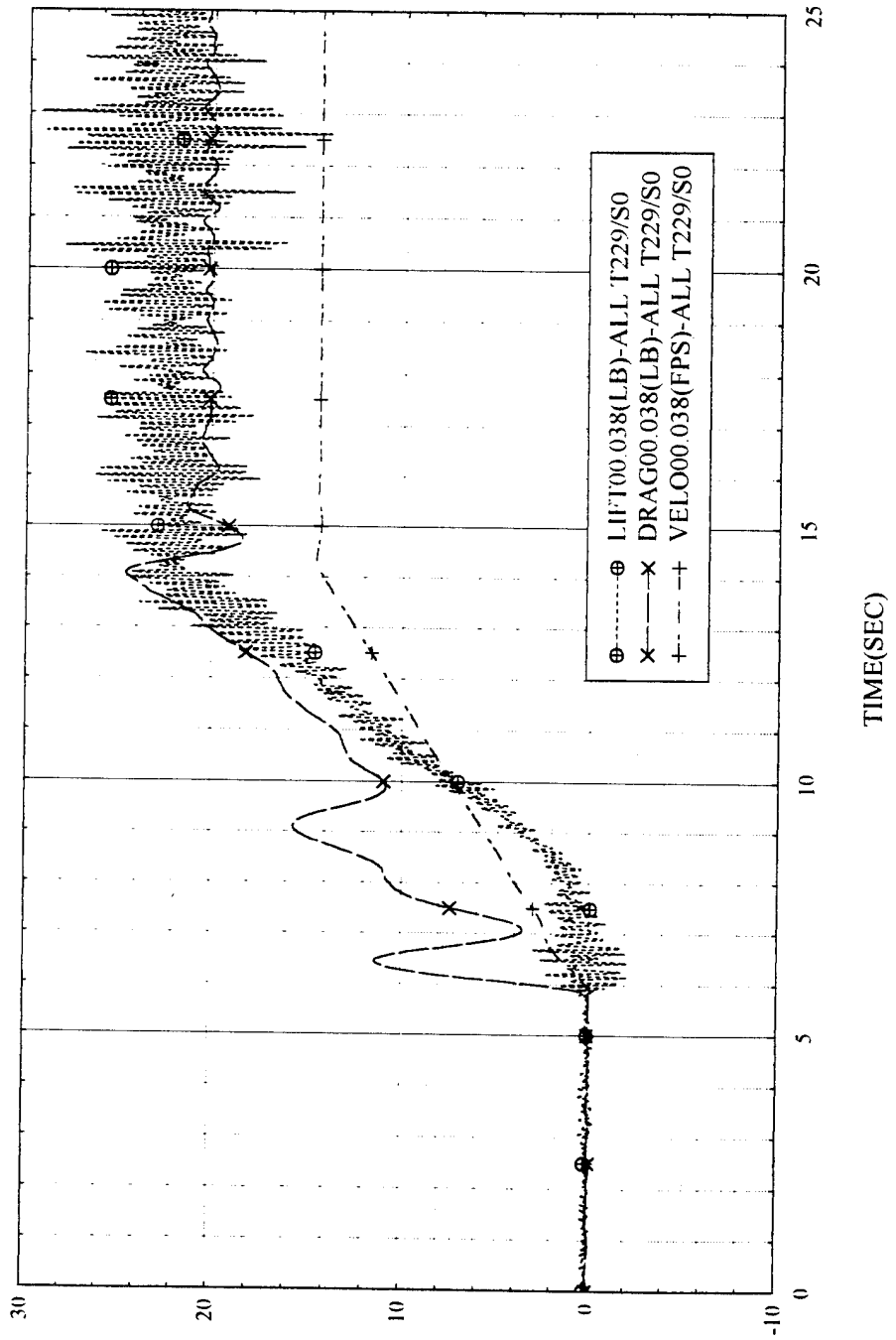
TEST: Model M-2 Test 1 RUN NO:R38
05/30/95 13:52:14

LIFT00.R38(LB)-ALL T229/S0
DRAG00.R38(LB)-ALL T229/S0
VELO00.R38(FPS)-ALL T229/S0

TIME(SEC)
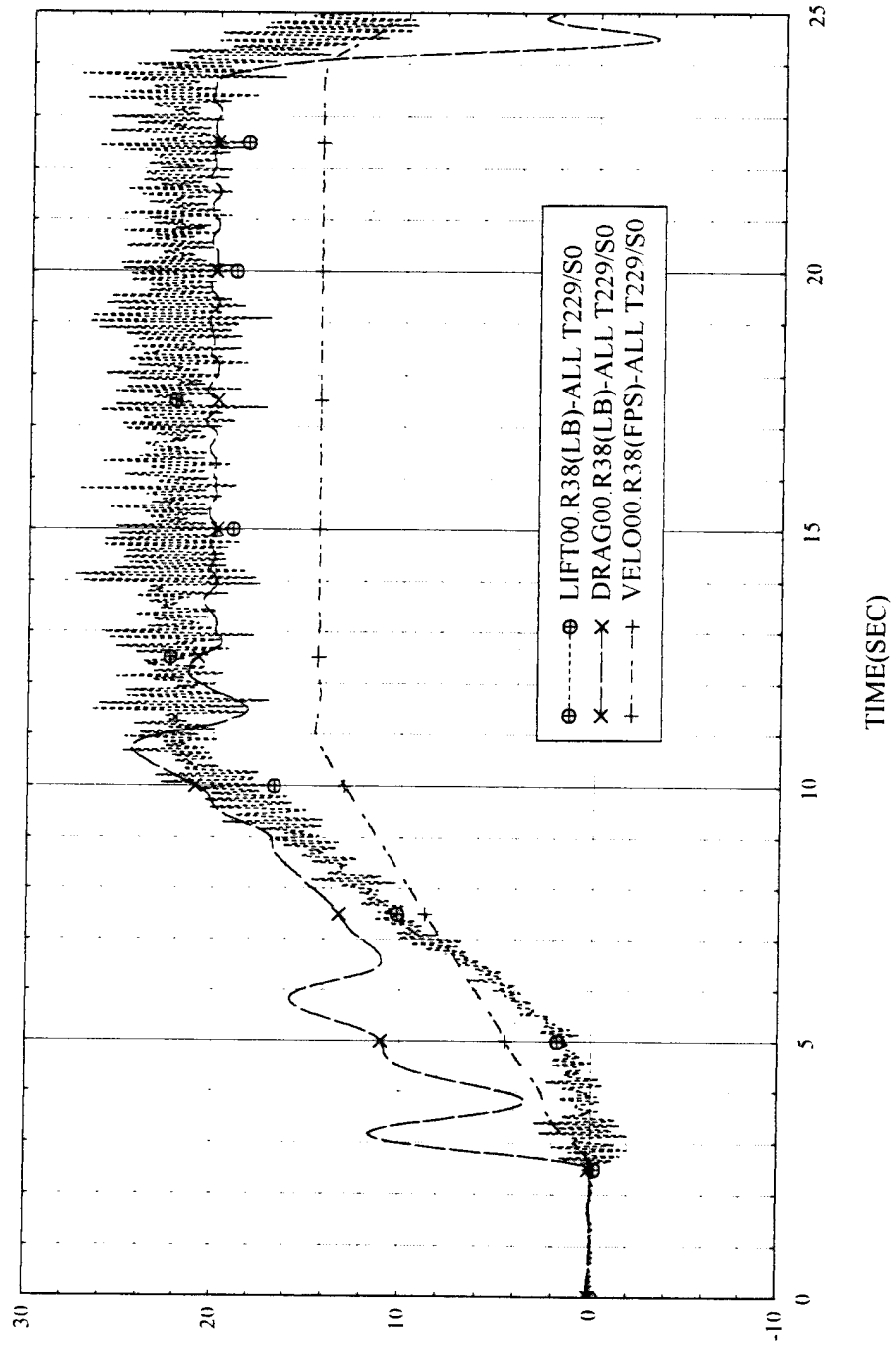
TEST:Model M-2 Test 1 RUN NO:040
05/30/95 13:53:50

LIFT00.040(LB)-ALL T229/S0
DRAG00.040(LB)-ALL T229/S0
VELO00.040(FPS)-ALL T229/S0

TIME(SEC)
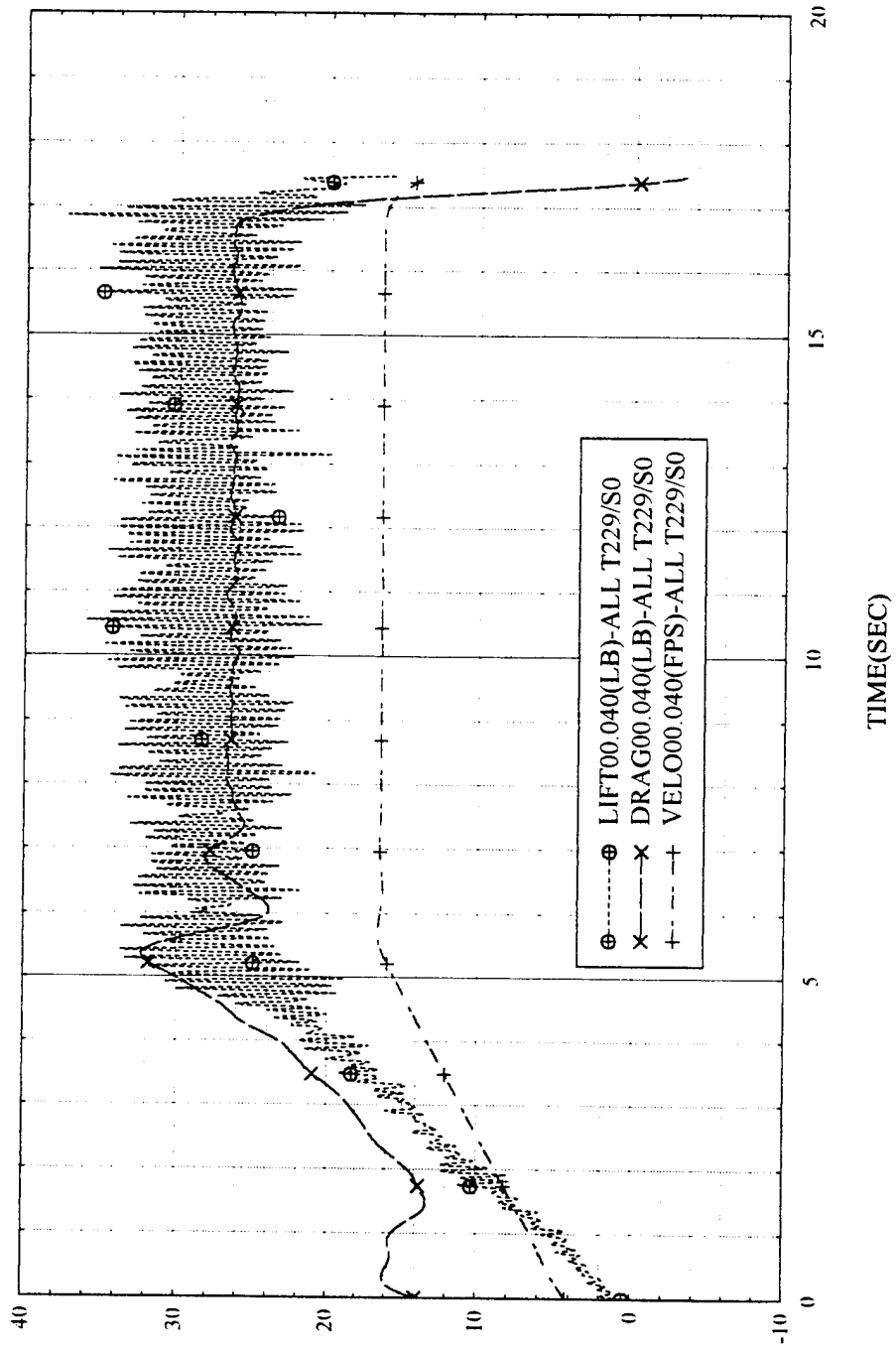
TEST: Model M-2 Test 1 RUN NO:R40
05/30/95 13:55:24

LIFT00.R40(LB)-ALL T229/S0
DRAG00 R40(LB)-ALL T229/S0
VELO00.R40(FPS)-ALL T229/S0

TIME(SEC)
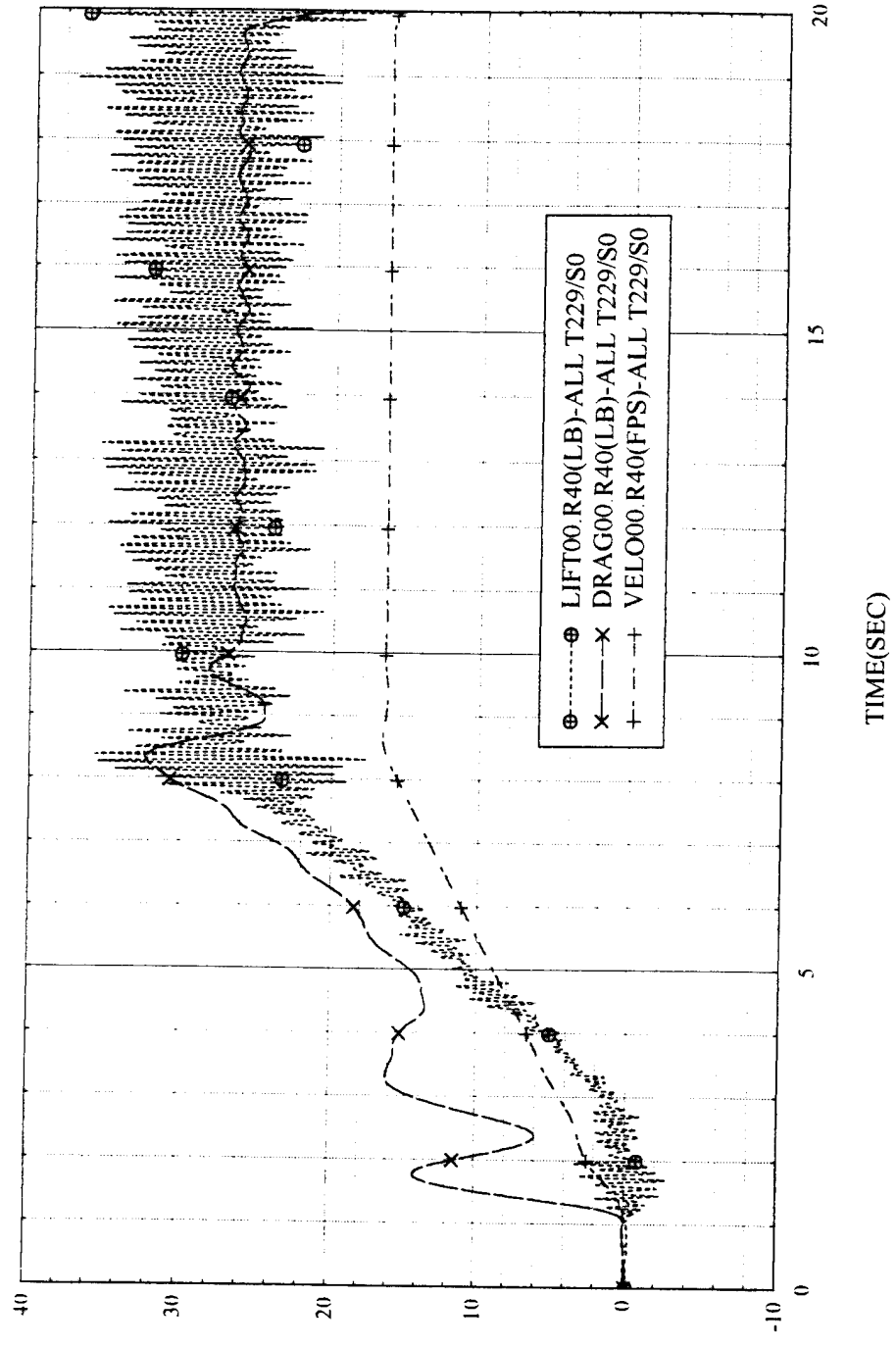
TEST:Model M-2 Test 1 RUN NO:042
05/30/95 13:57:01

Legend:
- ⊕ LIFT00.042(LB)-ALL T229/S0
- ✕ DRAG00.042(LB)-ALL T229/S0
- + VELO00.042(FPS)-ALL T229/S0

TIME(SEC)
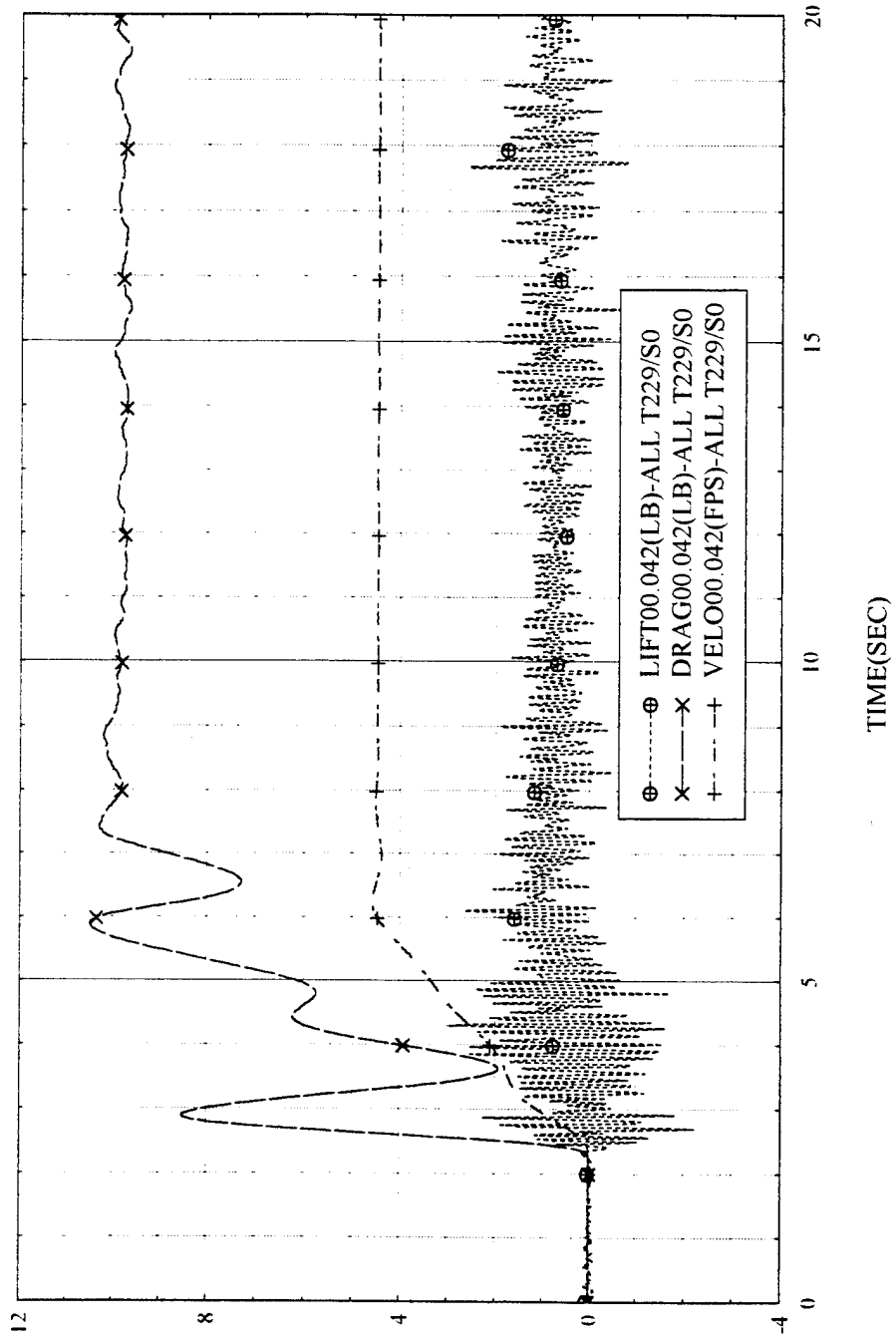
TEST:Model M-2 Test 1 RUN NO:043
05/30/95 15:24:48

LIFT00.043(LB)-ALL T229/S0
DRAG00.043(LB)-ALL T229/S0
VELO00.043(FPS)-ALL T229/S0

TIME(SEC)
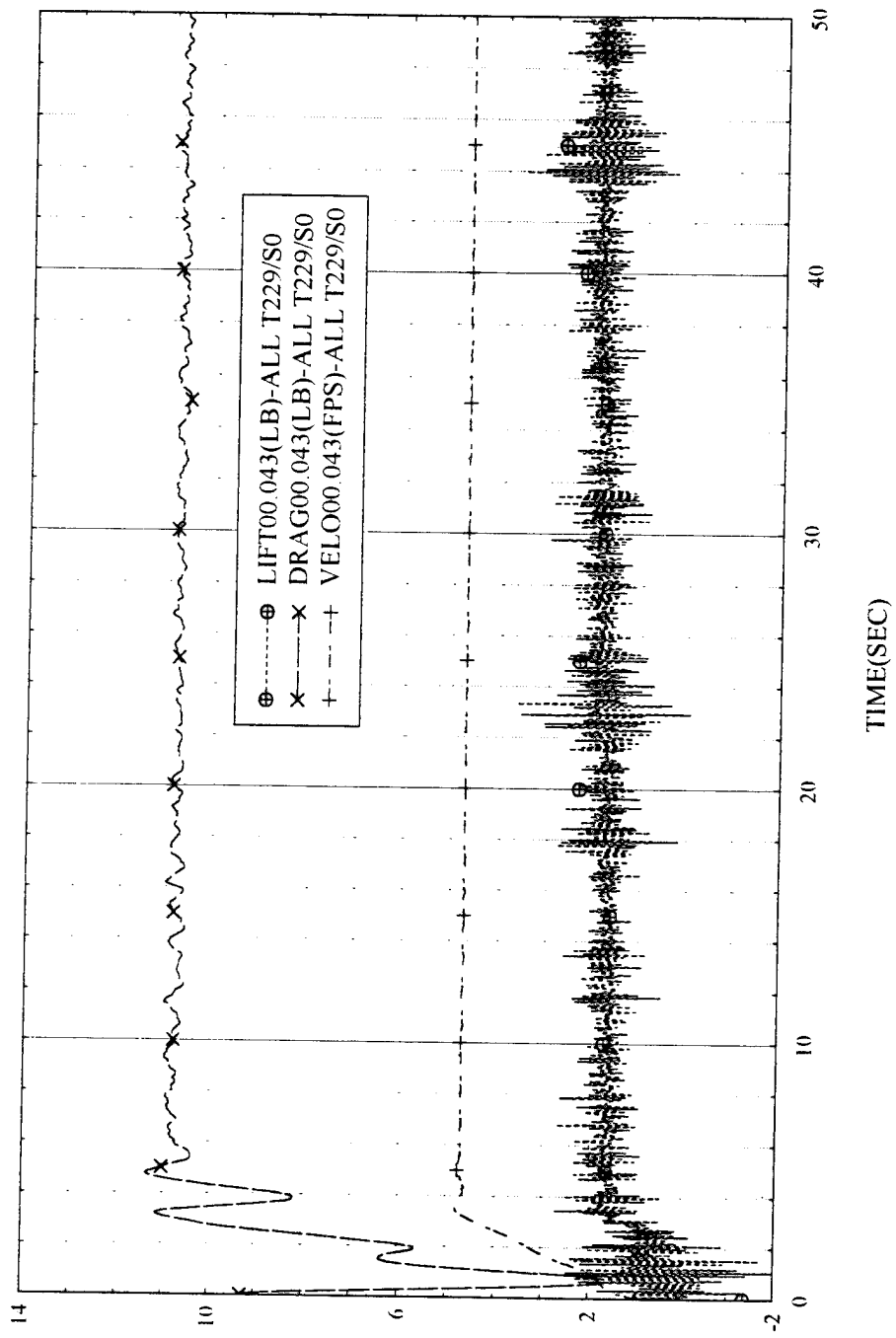
TEST:Model M-2 Test 1 RUN NO:044
05/30/95 15:26:38

Legend:
⊕ LIFT00.044(LB)-ALL T229/S0
✕ DRAG00.044(LB)-ALL T229/S0
+ VELO00.044(FPS)-ALL T229/S0

TIME(SEC)
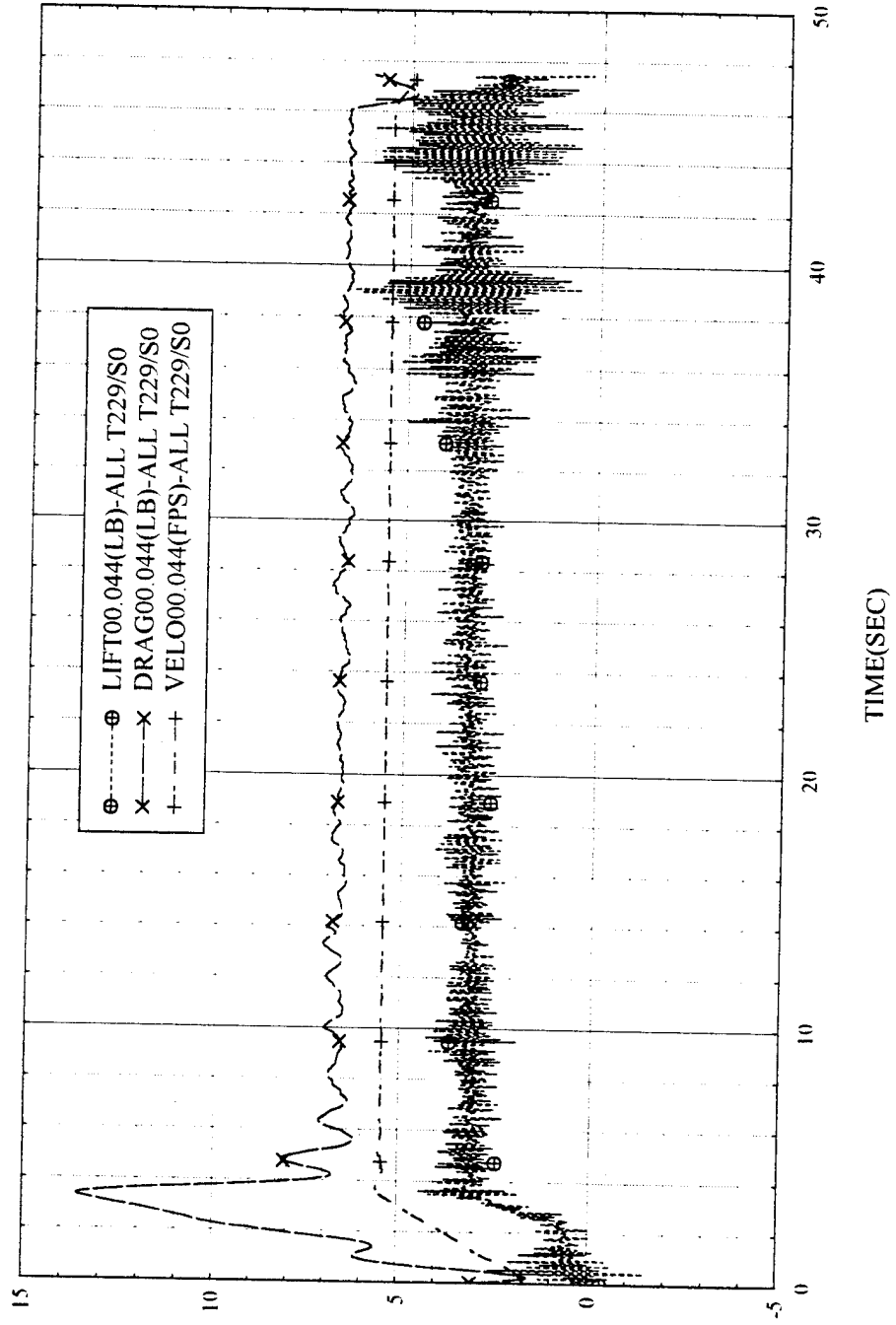
TEST:Model M-2 Test 1 RUN NO:045
05/30/95 15:28:28

LIFT00.045(LB)-ALL T229/S0
DRAG00.045(LB)-ALL T229/S0
VELO00.045(FPS)-ALL T229/S0

TIME(SEC)

TEST:Model M-2 Test 1 RUN NO:046
05/30/95 15:30:15

LIFT00.046(LB)-ALL T229/S0
DRAG00.046(LB)-ALL T229/S0
VELO00.046(FPS)-ALL T229/S0

TIME(SEC)

TEST: Model M-3 Test 1 RUN NO:049
05/30/95 15:34:28

LIFT00.049(LB)-ALL T229/S0
DRAG00.049(LB)-ALL T229/S0
VELO00.049(FPS)-ALL T229/S0

TIME(SEC)
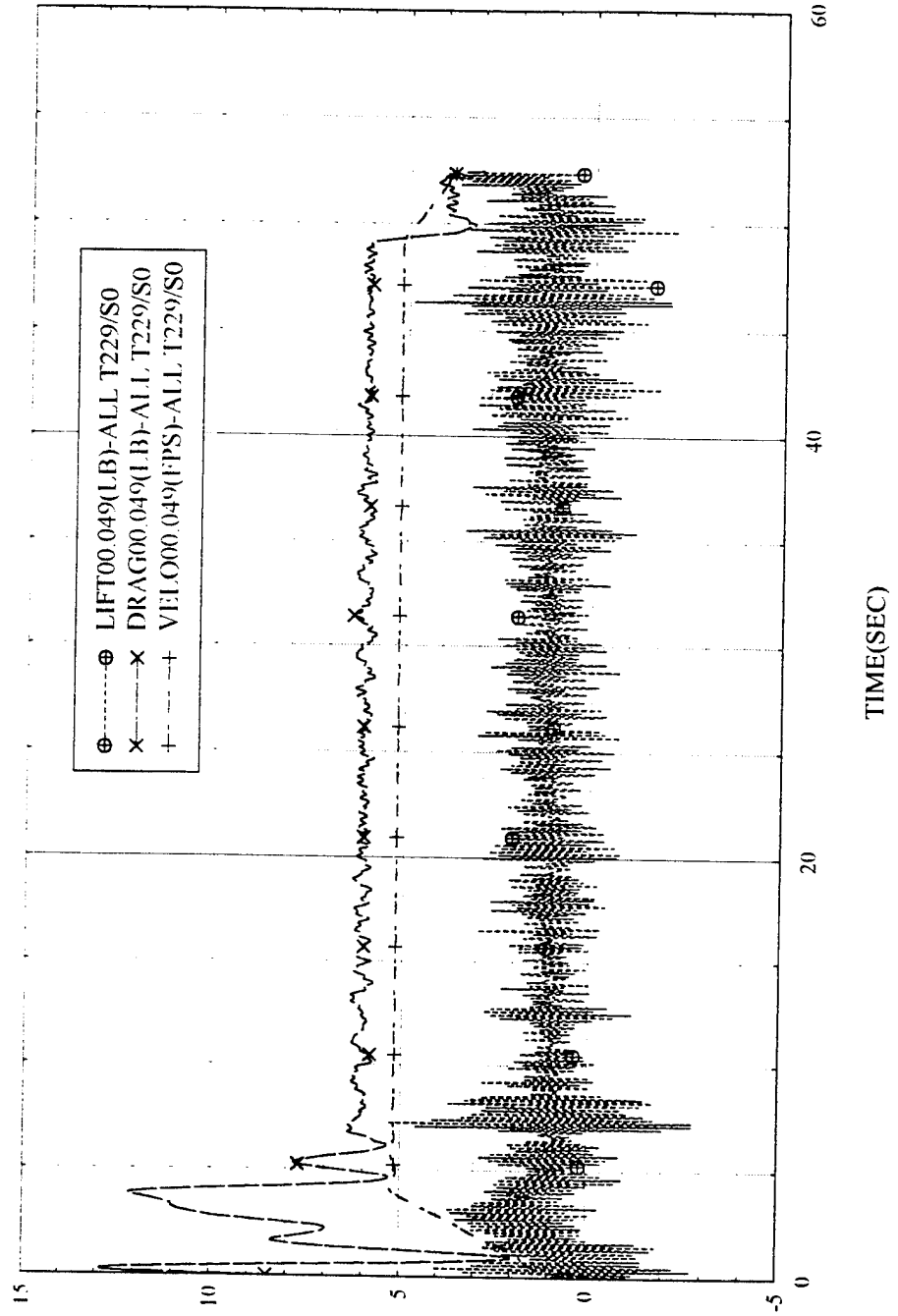
TEST: Model M-3 Test 1 RUN NO:053
05/30/95 15:36:25

TIME(SEC)

⊕ LIFT00.053(LB)-ALL T229/S0
✕ DRAG00.053(LB)-ALL T229/S0
+ VELO00.053(FPS)-ALL T229/S0
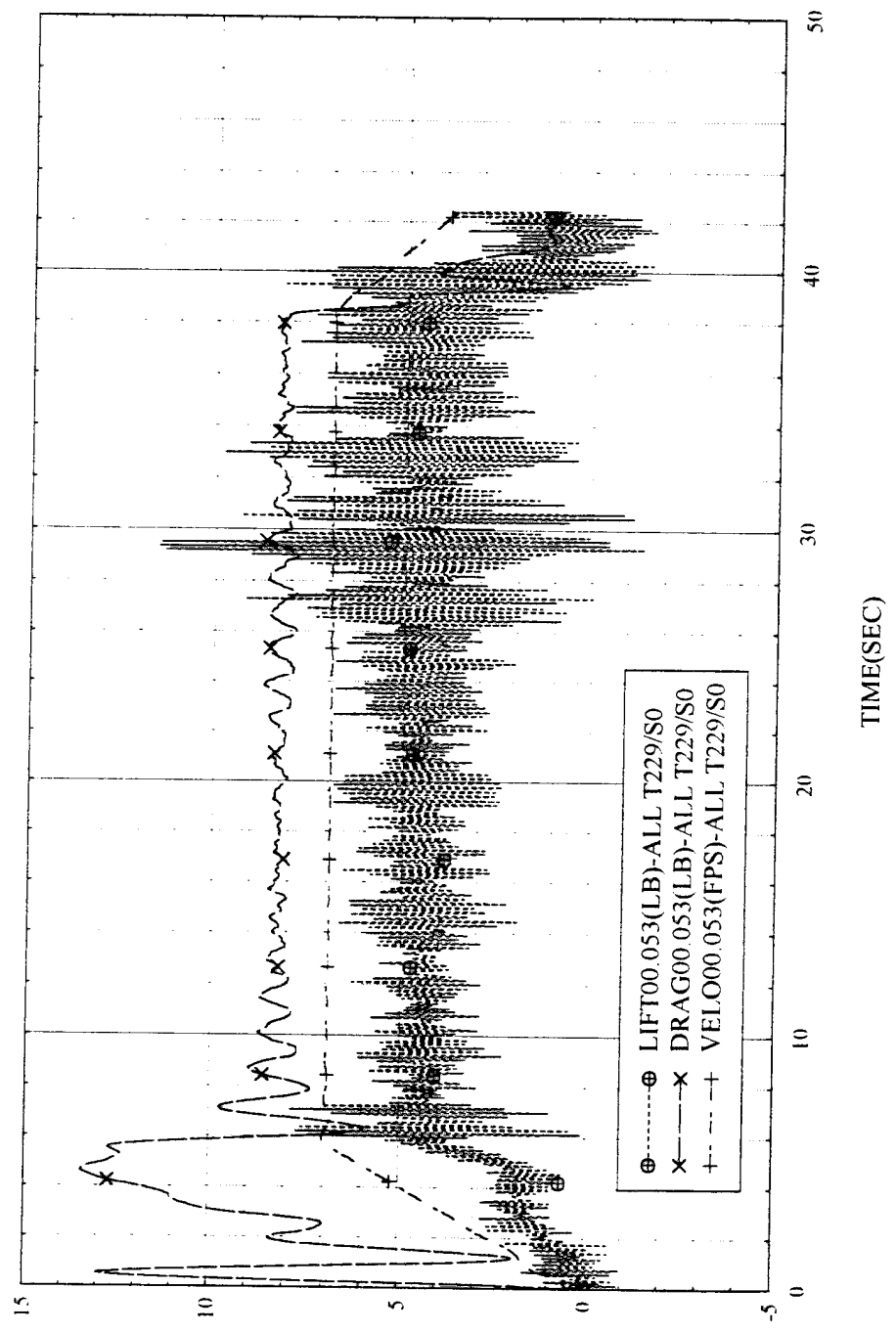
TEST: Model M-3 Test 1 RUN NO:055
05/30/95 15:39:42
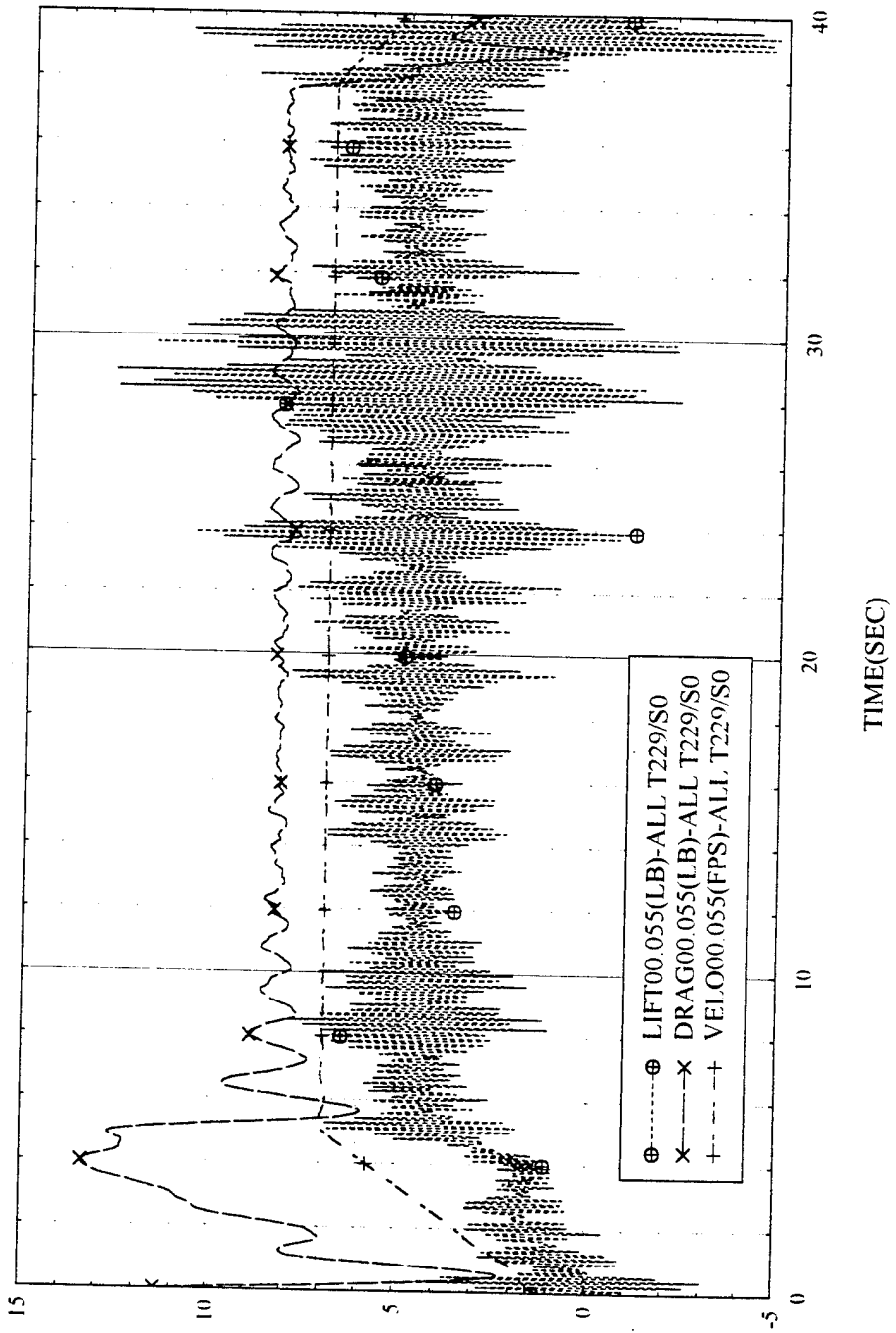
TEST:Model M-3 Test 1 RUN NO:056
05/30/95 15:49:51
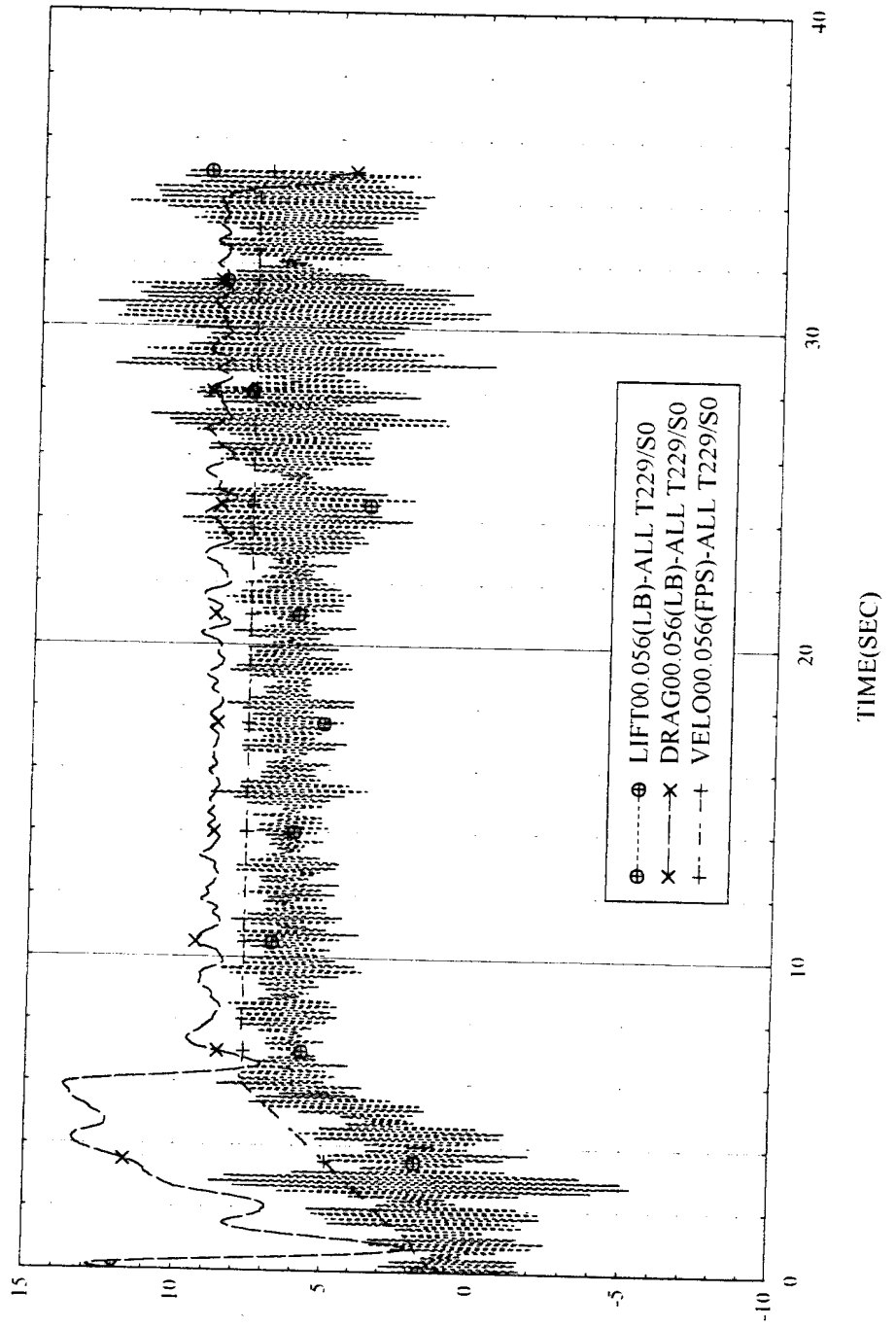
TEST: Model M-3 Test 1 RUN NO:057
05/30/95 15:59:04

TIME(SEC)

⊕ ...... ⊕ LIFT00.057(LB)-ALL T229/S0
✕ — ✕ DRAG00.057(LB)-ALL T229/S0
+ — + VELO00.057(FPS)-ALL T229/S0
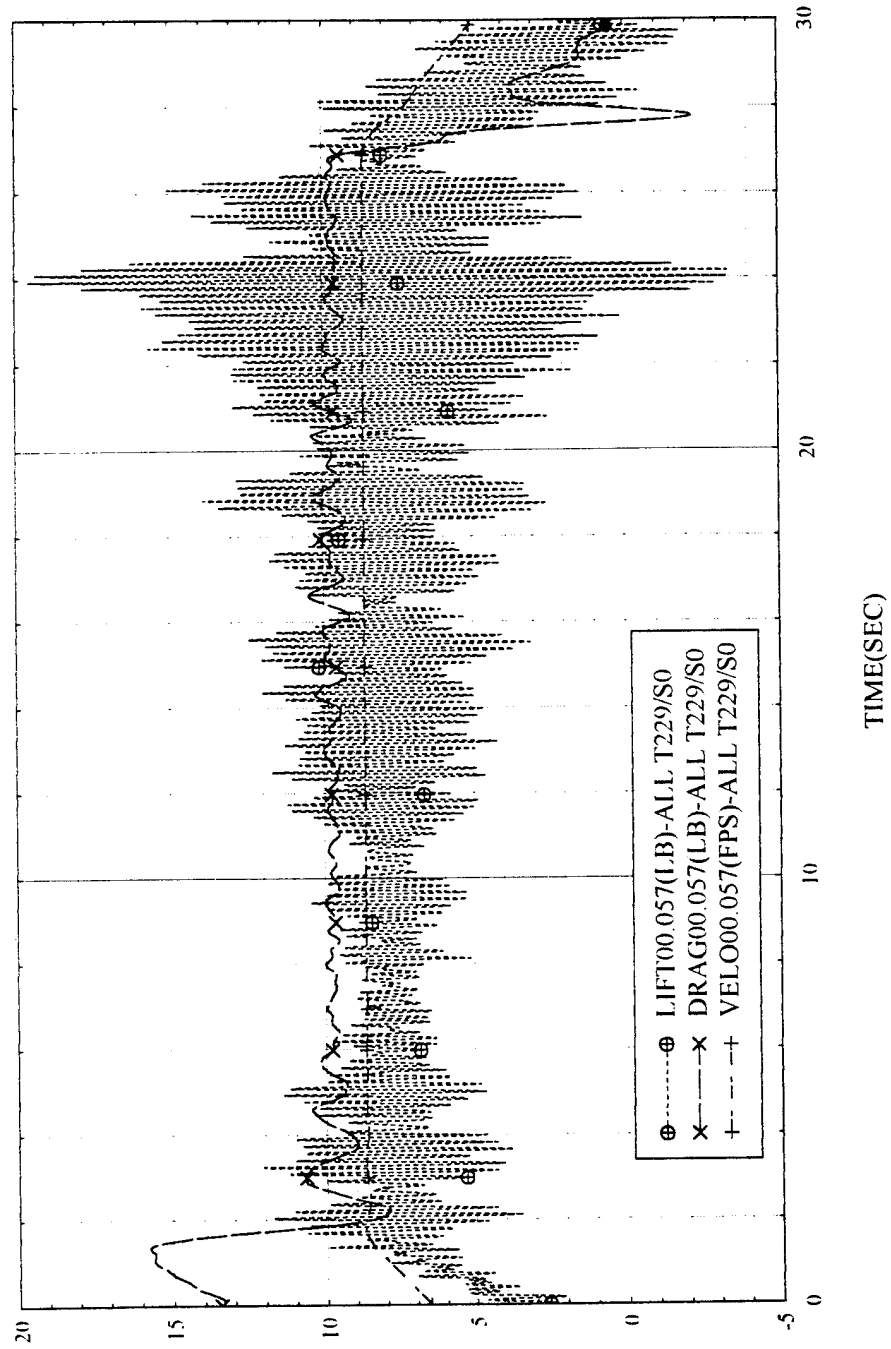
TEST: Model M-3 Reverse Direction Data Point RUN NO:058
05/30/95 16:02:36

LIFT00.058(LB)-ALL T229/S0
DRAG00.058(LB)-ALL T229/S0
VELO00.058(FPS)-ALL T229/S0

TIME(SEC)
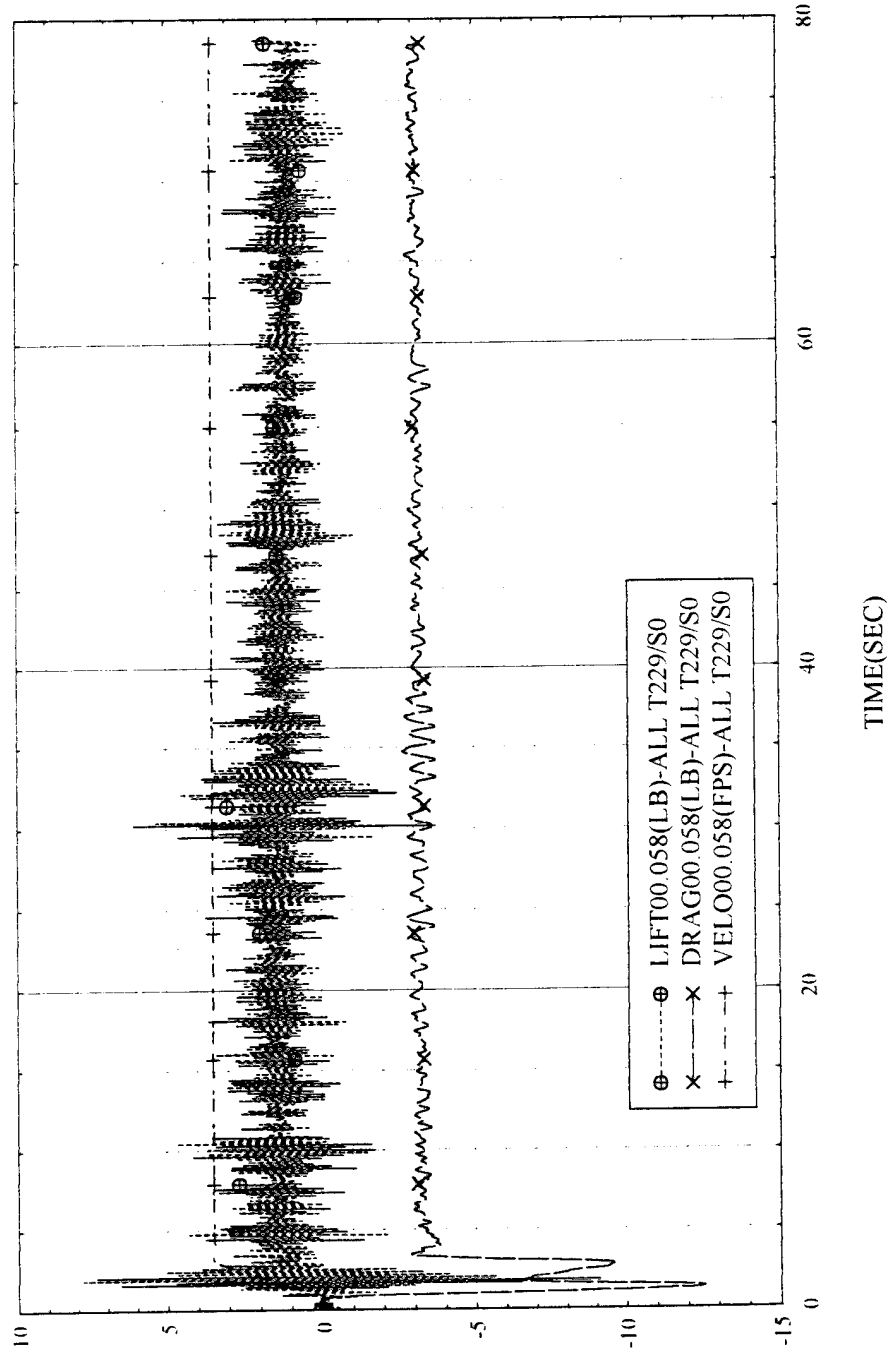
TEST: Model M-3 Test 1 RUN NO:059
05/30/95 16:04:38

TIME(SEC)

LIFT00.059(LB)-ALL T229/S0
DRAG00.059(LB)-ALL T229/S0
VELO00.059(FPS)-ALL T229/S0

TEST:229 RUN NO:R59

LIFT00.R59(LB)-ALL T229/S0
DRAG00.R59(LB)-ALL T229/S0
VELO00.R59(FPS)-ALL T229/S0

TIME(SEC)
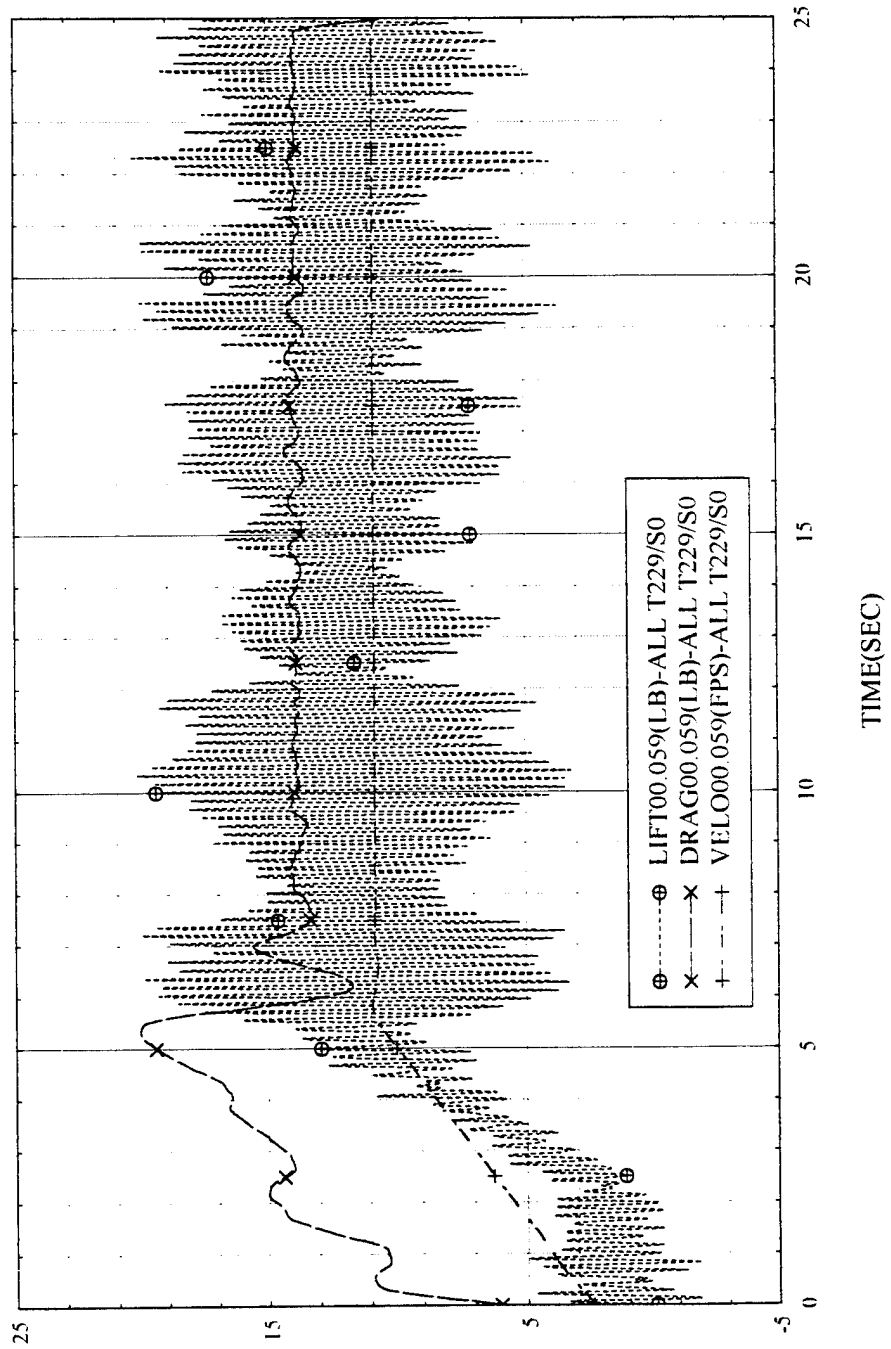
189
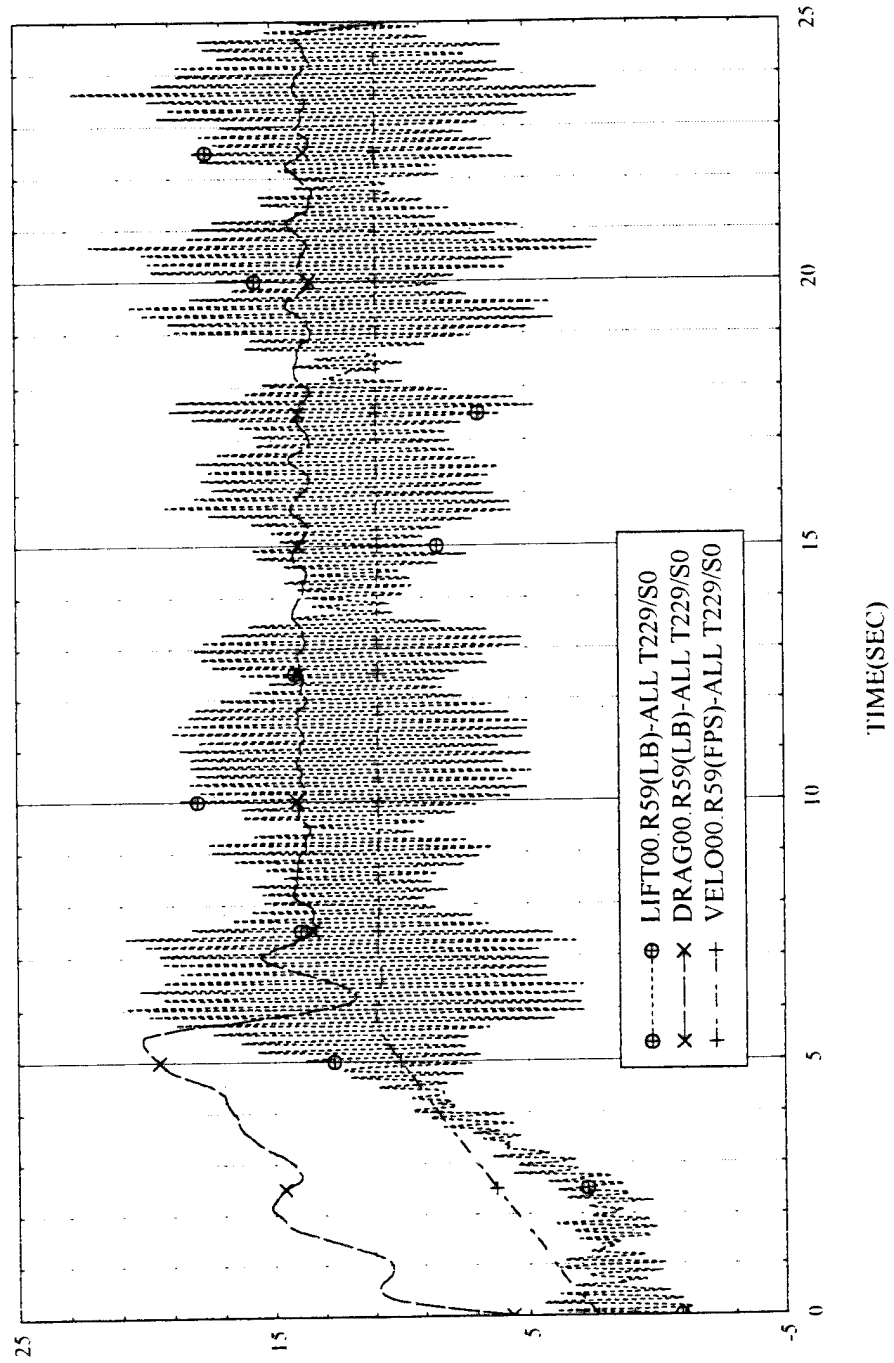
TEST: Model M-3 Test 1 RUN NO:061
05/30/95 16:09:20

LIFT00.061(LB)-ALL T229/S0
DRAG00.061(LB)-ALL T229/S0
VELO00.061(FPS)-ALL T229/S0

TIME(SEC)
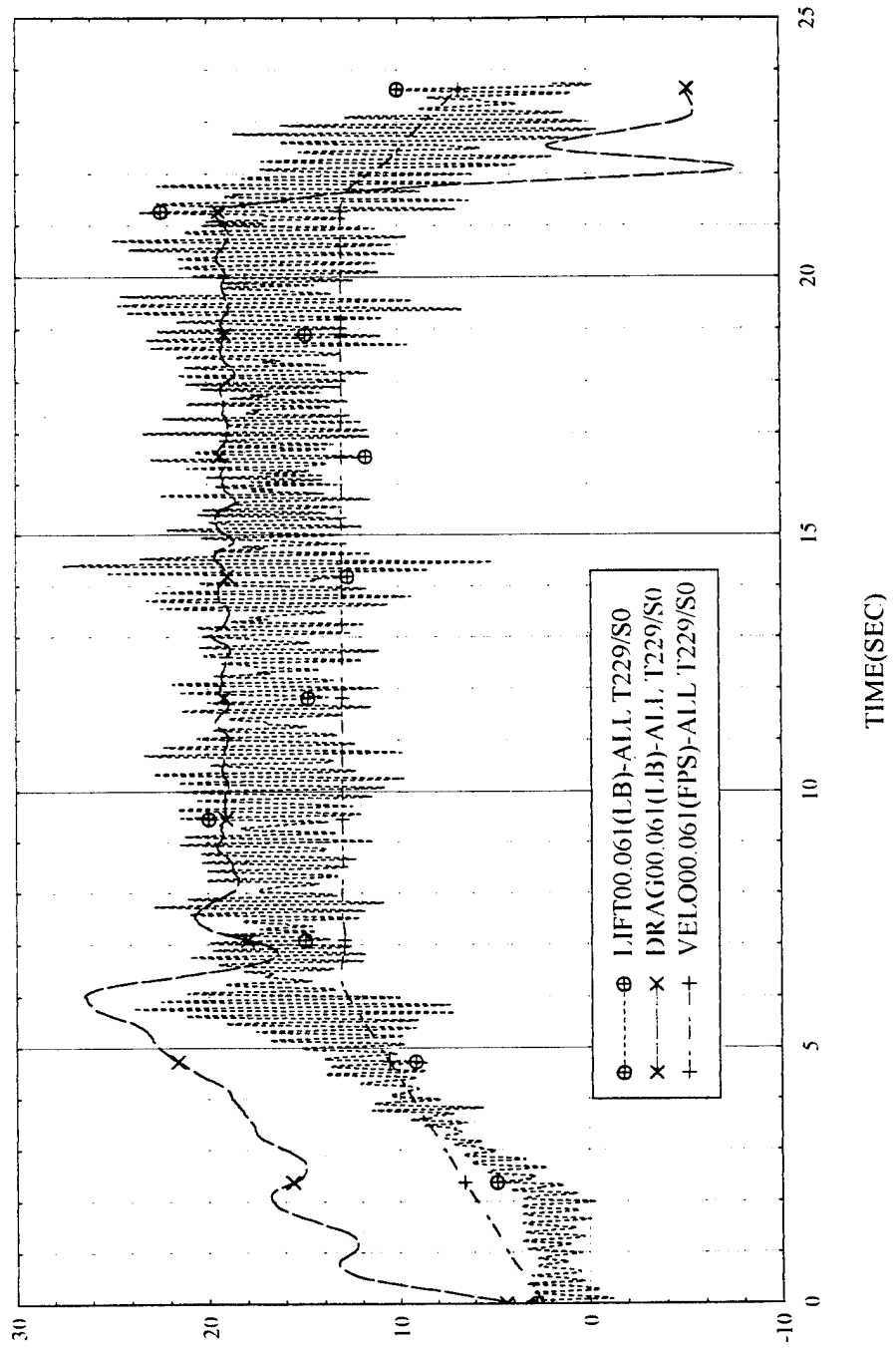
TEST:Model M-3 Test 1 RUN NO:R61
05/30/95 16:11:51
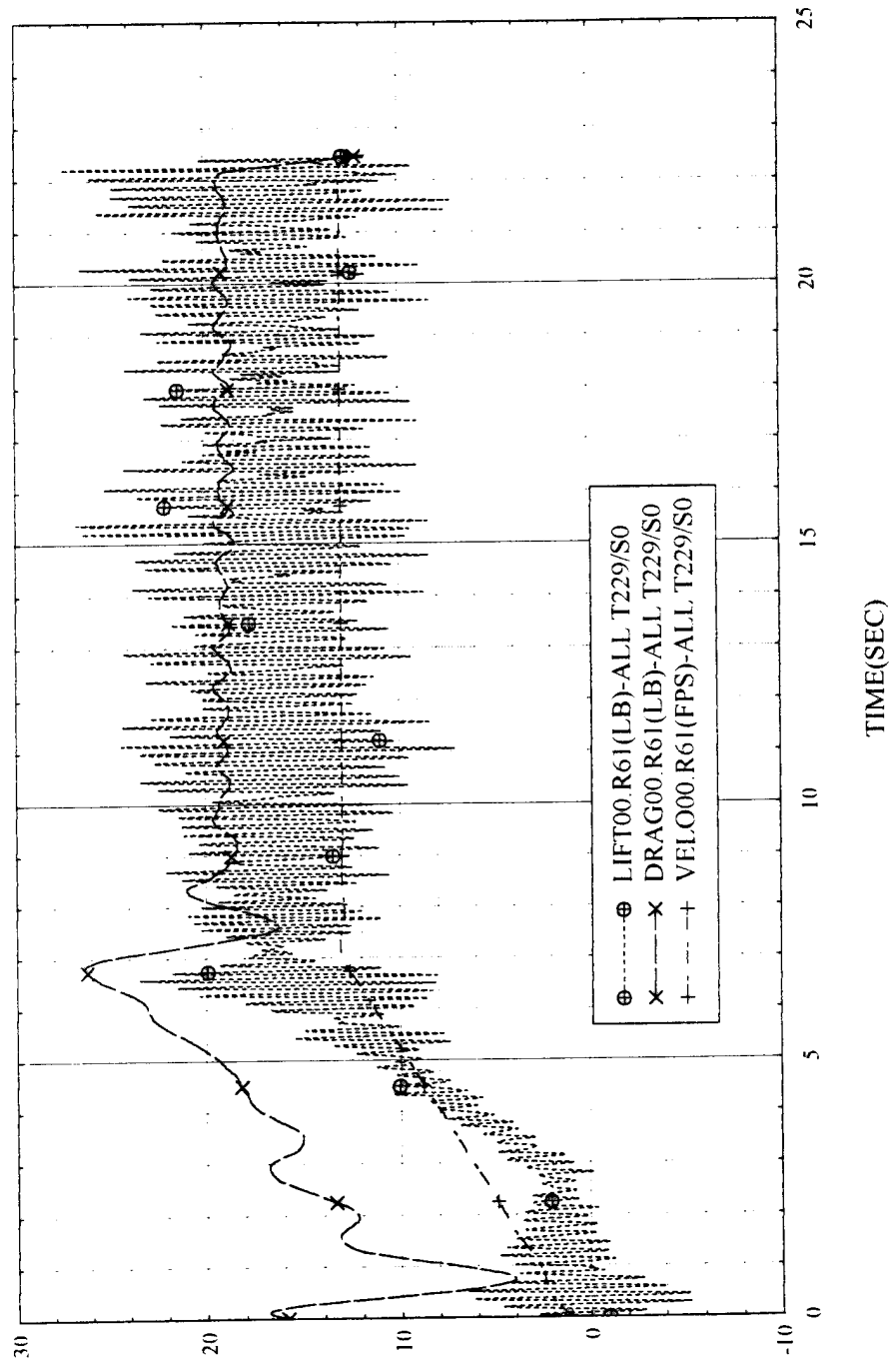
TEST:Model M-3 Test 1 RUN NO:063
05/30/95 16:13:45

LIFT00.063(LB)-ALL T229/S0
DRAG00.063(LB)-ALL T229/S0
VELO00.063(FPS)-ALL T229/S0

TIME(SEC)
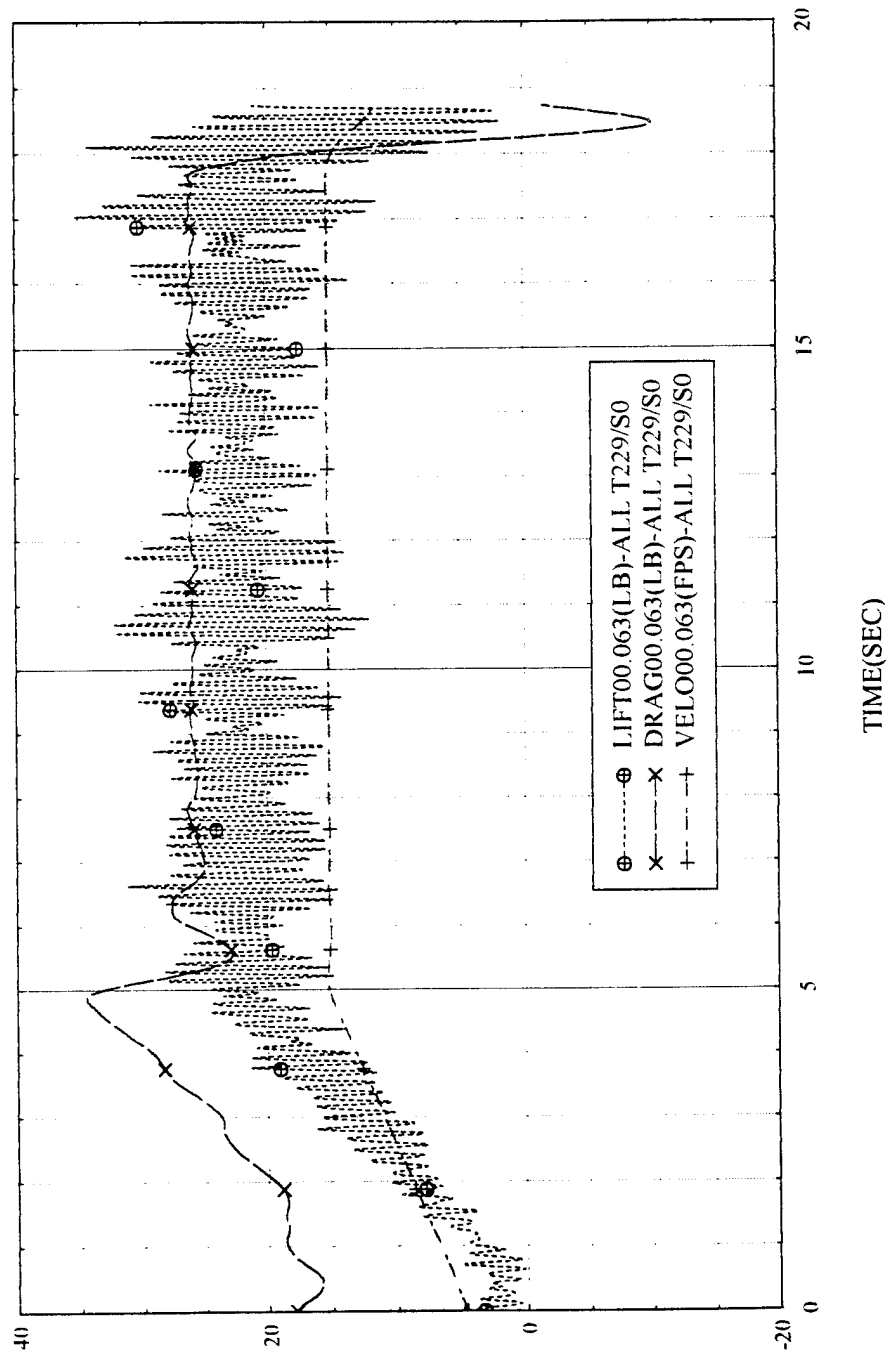
TEST:Model M-3 Test 1 RUN NO:R63
05/30/95 16:15:49

LIFT00.R63(LB)-ALL T229/S0
DRAG00.R63(LB)-ALL T229/S0
VELO00.R63(FPS)-ALL T229/S0

TIME(SEC)
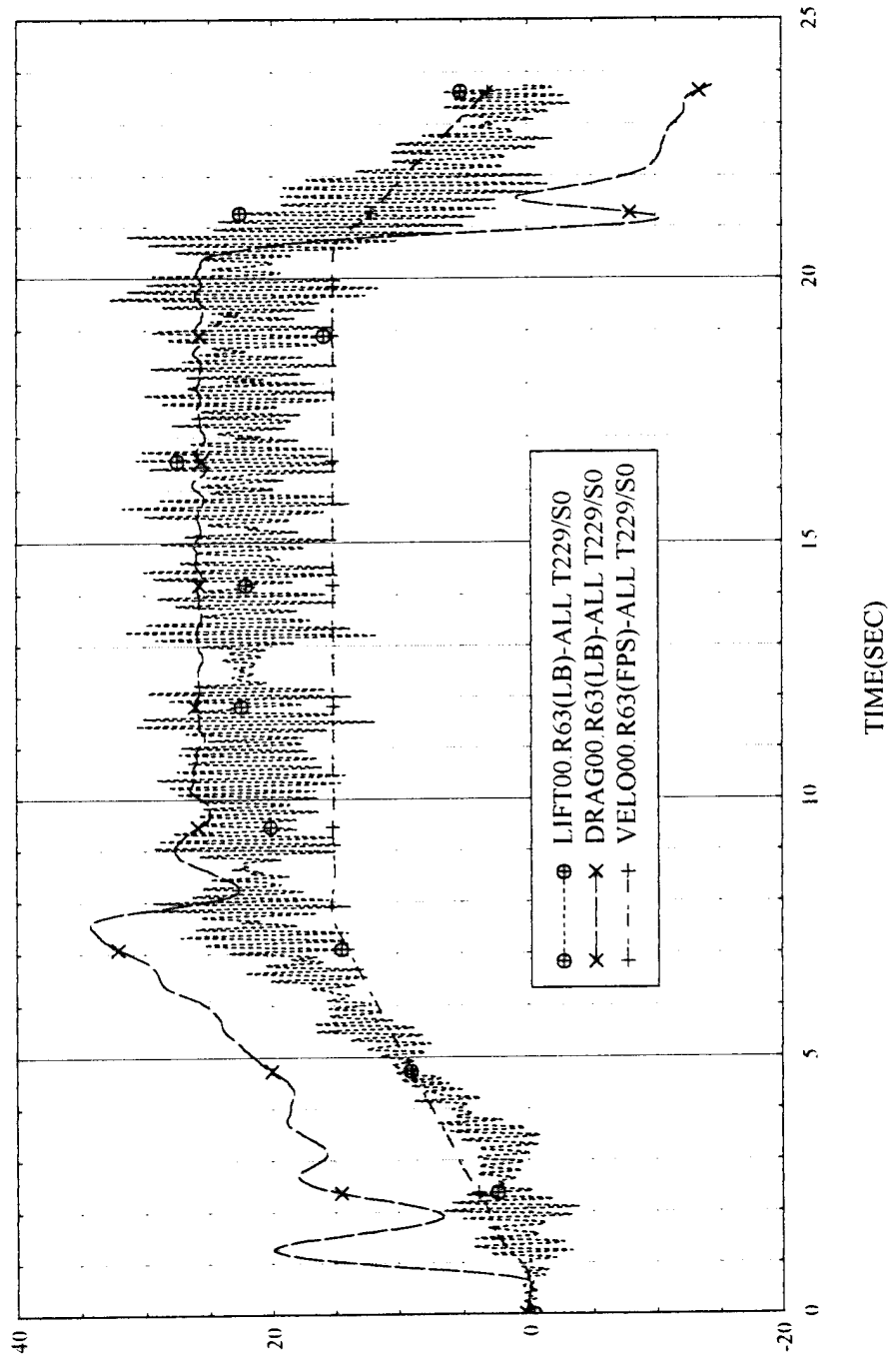
TEST: Model M-3 Test 1 RUN NO:066
05/30/95 16:17:49

TIME(SEC)

LIFT00.066(LB)-ALL T229/S0
DRAG00.066(LB)-ALL T229/S0
VELO00.066(FPS)-ALL T229/S0

194

TEST:Model M-3 Test 1 RUN NO:R66
05/30/95 16:19:38

LIFT00.R66(LB)-ALL T229/S0
DRAG00.R66(LB)-ALL T229/S0
VELO00.R66(FPS)-ALL T229/S0

TIME(SEC)
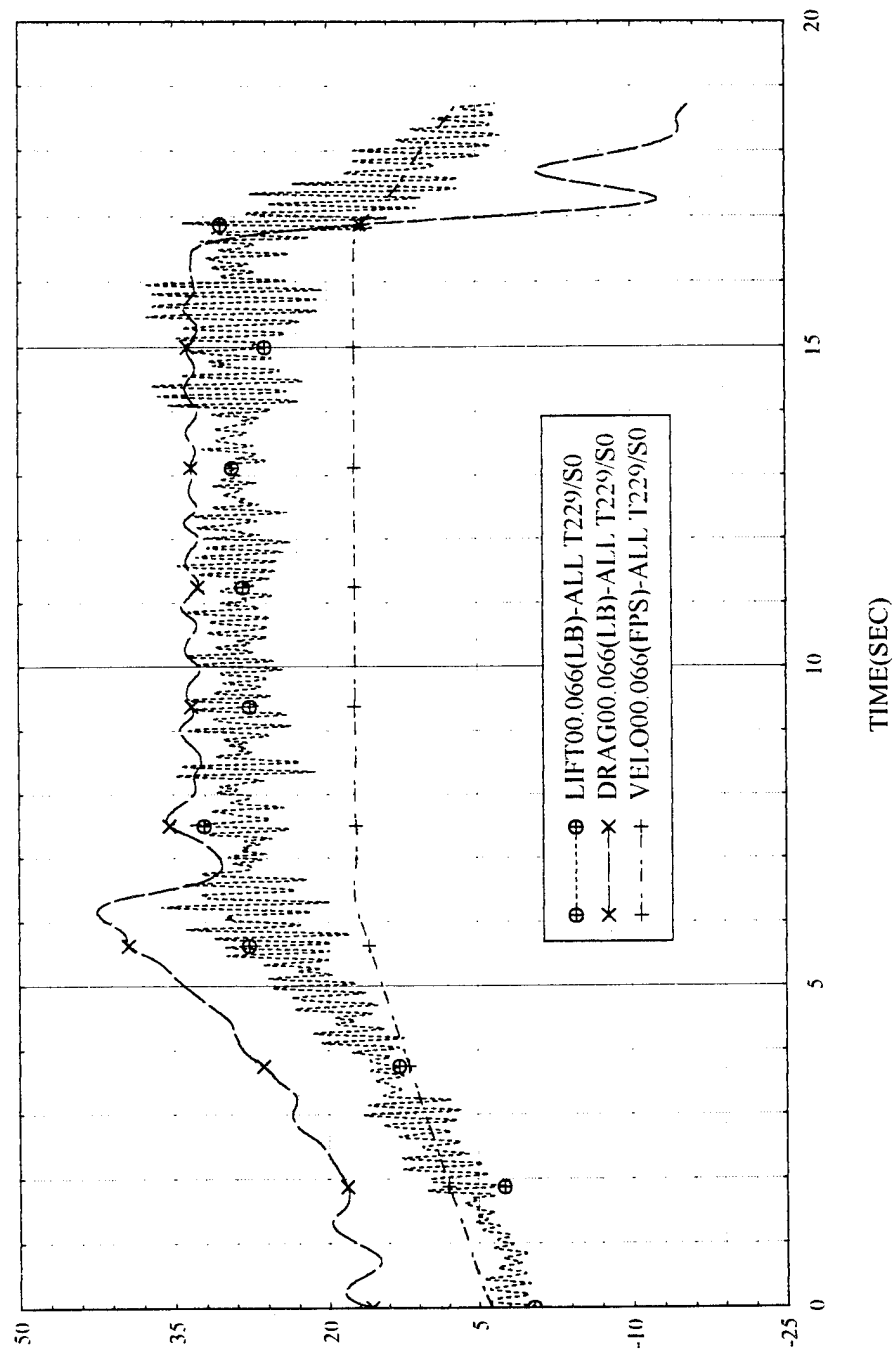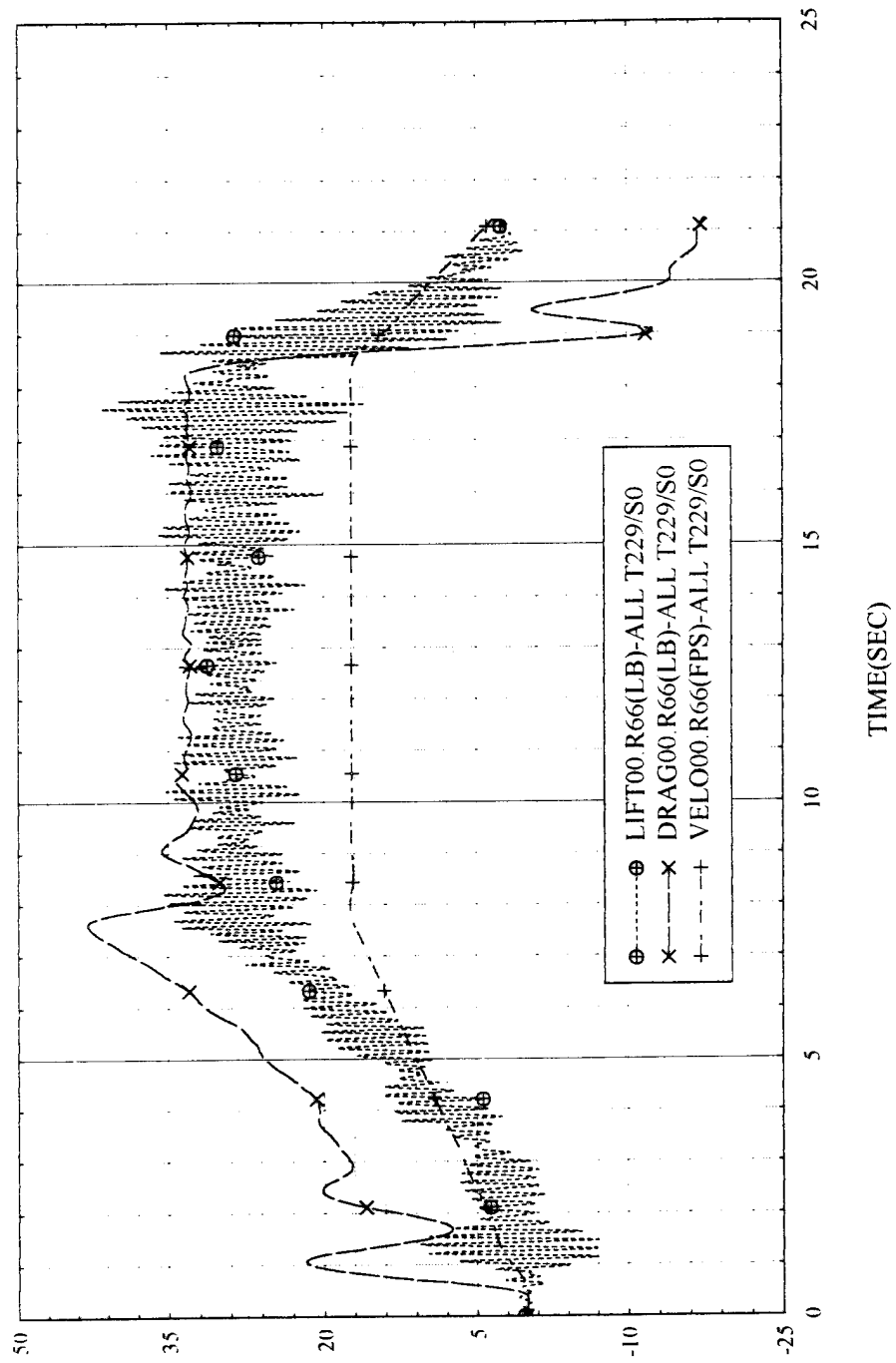
TEST:Model M-3 Test 1 RUN NO:068
05/30/95 16:21:34
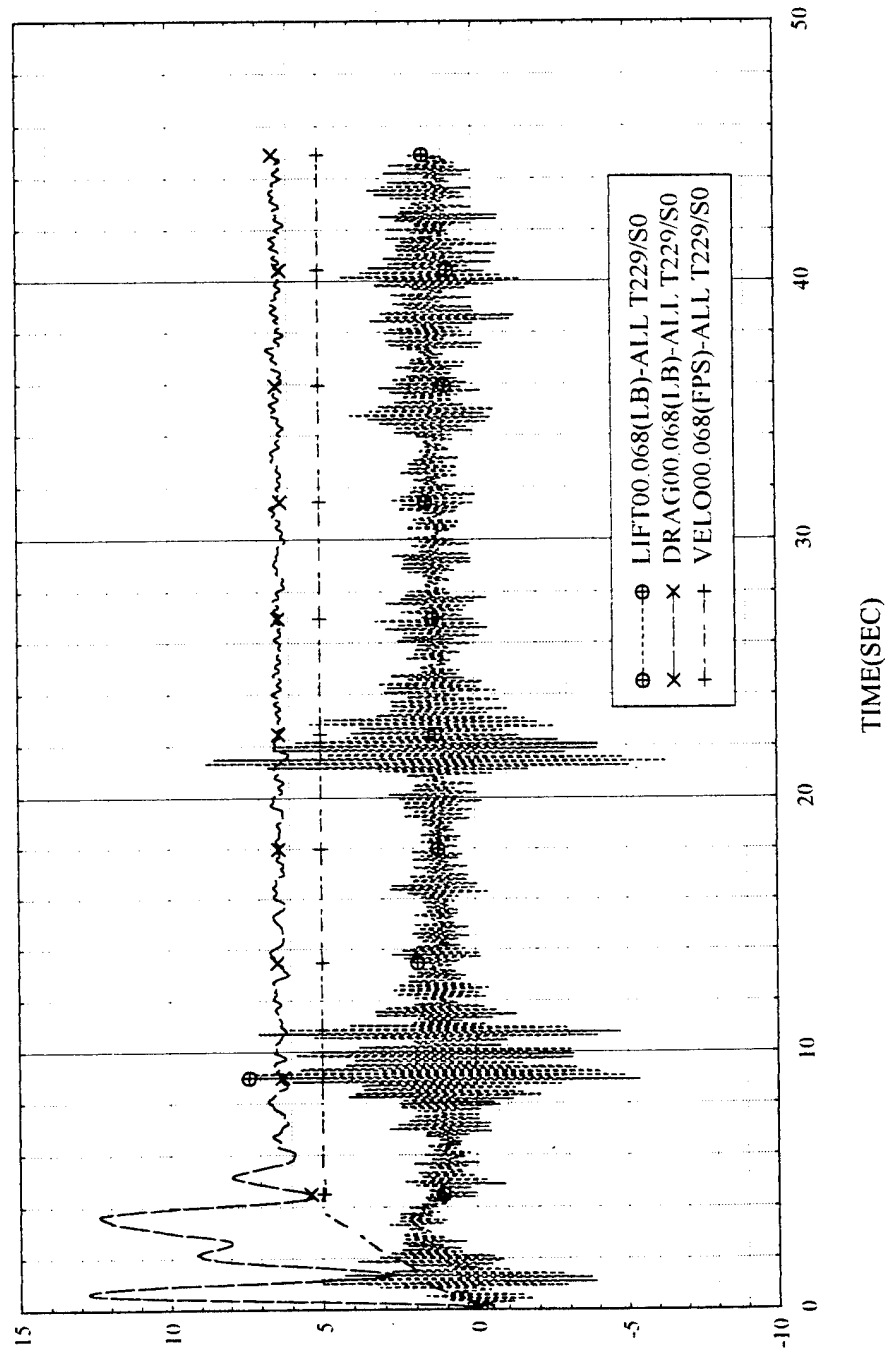
⊕ LIFT00.068(LB)-ALL T229/S0
✕ DRAG00.068(LB)-ALL T229/S0
+ VELO00.068(FPS)-ALL T229/S0

TIME(SEC)

TEST:Model M-3 Test 1 RUN NO:069
05/30/95 16:23:51

LIFT00.069(LB)-ALL T229/S0
DRAG00.069(LB)-ALL T229/S0
VELO00.069(FPS)-ALL T229/S0

TIME(SEC)

197

TEST: Model M-1 RUN NO:71

TIME(SEC)

⊕ LIFT00.071(LB)-ALL T229/S0
✕ DRAG00.071(LB)-ALL T229/S0
+ VELO00.071(FPS)-ALL T229/S0

198
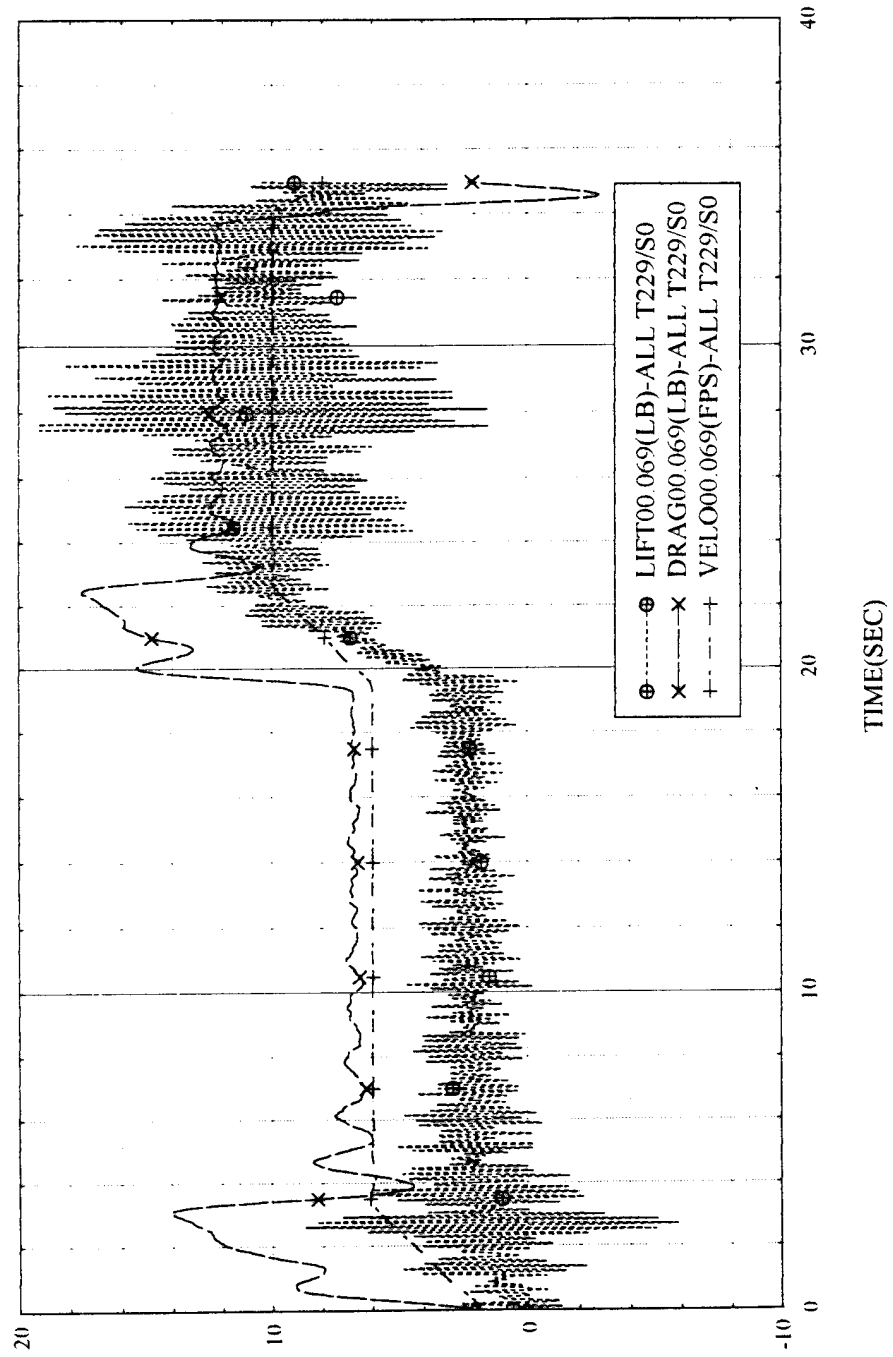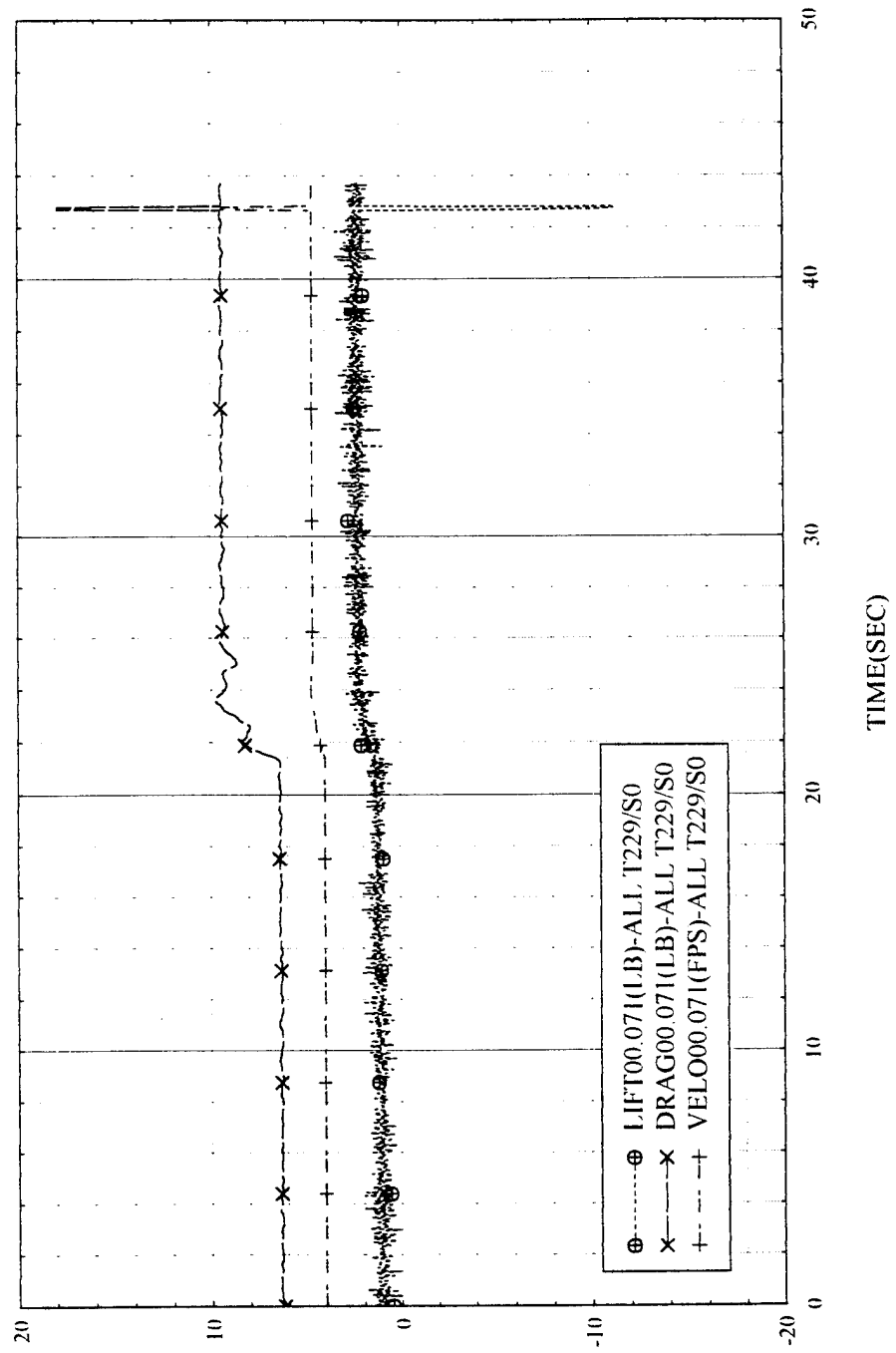
TEST: Model M-1 Draft Variation T+ 0.375" NO:R74

TIME(SEC)
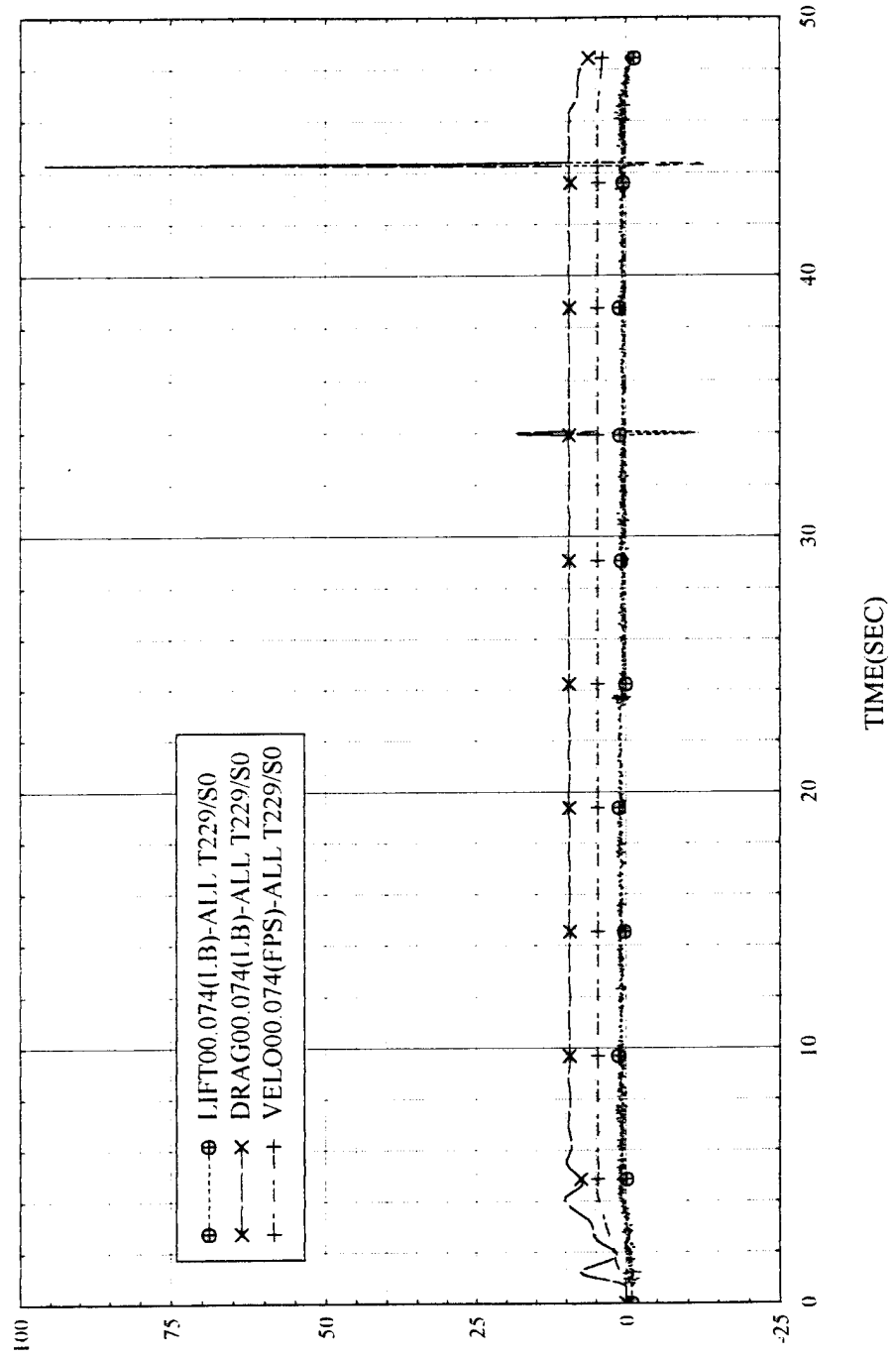
TEST:Model M-1 Draft Variation RUN NO:072
05/30/95 16:31:24

TIME(SEC)

LIFT00.072(LB)-ALL T229/S0
DRAG00.072(LB)-ALL T229/S0
VELO00.072(FPS)-ALL T229/S0
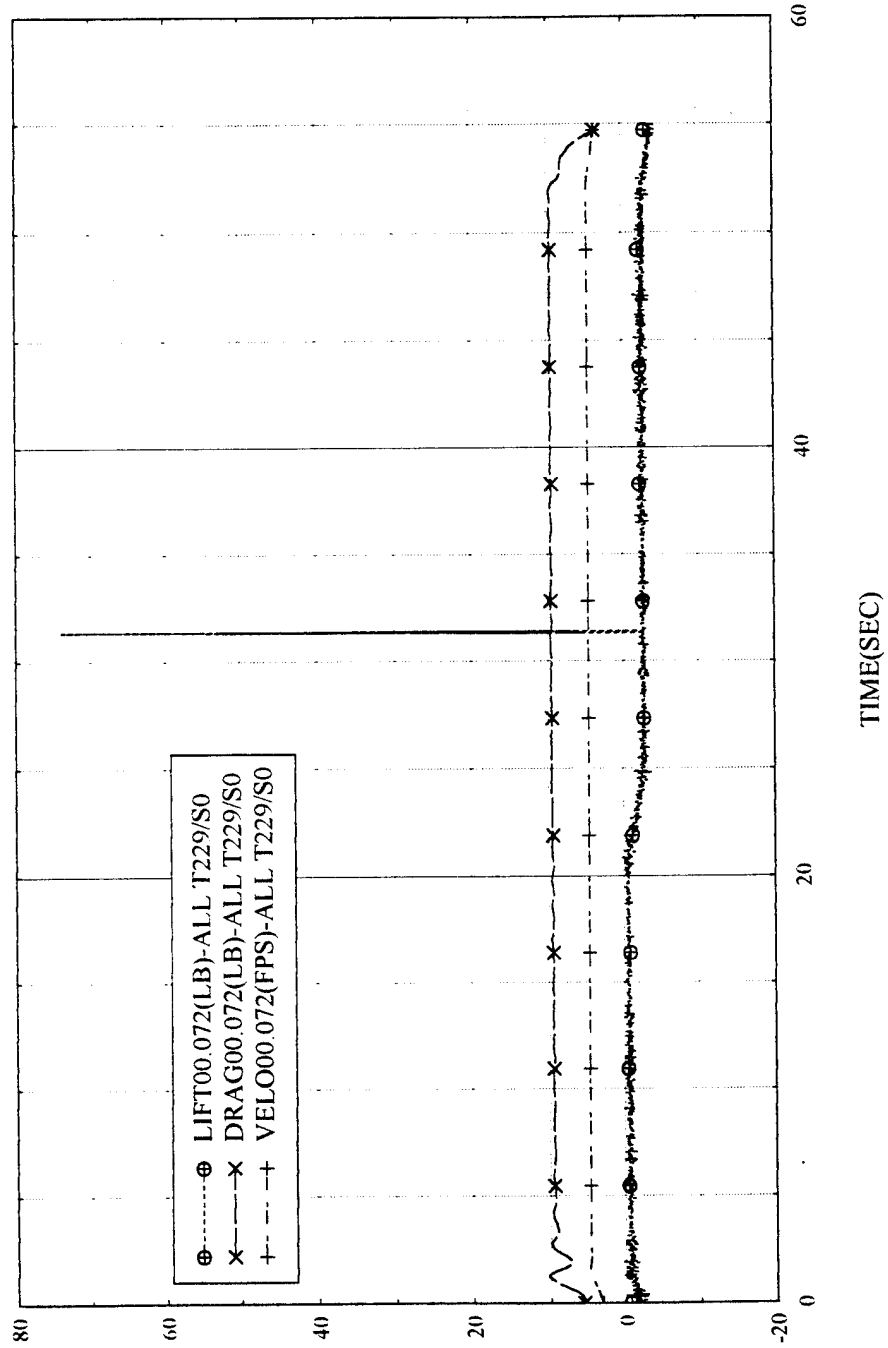
TEST:Model M-1 Draft Variation T=.25in RUN NO.74
05/30/95 16:33:46

TIME(SEC)
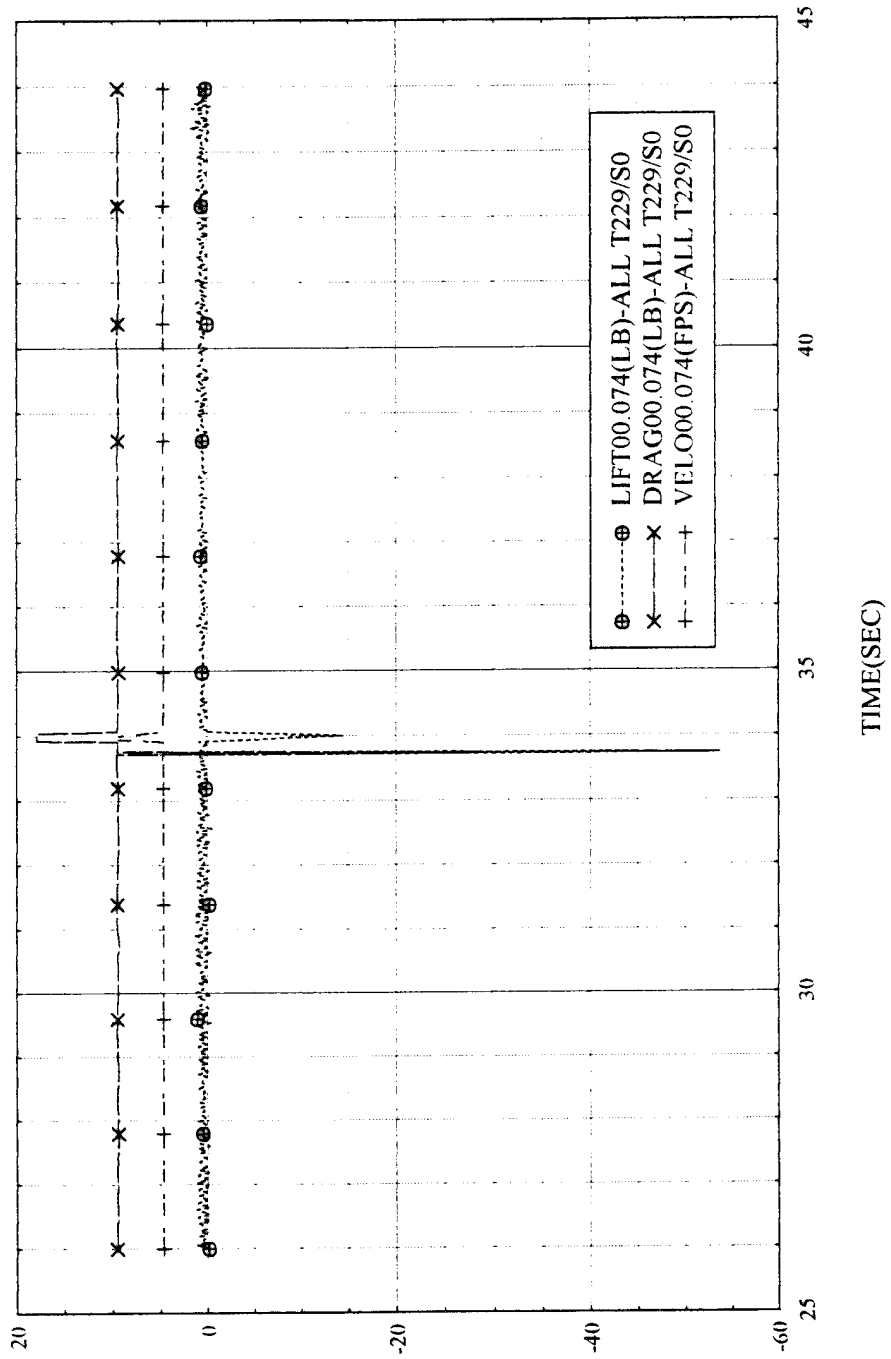
TEST:Model M-1 Test 1 RUN NO:083
Model Modified to In-Line Configuration
05/30/95 16:36:08

LIFT00.083(LB)–ALL T229/S0
DRAG00.083(LB)–ALL T229/S0
VELO00.083(FPS)–ALL T229/S0

TIME(SEC)

202
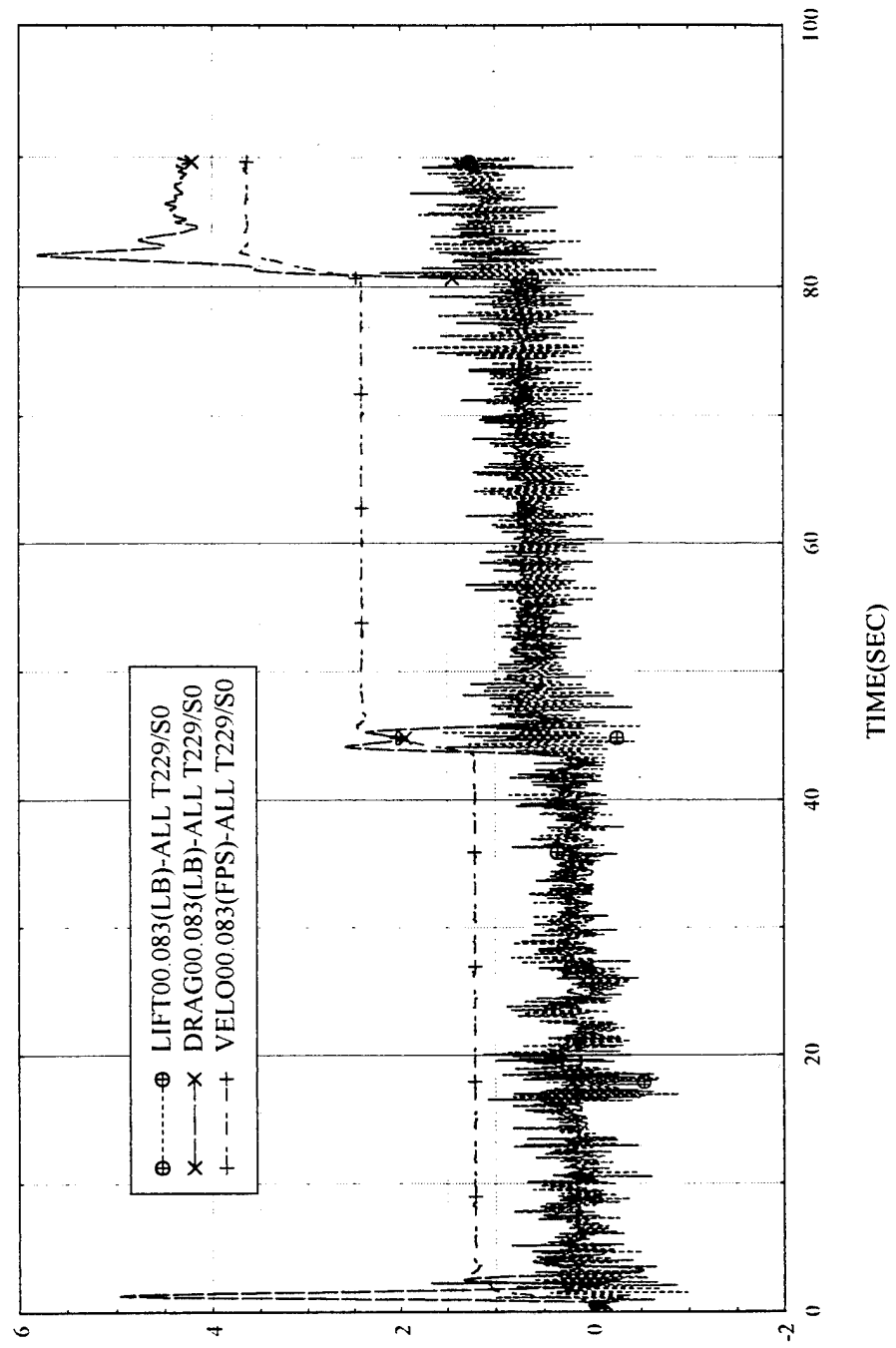
Appendix G

Data Scaling Worksheets

This Calculation Scales the Test Data obtained for Model M-1 to Full Scale.

NOTE: The System of Subscripts in this Routine can become rather bulky... "R", "C", "M", "S" are Resistance, Coefficient of Resistance, Measured and Ship respectively... where measured refers to the measured model (Model M-2 Data unscaled) and Ship refers to the full scale calculation. Also, "s", "p", "r", "f", "t" as subscripts are strut, pod, residual, frictional and total respectively. Other uses of symbols are defined as they arise.

Input Data Section

$i := 0 .. 16$ Sets the data range

$RM_{t1_i} := READ(m1t1fx)$ Total measured X component force for test #1: fixed in pitch and heave.

$VM_i := READ(m1t1v)$ Speed increments used in the test. (inputted in fps)

$\lambda := 17.26$ Scaling Factor for Lengths

$VM_{kts_i} := VM_i \cdot \dfrac{1}{1.688}$ Measured Velocity in Knots   (converts the inputs which are in fps)

$VS_{kts_i} := VM_{kts_i} \cdot \sqrt{\lambda}$ Scaled Velocity in Knots

$VS_i := VM_i \cdot \sqrt{\lambda}$ Equivalent Scaled Velocity in FPS

$\upsilon_{fw} := 1.2260 \cdot 10^{-5}$ ft^2/sec   Kinematic Viscosity of Fresh Water at 59 F (Test Temp)

$\upsilon_{sw} := 1.1794 \cdot 10^{-5}$ ft^2/sec   Kinematic Viscosity of Salt Water at 65 F (Assumed Operating Temp)

$\rho_{fw} := 1.9384$ lb sec^2/ft^4   Density of Fresh Water at 59 F (Test Temp)

$\rho_{sw} := 1.9890$ lb sec^2/ft^4   Density of Salt Water at 65 F (Assumed Operating Temp)

Geometry Section

$$LM_s = 1.39$$ feet Length of one Strut

$$SM_s = 0.715$$ ft^2 Wetted surface of one Strut

$$LM_p = 2.14$$ feet Length of one Pod

$$SM_p = 2.01$$ ft^2 Wetted Surface of one Pod

$$SM_t = 4 \cdot SM_s + 4 \cdot SM_p$$ ft^2 Wetted surface of the entire underwater body

Resistance Calculations

NOTE: In this section Rn is calculated for the pod and the strut separately since their lengths are different. Coefficients of friction are then calculated separately for each based on the 1957 ITTC Line. These are converted to Resistance Values and then subtracted from the Total Resistance value. Finally this is converted to a Coefficient of residuary resistance which is equal for the model and the ship.

$$RnM_{s_i} = \frac{VM_i \cdot LM_s}{\upsilon_{fw}}$$ operating Rn of the Strut

$$RnM_{p_i} = \frac{VM_i \cdot LM_p}{\upsilon_{fw}}$$ operating Rn of the Pod

$$CM_{fs_i} = \frac{0.075}{\left(\log\left(RnM_{s_i}\right) - 2\right)^2}$$ Coefficient of Frictional Resistance based on Strut Length and using the 1957 ITTC line.

$$CM_{fp_i} = \frac{0.075}{\left(\log\left(RnM_{p_i}\right) - 2\right)^2}$$ Coefficient of Frictional Resistance based on Pod Length and using the 1957 ITTC line.

$$RM_{fs_i} := CM_{fs_i} \cdot \frac{1}{2} \cdot \rho_{fw} \cdot \left(VM_i\right)^2 \cdot 4 \cdot SM_s \qquad \text{Frictional Resistance of four Struts}$$

$$RM_{fp_i} := CM_{fp_i} \cdot \frac{1}{2} \cdot \rho_{fw} \cdot \left(VM_i\right)^2 \cdot 4 \cdot SM_p \qquad \text{Frictional Resistance of four Pods}$$

$$RM_{r_i} := RM_{tl_i} - RM_{fs_i} - RM_{fp_i} \qquad \text{Residual Resistance for the Model as measured.}$$

$$CM_{r_i} := \frac{RM_{r_i}}{\left[\frac{1}{2} \cdot \rho_{fw} \cdot \left(VM_i\right)^2 \cdot SM_t\right]}$$

RnM_{s_i}	RnM_{p_i}	RM_{tl_i}	RM_{fs_i}	RM_{fp_i}	RM_{r_i}	CM_{fs_i}	CM_{fp_i}	CM_{r_i}
137186	211207	0.151	0.031	0.077	0.043	0.008	0.007	0.003
273238	420669	0.689	0.102	0.258	0.328	0.006	0.006	0.005
412692	635367	4.24	0.211	0.535	3.494	0.006	0.005	0.025
459176	706933	6.29	0.254	0.647	5.389	0.006	0.005	0.031
462577	712170	6.46	0.258	0.655	5.547	0.006	0.005	0.032
504527	776754	8.91	0.3	0.765	7.845	0.005	0.005	0.038
530604	816900	9.43	0.328	0.836	8.265	0.005	0.005	0.036
549878	846574	9.08	0.35	0.891	7.839	0.005	0.005	0.032
595228	916395	6.86	0.402	1.026	5.432	0.005	0.005	0.019
620171	954796	6.16	0.432	1.104	4.624	0.005	0.005	0.015
641713	987961	5.65	0.459	1.173	4.017	0.005	0.005	0.012
733548	1129347	5.61	0.582	1.489	3.538	0.005	0.005	0.008
916085	1410375	7.18	0.865	2.216	4.099	0.005	0.004	0.006
1146240	1764715	10.645	1.29	3.312	6.043	0.005	0.004	0.006
1375261	2117308	19.465	1.786	4.595	13.084	0.004	0.004	0.008
1603148	2468157	28.82	2.351	6.057	20.413	0.004	0.004	0.01
1834437	2824241	35.35	2.994	7.723	24.633	0.004	0.004	0.009

Note: these values for Rn are Low for ITTC 1957 use. Should be on order of 10^7

Scaled Resistance Calculations

$$CS_{r_i} := CM_{r_i}$$ Residual Resistance Coefficient remains the same in the saling.

$$RnS_{s_i} := \frac{VS_i \cdot LM_s \cdot \lambda}{\upsilon_{sw}}$$ operating Rn of the Strut in the new scale

$$RnS_{p_i} = \frac{VS_i \cdot LM_p \cdot \lambda}{\upsilon_{sw}}$$ operating Rn of the Pod in the new scale

$$CS_{fs_i} := \frac{0.075}{\left(\log\left(RnS_{s_i}\right) - 2\right)^2}$$ Coefficient of Frictional Resistance based on scaled Strut Length and using the 1957 ITTC line.

$$CS_{fp_i} = \frac{0.075}{\left(\log\left(RnS_{p_i}\right) - 2\right)^2}$$ Coefficient of Frictional Resistance based on scaled Pod Length and using the 1957 ITTC line.

$$CS_a := 0.0004$$ Correlation Allowance

$$RS_{fs_i} = CS_{fs_i} \cdot \frac{1}{2} \cdot \rho_{sw} \cdot \left(VS_i\right)^2 \cdot 4 \cdot SM_s \cdot \lambda^2$$ Frictional Resistance of the Struts

$$RS_{fp_i} = CS_{fp_i} \cdot \frac{1}{2} \cdot \rho_{sw} \cdot \left(VS_i\right)^2 \cdot 4 \cdot SM_p \cdot \lambda^2$$ Frictional Resistance of the Pods

$$RS_{r_i} := CS_{r_i} \cdot \frac{1}{2} \cdot \rho_{sw} \cdot \left(VS_i\right)^2 \cdot SM_t \cdot \lambda^2$$ Scaled Residual Resistance

$$RS_{a_i} := CS_a \cdot \frac{1}{2} \cdot \rho_{sw} \cdot \left(VS_i\right)^2 \cdot SM_t \cdot \lambda^2$$ Correlation

$$RS_{t_i} := RS_{fs_i} + RS_{fp_i} + RS_{r_i} + RS_{a_i}$$

207

Scaled Speed (fps)	Scaled Speed (knots)	Total M-2 Resistance at Full Scale	Residual Component	PodFrictional Component	StrutFrictional Component	Reynolds # of the Strut	Reynolds # of the Pod
VS_i	VS_{kts_i}	RS_{t_i}	RS_{r_i}	RS_{fp_i}	RS_{fs_i}	RnS_{s_i}	RnS_{p_i}
5.03	2.978	488.89	225.11	167.14	63.99	10225869	15743425
10.01	5.932	2680.46	1732.1	592.83	226.03	20367227	31356738
15.12	8.959	20480.51	18434.19	1268.39	482.53	30762119	47360385
16.83	9.968	30929.77	28431.8	1544.88	587.39	34227083	52694933
16.95	10.042	31798.85	29266.18	1566.09	595.44	34480617	53085266
18.49	10.952	44370.38	41391.37	1838.72	698.78	37607536	57899371
19.44	11.518	46882.96	43609.44	2018.35	766.85	39551296	60891923
20.15	11.937	44860.57	41361.02	2156.07	819.03	40987988	63103809
21.81	12.921	32717.51	28658.3	2496.66	948.04	44368441	68308247
22.73	13.463	28777.95	24394.36	2693.8	1022.69	46227690	71170688
23.51	13.93	25868.95	21195.81	2869.63	1089.26	47833405	73642796
26.88	15.924	24672.03	18667.49	3676.58	1394.66	54678821	84181783
33.57	19.887	30738.84	21627.81	5551.69	2103.76	68285143	10512964
42	24.883	45766.63	31883.98	8417.37	3186.42	85440940	13154216
50.39	29.854	88587.27	69030.12	11809.69	4466.99	102512226	15782457
58.74	34.801	133802.96	107699.01	15708.47	5937.76	119499001	18397687
67.22	39.822	163618.18	129965.39	20189.01	7627.04	136739309	21051951

$\text{WRITE}(mlfulfx) := RS_{t_i} \qquad \text{WRITE}(mlfulv) := VS_{kts_i}$ Writes the scaled data to a file for future use.

$$RS_{ft_i} = RS_{fp_i} + RS_{fs_i} \qquad FF_i = \frac{RS_{ft_i}}{RS_{t_i}} \qquad RF_i = \frac{RS_{r_i}}{RS_{t_i}}$$ Percent of total resistance attributable to friction/wave.

$$CA_i = \frac{RS_{a_i}}{RS_{t_i}}$$ percent of total resistance that is attributable to correlation allowance

$\text{WRITE}(mlfulfp) := FF_i \qquad \text{WRITE}(mlfulrp) := RF_i \qquad \text{WRITE}(mlfulcap) = CA_i$

This Calculation Scales the Test Data obtained for Model M-2 to the scale that Model M-1 is built to. This enables a direct comparison of the Data obtained from the two models.

NOTE: The System of Subscripts in this Routine can become rather bulky... "R", "C", "M", "S" are Resistance, Coefficient of Resistance, Measured and Scaled respectively... where measured refers to the measured model (Model M-2 Data unscaled) and Scaled refers to the Model M-2 data scaled to the Model M-1 scale factor. Also, "s", "p", "r", "f", "t" as subscripts are strut, pod, residual, frictional and total respectively. Other uses of symbols are defined as they arise.

Input Data Section

$i := 0 .. 15$ Sets the data range

$RM_{t1_i} := READ(m2t1fx)$ Total measured X component force for test #1: fixed in pitch and heave.

$VM_i := READ(m2t1v)$ Speed increments used in the test. (inputted in fps)

$\lambda := \dfrac{16.68}{17.26}$ Scaling Factor for Lengths   M2/M1 scale factor.

$VM_{kts_i} := VM_i \cdot \dfrac{1}{1.688}$ Measured Velocity in Knots (converts the inputs which are in fps)

$VS_{kts_i} := VM_{kts_i} \cdot \overline{\lambda}$ Scaled Velocity in Knots

$VS_i := VM_i \cdot \sqrt{\lambda}$ Equivalent Scaled Velocity in FPS

$\upsilon_{fw} := 1.2260 \cdot 10^{-5}$ ft^2/sec   Kinematic Viscosity of Fresh Water at 59 F (Test Temp)

$\upsilon_{sw} := 1.1794 \cdot 10^{-5}$ ft^2/sec   Kinematic Viscosity of Salt Water at 65 F (Assumed Operating Temp)

$\rho_{fw} := 1.9384$ lb sec^2/ft^4 Density of Fresh Water at 59 F (Test Temp)

$\rho_{sw} := 1.9890$ lb sec^2/ft^4 Density of Salt Water at 65 F (Assumed Operating Temp)

Geometry Section

$$LM_s := 1.4375 \qquad \text{feet} \quad \text{Length of one Strut}$$

$$SM_s := 1.059 \qquad \text{ft\^{}2} \quad \text{Wetted surface of one Strut}$$

$$LM_p := 2.32 \qquad \text{feet} \quad \text{Length of one Pod}$$

$$SM_p := 2.642 \qquad \text{ft\^{}2} \quad \text{Wetted Surface of one Pod}$$

$$SM_t := 4 \cdot SM_s - 4 \cdot SM_p \qquad \text{ft\^{}2} \quad \text{Wetted surface of the entire underwater body}$$

Resistance Calculations

<u>NOTE:</u> In this section Rn is calculated for the pod and the strut separately since their lengths are different. Coefficients of friction are then calculated separately for each based on the 1957 ITTC Line. These are converted to Resistance Values and then subtracted from the Total Resistance value. Finally this is converted to a Coefficient of residuary resistance which is equal for the model and the ship.

$$RnM_{s_i} = \frac{VM_i \cdot LM_s}{\upsilon_{fw}} \qquad \text{operating Rn of the Strut}$$

$$RnM_{p_i} = \frac{VM_i \cdot LM_p}{\upsilon_{fw}} \qquad \text{operating Rn of the Pod}$$

$$CM_{fs_i} = \frac{0.075}{\left(\log\left(RnM_{s_i}\right) - 2\right)^2} \qquad \text{Coefficient of Frictional Resistance based on Strut Length and using the 1957 ITTC line.}$$

$$CM_{fp_i} = \frac{0.075}{\left(\log\left(RnM_{p_i}\right) - 2\right)^2} \qquad \text{Coefficient of Frictional Resistance based on Pod Length and using the 1957 ITTC line.}$$

$$RM_{fs_i} = CM_{fs_i} \cdot \frac{1}{2} \cdot \rho_{fw} \cdot \left(VM_i\right)^2 \cdot 4 \cdot SM_s$$ **Frictional Resistance of four Struts**

$$RM_{fp_i} = CM_{fp_i} \cdot \frac{1}{2} \cdot \rho_{fw} \cdot \left(VM_i\right)^2 \cdot 4 \cdot SM_p$$ **Frictional Resistance of four Pods**

$$RM_{r_i} = RM_{tl_i} - RM_{fs_i} - RM_{fp_i}$$ **Residual Resistance for the Model as measured.**

$$CM_{r_i} = \frac{RM_{r_i}}{\left[\frac{1}{2} \cdot \rho_{fw} \cdot \left(VM_i\right)^2 \cdot SM_t\right]}$$

RnM_{s_i}	RnM_{p_i}	RM_{tl_i}	RM_{fs_i}	RM_{fp_i}	RM_{r_i}	CM_{fs_i}	CM_{fp_i}	CM_{r_i}
143046	230865	0.172	0.046	0.101	0.025	0.008	0.007	0.001
288438	465514	0.673	0.156	0.346	0.172	0.006	0.006	0.002
431485	696378	4.52	0.316	0.704	3.5	0.006	0.005	0.018
481903	777749	6.83	0.383	0.857	5.589	0.006	0.005	0.023
524113	845873	9.81	0.445	0.995	8.37	0.005	0.005	0.029
553426	893181	10.78	0.49	1.096	9.194	0.005	0.005	0.029
578049	932920	9.84	0.529	1.185	8.126	0.005	0.005	0.023
612051	987798	7.85	0.585	1.312	5.953	0.005	0.005	0.015
641364	1035106	6.68	0.636	1.426	4.619	0.005	0.005	0.011
699990	1129723	6.05	0.742	1.667	3.641	0.005	0.005	0.007
771513	1245155	6.29	0.882	1.983	3.425	0.005	0.004	0.006
964978	1557390	7.255	1.314	2.96	2.981	0.005	0.004	0.003
1205343	1945318	10.21	1.954	4.413	3.843	0.005	0.004	0.003
1448053	2337031	14.49	2.713	6.139	5.638	0.004	0.004	0.003
1688418	2724959	20.18	3.573	8.097	8.51	0.004	0.004	0.003
1928783	3112887	26.39	4.537	10.297	11.556	0.004	0.004	0.003

Scaled Resistance Calculations

$$CS_{r_i} = CM_{r_i}$$

Residual Resistance Coefficient remains the same in the saling.

$$RnS_{s_i} = \frac{VS_i \cdot LM_s \cdot \lambda}{\upsilon_{fw}}$$

operating Rn of the Strut in the new scale

$$RnS_{p_i} = \frac{VS_i \cdot LM_p \cdot \lambda}{\upsilon_{fw}}$$

operating Rn of the Pod in the new scale

$$CS_{fs_i} = \frac{0.075}{\left(\log\left(RnS_{s_i}\right) - 2\right)^2}$$

Coefficient of Frictional Resistance based on scaled Strut Length and using the 1957 ITTC line.

$$CS_{fp_i} = \frac{0.075}{\left(\log\left(RnS_{p_i}\right) - 2\right)^2}$$

Coefficient of Frictional Resistance based on scaled Pod Length and using the 1957 ITTC line.

$$CS_a = 0$$

Correlation Allowance

$$RS_{fs_i} = CS_{fs_i} \cdot \frac{1}{2} \cdot \rho_{fw} \cdot \left(VS_i\right)^2 \cdot 4 \cdot SM_s \cdot \lambda^2$$

Frictional Resistance of the Struts

$$RS_{fp_i} = CS_{fp_i} \cdot \frac{1}{2} \cdot \rho_{fw} \cdot \left(VS_i\right)^2 \cdot 4 \cdot SM_p \cdot \lambda^2$$

Frictional Resistance of the Pods

$$RS_{r_i} = CS_{r_i} \cdot \frac{1}{2} \cdot \rho_{fw} \cdot \left(VS_i\right)^2 \cdot SM_t \cdot \lambda^2$$

Scaled Residual Resistance

$$RS_{t_i} = RS_{fs_i} + RS_{fp_i} - RS_{r_i}$$

212

Scaled Speed (fps)	Scaled Speed (knots)	Total M-2 Resistance at 17.26:1 Scale	Residual Component	PodFrictional Component	StrutFrictional Component	Reynolds # of the Strut	Reynolds # of the Pod
VS_i	$VS\,kts_i$	$RS\,t_i$	$RS\,r_i$	$RS\,fp_i$	$RS\,fs_i$	$RnS\,s_i$	$RnS\,p_i$
1.2	0.711	0.16	0.02	0.09	0.04	135897	219326
2.42	1.433	0.61	0.16	0.32	0.14	274022	442248
3.62	2.143	4.09	3.16	0.64	0.29	409919	661574
4.04	2.394	6.18	5.04	0.78	0.35	457817	738877
4.39	2.603	8.87	7.55	0.91	0.41	497918	803596
4.64	2.749	9.75	8.3	1	0.45	525766	848540
4.85	2.871	8.9	7.33	1.08	0.48	549158	886293
5.13	3.04	7.1	5.37	1.2	0.53	581461	938428
5.38	3.186	6.05	4.17	1.3	0.58	609309	983372
5.87	3.477	5.48	3.29	1.52	0.68	665005	1073259
6.47	3.832	5.71	3.09	1.81	0.81	732953	1182922
8.09	4.793	6.59	2.69	2.7	1.2	916748	1479552
10.11	5.987	9.28	3.47	4.02	1.78	1145100	1848092
12.14	7.192	13.16	5.09	5.6	2.47	1375679	2220227
14.16	8.386	18.32	7.68	7.38	3.26	1604031	2588767
16.17	9.58	23.95	10.43	9.39	4.14	1832383	2957306

$$\text{WRITE(m2sclfx)} = RS_{t_i} \qquad \text{WRITE(m2sclv)} = VS_i \qquad \text{Writes the scaled data to a file for future use.}$$

$$RS_{ft_i} = RS_{fp_i} - RS_{fs_i} \qquad FF_i = \frac{RS_{ft_i}}{RS_{t_i}} \qquad RF_i = 1 - FF_i \qquad \text{Percent of total resistance attributable to friction/wave.}$$

$$\text{WRITE(m2ff)} = FF_i \qquad \text{WRITE(m2rf)} = RF_i$$

This Calculation Scales the Test Data obtained for Model M-2 to Full Scale.

NOTE: The System of Subscripts in this Routine can become rather bulky... "R", "C", "M", "S" are Resistance, Coefficient of Resistance, Measured and Ship respectively... where measured refers to the measured model (Model M-2 Data unscaled) and Ship refers to the full scale calculation. Also, "s", "p", "r", "f", "t" as subscripts are strut, pod, residual, frictional and total respectively. Other uses of symbols are defined as they arise.

Input Data Section

$i := 0 .. 15$ Sets the data range

$RM_{t1_i} := READ(m2t1fx)$ Total measured X component force for test #1: fixed in pitch and heave.

$VM_i := READ(m2t1v)$ Speed increments used in the test. (inputted in fps)

$\lambda := 16.68$ Scaling Factor for Lengths   M2/M1 scale factor.

$VM_{kts_i} := VM_i \cdot \dfrac{1}{1.688}$ Measured Velocity in Knots   (converts the inputs which are in fps)

$VS_{kts_i} := VM_{kts_i} \cdot \sqrt{\lambda}$ Scaled Velocity in Knots

$VS_i := VM_i \cdot \sqrt{\lambda}$ Equivalent Scaled Velocity in FPS

$\upsilon_{fw} := 1.2260 \cdot 10^{-5}$ ft^2/sec   Kinematic Viscosity of Fresh Water at 59 F (Test Temp)

$\upsilon_{sw} := 1.1794 \cdot 10^{-5}$ ft^2/sec   Kinematic Viscosity of Salt Water at 65 F (Assumed Operating Temp)

$\rho_{fw} := 1.9384$ lb sec^2/ft^4 Density of Fresh Water at 59 F (Test Temp)

$\rho_{sw} := 1.9890$ lb sec^2/ft^4 Density of Salt Water at 65 F (Assumed Operating Temp)

Geometry Section

$$LM_s := 1.4375 \qquad \text{feet} \quad \text{Length of one Strut}$$

$$SM_s := 1.059 \qquad \text{ft\textasciicircum2} \quad \text{Wetted surface of one Strut}$$

$$LM_p := 2.32 \qquad \text{feet} \quad \text{Length of one Pod}$$

$$SM_p := 2.642 \qquad \text{ft\textasciicircum2} \quad \text{Wetted Surface of one Pod}$$

$$SM_t := 4 \cdot SM_s + 4 \cdot SM_p \qquad \text{ft\textasciicircum2} \quad \text{Wetted surface of the entire underwater body}$$

Resistance Calculations

NOTE: In this section Rn is calculated for the pod and the strut separately since their lengths are different. Coefficients of friction are then calculated separately for each based on the 1957 ITTC Line. These are converted to Resistance Values and then subtracted from the Total Resistance value. Finally this is converted to a Coefficient of residuary resistance which is equal for the model and the ship.

$$RnM_{s_i} = \frac{VM_i \cdot LM_s}{\upsilon_{fw}} \qquad \text{operating Rn of the Strut}$$

$$RnM_{p_i} = \frac{VM_i \cdot LM_p}{\upsilon_{fw}} \qquad \text{operating Rn of the Pod}$$

$$CM_{fs_i} = \frac{0.075}{\left(\log\left(RnM_{s_i}\right) - 2\right)^2} \qquad \text{Coefficient of Frictional Resistance based on Strut Length and using the 1957 ITTC line.}$$

$$CM_{fp_i} = \frac{0.075}{\left(\log\left(RnM_{p_i}\right) - 2\right)^2} \qquad \text{Coefficient of Frictional Resistance based on Pod Length and using the 1957 ITTC line.}$$

$$RM_{fs_i} := CM_{fs_i} \cdot \frac{1}{2} \cdot \rho_{fw} \cdot \left(VM_i\right)^2 \cdot 4 \cdot SM_s \qquad \text{Frictional Resistance of four Struts}$$

$$RM_{fp_i} := CM_{fp_i} \cdot \frac{1}{2} \cdot \rho_{fw} \cdot \left(VM_i\right)^2 \cdot 4 \cdot SM_p \qquad \text{Frictional Resistance of four Pods}$$

$$RM_{r_i} := RM_{tl_i} - RM_{fs_i} - RM_{fp_i} \qquad \text{Residual Resistance for the Model as measured.}$$

$$CM_{r_i} = \frac{RM_{r_i}}{\left[\frac{1}{2} \cdot \rho_{fw} \cdot \left(VM_i\right)^2 \cdot SM_t\right]}$$

RnM_{s_i}	RnM_{p_i}	RM_{tl_i}	RM_{fs_i}	RM_{fp_i}	RM_{r_i}	CM_{fs_i}	CM_{fp_i}	CM_{r_i}
143046	230865	0.172	0.046	0.101	0.025	0.008	0.007	0.001
288438	465514	0.673	0.156	0.346	0.172	0.006	0.006	0.002
431485	696378	4.52	0.316	0.704	3.5	0.006	0.005	0.018
481903	777749	6.83	0.383	0.857	5.589	0.006	0.005	0.023
524113	845873	9.81	0.445	0.995	8.37	0.005	0.005	0.029
553426	893181	10.78	0.49	1.096	9.194	0.005	0.005	0.029
578049	932920	9.84	0.529	1.185	8.126	0.005	0.005	0.023
612051	987798	7.85	0.585	1.312	5.953	0.005	0.005	0.015
641364	1035106	6.68	0.636	1.426	4.619	0.005	0.005	0.011
699990	1129723	6.05	0.742	1.667	3.641	0.005	0.005	0.007
771513	1245155	6.29	0.882	1.983	3.425	0.005	0.004	0.006
964978	1557390	7.255	1.314	2.96	2.981	0.005	0.004	0.003
1205343	1945318	10.21	1.954	4.413	3.843	0.005	0.004	0.003
1448053	2337031	14.49	2.713	6.139	5.638	0.004	0.004	0.003
1688418	2724959	20.18	3.573	8.097	8.51	0.004	0.004	0.003
1928783	3112887	26.39	4.537	10.297	11.556	0.004	0.004	0.003

Note: these values for Rn are Low for ITTC 1957 use. Should be on order of 10^7

Scaled Resistance Calculations

$$CS_{r_i} := CM_{r_i}$$ Residual Resistance Coefficient remains the same in the saling.

$$RnS_{s_i} := \frac{VS_i \cdot LM_s \cdot \lambda}{\upsilon_{sw}}$$ operating Rn of the Strut in the new scale

$$RnS_{p_i} := \frac{VS_i \cdot LM_p \cdot \lambda}{\upsilon_{sw}}$$ operating Rn of the Pod in the new scale

$$CS_{fs_i} := \frac{0.075}{\left(\log\left(RnS_{s_i}\right) - 2\right)^2}$$ Coefficient of Frictional Resistance based on scaled Strut Length and using the 1957 ITTC line.

$$CS_{fp_i} := \frac{0.075}{\left(\log\left(RnS_{p_i}\right) - 2\right)^2}$$ Coefficient of Frictional Resistance based on scaled Pod Length and using the 1957 ITTC line.

$$CS_a := 0.0004$$ Correlation Allowance

$$RS_{fs_i} := CS_{fs_i} \cdot \frac{1}{2} \cdot \rho_{sw} \cdot \left(VS_i\right)^2 \cdot 4 \cdot SM_s \cdot \lambda^2$$ Frictional Resistance of the Struts

$$RS_{fp_i} := CS_{fp_i} \cdot \frac{1}{2} \cdot \rho_{sw} \cdot \left(VS_i\right)^2 \cdot 4 \cdot SM_p \cdot \lambda^2$$ Frictional Resistance of the Pods

$$RS_{r_i} := CS_{r_i} \cdot \frac{1}{2} \cdot \rho_{sw} \cdot \left(VS_i\right)^2 \cdot SM_t \cdot \lambda^2$$ Scaled Residual Resistance

$$RS_{a_i} := CS_a \cdot \frac{1}{2} \cdot \rho_{sw} \cdot \left(VS_i\right)^2 \cdot SM_t \cdot \lambda^2$$ Correlation

$$RS_{t_i} := RS_{fs_i} - RS_{fp_i} + RS_{r_i} + RS_{a_i}$$

217

Scaled Speed (fps)	Scaled Speed (knots)	Total M-2 Resistance at Full Scale	Residual Component	PodFrictional Component	StrutFrictional Component	Reynolds # of the Strut	Reynolds # of the Pod
VS_i	$VS\,kts_i$	RS_{t_i}	RS_{r_i}	RS_{fp_i}	RS_{fs_i}	RnS_{s_i}	RnS_{p_i}
4.98	2.952	446.65	118.56	200.31	87.1	10129794	16348607
10.05	5.952	2025.26	818.18	727.02	314.68	20425651	32965225
15.03	8.904	19224.96	16666.37	1528.5	659.99	30555445	49313832
16.79	9.944	29761.5	26616	1874.83	809.02	34125783	55076046
18.26	10.815	43537.84	39857.57	2189.74	944.46	37114902	59900225
19.28	11.42	47855.66	43780.95	2421.67	1044.18	39190680	63250349
20.13	11.928	43117.98	38697.41	2624.82	1131.5	40934333	66064454
21.32	12.63	33268.15	28348.32	2917.76	1257.39	43342235	69950598
22.34	13.235	27363.12	21992.81	3181.78	1370.81	45418013	73300723
24.38	14.444	23664.57	17337.95	3741.42	1611.16	49569568	80000972
26.87	15.92	23900	16307.54	4480.68	1928.51	54634465	88175275
33.61	19.912	25749.59	14195.24	6785.95	2917.3	68334597	110286097
41.98	24.872	35850.64	18300.87	10257.03	4404.6	85355972	137757117
50.44	29.881	51632.94	26848.18	14426.78	6189.62	102543410	165496147
58.81	34.841	73622.44	40524.35	19199.71	8231.34	119564786	192967168
67.18	39.801	97565.13	55028.49	24600.85	10540.35	136586162	220438188

$\text{WRITE}(m2fulfx) := RS_{t_i}$ $\text{WRITE}(m2fulv) := VS\,kts_i$ Writes the scaled data to a file for future use.

$$RS_{ft_i} = RS_{fp_i} + RS_{fs_i} \qquad FF_i := \frac{RS_{ft_i}}{RS_{t_i}} \qquad RF_i := \frac{RS_{r_i}}{RS_{t_i}}$$

Percent of total resistance attributable to friction/wave.

$$CA_i := \frac{RS_{a_i}}{RS_{t_i}}$$ percent of total resistance that is attributable to correlation allowance

$\text{WRITE}(m2fulfp) := FF_i$ $\text{WRITE}(m2fulrp) := RF_i$ $\text{WRITE}(m2fulcap) := CA_i$

$$EHP\,ship_i := \frac{RS_{t_i} \cdot VS_i}{550}$$

VS_i	VS_{kts_i}	EHP_{ship_i}
4.983	2.952	4.046
10.047	5.952	36.996
15.03	8.904	525.35
16.786	9.944	908.305
18.256	10.815	1445.139
19.277	11.42	1677.3
20.135	11.928	1578.486
21.319	12.63	1289.539
22.34	13.235	1111.446
24.382	14.444	1049.079
26.873	15.92	1167.775
33.612	19.912	1573.641
41.985	24.872	2736.688
50.439	29.881	4735.1
58.811	34.841	7872.416
67.184	39.801	11917.794

M-2 in full scale

This Calculation Scales the Test Data obtained for Model M-3 to the scale that Model M-1 is built to. This enables a direct comparison of the Data obtained from the two models.

NOTE: The System of Subscripts in this Routine can become rather bulky... "R", "C", "M", "S" are Resistance, Coefficient of Resistance, Measured and Scaled respectively... where measured refers to the measured model (Model M-3 Data unscaled) and Scaled refers to the Model M-3 data scaled to the Model M-1 scale factor. Also, "s", "p", "r", "f", "t" as subscripts are strut, pod, residual, frictional and total respectively. Other uses of symbols are defined as they arise.

Input Data Section

$i := 0.. 16$ Sets the data range

$RM_{t1_i} = READ(m3t1fx)$ Total measured X component force for test #1: fixed in pitch and heave.

$VM_i = READ(m3t1v)$ Speed increments used in the test. (inputted in fps)

$\lambda := \dfrac{15.1}{17.26}$ Scaling Factor for Lengths M3/M1 scale factor.

$VM_{kts_i} = VM_i \cdot \dfrac{1}{1.688}$ Measured Velocity in Knots (converts the inputs which are in fps)

$VS_{kts_i} = VM_{kts_i} \cdot \sqrt{\lambda}$ Scaled Velocity in Knots

$VS_i := VM_i \cdot \sqrt{\lambda}$ Equivalent Scaled Velocity in FPS

$\upsilon_{fw} = 1.2260 \cdot 10^{-5}$ ft^2/sec Kinematic Viscosity of Fresh Water at 59 F (Test Temp)

$\upsilon_{sw} = 1.1794 \cdot 10^{-5}$ ft^2/sec Kinematic Viscosity of Salt Water at 65 F (Assumed Operating Temp)

$\rho_{fw} = 1.9384$ lb sec^2/ft^4 Density of Fresh Water at 59 F (Test Temp)

$\rho_{sw} = 1.9890$ lb sec^2/ft^4 Density of Salt Water at 65 F (Assumed Operating Temp)

Geometry Section

$$LM_s = 1.589 \qquad \text{feet Length of one Strut}$$

$$SM_s = 1.716 \qquad \text{ft\^2 Wetted surface of one Strut}$$

$$LM_p = 5.958 \qquad \text{feet Length of one Demihull}$$

$$SM_p = 6.45 \qquad \text{ft\^2 Wetted Surface of one Demihull}$$

$$SM_t = 4 \cdot SM_s + 2 \cdot SM_p \qquad \text{ft\^2 Wetted surface of the entire underwater body}$$

Resistance Calculations

<u>NOTE:</u> In this section Rn is calculated for the pod and the strut separately since their lengths are different. Coefficients of friction are then calculated separately for each based on the 1957 ITTC Line. These are converted to Resistance Values and then subtracted from the Total Resistance value. Finally this is converted to a Coefficient of residuary resistance which is equal for the model and the ship.

$$RnM_{s_i} = \frac{VM_i \cdot LM_s}{\upsilon_{fw}} \qquad \text{operating Rn of the Strut}$$

$$RnM_{p_i} = \frac{VM_i \cdot LM_p}{\upsilon_{fw}} \qquad \text{operating Rn of the Demihull}$$

$$CM_{fs_i} = \frac{0.075}{\left(\log\left(RnM_{s_i}\right) - 2\right)^2} \qquad \begin{array}{l}\text{Coefficient of Frictional Resistance based on Strut Length}\\ \text{and using the 1957 ITTC line.}\end{array}$$

$$CM_{fp_i} = \frac{0.075}{\left(\log\left(RnM_{p_i}\right) - 2\right)^2} \qquad \begin{array}{l}\text{Coefficient of Frictional Resistance based on Demihull Length}\\ \text{and using the 1957 ITTC line.}\end{array}$$

$$RM_{fs_i} = CM_{fs_i} \cdot \left(\frac{1}{2} \cdot \rho_{fw} \cdot VM_i\right)^2 \cdot 4 \cdot SM_s$$

Frictional Resistance of four Struts

$$RM_{fp_i} = CM_{fp_i} \cdot \left(\frac{1}{2} \cdot \rho_{fw} \cdot VM_i\right)^2 \cdot 2 \cdot SM_p$$

Frictional Resistance of two Demihulls

$$RM_{r_i} = RM_{tl_i} - RM_{fs_i} - RM_{fp_i}$$

Residual Resistance for the Model as measured.

$$CM_{r_i} = \frac{RM_{r_i}}{\left[\frac{1}{2} \cdot \rho_{fw} \cdot VM_i^2 \cdot SM_t\right]}$$

RnM_{s_i}	RnM_{p_i}	RM_{tl_i}	RM_{fs_i}	RM_{fp_i}	RM_{r_i}	CM_{fs_i}	CM_{fp_i}	CM_{r_i}
334390	1253804	0.801	0.267	0.372	0.162	0.006	0.004	0.001
451038	1691178	3.17	0.453	0.635	2.082	0.006	0.004	0.009
502881	1885566	4.22	0.548	0.772	2.899	0.005	0.004	0.01
540467	2026498	6.01	0.623	0.879	4.508	0.005	0.004	0.014
593607	2225746	7.14	0.735	1.041	5.364	0.005	0.004	0.013
619529	2322940	6.75	0.793	1.124	4.833	0.005	0.004	0.011
644154	2415274	6.35	0.849	1.206	4.295	0.005	0.004	0.009
671372	2517328	6.08	0.914	1.299	3.867	0.005	0.004	0.008
773763	2901245	6.74	1.176	1.678	3.886	0.005	0.004	0.006
896243	3360487	8.23	1.527	2.188	4.514	0.005	0.004	0.005
1008354	3780852	8.93	1.884	2.709	4.337	0.005	0.004	0.004
1121113	4203646	9.74	2.276	3.282	4.182	0.005	0.004	0.003
1289604	4835408	12.2	2.924	4.231	5.046	0.004	0.003	0.003
1401068	5253343	13.865	3.391	4.918	5.556	0.004	0.003	0.002
1684910	6317618	19.08	4.72	6.877	7.483	0.004	0.003	0.002
1960976	7352736	25.875	6.199	9.064	10.612	0.004	0.003	0.002
2240931	8402432	33.185	7.881	11.56	13.744	0.004	0.003	0.002

Note: these values for Rn are Low for ITTC 1957 use. Should be on order of 10^7

222

Scaled Resistance Calculations

$$CS_{r_i} = CM_{r_i}$$ Residual Resistance Coefficient remains the same in the saling.

$$RnS_{s_i} = \frac{VS_i \cdot LM_s \cdot \lambda}{\upsilon_{fw}}$$ operating Rn of the Strut in the new scale

$$RnS_{p_i} = \frac{VS_i \cdot LM_p \cdot \lambda}{\upsilon_{fw}}$$ operating Rn of the Pod in the new scale

$$CS_{fs_i} = \frac{0.075}{\left(\log\left(RnS_{s_i}\right) - 2\right)^2}$$ Coefficient of Frictional Resistance based on scaled Strut Length and using the 1957 ITTC line.

$$CS_{fp_i} = \frac{0.075}{\left(\log\left(RnS_{p_i}\right) - 2\right)^2}$$ Coefficient of Frictional Resistance based on scaled Pod Length and using the 1957 ITTC line.

$$CS_a = 0$$ Correlation Allowance

$$RS_{fs_i} = CS_{fs_i} \cdot \frac{1}{2} \cdot \rho_{fw} \cdot \left(VS_i\right)^2 \cdot 4 \cdot SM_s \cdot \lambda^2$$ Frictional Resistance of the Struts

$$RS_{fp_i} = CS_{fp_i} \cdot \frac{1}{2} \cdot \rho_{fw} \cdot \left(VS_i\right)^2 \cdot 2 \cdot SM_p \cdot \lambda^2$$ Frictional Resistance of the Demi Hulls

$$RS_{r_i} = CS_{r_i} \cdot \frac{1}{2} \cdot \rho_{fw} \cdot \left(VS_i\right)^2 \cdot SM_t \cdot \lambda^2$$ Scaled Residual Resistance

$$RS_{t_i} = RS_{fs_i} + RS_{fp_i} + RS_{r_i}$$

223

Scaled Speed (fps)	Scaled Speed (knots)	Total M-3 Resistance at 17.26:1 Scale	Residual Component	PodFrictional Component	StrutFrictional Component	Reynolds # of the Strut	Reynolds # of the Pod
VS_i	VS_{kts_i}	RS_{t_i}	RS_{r_i}	RS_{fp_i}	RS_{fs_i}	RnS_{s_i}	RnS_{p_i}
2.41	1.43	0.56	0.11	0.26	0.19	273626	1025968
3.25	1.928	2.16	1.39	0.44	0.32	369077	1383864
3.63	2.15	2.87	1.94	0.54	0.38	411500	1542929
3.9	2.311	4.07	3.02	0.61	0.44	442256	1658251
4.28	2.538	4.83	3.59	0.73	0.52	485739	1821293
4.47	2.649	4.58	3.24	0.78	0.56	506951	1900825
4.65	2.754	4.31	2.88	0.84	0.6	527101	1976381
4.85	2.87	4.14	2.59	0.91	0.64	549373	2059890
5.58	3.308	4.59	2.6	1.17	0.82	633158	2374043
6.47	3.832	5.62	3.02	1.52	1.07	733381	2749834
7.28	4.311	6.11	2.9	1.88	1.32	825120	3093812
8.09	4.793	6.67	2.8	2.28	1.59	917390	3439778
9.31	5.513	8.36	3.38	2.94	2.04	1055263	3956738
10.11	5.99	9.51	3.72	3.42	2.37	1146472	4298728
12.16	7.203	13.08	5.01	4.78	3.29	1378736	5169608
14.15	8.384	17.72	7.11	6.29	4.32	1604636	6016628
16.17	9.581	22.72	9.2	8.02	5.49	1833718	6875579

$$\text{WRITE(m3sclfx)} = RS_{t_i} \qquad \text{WRITE(m3sclv)} = VS_i \qquad \text{Writes the scaled data to a file for future use.}$$

$$RS_{ft_i} = RS_{fp_i} + RS_{fs_i} \qquad FF_i = \frac{RS_{ft_i}}{RS_{t_i}} \qquad RF_i = 1 - FF_i \qquad \text{Percent of total resistance attributable to friction/wave.}$$

$$\text{WRITE(m3ff)} = FF_i \qquad \text{WRITE(m3rf)} = RF_i$$

This Calculation Scales the Test Data obtained for Model M-3 to full scale.

NOTE: The System of Subscripts in this Routine can become rather bulky... "R", "C", "M", "S" are Resistance, Coefficient of Resistance, Measured and Scaled respectively... where measured refers to the measured model (Model M-3 Data unscaled) and Scaled refers to the Model M-3 data scaled to the Model M-1 scale factor. Also, "s", "p", "r", "f", "t" as subscripts are strut, pod, residual, frictional and total respectively. Other uses of symbols are defined as they arise.

Input Data Section

$i := 0 .. 16$ Sets the data range

$RM_{t1_i} = READ(m3t1fx)$ Total measured X component force for test #1: fixed in pitch and heave.

$VM_i := READ(m3t1v)$ Speed increments used in the test. (inputted in fps)

$\lambda := 15.1$ Scaling Factor for Lengths   M3/M1 scale factor.

$VM_{kts_i} = VM_i \cdot \dfrac{1}{1.688}$ Measured Velocity in Knots   (converts the inputs which are in fps)

$VS_{kts_i} := VM_{kts_i} \cdot \sqrt{\lambda}$ Scaled Velocity in Knots

$VS_i := VM_i \cdot \sqrt{\lambda}$ Equivalent Scaled Velocity in FPS

$\upsilon_{fw} = 1.2260 \cdot 10^{-5}$ ft^2/sec   Kinematic Viscosity of Fresh Water at 59 F (Test Temp)

$\upsilon_{sw} = 1.1794 \cdot 10^{-5}$ ft^2/sec   Kinematic Viscosity of Salt Water at 65 F (Assumed Operating Temp)

$\rho_{fw} = 1.9384$ lb sec^2/ft^4 Density of Fresh Water at 59 F (Test Temp)

$\rho_{sw} = 1.9890$ lb sec^2/ft^4 Density of Salt Water at 65 F (Assumed Operating Temp)

Geometry Section

$$LM_s = 1.589 \qquad \text{feet Length of one Strut}$$

$$SM_s = 1.716 \qquad \text{ft\^{}2 Wetted surface of one Strut}$$

$$LM_p = 5.958 \qquad \text{feet Length of one Demihull}$$

$$SM_p = 6.45 \qquad \text{ft\^{}2 Wetted Surface of one Demihull}$$

$$SM_t = 4 \cdot SM_s - 2 \cdot SM_p \qquad \text{ft\^{}2 Wetted surface of the entire underwater body}$$

Resistance Calculations

NOTE: In this section Rn is calculated for the pod and the strut separately since their lengths are different. Coefficients of friction are then calculated separately for each based on the 1957 ITTC Line. These are converted to Resistance Values and then subtracted from the Total Resistance value. Finally this is converted to a Coefficient of residuary resistance which is equal for the model and the ship.

$$RnM_{s_i} := \frac{VM_i \cdot LM_s}{\upsilon_{fw}} \qquad \text{operating Rn of the Strut}$$

$$RnM_{p_i} := \frac{VM_i \cdot LM_p}{\upsilon_{fw}} \qquad \text{operating Rn of the Demihull}$$

$$CM_{fs_i} := \frac{0.075}{\left(\log\left(RnM_{s_i}\right) - 2\right)^2} \qquad \text{Coefficient of Frictional Resistance based on Strut Length and using the 1957 ITTC line.}$$

$$CM_{fp_i} := \frac{0.075}{\left(\log\left(RnM_{p_i}\right) - 2\right)^2} \qquad \text{Coefficient of Frictional Resistance based on Demihull Length and using the 1957 ITTC line.}$$

$$RM_{fs_i} = CM_{fs_i} \cdot \frac{1}{2} \cdot \rho_{fw} \cdot \left(VM_i\right)^2 \cdot 4 \cdot SM_s \qquad \text{Frictional Resistance of four Struts}$$

$$RM_{fp_i} = CM_{fp_i} \cdot \frac{1}{2} \cdot \rho_{fw} \cdot \left(VM_i\right)^2 \cdot 2 \cdot SM_p \qquad \text{Frictional Resistance of two Demihulls}$$

$$RM_{r_i} = RM_{tl_i} - RM_{fs_i} - RM_{fp_i} \qquad \text{Residual Resistance for the Model as measured.}$$

$$CM_{r_i} = \frac{RM_{r_i}}{\left[\frac{1}{2} \cdot \rho_{fw} \cdot \left(VM_i\right)^2 \cdot SM_t\right]}$$

RnM_{s_i}	RnM_{p_i}	RM_{tl_i}	RM_{fs_i}	RM_{fp_i}	RM_{r_i}	CM_{fs_i}	CM_{fp_i}	CM_{r_i}
334390	1253804	0.801	0.267	0.372	0.162	0.006	0.004	0.001
451038	1691178	3.17	0.453	0.635	2.082	0.006	0.004	0.009
502881	1885566	4.22	0.548	0.772	2.899	0.005	0.004	0.01
540467	2026498	6.01	0.623	0.879	4.508	0.005	0.004	0.014
593607	2225746	7.14	0.735	1.041	5.364	0.005	0.004	0.013
619529	2322940	6.75	0.793	1.124	4.833	0.005	0.004	0.011
644154	2415274	6.35	0.849	1.206	4.295	0.005	0.004	0.009
671372	2517328	6.08	0.914	1.299	3.867	0.005	0.004	0.008
773763	2901245	6.74	1.176	1.678	3.886	0.005	0.004	0.006
896243	3360487	8.23	1.527	2.188	4.514	0.005	0.004	0.005
1008354	3780852	8.93	1.884	2.709	4.337	0.005	0.004	0.004
1121113	4203646	9.74	2.276	3.282	4.182	0.005	0.004	0.003
1289604	4835408	12.2	2.924	4.231	5.046	0.004	0.003	0.003
1401068	5253343	13.865	3.391	4.918	5.556	0.004	0.003	0.002
1684910	6317618	19.08	4.72	6.877	7.483	0.004	0.003	0.002
1960976	7352736	25.875	6.199	9.064	10.612	0.004	0.003	0.002
2240931	8402432	33.185	7.881	11.56	13.744	0.004	0.003	0.002

Scaled Resistance Calculations

$$CS_{r_i} = CM_{r_i}$$ Residual Resistance Coefficient remains the same in the saling.

$$RnS_{s_i} = \frac{VS_i \cdot LM_s \cdot \lambda}{\upsilon_{sw}}$$ operating Rn of the Strut in the new scale

$$RnS_{p_i} = \frac{VS_i \cdot LM_p \cdot \lambda}{\upsilon_{sw}}$$ operating Rn of the Pod in the new scale

$$CS_{fs_i} = \frac{0.075}{\left(\log\left(RnS_{s_i}\right) - 2\right)^2}$$ Coefficient of Frictional Resistance based on scaled Strut Length and using the 1957 ITTC line.

$$CS_{fp_i} = \frac{0.075}{\left(\log\left(RnS_{p_i}\right) - 2\right)^2}$$ Coefficient of Frictional Resistance based on scaled Pod Length and using the 1957 ITTC line.

$$CS_a = 0.0004$$ Correlation Allowance

$$RS_{fs_i} = CS_{fs_i} \cdot \frac{1}{2} \cdot \rho_{sw} \cdot \left(VS_i\right)^2 \cdot 4 \cdot SM_s \cdot \lambda^2$$ Frictional Resistance of the Struts

$$RS_{fp_i} = CS_{fp_i} \cdot \frac{1}{2} \cdot \rho_{sw} \cdot \left(VS_i\right)^2 \cdot 2 \cdot SM_p \cdot \lambda^2$$ Frictional Resistance of the Demi Hulls

$$RS_{r_i} = CS_{r_i} \cdot \frac{1}{2} \cdot \rho_{sw} \cdot \left(VS_i\right)^2 \cdot SM_t \cdot \lambda^2$$ Scaled Residual Resistance

$$RS_{a_i} = CS_a \cdot \frac{1}{2} \cdot \rho_{sw} \cdot \left(VS_i\right)^2 \cdot SM_t \cdot \lambda^2$$ Correlation

$$RS_{t_i} = RS_{fs_i} + RS_{fp_i} + RS_{r_i} + RS_{a_i}$$

228

Scaled Speed (fps)	Scaled Speed (knots)	Total M-3 Resistance at Full Scale	Residual Component	PodFrictional Component	StrutFrictional Component	Reynolds # of the Strut	Reynolds # of the Pod
VS_i	VS_{kts_i}	RS_{t_i}	RS_{r_i}	RS_{fp_i}	RS_{fs_i}	RnS_{s_i}	RnS_{p_i}
10.03	5.939	1805.61	572.22	637.02	416.2	20396136	76475883
13.52	8.011	9515.06	7356.37	1109.41	721.46	27511067	10315351
15.08	8.932	12890.08	10243.43	1357.69	881.47	30673259	11501024
16.2	9.6	18956.26	15926.77	1552.15	1006.64	32965848	12360637
17.8	10.543	22563.11	18951.13	1847.58	1196.59	36207094	13575951
18.57	11.004	20988.62	17075.09	2000.34	1294.71	37788190	14168787
19.31	11.441	19383.41	15172.89	2150.67	1391.23	39290231	14731982
20.13	11.925	18211.4	13660.76	2322.7	1501.61	40950382	15354460
23.2	13.743	19668.69	13727.86	3024.61	1951.46	47195710	17696163
26.87	15.919	23779.04	15948.15	3976.3	2560.23	54666388	20497315
30.23	17.91	25097.62	15322.77	4952.65	3183.76	61504627	23061332
33.61	19.913	26706.78	14773.05	6034.61	3873.76	68382394	25640170
38.66	22.905	33361.84	17826.12	7835.39	5020.44	78659517	29493606
42.01	24.885	37792.85	19629.28	9146.31	5854.09	85458229	32042802
50.52	29.927	52161.65	26437.11	12907.73	8242.17	102771228	38534359
58.79	34.83	71750.23	37490.84	17139.31	10923.55	119609899	44848066
67.19	39.803	92642.78	48556.41	21997.35	13996.93	136685734	51250698

$$\text{WRITE}(\text{m3fulfx}) := RS_{t_i} \qquad \text{WRITE}(\text{m3fulv}) := VS_{kts_i} \qquad \text{Writes the scaled data to a file for future use.}$$

$$RS_{ft_i} = RS_{fp_i} + RS_{fs_i} \qquad FF_i := \frac{RS_{ft_i}}{RS_{t_i}} \qquad RF_i := \frac{RS_{r_i}}{RS_{t_i}} \qquad \text{Percent of total resistance attributable to friction/wave.}$$

$$CA_i = \frac{RS_{a_i}}{RS_{t_i}} \qquad \text{percent of total resistance that is attributable to correlation allowance}$$

229

$$\text{WRITE}(m3fulfp) := FF_i \qquad \text{WRITE}(m3fulrp) := RF_i \qquad \text{WRITE}(m3fulcap) := CA_i$$

$$EHP_{ship_i} = \frac{RS_{t_i} \cdot VS_i}{550}$$

VS_i	VS_{kts_i}	EHP_{ship_i}
10.026	5.939	32.913
13.523	8.011	233.946
15.077	8.932	353.357
16.204	9.6	558.489
17.797	10.543	730.113
18.574	11.004	708.823
19.313	11.441	680.632
20.129	11.925	666.498
23.199	13.743	829.613
26.871	15.919	1161.749
30.232	17.91	1379.551
33.613	19.913	1632.163
38.664	22.905	2345.303
42.006	24.885	2886.43
50.516	29.927	4790.937
58.793	34.83	7669.871
67.187	39.803	11317.027

M-3 in full scale

230

Appendix H

Approximation of Impingement Force

This Worksheet approximates the impingement force created by the rooster tail on the towing frame.

$$\rho = 64 \cdot \frac{lb}{ft^3}$$

density of water

$$V_{xr} = 10 \cdot \frac{ft}{sec}$$

estimate of the maximum relative x component of velocity between the frame and water before impact.

$$V_{xa} = 0 \cdot \frac{ft}{sec}$$

water x component of velocity after the impact.

$$t = .25 \cdot sec$$

an approximation for the time of impact of the water on the frame

$$a_x = \frac{V_{xr} - V_{xa}}{t}$$

acceleration of the water

$$a_x = 40 \cdot ft \cdot sec^{-2}$$

$$vol = 1.25 \cdot in \cdot 6 \cdot in \cdot \left(V_{xr} \cdot t\right)$$

an approximation for the volume of water that is impacted during the impact period.

$$vol = 0.13 \cdot ft^3$$

$$m_w = \rho \cdot vol$$

$$m_w = 8.333 \cdot lb$$

mass of the water that is impacted during the impact period.

$$F_{impact} = m_w \cdot a_x$$

Approximated Impact Force on the frame.

$$F_{impact} = 10.36 \cdot lbf$$

Appendix I

Numerical Codes

```
% This routine solves for the total resistance of an 8 bodied SLICE type
% vessel. Solution to the friction resistance is based on the ITTC 1957
% friction line. Solution to the wave resistance portion is based on the
% solution to Mitchell's Integral proposed by Lunde in 1951 and expanded
% by Wilson.


% GENERAL INPUTS SECTION

ls= input('Input the slowest integer speed as x.xx (f/s) =');
hs=input('The number of increments=');
lani=input('The incrementation (decimal)=');

g=32.2;


water=input('For Fresh Water enter 1, Salt Water enter 2:  ');
  if water==1;
    rho= 1.9367;
    nu= 1.0804E-5;
  elseif water==2;
    rho= 1.9912;
    nu= 1.3343E-5;
  else
    disp('                                ')
    disp('                                ')
    disp('******************************************')
    disp('A valid entry was not made for water type')
    disp('The program may not provide valid results')
    disp('******************************************')
  end


  end



disp('  ')
disp('  ')
disp('  ')
disp('The body numbering is: 1=fwd stbd strut')
disp('                       2=fwd port strut')
```

```matlab
disp('                    3=aft stbd strut')
disp('                    4=aft port strut')
disp('                    5=fwd stbd pod')
disp('                    6=fwd port pod')
disp('                    7=aft stbd pod')
disp('                    8=aft port pod')
disp('  ')
disp('  ')
disp('  ')
disp('The global coordinate system is:')
disp('           x positive in the direction of motion')
disp('           y positive to port')
disp('           z positive upward')
disp('           The origin is at the undisturbed free surface')


TS= input('The height of the struts (ft)=');
LS= input('The length of the struts (ft)=');
%WSS=input('The wetted Surface of one strut (ft^2)=');

cs6=input('The 6th power coefficient for the strut potential fn=');
cs5=input('The 5th power coefficient for the strut potential fn=');
cs4=input('The 4th power coefficient for the strut potential fn=');
cs3=input('The 3rd power coefficient for the strut potential fn=');
cs2=input('The 2nd power coefficient for the strut potential fn=');
cs1=input('The 1st power coefficient for the strut potential fn=');
cs0=input('The 0th power coefficient for the strut potential fn=');

TP= input('The max diameter of the pods (ft)=');
LP= input('The length of the pods (ft)=');
%WSP=input('The wetted surface of one pod (ft^2)=');

cp6=input('The 6th power coefficient for the pod potential fn=');
cp5=input('The 5th power coefficient for the pod potential fn=');
cp4=input('The 4th power coefficient for the pod potential fn=');
cp3=input('The 3rd power coefficient for the pod potential fn=');
cp2=input('The 2nd power coefficient for the pod potential fn=');
cp1=input('The 1st power coefficient for the pod potential fn=');
cp0=input('The 0th power coefficient for the pod potential fn=');


sb1=input('The x setback of body 1 (+ or - ft)=');
os1=input('The y offset of body 1 (+ or - ft)=');
sub1=input('The z submergence of body1 (- or - ft)=');
```

```
sb2=input('The x setback of body 2 (- or - ft)=');
os2=input('The y offset of body 2 (+ or - ft)=');
sub2=input('The z submergence of body2 (+ or - ft)=');


sb3=input('The x setback of body 3 (- or - ft)=');
os3=input('The y offset of body 3 (+ or - ft)=');
sub3=input('The z submergence of body3 (+ or - ft)=');


sb4=input('The x setback of body 4 (- or - ft)=');
os4=input('The y offset of body 4 (+ or - ft)=');
sub4=input('The z submergence of body4 (+ or - ft)=');


sb5=input('The x setback of body 5 (- or - ft)=');
os5=input('The y offset of body 5 (- or - ft)=');
sub5=input('The z submergence of body5 (+ or - ft)=');


sb6=input('The x setback of body 6 (- or - ft)=');
os6=input('The y offset of body 6 (+ or - ft)=');
sub6=input('The z submergence of body6 (+ or - ft)=');


sb7=input('The x setback of body 7 (- or - ft)=');
os7=input('The y offset of body 7 (+ or - ft)=');
sub7=input('The z submergence of body7 (+ or - ft)=');


sb8=input('The x setback of body 8 (- or - ft)=');
os8=input('The y offset of body 8 (+ or - ft)=');
sub8=input('The z submergence of body8 (+ or - ft)=');




tseg=input('The number of Theta Segments=');
zseg= input('The number of segments in Z=');
xseg= input('The number of segments in X=');
```

% This section calls the routines that computes the Rw value
% for each of the body and interface terms and the Rf value for
% the body terms only.

```
Rwb=0;
Rw11=0;
Rw22=0;
Rw33=0;
Rw44=0;
Rw55=0;
Rw66=0;
Rw77=0;
Rw88=0;
Rws=0;
Rw15=0;
Rw26=0;
Rw37=0;
Rw48=0;
Rwl=0;
Rw13=0;
Rw17=0;
Rw53=0;
Rw57=0;
Rw24=0;
Rw28=0;
Rw64=0;
Rw68=0;
Rwd=0;
Rw14=0;
Rw18=0;
Rw54=0;
Rw58=0;
Rw23=0;
Rw27=0;
Rw63=0;
Rw67=0;
Rwt=0;
Rw12=0;
Rw16=0;
Rw52=0;
Rw56=0;
Rw34=0;
Rw38=0;
Rw74=0;
```

```
Rw78=0;
Rf=0;
Rfs=0;
Rfp=0;
Rt=0;


%*********** BODY TERMS*********
oneone
twotwo
thrthr
forfor
fivfiv
sixsix
sevsev
ateate

%*******SAME CORNER INTERACTION TERMS******
onefiv
twosix
thrsev
forate

%******LONGITUDINAL INTERACTION TERMS*********
onethr
onesev
fivthr
fivsev
twofor
twoate
sixfor
sixate

%*****DIAGONAL INTERACTION TERMS*********
onefor
oneate
fivfor
fivate
twothr
twosev
sixthr
sixsev

%******TRANSVERSE DIAGONAL TERMS***********
```

```
onetwo
onesix
fivtwo
fivsix
thrfor
thrate
sevfor
sevate

Rwb=Rw11+Rw22+Rw33+Rw44+Rw55+Rw66+Rw77+Rw88;
Rws=Rw15+Rw26+Rw37+Rw48;
Rwl=Rw13+Rw17+Rw53+Rw57+Rw24+Rw28+Rw64+Rw68;
Rwd=Rw14+Rw18+Rw54+Rw58+Rw23+Rw27+Rw63+Rw67;
Rwt=Rw12+Rw16+Rw52+Rw56+Rw34+Rw38+Rw74+Rw78;

Rw=Rwb+Rws+Rwl+Rwd+Rwt

Rf=Rfs+Rfp

Rt=Rw+Rf

plot(V,Rt,'-',V,Rw,'-.')
```

```
%       *****************PODGEO*************************
%
%   This file creates the offsets for the pod by obtaining nose
%   tail and parallel midbody information. The nose is formed
%   using an ellipse and the tail is formed using a parabola.
%   This is then fit to a seventh order polynomial and the results compared.

seg=input('The min number of segments (must be even) for the pod = ');
D=input('The max. diameter(ft) of the pod = ');
L2D=input('The desired Legnth to Diameter ratio of the pod = ');
Lpmb=input(' The amount of Parallel Midbody(ft) in the pod = ');
Pn=input(' The decimal amount of the pod that is nose section = ');

  Lpod= D*L2D;
  Ln= Pn*(Lpod-Lpmb);
  Lt= Lpod-Ln-Lpmb;




npn=input(' The nose shape exponent.(bigger is fuller) = ');
npt=input(' The tail shape exponent.(bigger is fuller) = ');

ppod=zeros(1,8);
xn=zeros(1,seg*2);
offn=zeros(1,seg*2);
xpmb=zeros(1,seg/2);
offpmb=zeros(1,seg/2);
xt=zeros(1,seg*2);
offt=zeros(1,seg*2);
xpod=zeros(1,(seg*4+seg/2));
offpod=zeros(1,(seg*4+seg/2));
Xpod=zeros(1,seg*6);
OFFpod=zeros(1,seg*6);

  xn= (linspace(0,-Ln,seg*2))';
    offn= D/2*(1-((Ln-abs(xn))./Ln).^npn).^(1/npn);


  xpmb= (linspace(-Ln,-(Ln+Lpmb),seg/2))';
    offpmb= D/2*xpmb./xpmb;


  xt = (linspace(-(Ln+Lpmb),-Lpod,seg*2))';
```

```
offt= D/2*(1-((abs(xt)-Ln-Lpmb)./Lt).^npt);


xpod=[xn;xpmb;xt];
offpod=[offn;offpmb;offt];


ppod=polyfit(xpod,offpod,7)'


Xpod=(linspace(0,-Lpod,seg*6));
OFFpod=(ppod(1).*Xpod.^7)+(ppod(2).*Xpod.^6)+(ppod(3).*Xpod.^5)+...
    (ppod(4).*Xpod.^4)+(ppod(5).*Xpod.`3)+(ppod(6).*Xpod.^2)+...
    (ppod(7).*Xpod.^1)+ppod(8);


plot(Xpod.OFFpod,'-',Xpod,-OFFpod,':')
```

```
%      ****************STRUTGEO*********************
%
%   This file creates the offsets for the strut by obtaining nose
%   tail and parallel midbody information. The nose and tail are formed
%   using a parabola. This is then fit to a seventh order polynomial
%   and the results compared.

segs=input('The min number of segments (must be even) for the strut = ');
B=input('The max. beam(ft) of the strut = ');
L2Ds=input('The desired Legnth to Diameter ratio of the strut = ');
Lpmbs=input(' The amount of Parallel Midbody(ft) in the strut = ');
Pns=input(' The decimal amount of the strut that is nose section = ');

  Lstrut= B*L2Ds;
  Lns= Pns*(Lstrut-Lpmbs);
  Lts= Lstrut-Lns-Lpmbs;




nsn=input(' The nose shape exponent,(bigger is fuller) = ');
nst=input(' The tail shape exponent,(bigger is fuller) = ');


xns=zeros(1,segs*2);
offns=zeros(1,segs*2);
xpmbs=zeros(1,segs/2);
offpmbs=zeros(1,segs/2);
xts=zeros(1,segs*2);
offts=zeros(1,segs*2);
xstrut=zeros(1,(segs*4+segs/2));
offstrut=zeros(1,(segs*4+segs/2));
Xstrut=zeros(1,segs*6);
OFFstrut=zeros(1,segs*6);

  xns= (linspace(0,-Lns,segs*2))';
    offns= B/2*(1-((Lns-abs(xns))./Lns).^nsn);


  xpmbs= (linspace(-Lns,-(Lns+Lpmbs),segs/2))';
    offpmbs= B/2*xpmbs./xpmbs;


  xts = (linspace(-(Lns+Lpmbs),-Lstrut,segs*2))';
```

242

```
offts= B/2*(1-((abs(xts)-Lns-Lpmbs)./Lts).^nst);


xstrut=[xns;xpmbs;xts];
offstrut=[offns;offpmbs;offts];


ps=polyfit(xstrut,offstrut,7)'


Xstrut=(linspace(0,-Lstrut,segs*6))';
OFFstrut=(ps(1).*Xstrut.^7)+(ps(2).*Xstrut.^6)+(ps(3).*Xstrut.^5)+...
    (ps(4).*Xstrut.^4)+(ps(5).*Xstrut.^3)+(ps(6).*Xstrut.^2)+...
    (ps(7).*Xstrut)+(ps(8));


plot(Xstrut,OFFstrut,'--',xstrut,offstrut,'-');
```

```
theta1=zeros(tseg+1,1);
z1=zeros(zseg+1,1);
x1=zeros(xseg+1,1);
p1x=zeros(xseg+1,1);
q1x=zeros(xseg+1,1);
p1z=zeros(zseg+1,1);
q1z=zeros(zseg+1,1);
p1t=zeros(tseg+1,1);
q1t=zeros(tseg+1,1);
res11=zeros(tseg+1,1);
q1At=zeros(tseg+1,1);
p1At=zeros(tseg+1,1);
p1Az=zeros(zseg+1,1);
q1Az=zeros(zseg+1,1);
z1A=zeros(zseg+1,1);
p1Ax=zeros(xseg+1,1);
q1Ax=zeros(xseg+1,1);
x1A=zeros(xseg+1,1);
sara1=zeros(xseg+1,1);
katep1=zeros(xseg+1,1);
kateq1=zeros(xseg+1,1);
greg1=zeros(xseg+1,1);
sara1A=zeros(xseg+1,1);
katep1A=zeros(xseg+1,1);
kateq1A=zeros(xseg+1,1);
greg1A=zeros(xseg+1,1);
V=zeros(hs-1-ls,1);
Rw11=zeros(hs+1-ls,1);


for iv=1:hs;
  V(iv)=ls-(iv*lani);
  k=g/(V(iv)^2);
  w=-V(iv)/(2*pi);


  for it=1:tseg+1;
    theta1(it)=(pi/2)*((it-1)/tseg);
```

```
for iz1= 1:zseg+1;
  z1(iz1) = -TS*((iz1-1)/zseg);

    for ix1=1:xseg+1;
      x1(ix1) =-LS*((ix1-1)/xseg);



sara1(ix1)=w*((cs6*x1(ix1)^6)+(cs5*x1(ix1)^5)+(cs4*x1(ix1)^4)+(cs3*x1(ix1)^3)+(cs2
*x1(ix1)^2)+(cs1*x1(ix1))+cs0);
katep1(ix1)=cos(k*(sb1*cos(theta1(it))+os1*sin(theta1(it)))*(sec(theta1(it)))^2);
kateq1(ix1)=sin(k*(sb1*cos(theta1(it))-os1*sin(theta1(it)))*(sec(theta1(it)))^2);
greg1(ix1)=exp(k*sub1*(sec(theta1(it)))^2);

  p1x(ix1)=sara1(ix1)*katep1(ix1)*greg1(ix1);
  q1x(ix1)=sara1(ix1)*kateq1(ix1)*greg1(ix1);

end %this end closes the **** for ix1=1:xseg-1 loop ****

  p1z(iz1)=sum(p1x)/xseg;
  q1z(iz1)=sum(q1x)/xseg;

end %this end closes the **** for iz1=1:zseg-1 loop ****

  p1t(it)=sum(p1z)/zseg;
  q1t(it)=sum(q1z)/zseg;

% *******This starts the next body calculations inside the theta loop*****


    for iz1A= 1:zseg-1;
      z1A(iz1A) = -TS*((iz1A-1)/zseg);

      for ix1A=1:xseg+1;
        x1A(ix1A) =-LS*((ix1A-1)/xseg);

sara1A(ix1A)=w*((cs6*x1A(ix1A)^6)+(cs5*x1A(ix1A)^5)-(cs4*x1A(ix1A)^4)+(cs3*x
1A(ix1A)^3)+(cs2*x1A(ix1A)^2)+(cs1*x1A(ix1A))+cs0);
katep1A(ix1A)=cos(k*(sb1*cos(theta1(it))+os1*sin(theta1(it)))*(sec(theta1(it)))^2);
kateq1A(ix1A)=sin(k*(sb1*cos(theta1(it))+os1*sin(theta1(it)))*(sec(theta1(it)))^2);
greg1A(ix1A)=exp(k*sub1*(sec(theta1(it)))^2);

  p1Ax(ix1A)=sara1A(ix1A)*katep1A(ix1A)*greg1A(ix1A);
```

245

```
qlAx(ixlA)=saralA(ixlA)*kateqlA(ixlA)*greglA(ixlA);

end %this end closes the **** for ixlA=1:xseg+1 loop ****

    plAz(izlA)=sum(plAx)/xseg;
    qlAz(izlA)=sum(qlAx)/xseg;

end %this end closes the **** for izlA=1:zseg+1 loop ****

    plAt(it)=sum(plAz)/zseg;
    qlAt(it)=sum(qlAz)/zseg;

res11(it)=16*pi*rho*k^2*((plt(it)*plAt(it))+(qlt(it)*qlAt(it)))*(sec(theta1(it))^3);


end %this end closes the **** for it= 1:tseg+1 loop ****


    Rw11(iv)= sum(res11)/tseg

end   % this closes the **** for iv = ... loop *****
```

```
%*****************SIXSIX.m*********************

Rw66=zeros(hs-1-ls,1);
res66=zeros(tseg-1,1);
theta1=zeros(tseg-1,1);
z1=zeros(zseg+1,1);
x1=zeros(xseg+1,1);
p1x=zeros(xseg+1,1);
q1x=zeros(xseg-1,1);
p1z=zeros(zseg+1,1);
q1z=zeros(zseg+1,1);
p1t=zeros(tseg+1,1);
q1t=zeros(tseg+1,1);
q1At=zeros(tseg-1,1);
p1At=zeros(tseg-1,1);
p1Az=zeros(zseg-1,1);
q1Az=zeros(zseg-1,1);
z1A=zeros(zseg-1,1);
p1Ax=zeros(xseg-1,1);
q1Ax=zeros(xseg-1,1);
x1A=zeros(xseg-1,1);
sara1=zeros(xseg-1,1);
katep1=zeros(xseg-1,1);
kateq1=zeros(xseg-1,1);
greg1=zeros(xseg-1,1);
sara1A=zeros(xseg-1,1);
katep1A=zeros(xseg-1,1);
kateq1A=zeros(xseg-1,1);
greg1A=zeros(xseg-1,1);
V=zeros(hs+1-ls,1);


for iv=1:hs;
 V(iv)=ls+(iv*lani);

 k=g/(V(iv)^2);
 w=-V(iv)/(2*pi);


  for it=1:tseg+1;
    theta1(it)=(pi/2)*((it-1)/tseg);

      for iz1= 1:zseg+1;
        z1(iz1) = -TP*((iz1-1)/zseg);
```

247

```
        for ix1=1:xseg+1;
          x1(ix1) =-LP*((ix1-1)/xseg);



sara1(ix1)=w*((cp6*x1(ix1)^6)+(cp5*x1(ix1)^5)+(cp4*x1(ix1)^4)+(cp3*x1(ix1)^3)+(cp
2*x1(ix1)^2)+(cp1*x1(ix1))+cp0);
katep1(ix1)=cos(k*(sb6*cos(theta1(it))+os6*sin(theta1(it))))*(sec(theta1(it)))^2);
kateq1(ix1)=sin(k*(sb6*cos(theta1(it))+os6*sin(theta1(it))))*(sec(theta1(it)))^2);
greg1(ix1)=exp(k*sub6*(sec(theta1(it)))^2);

      p1x(ix1)=sara1(ix1)*katep1(ix1)*greg1(ix1);
      q1x(ix1)=sara1(ix1)*kateq1(ix1)*greg1(ix1);

end %this end closes the **** for ix1=1:xseg+1 loop ****

      p1z(iz1)=sum(p1x)/xseg;
      q1z(iz1)=sum(q1x)/xseg;

end %this end closes the **** for iz1=1:zseg+1 loop ****

      p1t(it)=sum(p1z)/zseg;
      q1t(it)=sum(q1z)/zseg;

% *******This starts the next body calculations inside the theta loop*****


        for iz1A= 1:zseg+1;
          z1A(iz1A) = -TP*((iz1A-1)/zseg);

          for ix1A=1:xseg+1;
            x1A(ix1A) =-LP*((ix1A-1)/xseg);

sara1A(ix1A)=w*((cp6*x1A(ix1A)^6)+(cp5*x1A(ix1A)^5)+(cp4*x1A(ix1A)^4)+(cp3*
x1A(ix1A)^3)+(cp2*x1A(ix1A)^2)+(cp1*x1A(ix1A))+cp0);
katep1A(ix1A)=cos(k*(sb6*cos(theta1(it))+os6*sin(theta1(it))))*(sec(theta1(it)))^2);
kateq1A(ix1A)=sin(k*(sb6*cos(theta1(it))+os6*sin(theta1(it))))*(sec(theta1(it)))^2);
greg1A(ix1A)=exp(k*sub6*(sec(theta1(it)))^2);

      p1Ax(ix1A)=sara1A(ix1A)*katep1A(ix1A)*greg1A(ix1A);
      q1Ax(ix1A)=sara1A(ix1A)*kateq1A(ix1A)*greg1A(ix1A);

end %this end closes the **** for ix1A=1:xseg+1 loop ****
```

```matlab
        p1Az(iz1A)=sum(p1Ax)/xseg;
        q1Az(iz1A)=sum(q1Ax)/xseg;

end %this end closes the **** for iz1A=1:zseg+1 loop ****

        p1At(it)=sum(p1Az)/zseg;
        q1At(it)=sum(q1Az)/zseg;

res66(it)=16*pi*rho*k^2*((p1t(it)*p1At(it))-(q1t(it)*q1At(it)))*(sec(theta1(it))^3);


end %this end closes the **** for it= 1:tseg+1 loop ****


    Rw66(iv)= sum(res66)/tseg

end   %this closes the **** for iv = ... loop *****
```

```
Rw16=zeros(hs+1-ls,1);
res16=zeros(tseg+1,1);
theta1=zeros(tseg+1,1);
z1=zeros(zseg+1,1);
x1=zeros(xseg+1,1);
p1x=zeros(xseg+1,1);
q1x=zeros(xseg+1,1);
p1z=zeros(zseg+1,1);
q1z=zeros(zseg+1,1);
p1t=zeros(tseg+1,1);
q1t=zeros(tseg+1,1);
q1At=zeros(tseg+1,1);
p1At=zeros(tseg+1,1);
p1Az=zeros(zseg+1,1);
q1Az=zeros(zseg+1,1);
z1A=zeros(zseg+1,1);
p1Ax=zeros(xseg+1,1);
q1Ax=zeros(xseg+1,1);
x1A=zeros(xseg+1,1);
sara1=zeros(xseg+1,1);
katep1=zeros(xseg+1,1);
kateq1=zeros(xseg+1,1);
greg1=zeros(xseg+1,1);
sara1A=zeros(xseg+1,1);
katep1A=zeros(xseg+1,1);
kateq1A=zeros(xseg+1,1);
greg1A=zeros(xseg+1,1);
V=zeros(hs+1-ls,1);


for iv=1:hs;
  V(iv)=ls+(iv*lani);

  k=g/(V(iv)^2);
  w=-V(iv)/(2*pi);


  for it=1:tseg+1;
    theta1(it)=(pi/2)*((it-1)/tseg);

      for iz1= 1:zseg+1;
        z1(iz1) = -TP*((iz1-1)/zseg);
```

```matlab
        for ix1=1:xseg+1;
          x1(ix1) =-LP*((ix1-1)/xseg);



sara1(ix1)=w*((cs6*x1(ix1)^6)+(cs5*x1(ix1)^5)+(cs4*x1(ix1)^4)+(cs3*x1(ix1)^3)+(cs2
*x1(ix1)^2)+(cs1*x1(ix1))+cs0);
katep1(ix1)=cos(k*(sb1*cos(theta1(it))+os1*sin(theta1(it)))*(sec(theta1(it)))^2);
kateq1(ix1)=sin(k*(sb1*cos(theta1(it))+os1*sin(theta1(it)))*(sec(theta1(it)))^2);
greg1(ix1)=exp(k*sub1*(sec(theta1(it)))^2);

  p1x(ix1)=sara1(ix1)*katep1(ix1)*greg1(ix1);
  q1x(ix1)=sara1(ix1)*kateq1(ix1)*greg1(ix1);

end %this end closes the **** for ix1=1:xseg+1 loop ****

  p1z(iz1)=sum(p1x)/xseg;
  q1z(iz1)=sum(q1x)/xseg;

end %this end closes the **** for iz1=1:zseg+1 loop ****

  p1t(it)=sum(p1z)/zseg;
  q1t(it)=sum(q1z)/zseg;

% *******This starts the next body calculations inside the theta loop*****


        for iz1A= 1:zseg+1;
         z1A(iz1A) = -TP*((iz1A-1)/zseg);

          for ix1A=1:xseg+1;
            x1A(ix1A) =-LP*((ix1A-1)/xseg);

sara1A(ix1A)=w*((cp6*x1A(ix1A)^6)+(cp5*x1A(ix1A)^5)+(cp4*x1A(ix1A)^4)+(cp3*
x1A(ix1A)^3)+(cp2*x1A(ix1A)^2)+(cp1*x1A(ix1A))+cp0);
katep1A(ix1A)=cos(k*(sb6*cos(theta1(it))+os6*sin(theta1(it)))*(sec(theta1(it)))^2);
kateq1A(ix1A)=sin(k*(sb6*cos(theta1(it))+os6*sin(theta1(it)))*(sec(theta1(it)))^2);
greg1A(ix1A)=exp(k*sub6*(sec(theta1(it)))^2);

  p1Ax(ix1A)=sara1A(ix1A)*katep1A(ix1A)*greg1A(ix1A);
  q1Ax(ix1A)=sara1A(ix1A)*kateq1A(ix1A)*greg1A(ix1A);

end %this end closes the **** for ix1A=1:xseg+1 loop ****
```

251

```
    p1Az(iz1A)=sum(p1Ax)/xseg;
    q1Az(iz1A)=sum(q1Ax)/xseg;

end %this end closes the **** for iz1A=1:zseg+1 loop ****

    p1At(it)=sum(p1Az)/zseg;
    q1At(it)=sum(q1Az)/zseg;

res16(it)=32*pi*rho*k^2*((p1t(it)*p1At(it))+(q1t(it)*q1At(it)))*(sec(theta1(it))^3);


end %this end closes the **** for it= 1:tseg+1 loop ****


    Rw16(iv)= sum(res16)/tseg

end   % this closes the **** for iv = ... loop *****
```
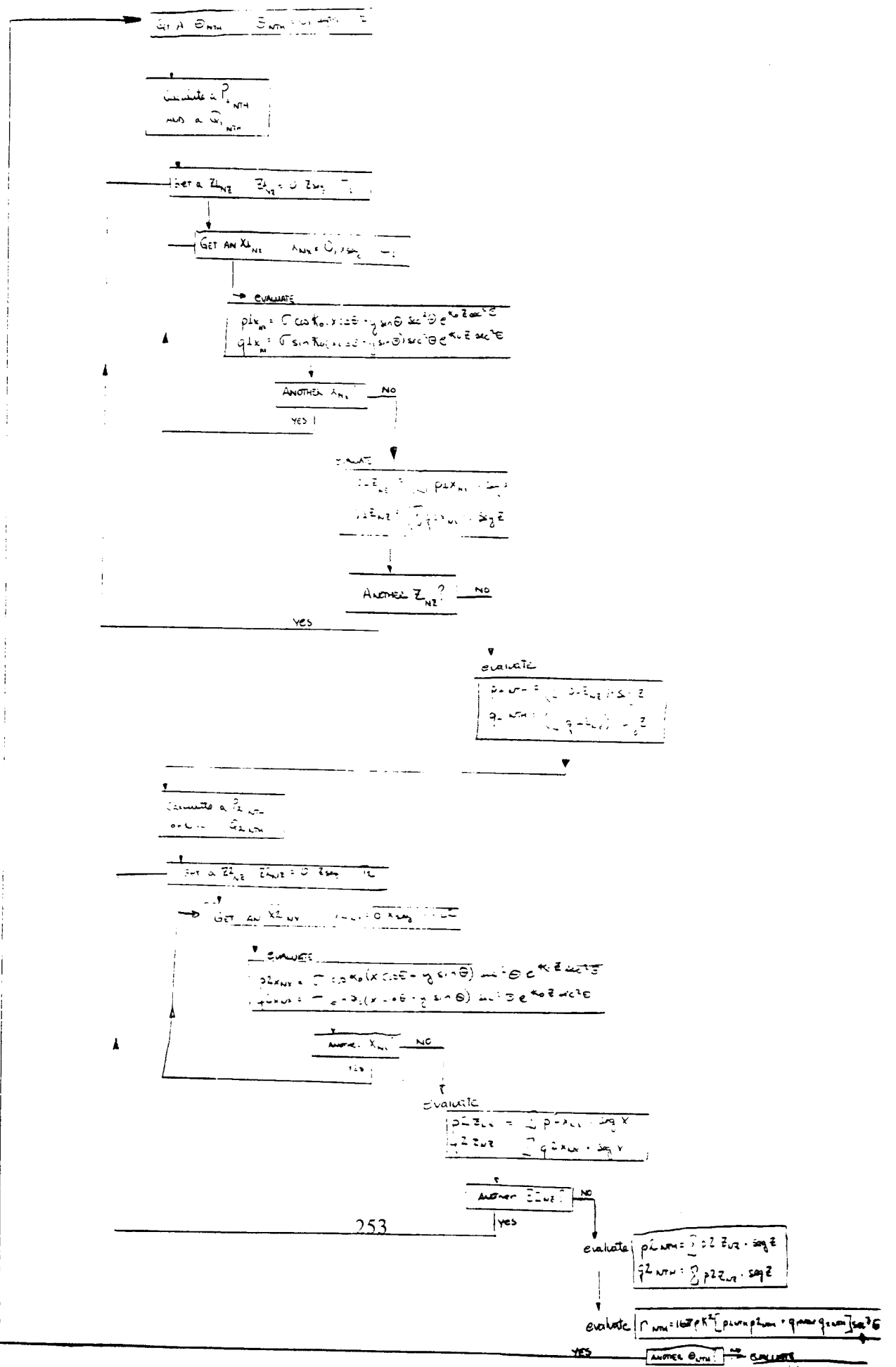
GET A Θ_{NTH} $\Xi_{NTH} = \ldots$

calculate a $P_{1_{NTH}}$
and a $Q_{1_{NTH}}$

GET a $Z_{1_{NZ}}$ $Z_{1_{NZ}} = 0 \; Z_{max} \; \ldots$

GET AN $X_{1_{NX}}$ $X_{NX} = 0, \ldots$

$\rightarrow$ EVALUATE

$$p1x_m = \sigma \cos K_0 \ldots$$
$$q1x_m = \sigma \sin K_0 \ldots$$

ANOTHER X_{NX} NO

YES

evaluate

$$\ldots = \sum p1x_{nx} \ldots$$
$$\ldots = \sum q1x_{nx} \ldots$$

ANOTHER Z_{NZ}?   NO

YES

evaluate

$$p \ldots = \ldots$$
$$q \ldots = \ldots$$

calculate a $P2_{N\ldots}$
and a $Q2_{NTH}$

GET a $Z2_{NZ}$ $Z2_{NZ} = 0 \; Z_{max} \; \ldots$

$\rightarrow$ GET AN $X2_{NX}$ $\ldots = 0 \; X_{max} \ldots$

EVALUATE

$$p2x_{NX} = \sigma \cos K_0 (x \cos \Theta - y \sin \Theta) \ldots \Theta e^{\ldots}$$
$$q2x_{NX} = \sigma \sin K_0 (x \cos \Theta + y \sin \Theta) \ldots \Theta e^{\ldots}$$

ANOTHER X_{NX} NO

YES

evaluate

$$p2z_{\ldots} = \sum p2x_{nx} \cdot \ldots X$$
$$q2z_{NZ} = \sum q2x_{nx} \cdot \ldots Y$$

ANOTHER $Z2_{NZ}$ NO

YES

evaluate $$p2_{NTH} = \sum p2z_{nz} \cdot \ldots$$
$$q2_{NTH} = \sum p2z_{nz} \cdot \ldots$$

evaluate $$\sigma_{NM} = 16 \pi K^2 [p1_{NTH} p2_{NTH} + q_{NTH} q1_{NTH}] \ldots$$

ANOTHER Θ_{NTH} NO

YES

253